TUNGSTEN-NITROGEN INTERACTIONS IN IRON

A dissertation submitted for the degree of

Doctor of Philosophy

of the University of Newcastle upon Tyne

by

Alan Stephenson

Department of Metallurgy

University of Newcastle upon Tyne

March 1973

PREFACE

This dissertation describes original work which has not been submitted for a degree at any other University.

The investigations were carried out in the Department of Metallurgy of the University of Newcastle upon Tyne during the period October 1969 to September 1972 under the supervision of Professor K.H. Jack and Dr. P. Grieveson.*

The main part of the thesis describes a study of precipitation in iron-tungsten-nitrogen alloys and is part of a wider investigation being carried out at Newcastle on the effect of substitutional alloying elements on the behaviour of interstitial solutes in iron.

Subsidiary topics are discussed in three appendices.

* Now Professor of Metallurgy at the University of Strathclyde, Glasgow.

ACKNOWLEDGEMENTS

I wish to thank Professor K.H. Jack and Professor P. Grieveson for advice, encouragement and general supervision of the work.

I also wish to express gratitude to:
Professor N.J. Petch for providing accommodation and facilities in the Department of Metallurgy of the University of Newcastle upon Tyne;
The Science Research Council for the award of a maintenance grant;
Professor Thirsk and his staff in the Department of Chemistry of the University of Newcastle upon Tyne for the use of electron microscope facilities;
Many colleagues in the Department of Metallurgy of the University of Newcastle upon Tyne for stimulating discussion and advice, in particular Dr. J.H. Driver for instruction in electron microscopy;
Mrs A. Rule for typing the script;
My wife for her encouragement.

March, 1973

ABSTRACT

Precipitation in iron-tungsten alloys containing nitrogen as the predominant interstitial constituent is studied by a variety of techniques including X-ray methods, optical metallography and electron microscopy.

Investigations into the tungsten-nitrogen system show the marked effect of oxygen on the formation of tungsten nitrides.

"Constant activity nitriding" of iron-tungsten alloys containing up to 9.3 wt.% W produces as many as six different equilibrium tungsten or iron-tungsten nitrides and oxy-nitrides. The phase produced depends upon the tungsten, nitrogen and oxygen potential as well the the temperature.

Alloys containing more than about 4.0 wt.% tungsten nitrided at 590-640°C in appropriate nitrogen potentials exhibit a precipitation sequence

GP zones ⟶ intermediate precipitate ⟶ equilibrium precipitate

The transition from zones to intermediate precipitate occurs by a continuous ordering process in which tungsten atoms replace those of iron in certain sites. The final stage occurs discontinuously.

Tungsten concentrations or nitrogen potentials lower than the critical values prevent rapid homogeneous precipitation and the intermediate phase is precipitated heterogeneously.

Metallographic studies of quench-aged tungsten-nitrogen-ferrites demonstrate that tungsten has a negligible effect on the para-precipitation of iron nitrides.

CONTENTS

INTRODUCTION

Small amounts of manganese together with nitrogen are known to improve the tensile strength and creep resistance of iron (Baird and Jamieson, 1963; Forrest and Hopkin, 1963; Baird and Mackenzie, 1964; Hopkin, 1965; Baird and Jamieson, 1966). An investigation at Newcastle showed that these improvements were at least partly due to the precipitation of manganese nitrides (see Pipkin, 1967).

More recently, similar investigations in the Fe-Mo-N system (see Speirs, 1969; Speirs et.al., 1971) and the Fe-Nb-N system (see Roberts, 1970) have produced materials of surprisingly high hardness. Although tungsten is not a common addition to steels, its behaviour on nitriding is in some ways similar to that of molybdenum. It was therefore thought that a systematic study of the precipitation of nitrides in iron-tungsten alloys might prove useful.

Any examination of a ternary system requires knowledge of the three component binary systems. Although the phases occurring in the Fe-N and Fe-W systems are well established, many uncertainties exist in the W-N system. Consequently a short study of the latter was undertaken in order to provide background information for the main topic.

The techniques used in the investigation include electron microscopy, X-ray diffraction and optical metallography. In addition, the application of thermodynamic principles, in particular the concepts of local and metastable equilibria, is necessary for the interpretation of results.

Chapter I

PREVIOUS INVESTIGATIONS

I.1 The iron-nitrogen phase diagram

Figure I.1 shows the iron-nitrogen phase diagram (Jack, 1951a) in which there are five stable phases (α - nitrogen ferrite, γ - nitrogen austenite, γ' - Fe_4N, ϵ - "Fe_3N" and ζ - Fe_2N) and two metastable phases (α' - nitrogen martensite and α'' - $Fe_{16}N_2$). Table I.1 summarises the characteristics of each phase.

The solid solutions of nitrogen in ferrite and austenite are isostructural with their carbon equivalents but some differences between the behaviour of carbon and nitrogen are significant. In particular the maximum solubility of nitrogen in ferrite is about 0.1 wt.% i.e. about an order of magnitude greater than that of carbon. The solubilities of Fe_4N and $Fe_{16}N_2$ in ferrite, together with that of molecular nitrogen at a pressure of one atmosphere are shown in Figure I.2. Nitrogen-austenite exists down to 590°C at which temperature it contains 2.35 wt.% nitrogen.

γ' - Fe_4N has a face-centred cubic arrangement of iron atoms like austenite, but the nitrogen atoms are fully ordered and occupy one quarter of the available octahedral interstices (see Figure I.3).

Table I.1

Unit-cell dimensions and composition limits of iron-nitrogen phases

phase symbol	crystal structure	composition limits	unit-cell dimensions	composition	references
α	b.c.c.	0-0.1 wt.%N; i.e. $Fe-FeN_{0.004}$	a=2.866 Å a=2.869 Å	Fe 0.1 wt.%N	Wreidt and Zwell (1962)
γ	f.c.c.	0-2.8 wt.%N; i.e. $Fe-FeN_{0.12}$	a=3.615 Å a=3.654 Å a=3.571 Å a=3.645 Å	1.5 wt.%N 2.8 wt.%N Fe 2.4 wt.%N	Paranjpe et.al. (1950) Jack (1951a)
γ'	cubic	5.29-5.7 wt.%N; i.e. $FeN_{0.23}-FeN_{0.24}$ 5.75-6.10 wt.%N; i.e. $FeN_{0.24}-FeN_{0.26}$	a=3.791 Å a=3.801 Å a=3.787 Å a=3.795 Å	5.29 wt.%N 5.71 wt.%N 5.75 wt.%N 6.10 wt.%N	Paranjpe et.al. (1950) Jack (1948)
ε	c.p. hexagonal (dimensions for pseudo-cell)	5.70-11.0 wt.%N; i.e. $FeN_{0.24}-FeN_{0.49}$	a=2.660; c=4.344 Å a=2.764; c=4.420 Å a=2.657; c=4.380 Å a=2.770; c=4.432 Å	5.70 wt.%N 11.0 wt.%N 7.30 wt.%N 11.0 wt.%N	Jack (1948) Paranjpe et.al. (1950)
ζ	orthor-hombic (dimensions for pseudo-cell)	11.1-11.3 wt.%N; i.e. $FeN_{0.50}-FeN_{0.51}$	a=2.762; b=4.830 c=4.416 Å	11.3 wt.%N	Jack (1948)
α'	b.c. tetragonal	as γ-austenite	a=2.851; c=3.071 Å	2.30 wt.%N	Jack (1951a)
α''	tetragonal	3.1 wt.%N; i.e. $FeN_{0.13}$	a=5.72; c=6.29 Å	3.1 wt.%N	Jack (1951b)

Fig. I.1

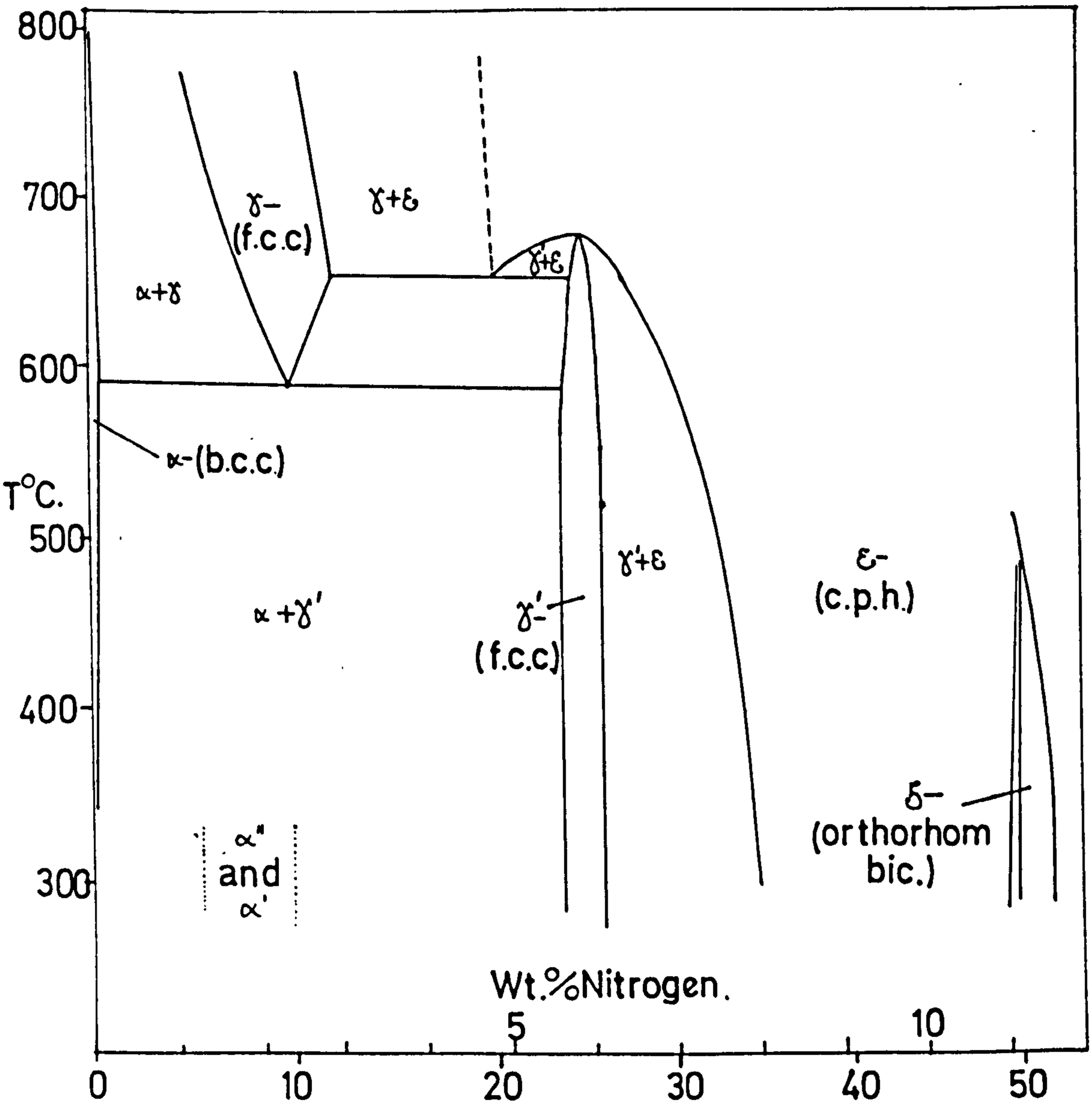

THE IRON-NITROGEN PHASE DIAGRAM.[After Jack, 1951].

Fig. I.2

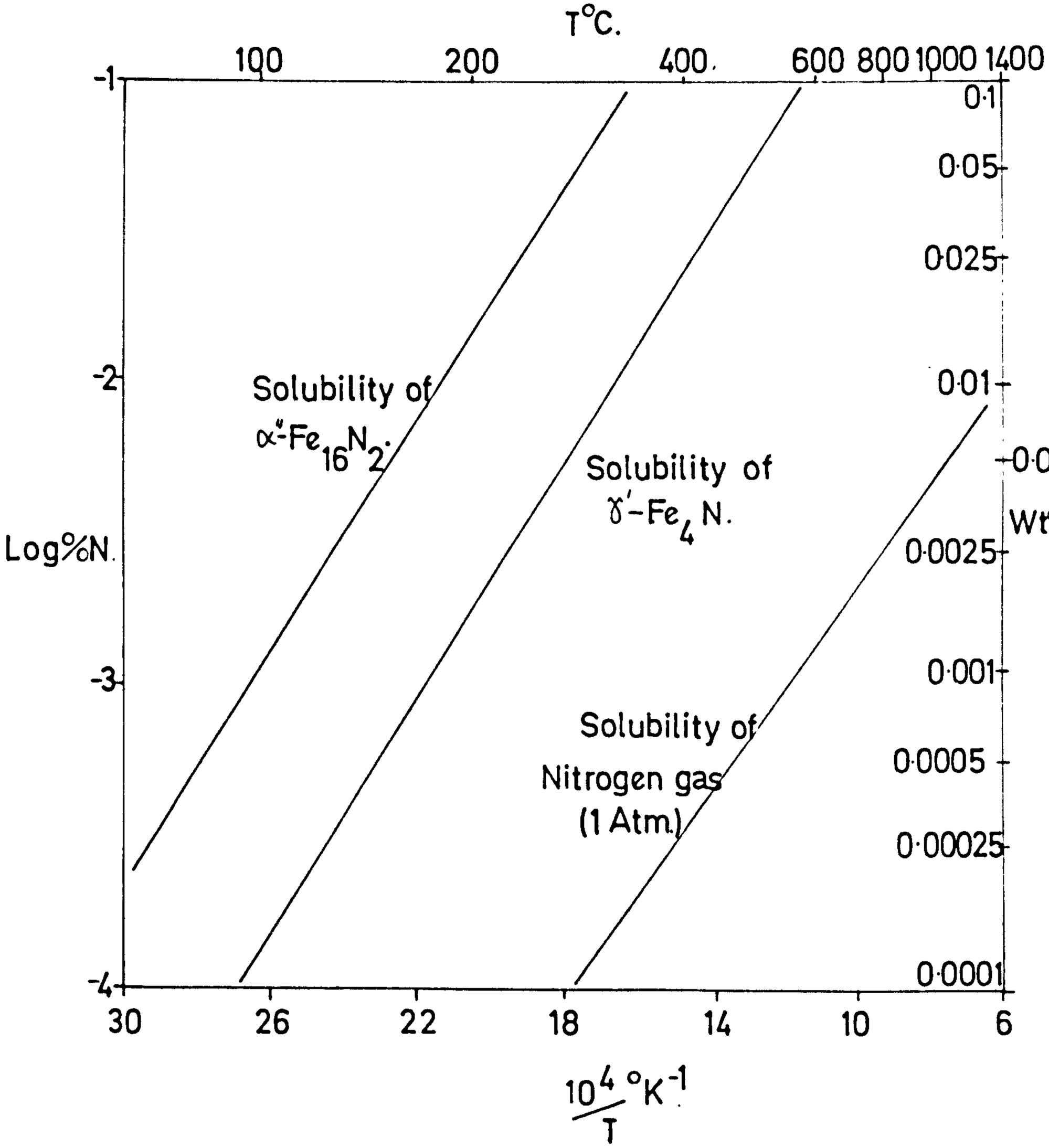

THE SOLUBILITY OF NITROGEN AND IRON NITRIDES IN α-IRON.

Fig. I.3

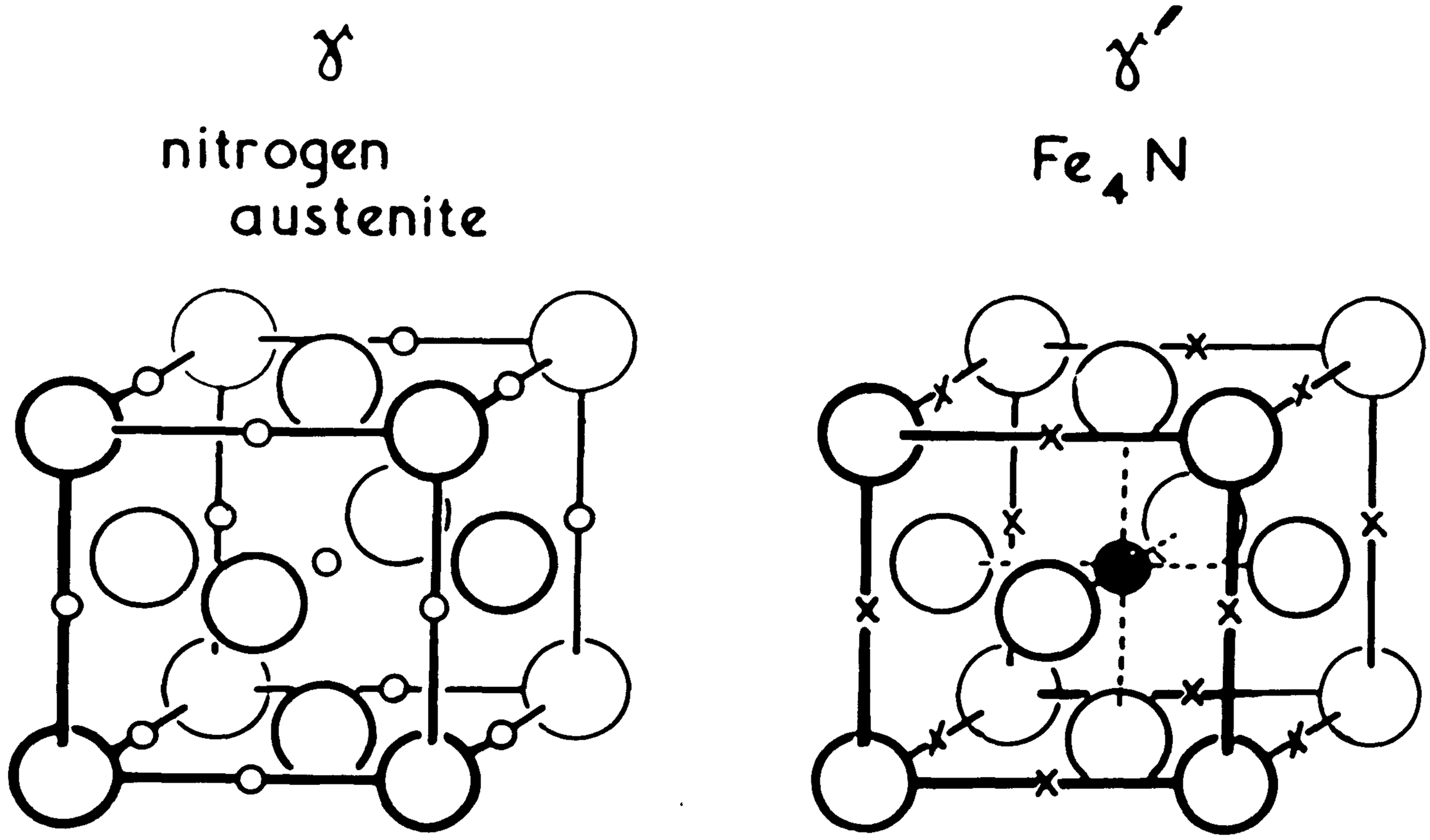
γ
nitrogen austenite
γ'
Fe_4N
Fe atoms
octahedral interstices
1 in 10 randomly filled
unoccupied interstices
N atom

The ε -phase which extends from about 5 to 11.1 wt.% nitrogen, that is approximately Fe_4N to Fe_2N, has a close-packed hexagonal arrangement of iron atoms. Orthorhombic ζ- Fe_2N is a distorted modification of ε formed by a change in the nitrogen-atom ordering. The ε -phase shows ordering over its complete homogeneity range and the $\varepsilon \longrightarrow \zeta$ transition is from one ordered nitrogen-atom arrangement to another equally ordered but different arrangement which causes an anisotropic distortion of the iron-atom lattice. The relationships between the hexagonal ε unit-cell dimensions $\underline{a}_\varepsilon$ and $\underline{c}_\varepsilon$ and the orthorhombic ζ dimensions $\underline{a}_\zeta$, $\underline{b}_\zeta$ and $\underline{c}_\zeta$ are:

$$\underline{a}_\zeta = \sqrt{3}\ \underline{a}_\varepsilon \ ; \quad \underline{b}_\zeta = 2\,\underline{a}_\varepsilon \ ; \quad \underline{c}_\zeta = \underline{c}_\varepsilon$$

Body-centred tetragonal nitrogen-martensite (α') is isostructural with carbon-martensite and is obtained by quenching nitrogen austenite. α'' - $Fe_{16}N_2$ occurs as an intermediate precipitate during the tempering of nitrogen-martensite or the aging of supersaturated nitrogen-ferrite.

I.2 The quench-aging of nitrogen-ferrite

Dijkstra (1949) showed that at 250°C the precipitation of nitrogen from quench-aged nitrogen-ferrite is a two stage process. Using X-ray techniques, Jack and Maxwell (1952) showed that the initial precipitate was α'' - $Fe_{16}N_2$, which had been previously characterised by Jack (1951b) during the

low temperature aging of nitrogen-martensite.

The structure of $Fe_{16}N_2$ can be considered merely as eight unit cells of body-centred cubic iron strained anisotropically due to the presence of nitrogen (see Figure I.4). The nitrogen atoms occupy one twenty-fourth of the available interstices but in such a manner as to expand the lattice in the c direction only. There is a consequent small contraction of the lattice in the a directions.

Electron microscope investigations (Booker, Norbury and Sutton, 1957; Keh and Wreidt, 1962; Hale and McLean, 1963) confirmed the orientation relationship proposed by Jack and Maxwell, that is

$$(100)_{\alpha''} \parallel (100)_{\alpha} \qquad [001]_{\alpha''} \parallel [001]_{\alpha}$$

The phase readily precipitates as discs because of the excellent lattice "fit" in two directions, and the large degree of "misfit" in the third ($\sim$11%).

In recent work at Newcastle Roberts, Grieveson and Jack (see Speirs et.al., 1971; see Roberts, 1970) have shown that at high supersaturations and at low temperatures ($\sim 20^{\circ}C$), precipitation of α''-$Fe_{16}N_2$ is homogeneous and occurs via Guinier-Preston zone formation. As the temperature is increased and the supersaturation decreased precipitation becomes heterogeneous (see Figure I.5).

The equilibrium phase γ'-Fe_4N precipitates at the

Fig. I.4

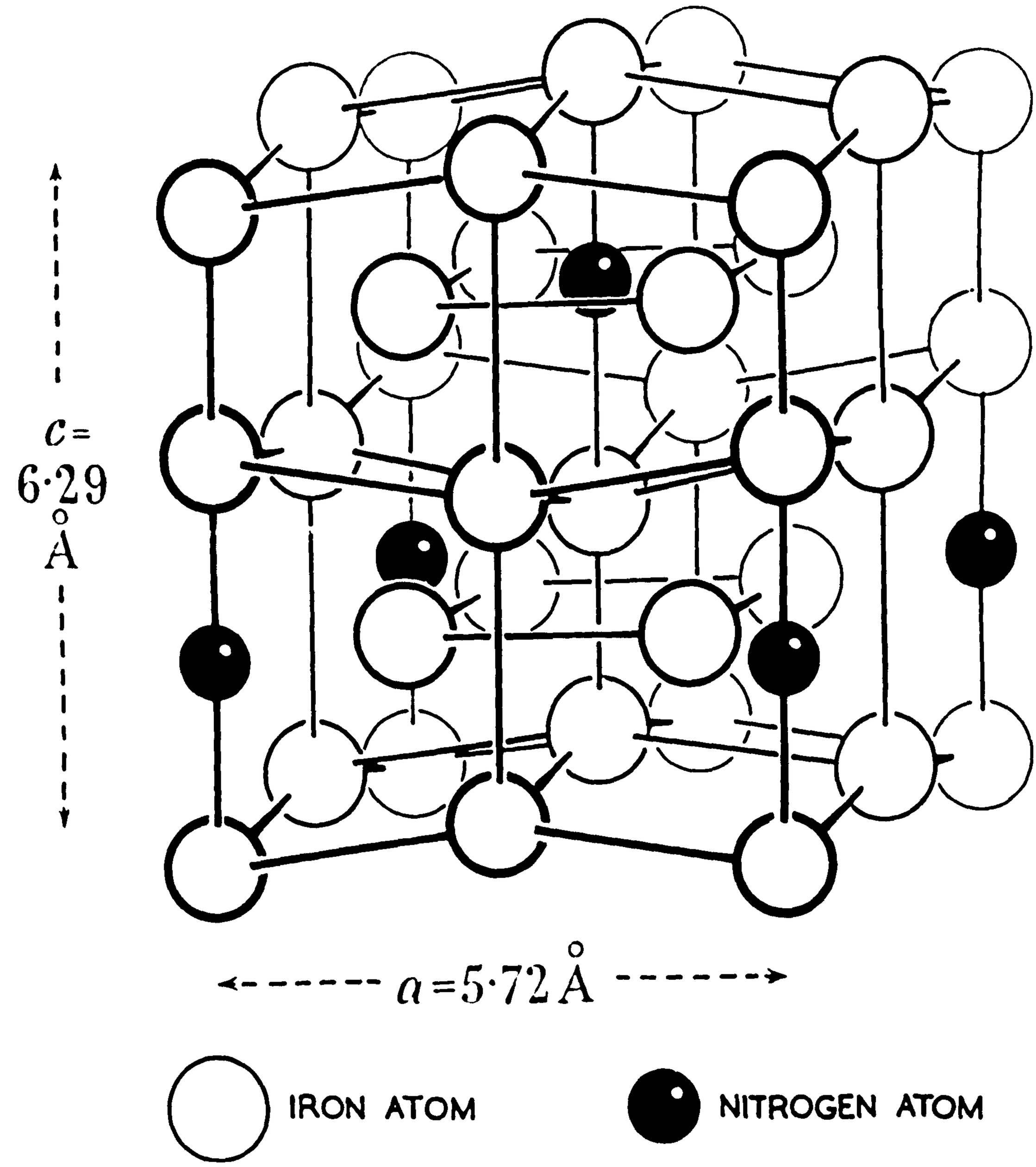

Fig. I.5

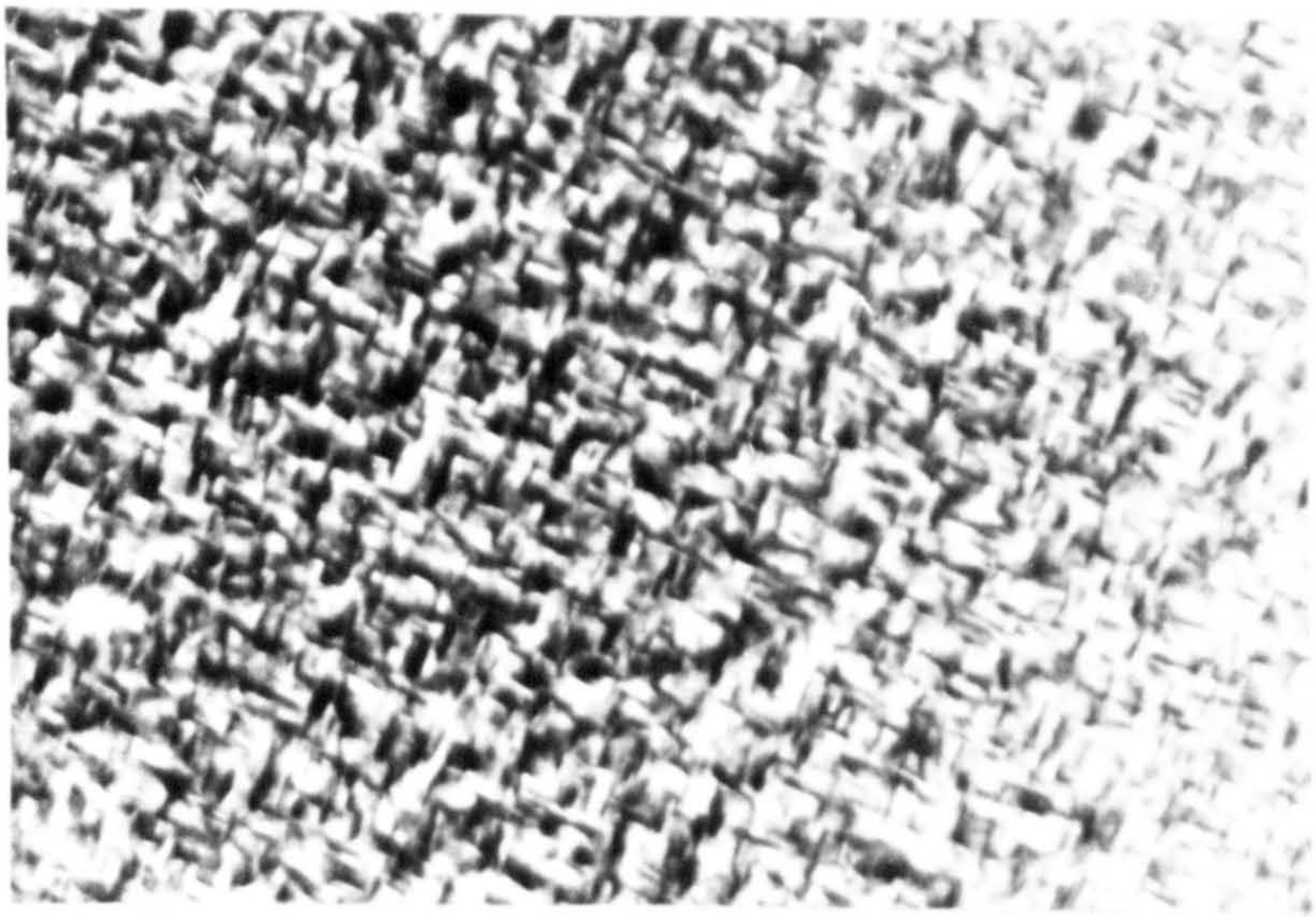

0·072%N. Aged 16h.21°C.

Homogeneous only

0·1μ

[010]

[100] (001)

0·072%N. Aged 1h.55°C.

Homogeneous +

Heterogeneous

0·5μ

[010]

(001)

[100]

0·009%N. Aged 23h.45°C.

Heterogeneous only

0·5μ

[3,$\bar{1}$0,1]

(311)

[$\bar{3}\bar{1}$,10]

Fig PRECIPITATION MODES IN IRON-NITROGEN ALLOYS.

[from Roberts, 1970]

expense of α''-$Fe_{16}N_2$ after longer aging times. However it also occurs as a grain boundary precipitate during the first stage of aging (see Roberts, 1970). The orientation relationship between γ'-Fe_4N and α-Fe has been shown by Mehl, Barrett and Jerabek (1934) and Booker, Norbury and Sutton (1957) to be

$$(112)_{\gamma'} \;||\; (210)_{\alpha} \qquad [110]_{\gamma'} \;||\; [001]_{\alpha}$$

and γ' grows as plates such that $(112)_{\gamma'}$ is parallel to the plate surface.

I.3 The tungsten-nitrogen system and the effect of oxygen

The phases reported in the tungsten-nitrogen system and tungsten-nitrogen-oxygen system are summarised in Table I.2.

Hägg (1930a) reported the existence of a face centred cubic phase whose lattice parameter was $\underline{a}$=4.118 kX. This was confirmed by Kiessling and Liu (1951) who obtained a value of $\underline{a}$=4.126 Å. Khitrova and Pinsker (1959) give the composition limits of this phase as WN - $WN_{0.67}$.

δ - WN has a simple hexagonal arrangement of tungsten atoms with cell dimensions $\underline{a}$=2.893 Å and $\underline{c}$=2.826 Å (Schönberg, 1954a).

δ - $W_{0.75}$ (N, O) has a pseudo-simple cubic arrangement of metal atoms with an ordered defect structure. It has a

Table I.2

Phases existing in the W-N and W-N-O systems

phase	crystal structure	unit-cell dimensions	references
β -$WN_{0.67}$-WN	f.c.c.	a=4.126 Å a=4.12-4.14 Å	Kiessling and Liu (1951) Khitrova and Pinsker (1959)
δ -WN	hexagonal	a=2.893; c=2.826 Å	Schönberg (1954a)
γ -$W_{0.75}(N,O)$	cubic (defective)	a=4.122-4.130 Å	Kiessling and Peterson (1954)
$W_{0.62}(N_{0.62}, O_{0.38})$	cubic (defective)	a=4.138 Å	Kiessling and Peterson (1954)
δ_H^I-$W_{1.2}N$	hexagonal	a=2.89; c=15.30 Å	Khitrova and Pinsker (1962)
δ_H^{II} -W_2N	hexagonal	a=2.89; c=22.85 Å	Characterised during electron diffraction of thin foils
δ_H^{III}-$W_{0.64}N$	hexagonal	a=2.87; c=11.00 Å	
δ_H^{IV}-$W_{0.6}N$	hexagonal	a=2.89; c=10.8 Å	
δ_R^V-$W_{0.5}N$	orthorhombic	a=2.89; c=16.4 Å	
δ_R^{VI}-$W_{1.2}N$	orthorhombic	a=2.89; c=23.35 Å	

similar structure to the face-centred cubic nitride but with no tungsten atoms occurring at the (0,0,0) positions (Kiessling and Peterson, 1954). The ordered defect structure is stable below 850°C. On annealing and quenching the phase from 890°C a face-centred cubic structure is obtained because the vacancies are randomly distributed. On subsequently annealing the phase below 850°C the ordered structure returns. The oxygen content of the phase is not known, but is considered to be small.

With increasing oxygen concentration the cubic structure becomes more defective. A phase $W_{0.62}$ $(N_{0.62}, O_{0.38})$ produced by nitriding either ammonium paratungstate or tungsten trioxide has a defect NaCl-type structure where the tungsten atoms occupy the four metal-atom sites but with 38% of them vacant. In this phase the vacancies are distributed randomly and hence only refections expected from a face-centred cubic structure are observed on X-ray diffraction patterns (Kiessling and Peterson, 1954).

A series of hexagonal nitrides of variable composition have been observed in electron diffraction studies of nitrided thin tungsten specimens. These are modifications of the simple hexagonal δ-WN and are identified as δ^{I}_{H} to δ^{VI}_{R} in Table I.2. They all have unit-cell a dimensions of 2.87-2.89 Å with c dimensions varying between 10.8 Å and 23.35 Å (Khitrova and Pinsker, 1962). The phases occur in localised regions of nitrided tungsten foils and hence have only been detected by electron diffraction.

I.4 The iron-tungsten-nitrogen and related systems

At least one ternary iron-tungsten-nitrogen phase exists; this is η_1-Fe_3W_3N. The preparation of ternary nitrides having the "high speed steel" eta carbide structure was mentioned by Schönberg (1955). The phase occurred in a number of systems including iron-tungsten-nitrogen but no details were published. In a later investigation of ternary nitride systems Grieveson (1960) prepared the phase η_1-Fe_3W_3N. As in previous preparations of the binary tungsten nitrides, this phase could not be prepared pure and so the composition was assumed by analogy with the corresponding iron-molybdenum-nitrogen phase η_1-Fe_3Mo_3N. Continuing the analogy, Grieveson attempted to prepare a ternary iron-tungsten-nitrogen phase having the β-manganese structure and isostructural with β^m-$Fe_7Mo_{13}N_4$. He was unable to do so, probably due to the inability to nitride the metal powders completely. β^m-$M'_7Mo_{13}N_4$ occurs in systems where M' = Mn, Fe, Co or Ni and replaces the η_2-carbide M'_2Mo_4C in the equivalent carbon systems (Evans, 1957; Grieveson, 1960).

Ternary eta-phases also exist where the interstitial atom is oxygen (Schönberg, 1954b). Grieveson (1960) prepared several eta-oxide phases of slightly smaller unit cell dimensions than had been obtained for η_1-carbides and nitrides (see Table I.3) but Nutter (1969) showed these phases to be of composition $M'_{12}M''_{12}$ (O,C.N) which he designated as η_3.

Table I.3

Lattice parameters of some η-phases

phase	unit-cell dimensions	references
Fe_3W_3N	$\underline{a}$=11.095 Å	Grieveson (1960)
Fe_3W_3C	$\underline{a}$=11.08 kX	Westgren (1933) Krainer (1950)
Fe_3Mo_3N	$\underline{a}$=11.065 - 11.095 Å	Evans (1957)
Ni_3Mo_3N	$\underline{a}$=11.020 - 11.027 Å	Grieveson (1960)
Ni_3Mo_3C	$\underline{a}$=11.05 Å	Kuo (1953)
Fe_6W_6C	$\underline{a}$=10.934 Å	Leciejewicz (1964)
Ni_6Mo_6C	$\underline{a}$=10.893 Å	Fraker (1967)
$Ni_{12}Mo_{12}(O,C,N)$	$\underline{a}$=10.889 Å	Nutter (1969)

No systematic study of the precipitation of tungsten nitrides in iron has been reported in the literature.

The precipitation of carbides in iron-tungsten-carbon martensite has been studied by Davenport and Honeycombe (1967). The phase transformations and metallography are similar to those observed in iron-molybdenum-carbon secondary hardening steels. The precipitation sequence on aging a Fe-6 wt.%W - 0.2 wt.%C alloy at 500-700°C after quenching to martensite is

$$Fe_3C \longrightarrow W_2C \longrightarrow Fe_3W_3C$$

W_2C is close packed hexagonal with $\underline{a}$=2.990 Å and $\underline{c}$=4.710 Å and grows as needles in ferrite. The orientation relationship is identical to the Pitsch-Schrader relationship suggested for ε-carbide in ferrite, that is

$$(011)_\alpha \parallel (001)W_2C; \quad (01\bar{1})_\alpha \parallel (010)W_2C; \quad (100)_\alpha \parallel (2\bar{1}0)W_2C$$

and the growth direction is <100>

Precipitation studies in other transition metal-iron-nitrogen systems carried out in this laboratory in recent years are probably more relevant to the present work than iron-tungsten-carbon, and these will be discussed appropriately in the text.

Chapter II

EXPERIMENTAL TECHNIQUES

II.1 The preparation of alloy samples

Iron-tungsten alloys supplied by the British Iron and Steel Research Association had tungsten concentrations 0.50, 1.00, 2.05, 5.05 and 9.30 wt.%. In addition two further alloy samples were prepared having nominal tungsten concentration of 3.5 and 4.0 wt.% respectively. The former was prepared by arc melting pure B.I.S.R.A.iron together with tungsten powder, and the latter was prepared from the 2.05 and 5.05 wt.% tungsten stock material. It was subsequently found that the Fe-0.50 wt.%W alloy also contained 0.16 wt.% vanadium (see Appendix II).

The "as-received" alloy bar was sectioned and cold rolled to a variety of thicknesses ranging from 0.005 to 0.050 in., the thicker material providing specimens for X-ray examination, optical metallography and accurate weight changes, and the thin material providing specimens for examination by electron microscopy.

All specimens were abraded, cleaned and degreased in benzene or "chemiclene" prior to nitriding.

II.2 Preparation of tungsten samples

Two qualities of tungsten wire were used in the investigation (a) 99.9%W supplied by Koch-Light Laboratories Ltd. and (b) 99.97%W supplied by Murex Ltd. All wires were abraded and degreased before nitriding.

Tungsten powder (min. 98%W) was dried under vacuum at 100°C in the presence of phosphorus pentoxide before use.

II.3 Ammonia-hydrogen nitriding

The nitrogen activity of an ammonia-hydrogen gas mixture is determined by the ratio of concentrations of ammonia and hydrogen; Lehrer (1930), Brunauer, Jefferson, Emmett and Hendricks (1931) and Paranjpe, Cohen, Bever and Floe (1950). The nitriding reaction is

$$NH_3\,(g) \rightleftharpoons \underline{N} + {}^3/_2\,H_2\,(g) \qquad \ldots\ldots (II).1$$

and at T°K, the equilibrium constant is given by

$$K_1 = \frac{a_{\underline{N}} \cdot p^{\frac{3}{2}}_{H_2}}{p_{NH_3}} \qquad \ldots\ldots (II).2$$

where $a_{\underline{N}}$ is the activity of nitrogen in the nitride phase and p_{NH_3} and p_{H_2} are the partial pressures of ammonia

and hydrogen respectively. A system can therefore be brought to equilibrium under a predetermined nitrogen activity by controlling the proportions of ammonia and hydrogen.

In the iron-nitrogen system at 630°C the successive phases formed with increasing nitrogen content are α-solid solution, γ-solid solution and γ'-Fe_4N. When an iron specimen is exposed to a nitriding atmosphere of sufficiently high nitrogen potential to form Fe_4N, the activity of the combined nitrogen will vary in the following manner. It will increase from zero in the pure α to a value of $a_{\underline{N}}^{\alpha\text{-max}}$ in the saturated nitrogen ferrite at which point austenite of composition γ-min will form. Since the two phases co-exist $a_{\underline{N}}^{\alpha\text{-max}}$ is equal to $a_{\underline{N}}^{\gamma\text{-min}}$. As the total nitrogen content increases, the activities remain constant and γ grows at the expense of α. When no α remains, the activity of γ increases and the composition of γ changes. Eventually the solubility limit of nitrogen in γ is reached and γ' forms such that $a_N^{\gamma\text{-max}}$ is equal to $a_N^{\gamma'\text{-min}}$. Thus the process is repeated until the system attains equilibrium with the gas phase, that is γ'-Fe_4N of a fixed composition in equilibrium with a gas mixture of fixed composition.

In any single nitride phase the nitrogen activity will vary regularly with composition, and since $a_{\underline{N}}$ is proportional to $p_{NH_3}/p^{\frac{3}{2}}_{H_2}$, then a gas mixture of fixed composition is in equilibrium with a nitride of fixed nitrogen content.

Considering the case of ferrite, the reaction is

$$NH_3 \rightleftharpoons \underline{N}^{\alpha} + {}^{3}/_{2}\, H_2 \qquad \ldots\ (II).3$$

for which, the equilibrium constant K_2, is given by

$$K_2 = \frac{a_{\underline{N}^{\alpha}} \cdot \rho^{\frac{3}{2}}_{H_2}}{\rho_{NH_3}} \qquad \ldots\ (II).4$$

rearranging $$a_{\underline{N}^{\alpha}} = \frac{\rho_{NH_3}}{\rho^{\frac{3}{2}}_{H_2}} \cdot K_2 \qquad \ldots\ (II).5$$

Since Henry's Law is applicable over the complete range of solubility of nitrogen in ferrite, then

$$a_{\underline{N}^{\alpha}} = k_h \cdot \text{wt.\%}\, \underline{N}^{\alpha} = \frac{\rho_{NH_3}}{\rho^{3/2}_{H_2}} \cdot K_2 \qquad \ldots\ (II).6$$

where k_h is Henry's Law constant. Therefore the wt.% nitrogen in solution in pure ferrite nitrided in an ammonia-hydrogen gas mixture is given by

$$\text{wt.\%}\, \underline{N}^{\alpha} = \frac{\rho_{NH_3}}{\rho^{3/2}_{H_2}} \cdot K_3 \qquad \ldots\ (II).7$$

where $K_3 = K_2 / k_h$.

The procedure is complicated by the "cracking" of ammonia

$$NH_3\ (g) \quad = \quad \tfrac{1}{2}\,N_2\ (g) \ + \ {}^3/2\ H_2\ (g) \qquad \ldots\ (II).8$$

where the equilibrium mixture contains only a few per cent of ammonia at normal nitriding temperatures. If the catalytic effect of the specimen and reaction tube is constant, then the degree to which the gas approaches its equilibrium NH_3-H_2-N_2 mixture is determined by its flow rate. With flow rates used in the present study the extent of "cracking" is negligible.

The diagrams compiled by Lehrer (1930) and shown in Figure II.1 proved useful in determining suitable nitriding conditions.

II.4 Nitrogen-hydrogen nitriding

The nitriding potential of a nitrogen-hydrogen gas mixture is determined only by the partial pressure of nitrogen. The nitriding reaction is

$$1/2\ N_2\ (g) \ \rightleftharpoons\ \underline{N} \qquad \ldots\ (II).9$$

for which the equilibrium constant at T^oK is

$$K_4 \quad = \quad a_{\underline{N}} \,/\, p^{\frac{1}{2}}_{N_2} \qquad \ldots\ (II).10$$

Fig. II.1

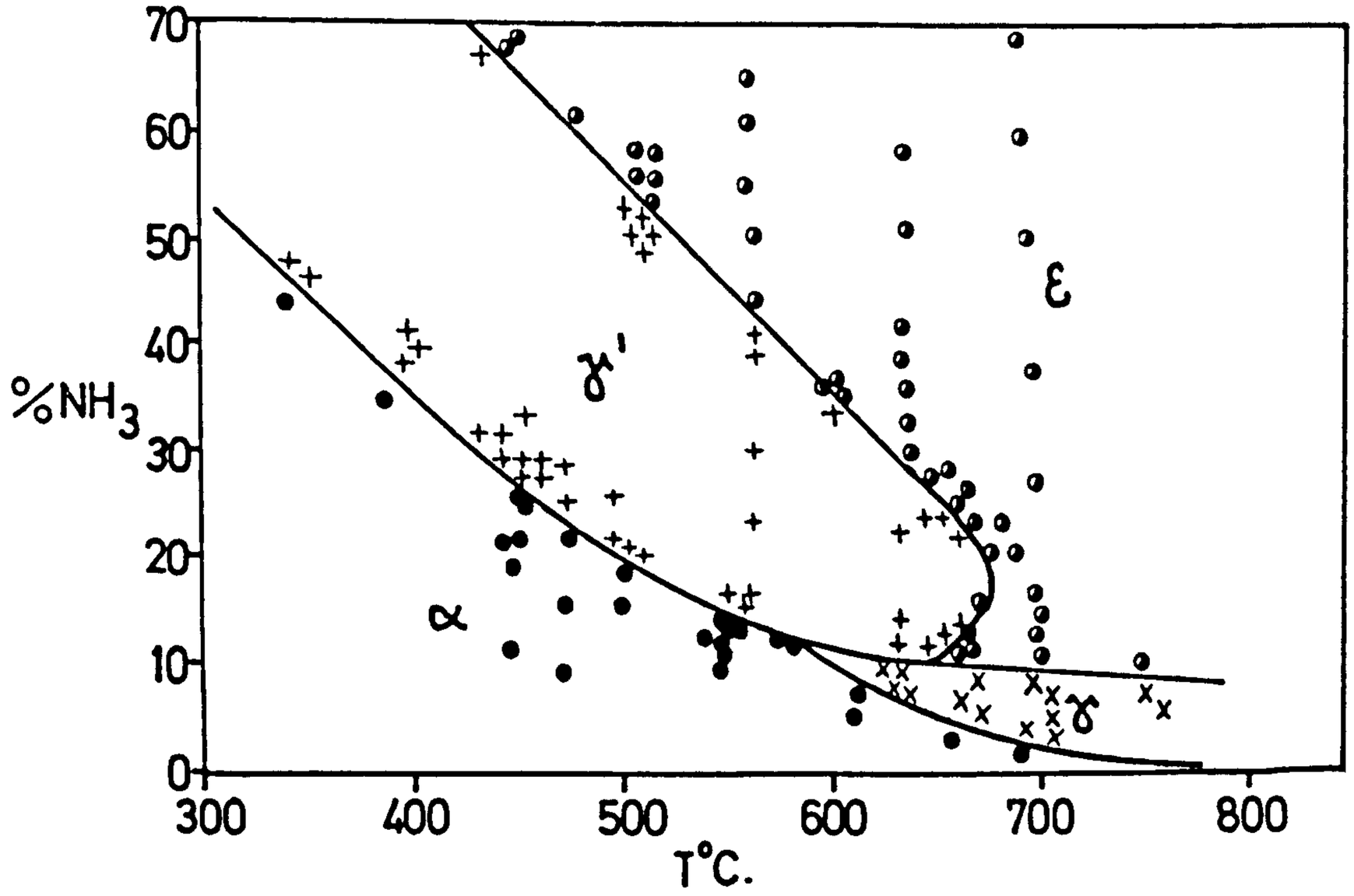

EQUILIBRIUM BETWEEN NH_3-H_2 MIXTURES [1 ATM.] AND SOLID PHASES OF THE IRON-NITROGEN SYSTEM [AFTER LEHRER (1930)].

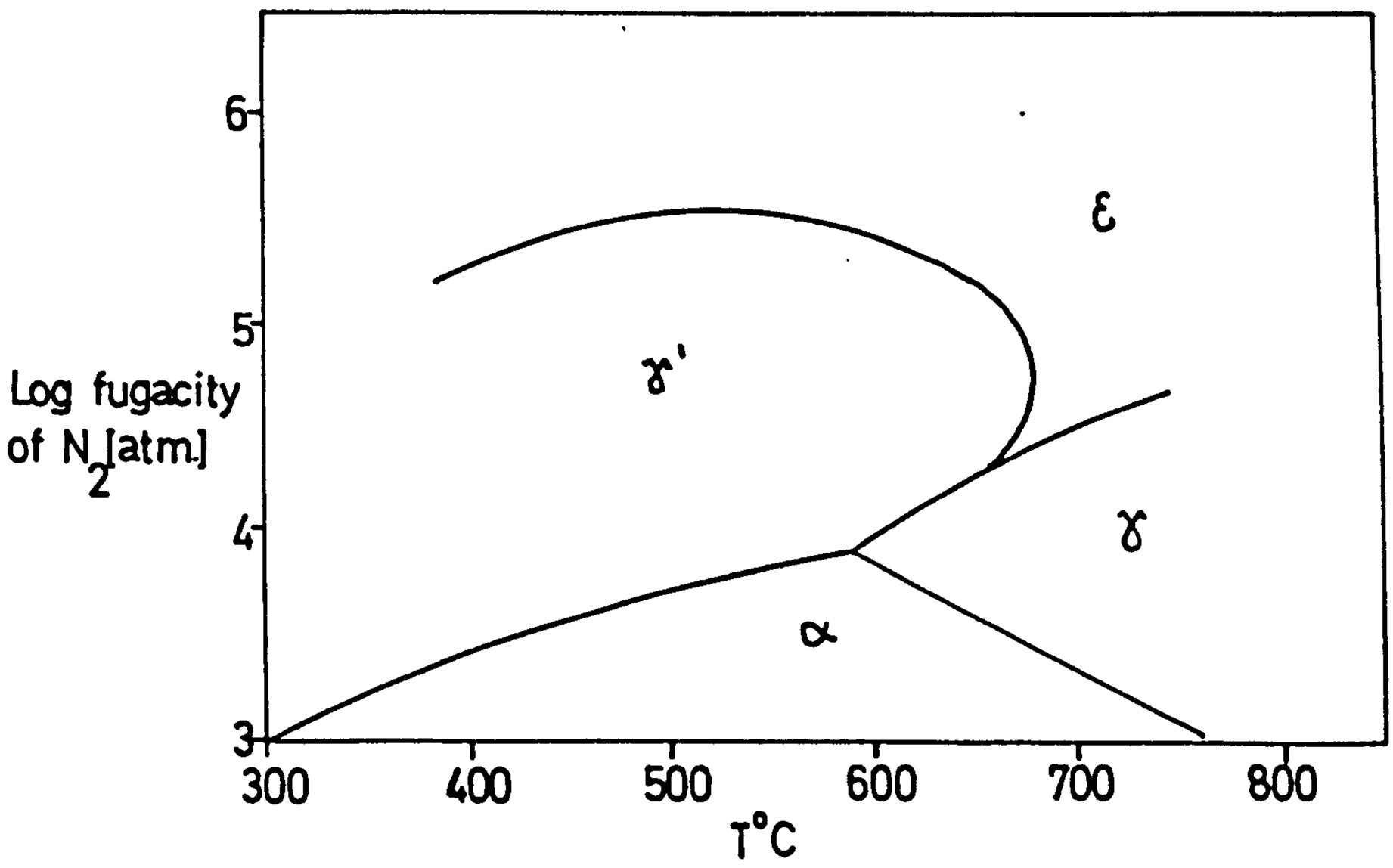

FUGACITY-TEMPERATURE DIAGRAM FOR THE IRON-NITROGEN SYSTEM USING DATA FROM THE PREVIOUS FIGURE.

where ρN_2 is the partial pressure of nitrogen.

The range of nitrogen potentials for which nitrogen-hydrogen nitriding is suitable is clearly small. The technique complements ammonia-hydrogen nitriding by allowing accurate nitrogen partial pressures up to about one atmosphere. The nitrogen partial pressures equivalent to ammonia-hydrogen mixtures in the region where ammonia can be accurately metered (greater than about 1% NH_3-H_2) is about 10^2 - 10^4 atmospheres of molecular nitrogen depending on the temperature.

As well as being a diluent, the hydrogen in the gas mixture reduces the oxygen potential of the system.

II.5 Apparatus

Nitriding apparatus with both vertical and horizontal reaction tubes are shown in Figures II.2 and II.3. Commercial hydrogen, nitrogen and ammonia were purified by standard methods (see Figure II.4). The calcium oxide was freshly prepared by decomposition of small marble chips at 950°C and the activated copper (received as oxide) was pre-reduced in hydrogen for two days at 160-180°C. During use, the activated copper was maintained at 120°C. Gas flows were measured by capillary flowmeters (see Figure II.5) calibrated by a bubble displacement technique. Gas velocities of 50cm min^{-1} gave no detectable cracking at 620°C.

Fig.II.2

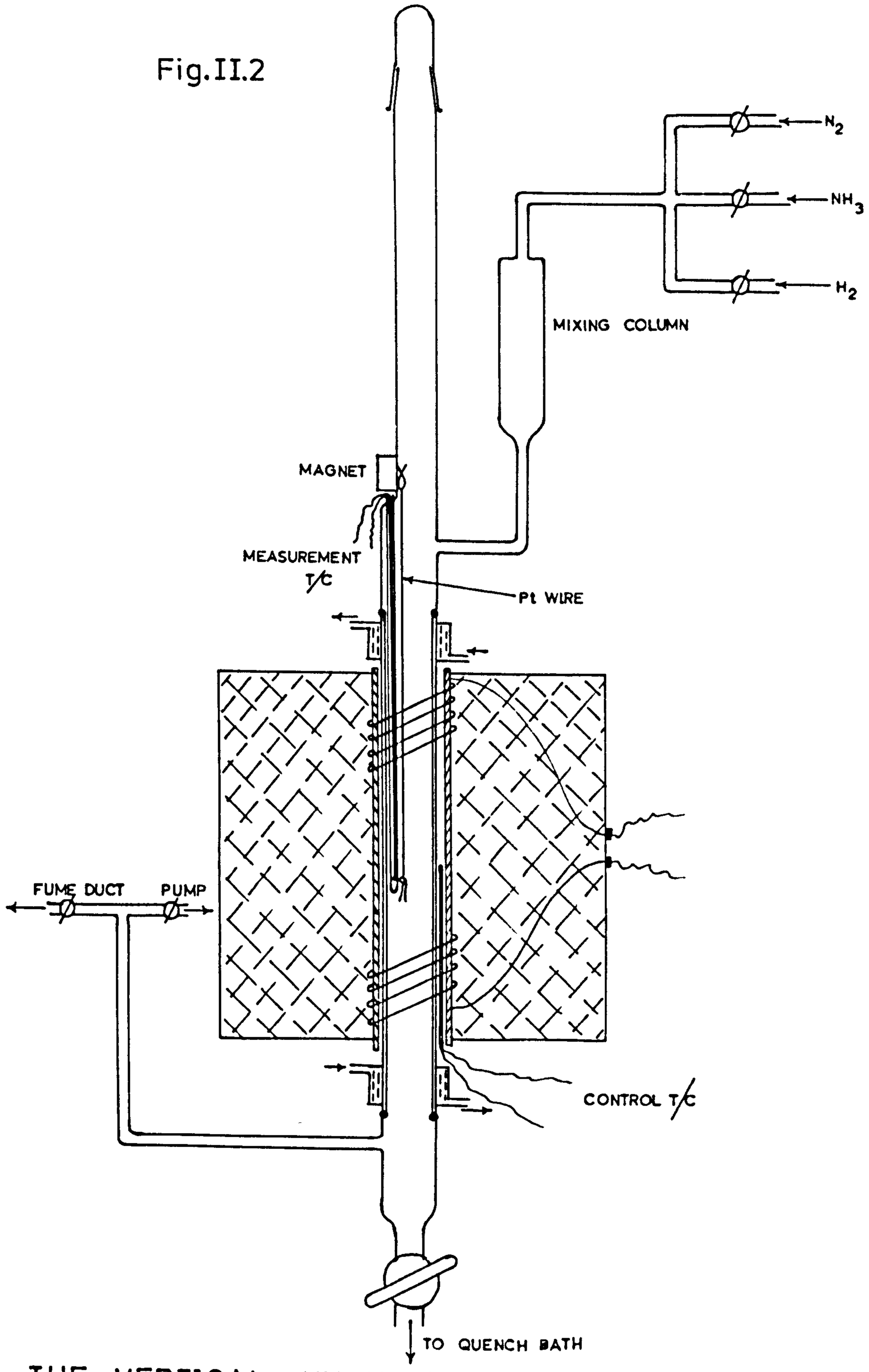

THE VERTICAL NH_3-H_2 AND N_2-H_2 EQUILIBRATION APPARATUS.

Fig. II.3

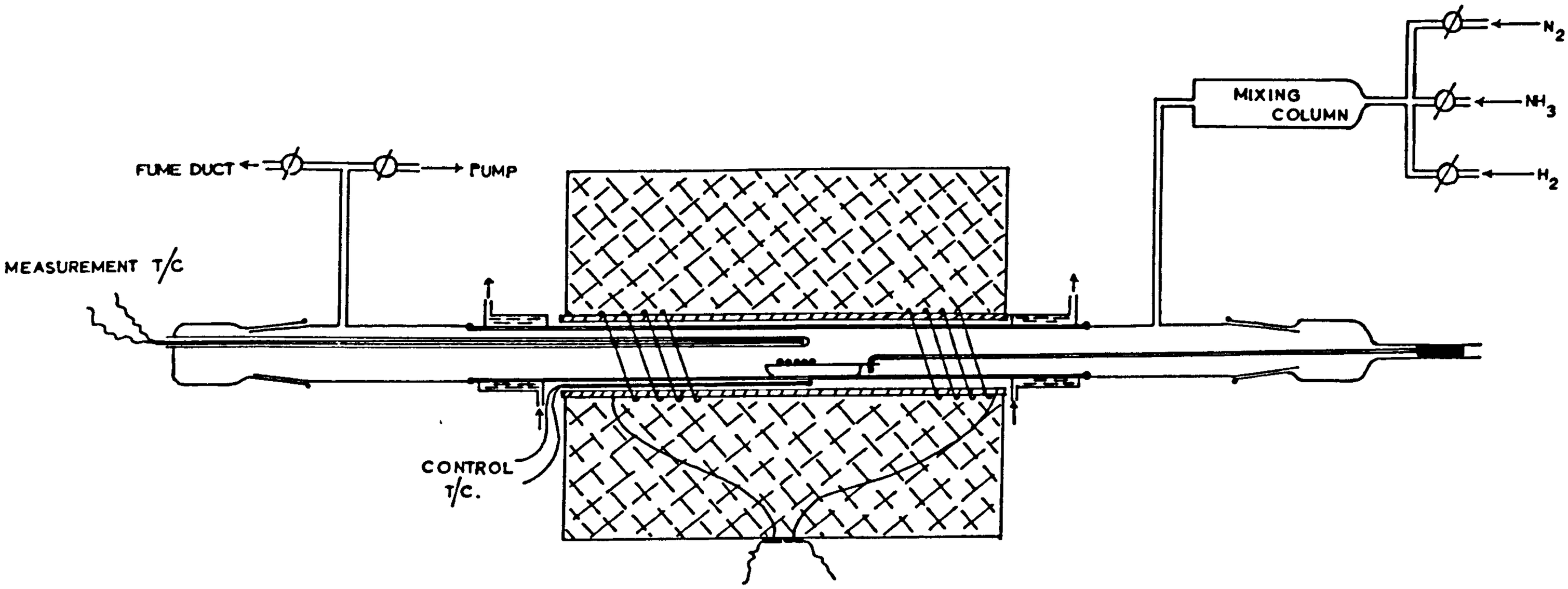

THE AMMONIA–HYDROGEN EQUILIBRATION APPARATUS [HORIZONTAL FURNACE].

Fig. II.4

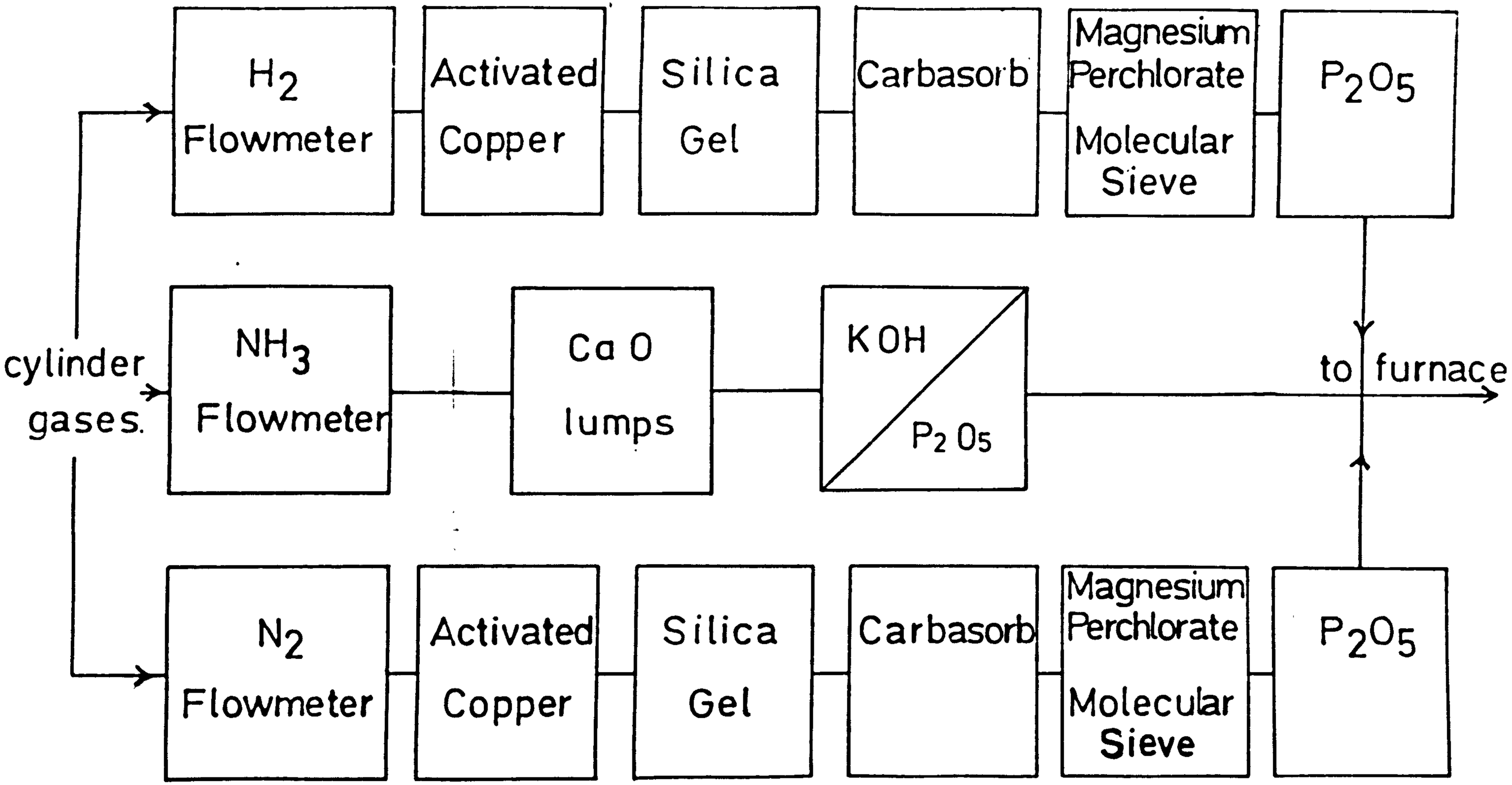

GAS FLOW SYSTEM FOR NH_3-H_2 AND N_2-H_2 EQUILIBRATION.

Fig. II.5

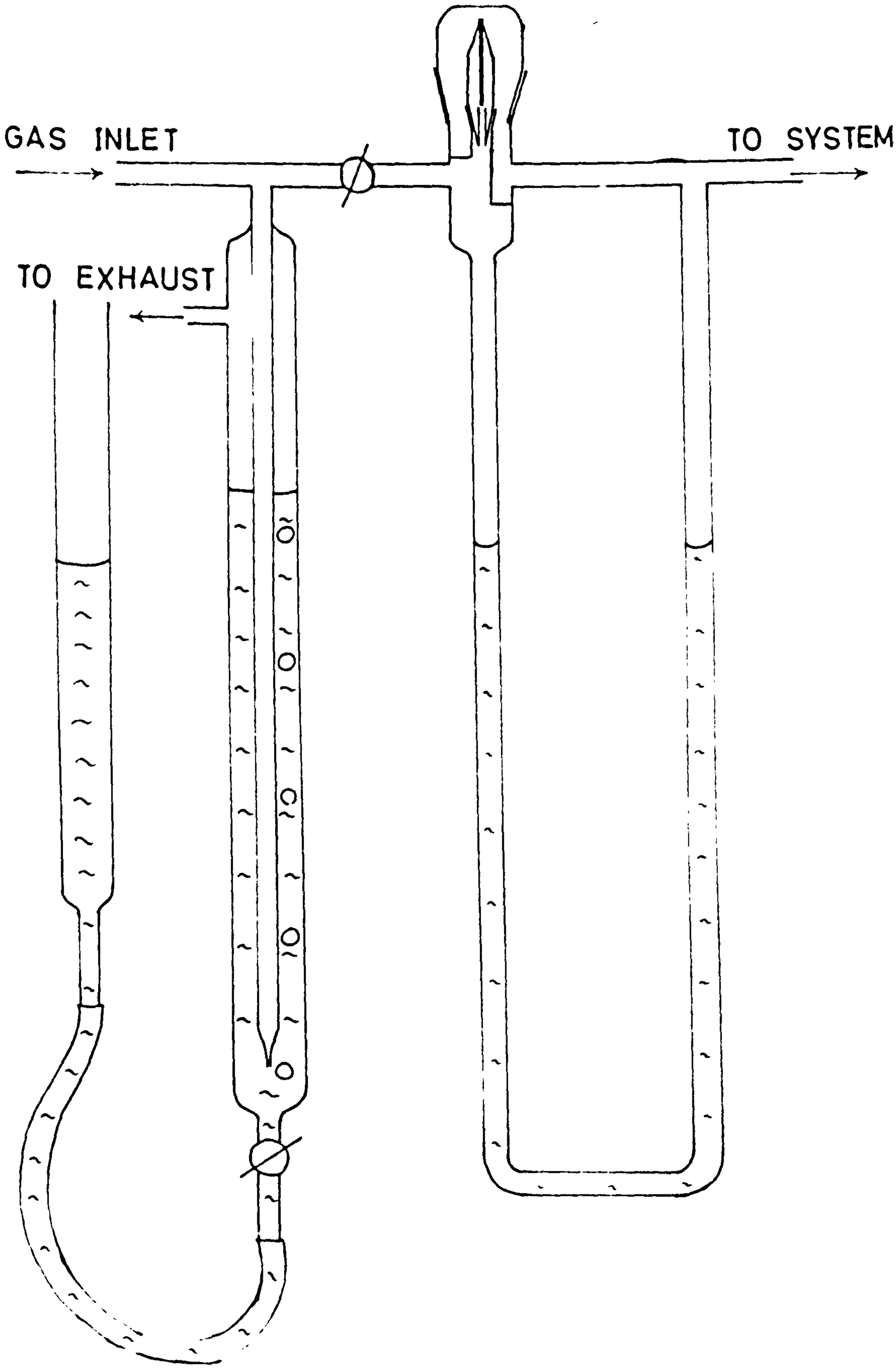

A CAPILLARY FLOWMETER [SCHEMATIC].

The furnace temperature was controlled to $\pm$ 5°C by a standard "Ether" controller using a built-in Pt/Pt-Rh thermocouple situated between the reaction tube and the furnace winding. The specimen temperature was monitored by a chromel/alumel thermocouple situated adjacent to the specimen in an alumina sheath.

The total gas pressure was maintained at slightly greater than atmospheric by 1-2cms. of oil in an exit bubbler. A column of potassium hydroxide placed between the reaction tube and the exit bubbler eliminated the risk of any back diffusion of atmospheric moisture.

The procedure adopted in the nitriding experiments was essentially the same for both types of furnace. After cleaning and weighing, the specimens were inserted into the furnace and placed at the cold end. The system was then evacuated and checked for leaks before being filled with nitrogen. Hydrogen was then allowed to flow through the furnace for about one hour before moving the specimens into the hot zone. After annealing the specimens in hydrogen for 3 hr. at 880°C, the furnace temperature was lowered to that required for nitriding and the nitriding gas mixture subsequently introduced.

After nitriding, the specimens were cooled in the following manner. In the horizontal furnace, the alumina boat was quickly moved to the furnace "cold end". Except for the thinnest specimens the cooling rate was too slow to prevent auto-tempering of saturated nitrogen ferrite.

In the vertical furnace an appreciable cooling rate was obtained by raising the specimens quickly and allowing them to quench in the incoming gas stream. For exceptional cooling rates, the specimens were released and allowed to fall into an oil bath included in the system.

II.6 Pressure nitriding

Figure II.6 shows the arrangement for nitriding in high pressures of molecular nitrogen (Jack, unpublished; see Evans, 1957). The source of nitrogen can be any nitride which decomposes fully below the required nitriding temperature. It is known that ε or ζ -Fe_2N, prepared by passing ammonia at high flowrates over 100 mesh iron powder at 450°C, provides a gas of high purity. As an alternative source of nitrogen θ -$MnN_{0.9}$ was also used. This was prepared by passing ammonia at high flow-rates over 300-mesh "electrolytic" manganese at 500°C.

The calculated amount of nitride was weighed out and pressed into a pellet before being placed in thick-walled silica tube of internal diameter 0.50cms. The silica tube was then evacuated to 10^{-5} torr and sealed. The specimens were nitrided in a vertical furnace and quenched by plunging the tube into a water bath. Nitriding of tungsten wires was carried out in the temperature range 800-950°C using nitrogen pressures of ~15-60 atmospheres.

Fig. II. 6

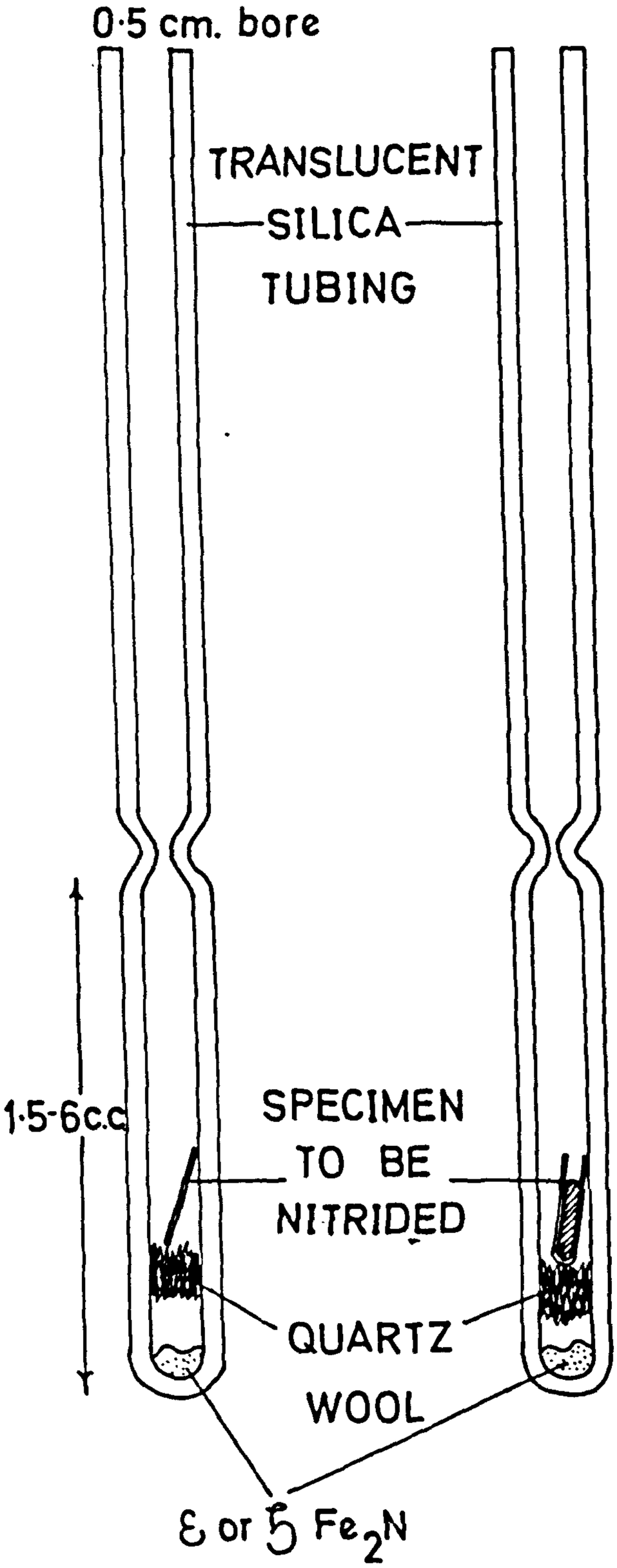

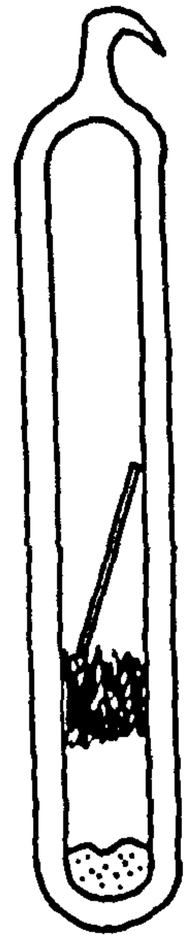

c)

a) Wires b) Powders

METHOD OF SEALING SPECIMENS IN PRESSURE NITRIDING EXPERIMENTS

Iron-tungsten alloys were nitrided in the same manner, and after quenching, were resealed in small evacuated silica capsules and aged in the temperature range 550-750°C.

In some experiments it was desirable to introduce a small oxygen potential during nitriding. This was done by including a small amount of Cr_2O_3 in the manganese or iron nitride pellet.

II.7 X-ray techniques

For "in situ" determination of precipitated phases in nitrided iron-tungsten alloys it was necessary to use monochromatic FeKα radiation reflected from a lithium fluoride single crystal. Diffraction patterns were recorded photographically using a 9cm. "Unicam" camera. Monochromatic radiation was essential in order to reduce background intensity during the long exposures necessary to obtain diffraction patterns from small volume fractions of precipitate.

For accurate lattice parameter determinations a Hägg-Guinier focussing camera was used together with pure monochromatic $CuK\alpha_1$ or $CrK\alpha_1$ radiation as appropriate.

For less critical work diffraction patterns were obtained using either manganese filtered FeKα radiation or nickel filtered CuKα radiation.

II.8 Metallographic examination

Alloy specimens in the form of strip or wire were mounted vertically in hot mounting compound and polished on two grades of emery paper followed by four grades of diamond down to 0.25μ . Specimens were etched in 2-5% nital for 5-25 seconds.

Low temperature aged specimens were of course mounted in cold mounting compound and subsequently prepared in the same manner.

A Reichert projection microscope was used for optical microscopy and photomicrography at a direct magnification up to 2,000 X.

II.9 Hardness measurements

Hardness measurements were made on etched and unetched metallographic specimens using a standard micro-hardness tester fitted to the Reichert microscope.

II.10 Preparation of specimens for electron microscopy

(a) In general thin foils of nitrided alloy specimens were prepared from 0.005in. thick strips using a standard window technique. Specimens were electropolished using a "Shandon" electropolisher power supply at 16-22 volts and

-2 to +3°C in a solution of 68% acetic acid/16% perchloric acid/16% 2-butoxy ethanol. When thicker specimens were used (e.g. 0.020in.) they were subjected to a prior chemical polish in a solution of 50 parts water/50 parts hydrogen peroxide/5 parts hydrofluoric acid. After polishing, the specimens were washed in methanol and ethanol, and thin foils removed.

(b) Extraction replicas were taken from thicker material (0.020in.) in the following manner. The nitrided alloy strip was given a light electropolish as in (a) and etched in 5% nital for 30-40 seconds at -10°C. This was found to be more successful than etching in 2% nital at room temperature. The specimens were then given a fairly thick coating of carbon using an Edwards evaporator, and subsequently scored with grid marks. The replicas were removed either in 2% nital or in ethanol after a short (5 second) electropolish at 18 volts and 0°C. The replicas were washed in a mixture of ethanol and water and placed on copper grids.

II.11 Electron microscopes

Most of the electron microscopy was carried out using a Philips E.M.300 equipped with a goniometer stage. Additional facilities were available in the form of a J.E.M. 100U microscope equipped with a goniometer stage and some of the earlier work was carried out on an A.E.I. E.M.6G instrument. equipped with a high resolution stage but having only

limited tilt facilities ($\pm 5^{\circ}$).

II.12 Extraction of precipitates

It was found that precipitates could be successfully extracted by dissolving nitrided alloy specimens in 20% sulphuric acid. The extract was subsequently washed in de-ionized water, centrifuged, and the supernatent liquid poured off. This process was repeated six or seven times using water and two or three times using ethanol before drying the extract. The precipitate was placed in a 0.5mm glass capillary and examined by X-ray diffraction.

II.13 Nitrogen analysis and sample weighings

Some nitrogen analysis was carried out using a standard micro-Kjeldahl apparatus with colorimetric determination of the distilled ammonia using Nessler's reagent and with ammonium chloride as a standard.

In general the nitrogen levels in nitrided alloys are much higher than those in steels (up to nearly 1.0 wt.% in the present study) and at these values weight differences before and after nitriding give exceptionally good reproducibility. Even at levels as low as 0.1 wt.% nitrogen using suitable specimens (2-3gms.) reproducibility was within $\pm$ 0.005 wt.%. Weighings to $\pm$ 0.0001g were made on an "Oertling" analytical balance and the average of at least

three values was taken as correct.

II.14 Internal friction measurements

0.017 in diameter wires were nitrided in a vertical furnace and quenched into an oil reservoir included in the system, but cooled externally by a jacket containing methanol and liquid nitrogen. Specimens were retained at -40°C until required. The internal friction apparatus was of the inverted torsional pendulum type (see Figure II.7), with the damping measured by the free decay method.

A mirror on the head of the pendulum reflects light from a suitably positioned light source onto the "spot-follower" of a continuous recorder. The pendulum was oscillated by means of two small electromagnets and allowed to decay freely. The frequency of oscillation was varied between 0.46 and 1.53 c.p.s. by means of counterweights placed on the pendulum arms. Small strain amplitudes were used to ensure that damping was amplitude independent.

Temperature control was by means of three furnace windings each in series with a variable resistance but supplied by one variable transformer. The test temperature was measured using two copper-constantan thermocouples whose hot junctions were adjacent to the wire, one at the top and one at the bottom.

The system was evacuated to 10^{-5} torr pior to each measurement.

Fig. II.7

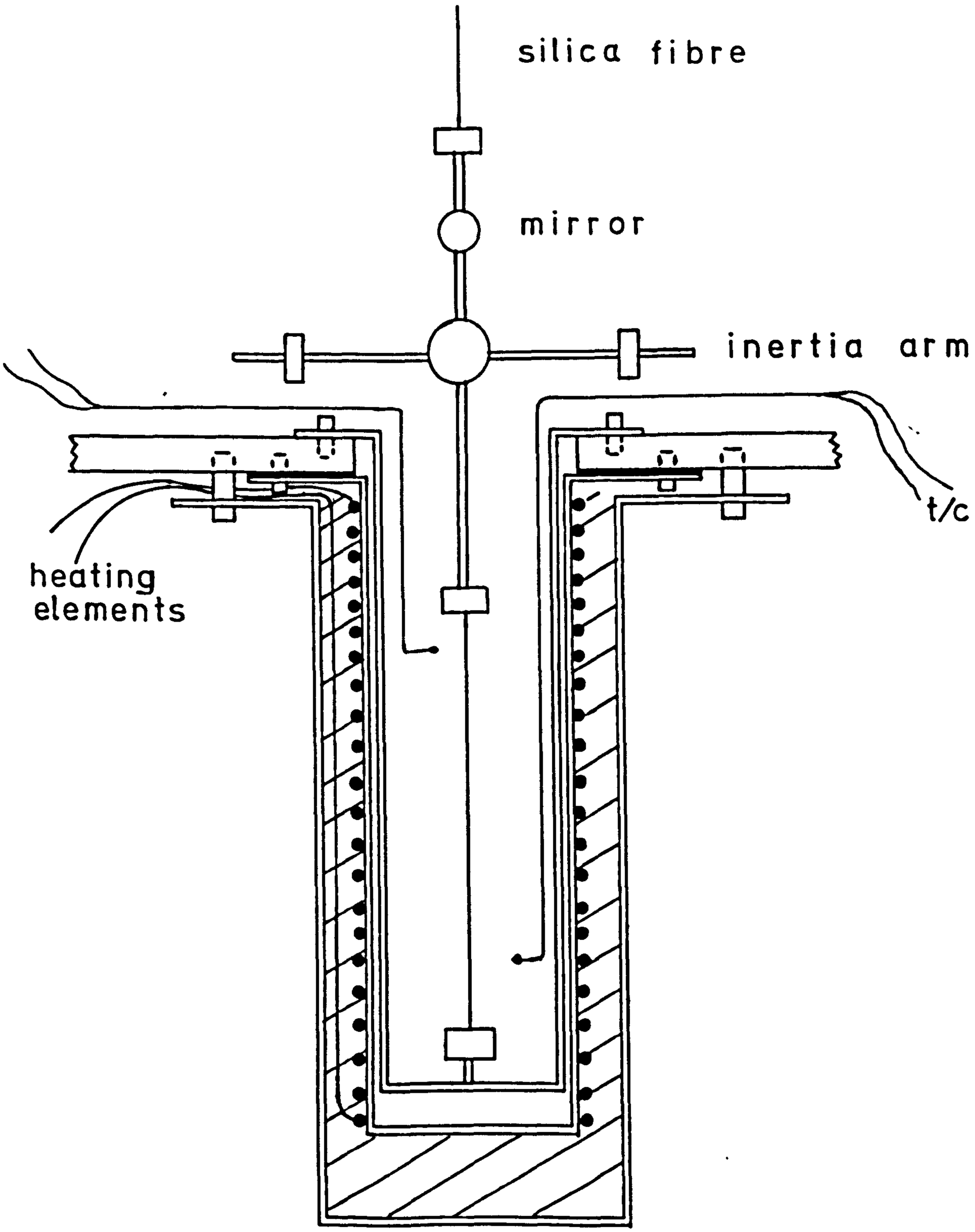

INTERNAL FRICTION APPARATUS

Chapter III

THE SCOPE OF THE PRESENT INVESTIGATION

Previous examinations of ternary Fe-X-N systems where X is Mn, Mo, Si, Nb and Cr have been primarily based on constant activity aging in ammonia-hydrogen gas mixtures described in Chapter II. This preparative technique coupled with the sensitive X-ray methods employed at Newcastle has allowed unequivocal characterisation of the phases produced. It has also been shown that in all systems except Fe-Si-N homogeneous precipitation of metastable phases precedes the formation of the equilibrium nitride if the conditions are carefully controlled. In the present thesis the interaction of tungsten and nitrogen in iron is examined and so contributes to the understanding of F-X-N systems.

The work on formation of nitrides on "pure" tungsten described in Chapter IV was carried out in order to provide a basis for the precipitation studies of Chapter V. The effects of variations in nitrogen, oxygen and tungsten activities and in temperature are emphasised and an interpretation of the observations is offered.

The various stages observed in the decomposition of tungsten-nitrogen ferrite are presented in Chapter VI, whilst in the following chapter the stability of the non-equilibrium phase is examined and a simple thermodynamic model is suggested which can be qualitatively extended to give some

indication of the conditions for homogeneous precipitation.

Chapter VIII presents the results of para-precipitation studies in tungsten-nitrogen-ferrites. In similar studies it has been observed that the distribution of iron-nitrides in alloy-ferrites is related to the magnitude of the alloy-nitrogen interaction and the present work is in good agreement with this.

In Chapter IX an attempt is made to relate all results to the general phenomena of nitride precipitation and pre-precipitation in ternary Fe-X-N systems.

Finally, as in every research, subsidiary topics arise are these are discussed in appendices.

Chapter IV

THE TUNGSTEN NITROGEN SYSTEM AND THE EFFECT OF OXYGEN

IV.1 Interstitial alloys

Interstitial alloys, that is compounds in which small non-metal atoms such as H, B, C and N occupy the interstices between relatively close-packed arrangements of larger metal atoms, were first classified by Hägg (1930b) who concluded that the structure type depended upon the radius ratio R = rx/rm, where rx and rm are the radii of the non-metal and metal atoms respectively. If R is less than 0.59, the metal atom arrangement is usually simple whereas for R greater than 0.59 the structures are "complex" and have less pronounced metallic properties than "normal" interstitial alloys.

Geometrical principles, whilst being a necessary condition for interstitial alloy formation, are not the only determiners. The fact that interstitial alloys are formed only by metal atoms with an inner incomplete electron shell implies that there is an "electronic" factor. It is also accepted (Seitz, 1945) that the electronegativity differences between the metal and non-metal plays some part in determining the possibility of interstitial alloy formation. Thus, oxides with relatively high oxygen concentrations are usually ionic or covalent and not metallic.

The radius ratio for tungsten and nitrogen is 0.53 and only simple metal-atom arrangements, or slight distortions of them, are expected in the tungsten-nitrogen system. Although some previous studies have been carried out in this system (see Chapter 1) the results seem inconclusive and with the exception of δ-$W_{0.75}(N,O)$ no reasons for the structural modifications observed have been suggested. Also, with the exception of δ-$W_{0.75}(N,O)$, the compositions of the phases are not known with certainty. The β-phase is reported as having a range W_3N_2-WN. In the present thesis it will be referred to as $W_{1.5}(N,O)$ although the composition range suggested is not disputed.

IV.2 Nitriding of tungsten in ammonia-hydrogen mixtures

No thermodynamic data are available for tungsten nitrides but by analogy with other transition element nitrides it is expected that the nitrogen potential required for their formation will be low ($<<1$ atm.) Therefore the phases produced under different nitriding conditions will be largely dependent on kinetics and oxygen potential.

The phases formed on nitriding tungsten wire in ammonia-hydrogen gas mixtures are listed in Table IV.1. Typical X-ray photographs are shown in Figures IV.1 and IV.2, and the unit-cell domensions of phases obtained are given in Table IV.2.

The conditions existing during ammonia-hydrogen

Table IV.1

Nitriding of tungsten with ammonia-hydrogen mixtures

run	starting material	$NH_3:H_2$	temp. °C	time days	X indicates phases observed			
					α-W	β-$W_{1.5}(N,O)$	γ-$W_{0.75}(N,O)$	δ-WN
1*	α-wire	100:0	800-950	1-5	X		X	
2	α-wire	50:50	950	5	X		X	
3	α-wire	50:50	850	2	X	X	X	
4	α-wire(as 3)	10:90	850	1	X	X	X	
5*	α-powder	50:50 100:0	800-950	2-5	X		X	
6	α-powder	100:0	900	5	X	X	X	
7	α-wire + δ	100:0	900	1	X		X	X
8	α-wire + δ	8:92	615	5	X			X

* runs 1 and 5 include experiments under conditions varied within the limits indicated.

Table IV.2

Unit-cell dimensions of tungsten nitrides observed in the present investigation

(a) ammonia-hydrogen nitriding

phase	crystal structure	unit-cell dimensions
γ-$W_{0.75}(N,O)$	cubic	$\underline{a}$ = 4.106-4.128 Å
β-$W_{1.5}(N,O)$	f.c. cubic	$\underline{a}$ = 4.128 Å

(b) pressure nitriding

phase	crystal structure	unit-cell dimensions
δ-WN	hexagonal	$\underline{a}$ = 2.898 Å $\underline{c}$ = 2.831 Å
* δ-WN(O)	hexagonal (faulted)	$\underline{a}$ = 2.898 Å $\underline{c}$ = 2.839 Å

* In this dissertation (O) represents accommodation of small quantities of oxygen in an otherwise "pure" nitride, whereas (N,O) represents an oxy-nitride whose existence depends on the presence of oxygen.

Fig. IV.1

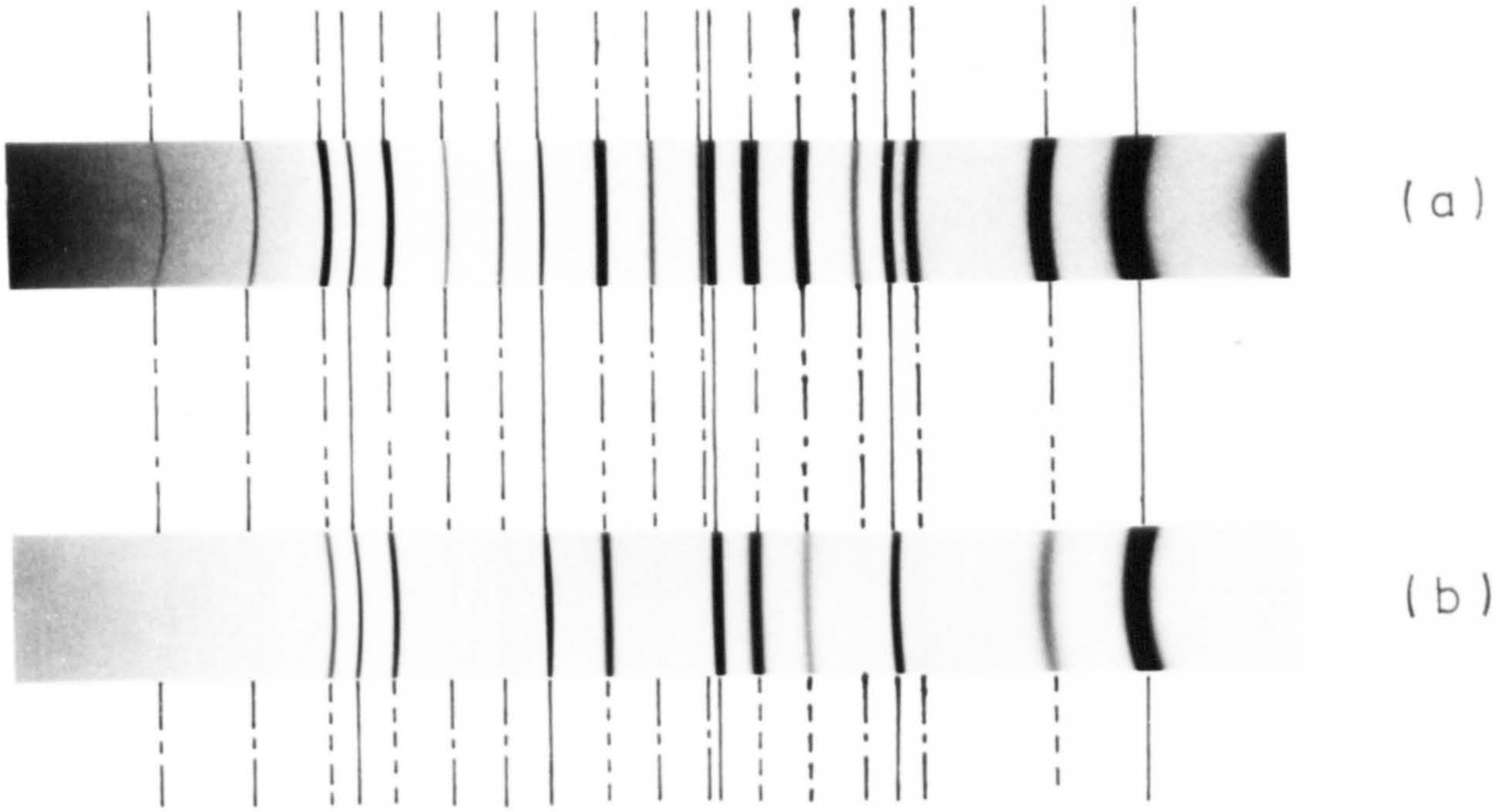

(a) 100% NH_3:H_2. 5 days at 900 °C

(b) 50% NH_3:H_2. 2 days at 850 °C

X-RAY PHOTOGRAPHS SHOWING TUNGSTEN OXY-NITRIDES PRODUCED BY NITRIDING TUNGSTEN WIRE IN AMMONIA – HYDROGEN MIXTURES [Fe Kα]

Fig. IV.2

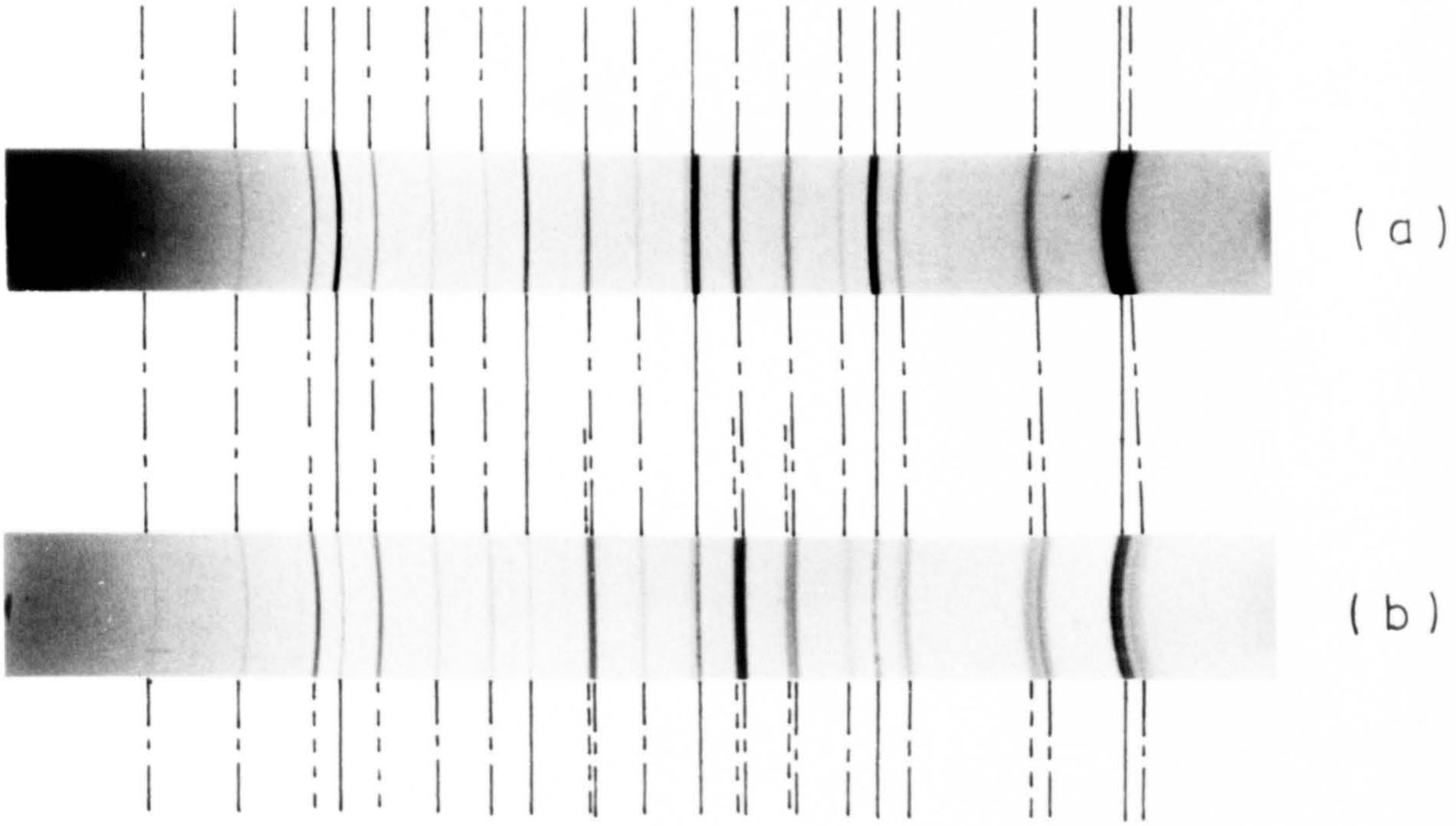

(a) 50% NH_3:H_2. 2 days at 900 °C

(b) 100% NH_3:H_2. 5 days at 900 °C

X-RAY PHOTOGRAPHS SHOWING TUNGSTEN OXY-NITRIDES PRODUCED BY NITRIDING TUNGSTEN POWDER IN AMMONIA–HYDROGEN MIXTURES [Fe Kα]

nitriding are such that the stable phase is γ-$W_{0.75}(N,O)$ although β-$W_{1.5}(N,O)$ is sometimes observed. The actual nitrogen potential is not known because at the high temperatures employed, ammonia is dissociated to a large extent. The small oxygen potentials required for oxynitride formation are assumed to be due to impurities in the ammonia. The difficulty in differentiating between the two oxynitrides can be appreciated from the X-ray photographs. The metal-atom structure of γ-phase is merely that of β-phase with vacant lattice sites substituted for the (0,0,0) tungsten atoms. Furthermore the range of observed lattice parameters overlap, so that the intense diffraction lines of γ-phase are often coincidental with those of β-phase. Indeed it is possible that a thin layer of β-$W_{1.5}(N,O)$ exists between γ-$W_{0.75}(N,O)$ and α-W on all specimens: this would rarely be observed on an X-ray photograph.

The general trend in nitrided wires is for the ratio of β : γ to increase as the ammonia content and hence the oxygen potential is reduced. The nitriding of powders usually produced only γ-phase even when the ammonia content of the gas was reduced. However, on one occasion (run 6) not only were the two phases observed together, but the lattice parameters differed sufficiently to cause "splitting" of the diffraction patterns (Figure IV.2). Surprisingly, this was with 100% ammonia. A specimen of δ-WN on tungsten wire was converted to γ when nitrided in ammonia (run 7). Successive etching with 70%HNO_3/30%HF with X-ray examination at each stage showed the sequence of nitride phases from

outside to inside as:

$$\gamma \longrightarrow \delta \longrightarrow \alpha$$

Etching the specimen from Figure IV.1b ($\beta+\gamma$) showed no difference in the phases present at different depths implying that ($\gamma+\beta$) exists as a duplex structure and not as successive layers. Hence their nitrogen potentials are similar but at least one of them is stabilised by impurities. Alternatively Figure IV.1b may in fact show only β -nitride in which case its structure must contain either ordered metal-atom vacancies (although a much smaller number than γ) or nitrogen in ordered positions. It is also possible that the faint superlattice reflections (320) and (321) exist on the pattern of β in Figure IV.2b. However Khitrova and Pinsker (1959, 1962) assert that the phase is free from defects and contains randomly distributed nitrogen.

It seems evident that both β and γ are oxynitrides with γ existing at slightly higher oxygen potentials than β while δ-WN is clearly unstable in the oxygen potentials produced in ammonia-hydrogen mixtures.

IV.3 Nitriding of tungsten in high-pressure molecular nitrogen

Oxygen-free phases in the molybdenum-nitrogen system are formed by pressure nitriding (Evans and Jack, 1957; see Evans, 1957) with pure molecular nitrogen obtained by decomposition of ϵ or ζ -Fe_2N (see Chapter II) provided that oxygen-free (i.e. wire) specimens are used. Preliminary

experiments on tungsten wire showed that the phases formed included ternary iron-tungsten nitrides (see Appendix I). In order to avoid the formation of these phases, it was necessary to use θ-$MnN_{0.9}$ as a source of nitrogen. Table IV.3 lists the phases observed on nitriding wire and powder and Figure IV.3 shows X-ray photographs of δ-WN.

The presence of a ternary η-phase on nitrided tungsten powder is also discussed in Appendix I. The only phase produced on tungsten wire was δ-WN. This phase has never been prepared sufficiently pure for analysis and is only assumed to be of composition WN by analogy with its isomorph WC.

The presence of a very low oxygen potential ($p_{O_2} \sim 10^{-25}$atm.) in the system, obtained by including a small amount of Cr_2O_3 in the reaction tube, causes s small increase in the c dimension of δ-WN and produces stacking faults in the crystal. This is demonstrated by the broadening of X-ray lines in Figure IV.3. X-ray line broadening due to stacking disorder has been observed in other hexagonal interstitial phases. Roberts (1970) studied faulting in ε-NbN(O) and concluded that the stacking of niobium atoms in AABB sequence was periodically interrupted by a sequence ABAB existing over several atom planes. Alternatively the structure could be described as coherent discs of δ-NbN(O) (ABAB) in a matrix of ε-NbN(O) (AABB). Since it was known that δ contained less oxygen than ε Roberts concluded that the phase was broken up into regions of "oxygen-rich" and "oxygen-poor" NbN. Mortimer (1971) obtained faulting in hexagonal $Mn_{22}C_6$

Table IV.3

Nitriding of tungsten in high pressure molecular nitrogen

run	starting material	~N_2 atm.	temp. °C	time days	X indicates phases observed		
					α-W	δ-WN	*η_3-Fe_6W_6N
1	α-powder	40	850	2	X		X
2	α-wire	20	850	2	X	X	
3	α-wire	40	850	2	X	X	
4	α-wire	60	850	2	X	X	
5	α-wire	40 ($+Cr_2O_3$)	850	2	X	X "WN(O)" (faulted)	

* This particular eta-phase had a lattice parameter the same as Fe_6W_6C (Leciejewicz, 1964) and similar to $Ni_{12}Mo_{12}(O,C,N)$ (Nutter, 1969). In the absence of conclusive proof of its composition it will be referred to as "η_3" - the term introduced by Nutter for the composition $M_{24}X$. The phase is discussed in Appendix I.

Fig. IV.3

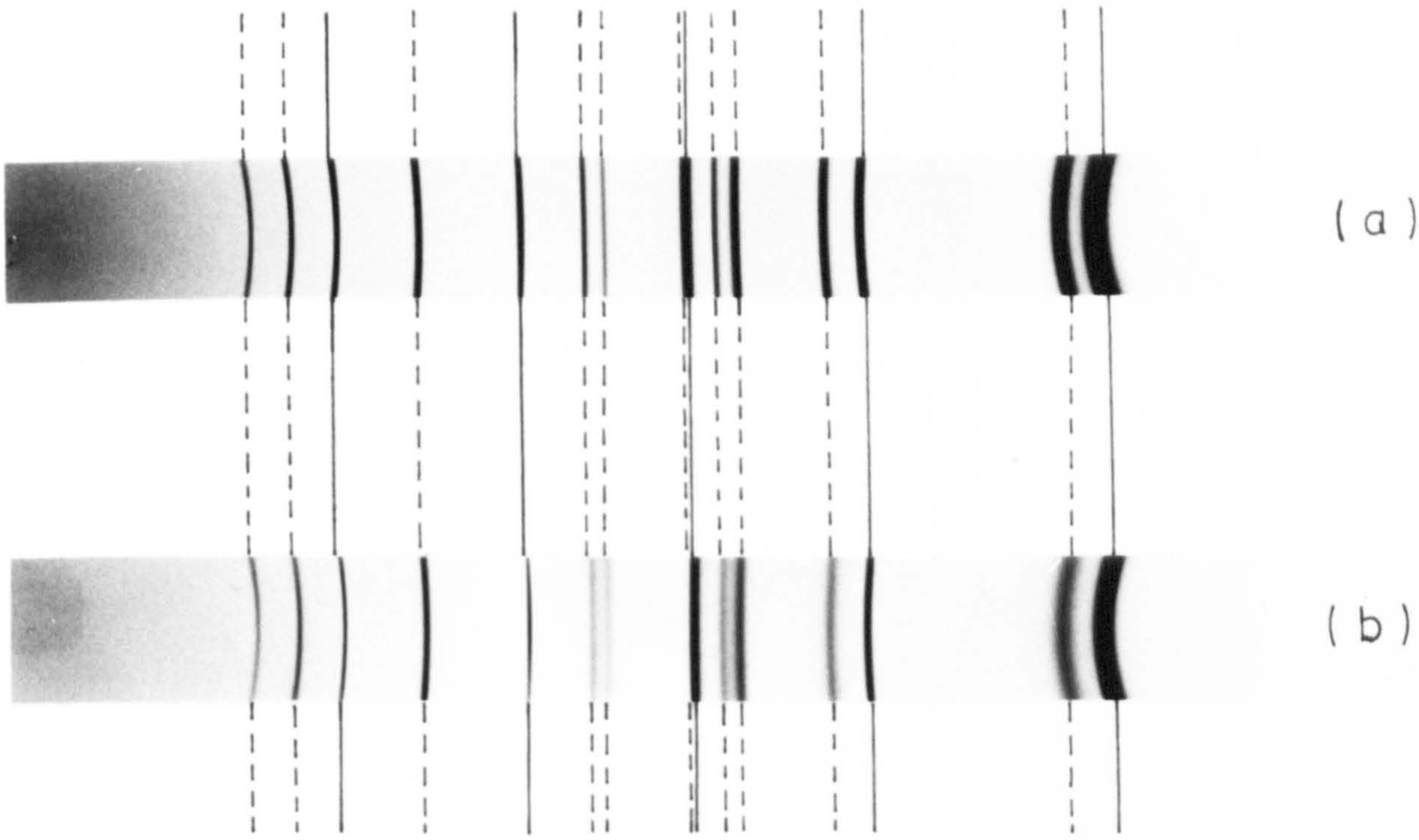

(a) ~40 atm. N_2. 2 days at 850 °C

(b) ~40 atm. N_2. 2 days at 850 °C
($+Cr_2O_3$)

X-RAY PHOTOGRAPHS SHOWING TUNGSTEN NITRIDES PRODUCED BY PRESSURE NITRIDING TUNGSTEN WIRE [Fe Kα]

and also showed the phase to be an oxy-carbide.

It is clear from the present experimental results that the only "pure" phase in the tungsten-nitrogen system is δ-WN. The presence of a small amount of oxygen is tolerated but at higher oxygen potentials (ammonia-hydrogen nitriding) the phase becomes unstable.

IV.4 Aging of tungsten nitride and oxy-nitride

In order to determine the relative stabilities of γ-$W_{0.75}(N,O)$ and δ-WN, specimens of each phase produced on wire were aged in evacuated sealed silica capsules.

It is reported that the vacant metal lattice sites in γ become randomly distributed on annealing at 890°C and hence give an X-ray diffraction pattern like that of β (Kiessling and Peterson, 1954). This was not observed in the present study. Instead, after aging for only one day at 900°C, γ decomposed according to the reaction

$$\underset{\gamma}{W_3(N,O)_4} = \underset{\delta}{3WN} + \frac{1}{2}N_2\,(O)$$

producing the "oxygen-free" δ-phase. The oxygen potential produced at high temperatures in evacuated silica tubes can be appreciable (Bell, Hetherington and Jack, 1962; Roberts, 1970) but evidently it is not high enough to stabilise γ or prevent the formation of δ.

Schönberg (1954a) obtained decomposition of δ-WN at 600°C in vacuum, but no details were given. He assumed the composition of β to be W_2N and gave the decomposition reaction as

$$2WN = W_2N + \frac{1}{2}N_2$$
$$\delta \quad \beta \quad \text{gas}$$

In the present study a specimen of δ-WN on the surface of α-wire was aged for 17 days at 900°C with no detectable decomposition. This is completely at variance with the observations of Schönberg. The only possible reason for the marked difference in behaviour is that the system used by Schönberg was at a higher oxygen potential than in the present case, and so stabilised β at the expense of δ.

IV.5 Discussion

The differences in behaviour observed on nitriding tungsten can be attributed to the effect of oxygen. The sequence of phases produced with increasing oxygen potential is δ-WN $\rightarrow$ β-$W_{1.5}(N,O)$ $\rightarrow$ γ-$W_{0.75}(N,O)$ $\rightarrow$ $W_{0.62}(N_{0,62},O_{0,38})$ with δ being "oxygen-free". The term "oxygen-free is of course relative and it is possible that δ can contain small concentrations of impurity before faulting is observed. The phase $W_{0.62}(N_{0.62},O_{0.38})$ was never observed in the present investigation because the oxygen potential was not high enough.

Kiessling (1954) suggested that as the oxygen content of the cubic oxy-nitrides increases, the tendency to form N-O bonds reduces the contribution of electrons by nitrogen to the tungsten lattice. In order to minimise the electron imbalance, defects are introduced in proportion to the oxygen content of the phase,

i.e. β - $W_{1.5}(N,O)$	0% vacant sites
γ - $W_{0.75}(N,O)$	25% vacant sites
$W_{0.62}(N_{0.62},O_{0,38})$	38% vacant sites

A similar effect occurs with the hexagonal nitride δ -WN and it is likely that all the defective phases reported by Khitrova and Pinsker (1962) are oxy-nitrides. One such phase (δ_{H}^{III}) has been confirmed in the present work but is not produced on "pure" α -tungsten. It is often observed as a precipitate in Fe-W-N alloys and is therefore discussed in Chapter V; it is certainly an oxy-nitride and has a defect structure.

A schematic ternary phase diagram for the W-N-O system which accounts for this and other work is shown in Figure IV.4. Since β -phase has been observed in equilibrium with gas (Hägg 1930a) then δ can not co-exist with γ (see Figure IV.4). Therefore in the conversion of δ to γ (run 7, Table IV.1) a layer of β must exist between γ and δ but it is too thin to be detected.

Fig. IV.4

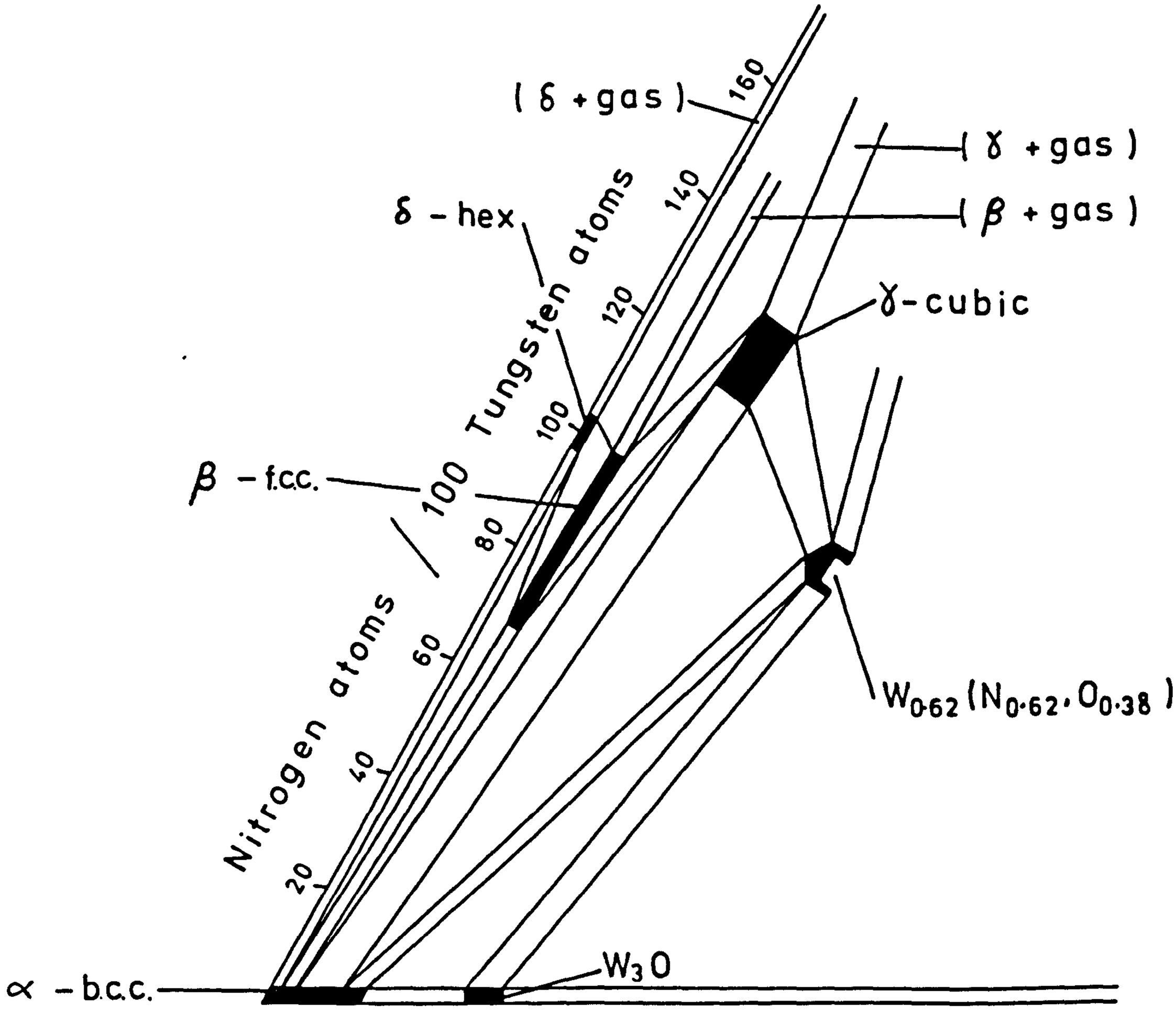

PROPOSED TERNARY PHASE DIAGRAM

FOR THE W-N-O SYSTEM (SCHEMATIC)

IV.6 Conclusions

(a) Three phases are observed by nitriding α-tungsten, namely δ-WN, β-$W_{1.5}(N,O)$ and γ-$W_{0.75}(N,O)$.

(b) A critical oxygen potential exists, above which stacking disorders are introduced into δ-WN. There is a second critical oxygen potential above which the δ-phase can not be formed.

(c) A schematic ternary phase diagram is suggested which shows the sequence of phases produced as the oxygen content is increased.

Chapter V

PRECIPITATION IN Fe-W-N ALLOYS: THE EQUILIBRIUM PHASE

V.1 Introduction

The two nitriding techniques discussed in Chapter II, that is, constant activity aging in $NH_3:H_2$ gas mixtures and pressure nitriding using molecular nitrogen, are complementary. By continuously supplying nitrogen constant activity aging allows all the substitutional solute to precipitate and unequivocal characterisation of the nitride is possible using sensitive X-ray methods. Pressure nitriding using pure molecular nitrogen has the advantage of eliminating oxy-nitrides.

V.2 A structural modification of δ-WN

Preliminary experiments using iron-tungsten alloys nitrided in $NH_3:H_2$ gas mixtures established the existence of a hexagonal oxy-nitride the unit cell of which is related to that of δ-WN. The phase, designated δ', is precipitated in the higher tungsten alloys at about 600°C using relatively high nitrogen potentials, typically about 6-10% $NH_3:H_2$.

X-ray and electron diffraction patterns of δ' extracted from iron alloys are shown in Figure V.1. All reflections are indexed on the basis of a hexagonal unit cell (see Table V.1)

Fig. V.1

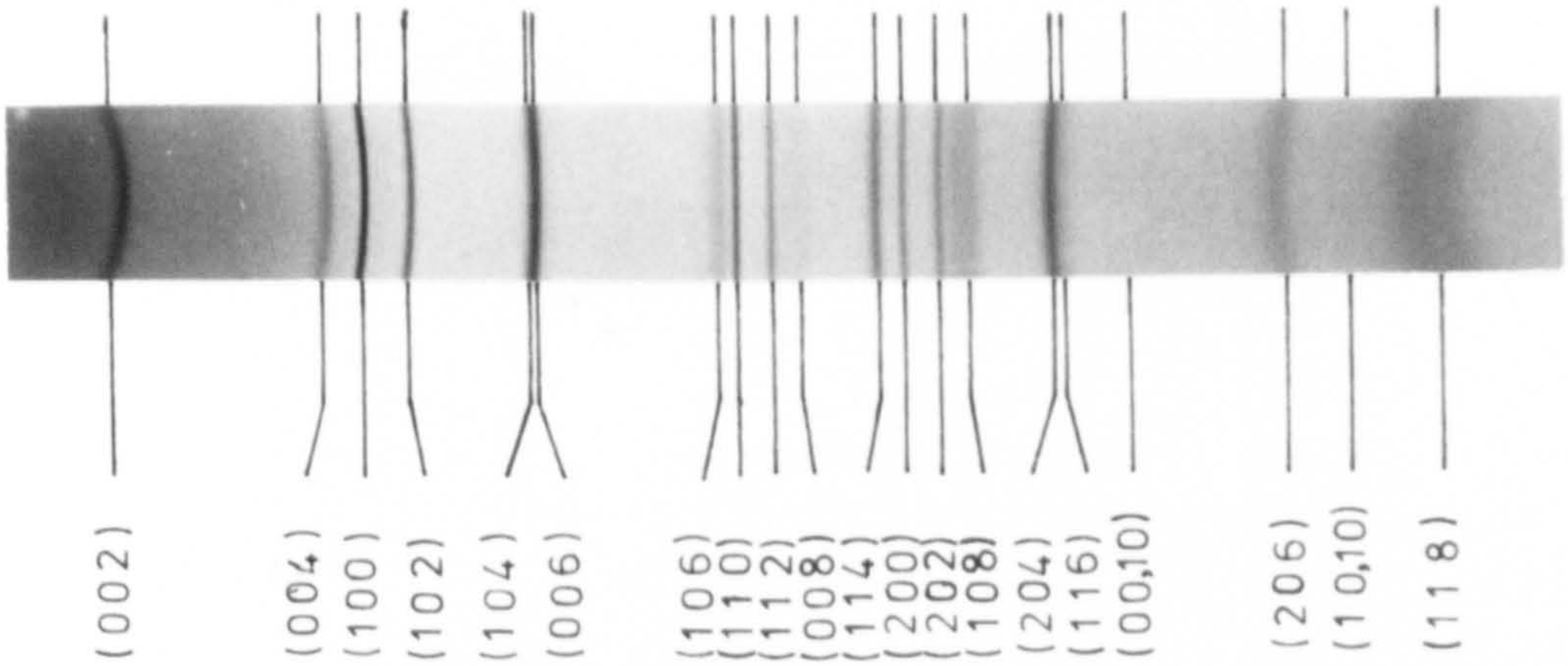

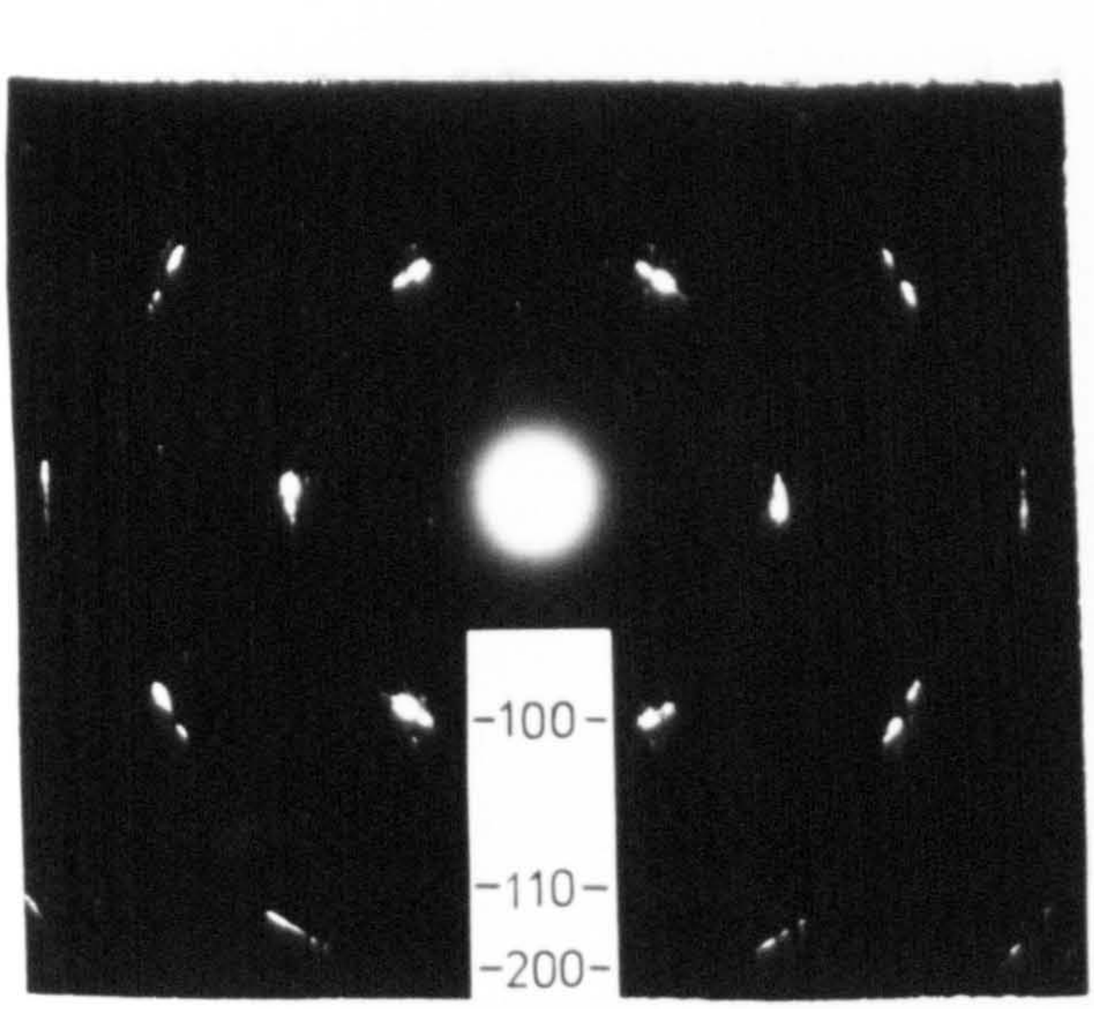

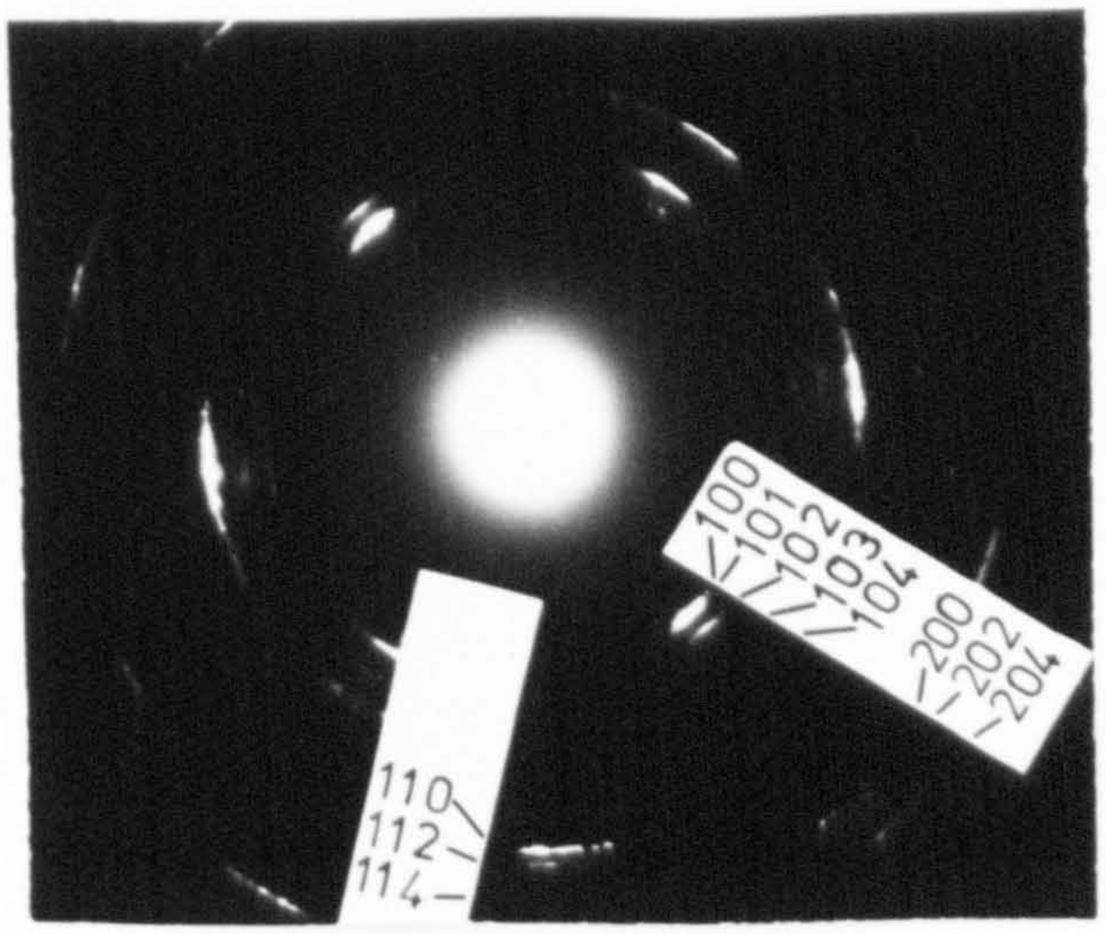

X-RAY AND ELECTRON DIFFRACTION PATTERNS OF δ'-$W_{0.9}(N,O)$ EXTRACTED FROM Fe-4·0 wt.% W NITRIDED AT 615 °C. IN 8% NH_3:H_2 FOR 10 DAYS.

Table V.1

X-ray data for δ'-$W_{0.9}(H,O)$

camera: Hägg-Guinier ($CuK\alpha_1$)

unit-cell: hexagonal $\underline{a} = 2.8760 \pm 0.0005$ Å

$\underline{c} = 10.86 \pm 0.02$ Å

$c/\underline{a} = 3.776$

No	I obs	breadth	$\sin^2\theta$ obs	$\sin^2\theta$ calc	{hkl}
1	W	b	0.0201	0.0201	002
2	W	vb	0.0814	0.0805	004
3	S	sh	0.0957	0.0957	100
4	M	b	0.1157	0.1158	102
5	M	vb	0.1764	0.1762	104
6	VW	vb	0.2783	0.2768	106
7	MS	sh	0.2869	0.2870	110
8	M	sh	0.3069	0.3071	112
9	M	b	0.3674	0.3674	114
10	M	sh	0.3826	0.3826	200
11	M	sh	0.4025	0.4027	202
12	VVW	vvb	0.4219	0.4176	108
13	M	b	0.4633	0.4631	204

with dimensions:

$$\underline{a} = 2.876\ \text{Å}; \qquad \underline{c} = 10.86\ \text{Å}; \qquad \underline{c}/\underline{a} = 3.776$$

δ' is usually precipitated in a heavily faulted condition causing severe line broadening on X-ray patterns. Consequent inaccuracies in determining the unit-cell dimensions (especially the $\underline{c}$ dimension) were minimised by using a Hägg-Guinier focussing camera. The broadening of all lines (hkl) where $l \neq 0$ is clearly seen in Figure V.1.

It seems that δ' is the phase characterised by Khitrova and Pinsker (1962) during electron diffraction studies and termed δ^{III}_{H}. The metal-atom arrangement of δ^{III}_{H} is merely a simple-hexagonal stacking of close-packed atom planes in the sequence A A' A A', where alternate planes have sites which are only 28% occupied (A'). The nitrogen atoms (one atom per simple-hexagonal sub-cell) are in trigonal-prisms and stacked in the sequence B C C B. Therefore with respect to the metal-atom lattice the unit cell consists of only two basic sub-cells and it is only the positions of the nitrogen atoms which make the true unit equal to four sub-cells. X-ray diffraction is insensitive to interstitial atoms especially in the presence of the heavy tungsten atoms and it is for this reason that the reflections (hkl) where l is odd are not seen on the X-ray pattern of Figure V.1; these are observed, however, on the electron diffraction pattern and clearly show the nitrogen superlattice.

The approximate formula for δ^{III}_{H} suggested by Khitrova

and Pinsker was $W_{0.64}N$. Nitrogen analysis of the extracted δ' precipitate (three determinations) gave a nitrogen content of 51.6 at.% corresponding to a formula of $W_{0.94}N$, assuming only tungsten and nitrogen to be present in substantial quantities. Weight increases of nitrided alloys give results in general agreement with the latter formula.

The fact that δ' is not produced on tungsten wire under the same experimental conditions as it is precipitated in alloys, suggests that iron is required to stabilise the phase. This conclusion is supported by the following observation. A specimen of the pure nitride δ-WN, on tungsten wire, aged in 8%NH_3:H_2 at 615°C is not converted to δ' even after aging for 7 days. However a specimen of (η_1-Fe_3W_3N + δ-WN) on tungsten wire, aged under the same conditions shows transformation to δ'-$W_{0.9}(N,O)$.

It has been shown in Chapter IV that the presence of impurity non-metal atoms can cause stacking disorders in δ-WN, probably by segregating within the crystal to regions of "high" and "low" impurity content. It seems possible that impurity metal-atoms, i.e. iron, can have a similar effect.

In conclusion, a hexagonal tungsten oxy-nitride hitherto regarded as a pure nitride and observed only in localised regions of nitrided tungsten foils, has been shown to exist if a sufficiently high oxygen potential is maintained. The phase is stabilised by the presence of iron and forms freely in nitrided iron-tungsten alloys. The composition is near

to $W_{0.9}(N,O)$ and the structure contains tungsten vacancies.

V.3 Ammonia-hydrogen nitriding

All alloys up to and including Fe-5.05 wt.%W. are single phase (α-iron) both in the "as-received" condition and after annealing in hydrogen at 800-900°C. This is in accordance with the Fe-W equilibrium diagram (Hansen, 1958) reproduced in Figure V.2. At about 600°C under equilibrium conditions all alloys in the range 5-62 wt.%W are two-phase, the intermetallic compound being Fe_2W, a Laves phase with the $MgZn_2$ structure. Surprisingly, the Fe-9.3 wt.%W in the "as received" condition consists of (α + η-oxide) and it is only after annealing the specimen in hydrogen at 800-900°C that the structure reverts to that predicted by the equilibrium diagram (see Figure V.3). The η-phase has a unit-cell dimension of $\underline{a}$ = 10.894 Å which is near to that of Fe_6W_6C, $\underline{a}$ = 10.934 (Leciejowicz, 1964) and $Ni_{12}Mo_{12}(O,C,N)$, $\underline{a}$ = 10.889 (Nutter, 1969) but considerably smaller than Fe_3W_3N, $\underline{a}$ = 11.05 Å. Annealing the specimens in hydrogen (3h. at 880°C) prior to nitriding is carried out for the following reasons:

(i) to reduce the oxygen content;

(ii) to allow recrystallisation and hence facilitate optical metallography;

(iii) to minimise the number of potential nucleation sites and so encourage homogeneous precipitation.

Fig.V.2

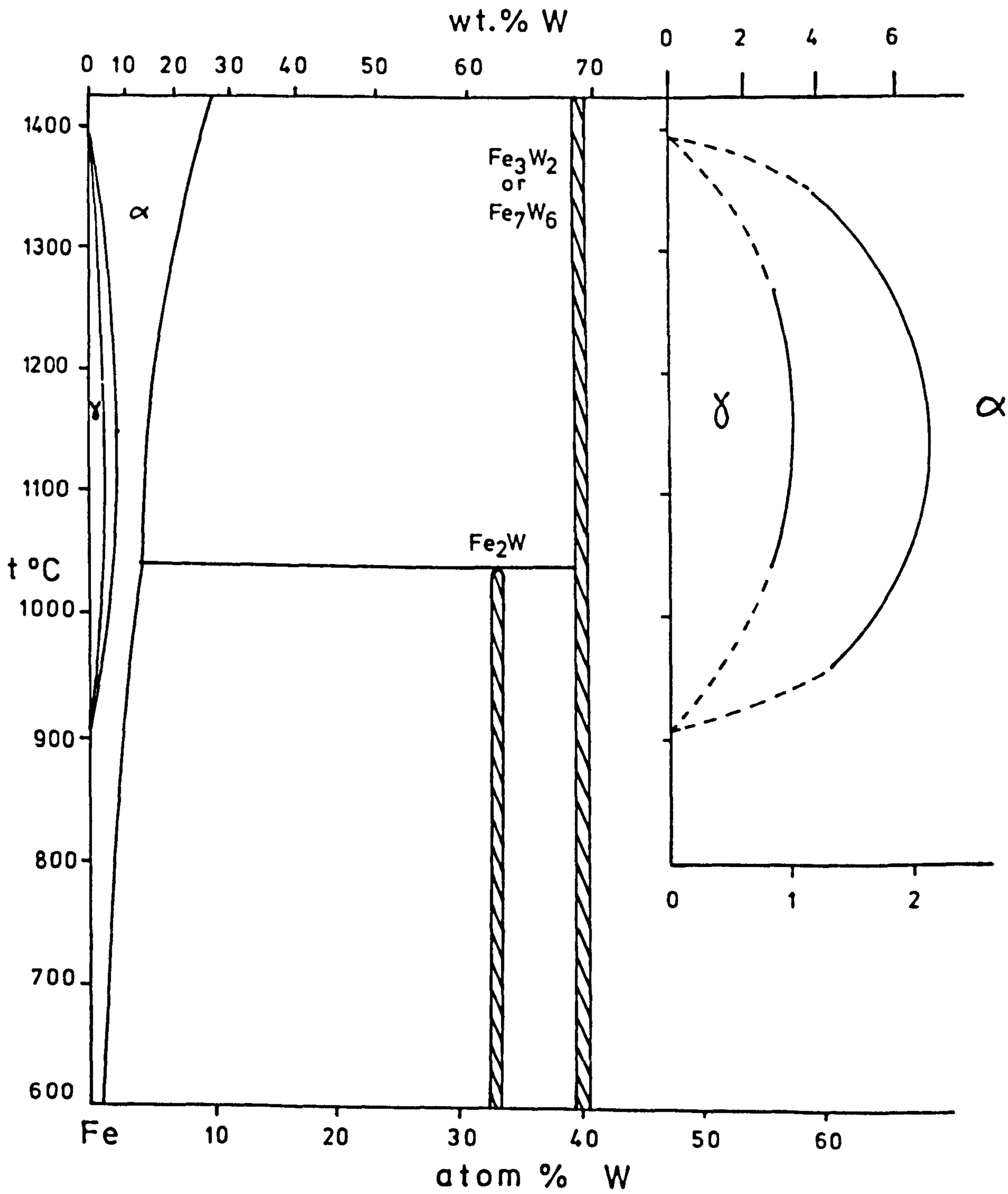

THE IRON-TUNGSTEN EQUILIBRIUM DIAGRAM.

[after HANSEN, 1958

Fig. V. 3

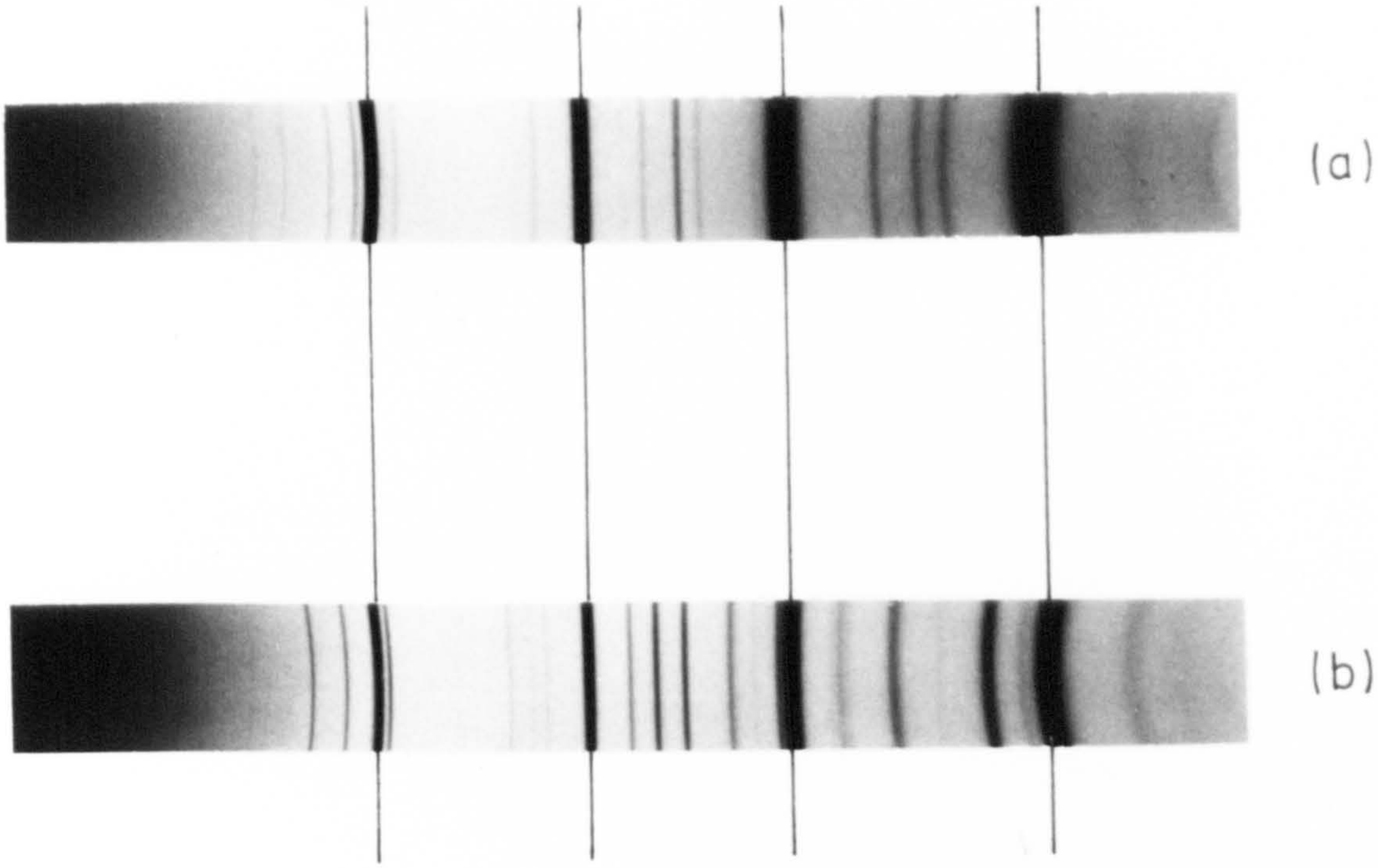

(a) as recieved

$\alpha - Fe + \eta_3 - oxide$

(b) annealed in purified H_2

$\alpha - Fe + Fe_2W$

X-RAY PHOTOGRAPHS SHOWING PHASES

PRECIPITATED IN Fe – 9·3 wt.% W.

Under certain nitriding conditions homogeneous precipitation does occur and this is more fully discussed in Chapter VI.

The phases produced by ammonia-hydrogen nitriding are summarised in Table V.2.

(a) Annealed alloys

At temperatures below 590°C there is no detectable precipitation in any alloys up to Fe-5 wt.%W in reasonable times (up to 14 days). However in Fe-9.3 wt.%W the Fe_2W particles transform to either η_1 or δ' accompanied by trace quantities of γ (runs 1 and 2). η_1 is favoured by low nitrogen (and hence oxygen) potentials whilst δ' predominates at higher values.

Between 590-650°C where precipitation can proceed under a wide range of nitrogen potentials, the predominant phase produced is δ'. Again η is seen as an alternative when the ammonia content of the gas is low (run 4). The nitride produced in the low tungsten alloys (1 and 2 wt.%W) is almost always γ (runs 4, 9 and 11), but the tungsten content above which δ' predominates is lowered as the nitrogen potential is increased (see Figure V.4). Conversely this critical level increases as the temperature is increased so that even when higher nitrogen potentials are used significant quantities of γ are seen in all alloys (runs 12-15). Although the activity of tungsten controls the precipitate

Table V.2

Precipitation in ammonia-hydrogen mixtures

run	$\%NH_3:\%H_2$	temperature °C	time, days	hydrogen anneal	wt.%W	phases observed in α-iron matrix					
						η_1	δ'	δ''	δ	δ_A	Fe_2W
1	14:86	565	11	yes	9.3		ẋ				
					5		no	phases	observed		
2	8:92	575	3	yes	9.3	ẋ	X		X		
3	4:96	590	6	yes	9.3	ẋ					X
					5	X					
4	"	"	4	no	9.3	X		ẋ	X		
					5			X	ẋ		
					2				X		
					1				X		
5	6:94	"	13	yes	9.3		ẋ		X		X
					5		X				
					2		no	phases	observed		
6	9:91	"	4	yes	9.3		ẋ		X		
					5		X				
					2		X				
7	11:89	"	9	yes	9.3		ẋ		X		
					5		X				
					2		X				

Table V.2 (continued)

run	$\%NH_3:\%H_2$	temperature °C	time, days	hydrogen anneal	wt.%N	phases observed in α-iron matrix						
						η_1	δ'	δ''	γ	γ_A	Fe_2W	α'
8	11:89	590	9	no	9.3		X					
					5		X					
9	8:92	615	2	yes	9.3		X				X	
					4		X					
					2				X			
					1				X			
10	"	"	1/3	no	9.3	X			X			
			4		"		X			X		
			1/3		5		X		X			
			4		"		X			X		
			1/3		4		X			X		
			4		"		X			X		X
11	5:95	640	4	yes	9.3	X	X		X			
					5		X					
					2				X			
12	1:99	650	3	yes	9.3				X		X	
					5				X			
13	2:98	"	4	yes	9.3			X	X			
					5				X			
					4				X			

Table V.2 (continued)

run	$\%NH_3:\%H_2$	temperature °C	time, days	hydrogen anneal	wt.% N	phases observed in α-iron matrix						
						η_1	δ'	δ''	γ	γ_A	Fe_2W	α'
14	4:96	650	3	yes	9.3		X		X			
					5	X	X		X			
					2				X			
15	5:95	"	"	yes	9.3			X	X		X	
16	8:92	"	4	yes	9.3		X		X	X		X
					5		X		X	X		X
					3.5		X		X	X		X
					2		X			X		X
					1					X		X
17	$1\frac{1}{2}:98\frac{1}{2}$	700	3	yes	5				X			
18a	2:98	"	4	yes	9.3			X	X			
					5			X	X			
					4				X			
					2				X			
					1				X			
18b	"	"	"	"	9.3	X		X	X			

Table V.2 (continued)

run	$\%NH_3:\%H_2$	temperature °C	time, days	hydrogen anneal	wt.%W	phases observed in α-iron matrix						
						η_1	δ'	δ'	γ	γ_A	Fe_2W	α'
19	6:94	700	4	yes	5			X	$\dot{X}$	X		X
					3.5			X	$\dot{X}$	X		X
					2					X		X
					1					X		X
20	2:98	740	2	yes	9.3			X	$\dot{X}$		X	
					5				X	X		
					2					X		X

Key to Table V.2

η_1 - Fe_3W_3N ; cubic

δ' - $W_{0.9}(N,O)$; hexagonal

δ'' - unknown ; probably hexagonal and of similar composition to

γ - $W_{0.75}(N,O)$; cubic

γ_A - nitrogen-austenite ; cubic

α' - nitrogen-martensite - tetragonal

Fe_2W - hexagonal

X - denotes phases present

$\dot{X}$ - denotes principle (oxy)-nitride present (excluding γ_A or α')

Fig. V.4

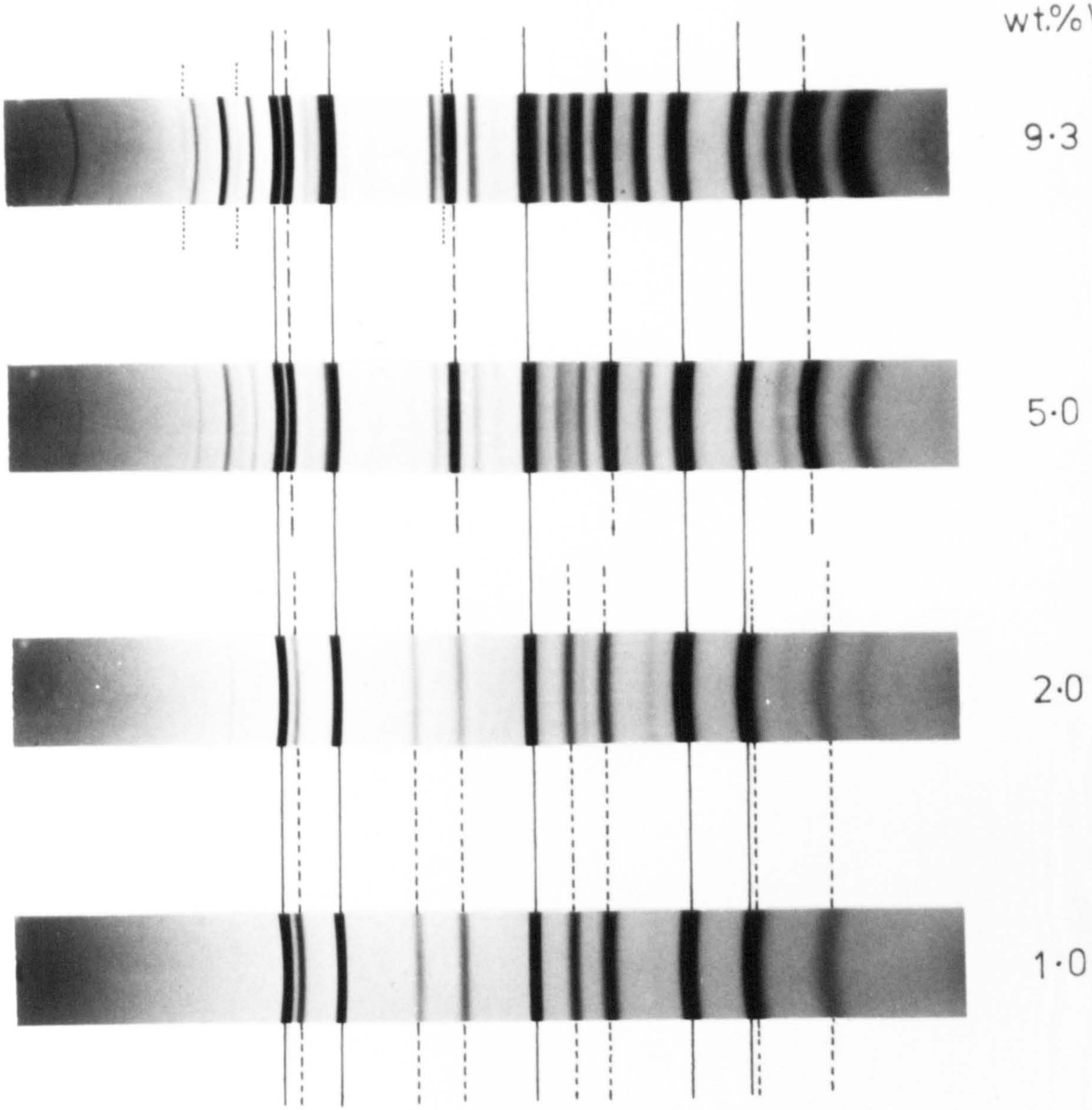

——— γ_n – Fe

–·–·–·– α – Fe

– – – – – – – – α' – martensite

..... γ – $W_{0\cdot75}$ (N,O)

unmarked δ' – $W_{0\cdot9}$ (N,O)

X-RAY PHOTOGRAPHS SHOWING PHASES PRECIPITATED IN Fe–W ALLOYS NITRIDED IN 8 % NH_3:H_2 AT 650 °C. FOR 4 DAYS

produced to a certain extent, the dominating factor appears to be the ammonia content of the gas mixture. In view of the results of Chapter IV it seems that oxygen also has a pronounced effect.

As the temperature increases, e.g. at 650-750°C, the same nitrogen potential is achieved with lower ammonia contents so that the oxygen potential, if proportional to the ammonia content, is reduced considerably. The combination of a temperature increase and reduced oxygen potential results in yet another modification of δ-WN, termed δ'' (runs 13, 15, 18, 19 and 20) (see Figure V.5). Only small amounts of the phase are formed and it is always observed with considerable quantities of other phases. Neither the composition nor the structure of δ'' is known, but a strong reflection on the diffraction patterns corresponds to a hexagonal unit-cell a dimension of 2.87 Å. It is thought that δ'' is stable at an oxygen potential lower than that required for δ' but higher than for the formation of η_1. Occasionally all three phases δ' (or δ''), γ and Fe_2W are detected in the same specimen. At high nitrogen potentials the matrix becomes austenitic but the precipitation sequence remains unchanged. Typical micrographs illustrating the different nitride distribution in 5.05 and 9.3 wt.%W are shown in Figure V.6.

(b) Cold-worked alloys

In order to facilitate precipitation several runs were repeated using alloys which were not previously annealed.

Fig. V. 5

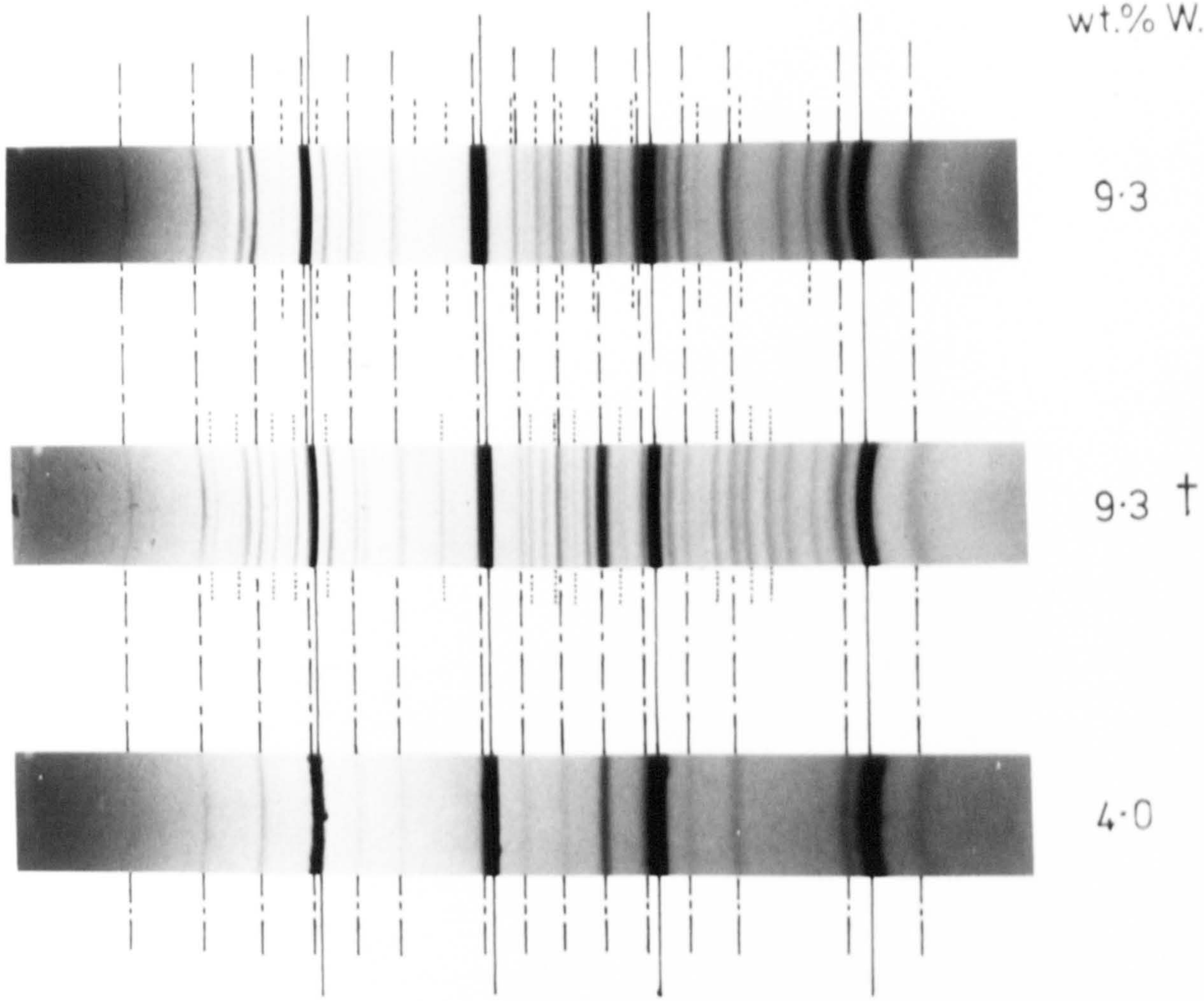

——— α – Fe

—·—·—·— γ – $W_{0.75}$ (N,O)

------ Fe_2W

..... η_1 – $Fe_3W_3N(O)$

unmarked δ''

repeat run †

X-RAY PHOTOGRAPHS SHOWING PHASES PRECIPITATED IN Fe-W ALLOYS NITRIDED IN 2% NH_3:H_2 AT 700 °C FOR 4 DAYS

Fig.V.6

(a) Fe-9·3 wt.% W

annealed 3h. at 880 °C

$\alpha + Fe_2W$

X 2600

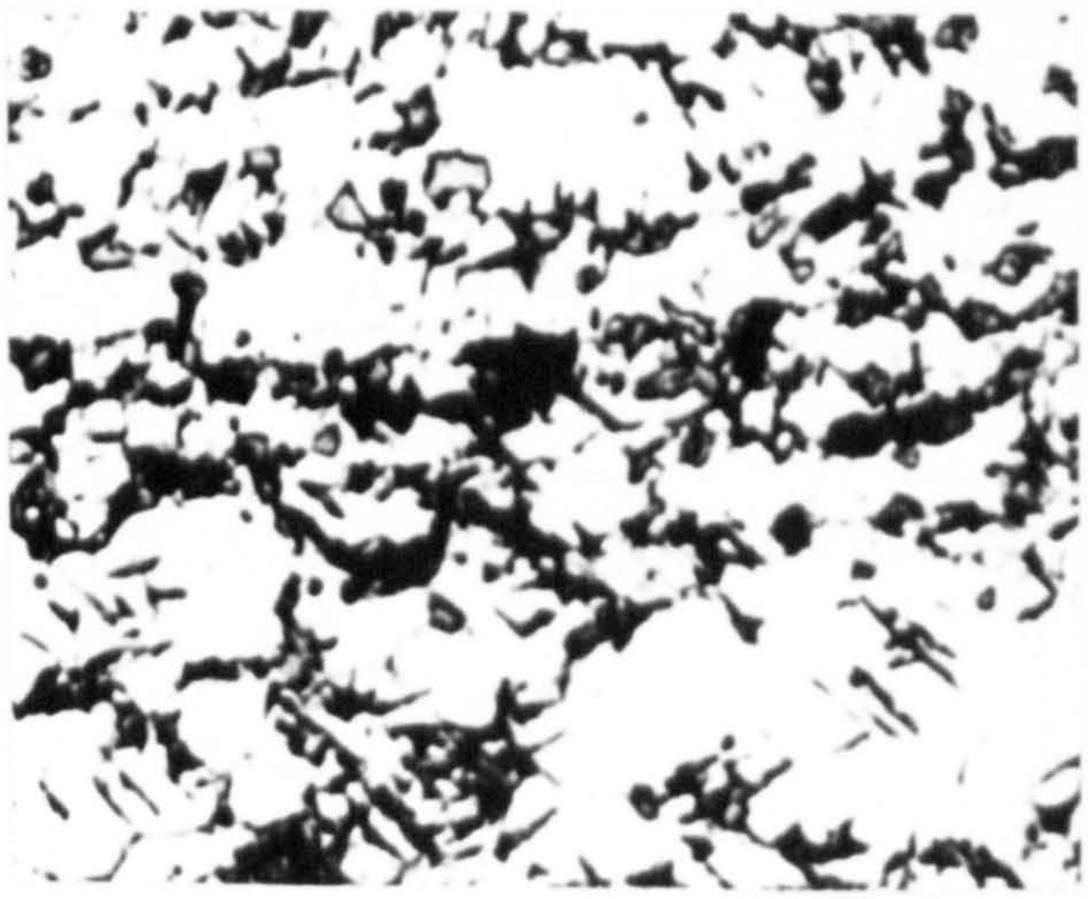

(b) as (a)

nitrided 4 d. in 5% NH_3:H_2

at 640 °C

$\alpha + \delta'$

X 2600

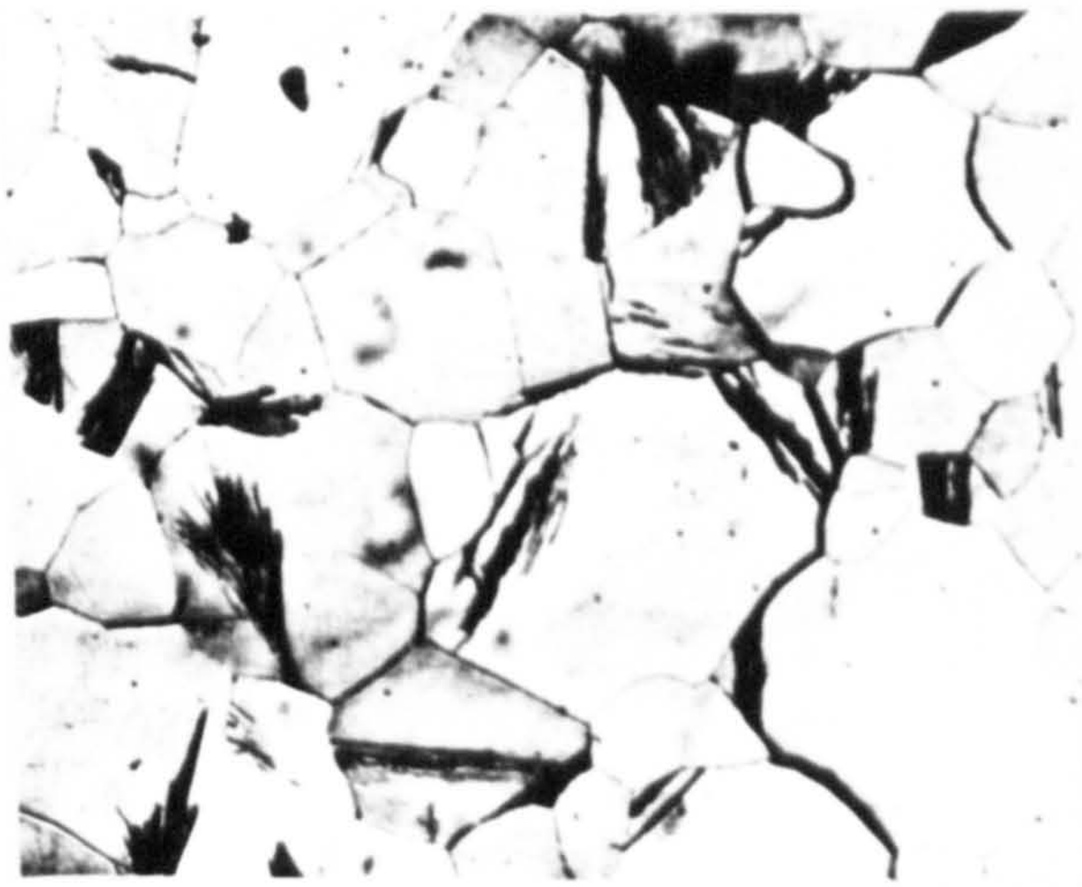

(c) Fe-5·05 wt.% W

annealed 3h.at 880 °C

nitrided 9 d. in 11% NH_3:H_2

at 590 °C

$\alpha + \delta'$

X 140

PHOTOMICROGRAPHS OF ANNEALED AND NITRIDED Fe-W ALLOYS.

The effect of the higher oxygen content is shown by run 4 where δ'' partially replaces η_1 in the 9.3 wt.%W alloy and completely replaces it in the 5.05 wt.%W alloy. δ is observed in the 2.05 and 5.05 wt.%W alloys because precipitation is more rapid than in the annealed alloys and the tungsten content decreases to a level where is stable.

The sequence of phases produced during nitriding is shown by interrupting the nitriding treatment at 615°C and 8% NH_3:H_2 (run 10). In the Fe-9.3 wt.%W alloy after only 8h. the original η-oxide has merely transformed to η_1-$Fe_3W_3N(O)$ with some formation of δ. However after 4 days under the same conditions both phases are unstable and only δ' remains (see Figure V.7). With only 4.0 and 5.05 wt.%W, δ' is nucleated directly (again with δ) because the alloys are single-phase before nitriding. As with the high-tungsten alloy δ' is the equilibrium phase, and δ is not present after 4 days. During run 10 the ammonia content of the gas mixture exceeded 8% resulting in the formation of δ-austenite, less of which is seen in the 9.3 wt.%W alloy because of the ferrite-stabilising effect of tungsten (Figure V.7).

V.4 Pressure-nitriding and quench-aging

X-ray examination of pressure-nitrided alloys without subsequent aging (runs 1 and 2, Table V.3) shows no nitride precipitation in alloys up to 5.05 wt.%W and both solutes

Fig. V. 7

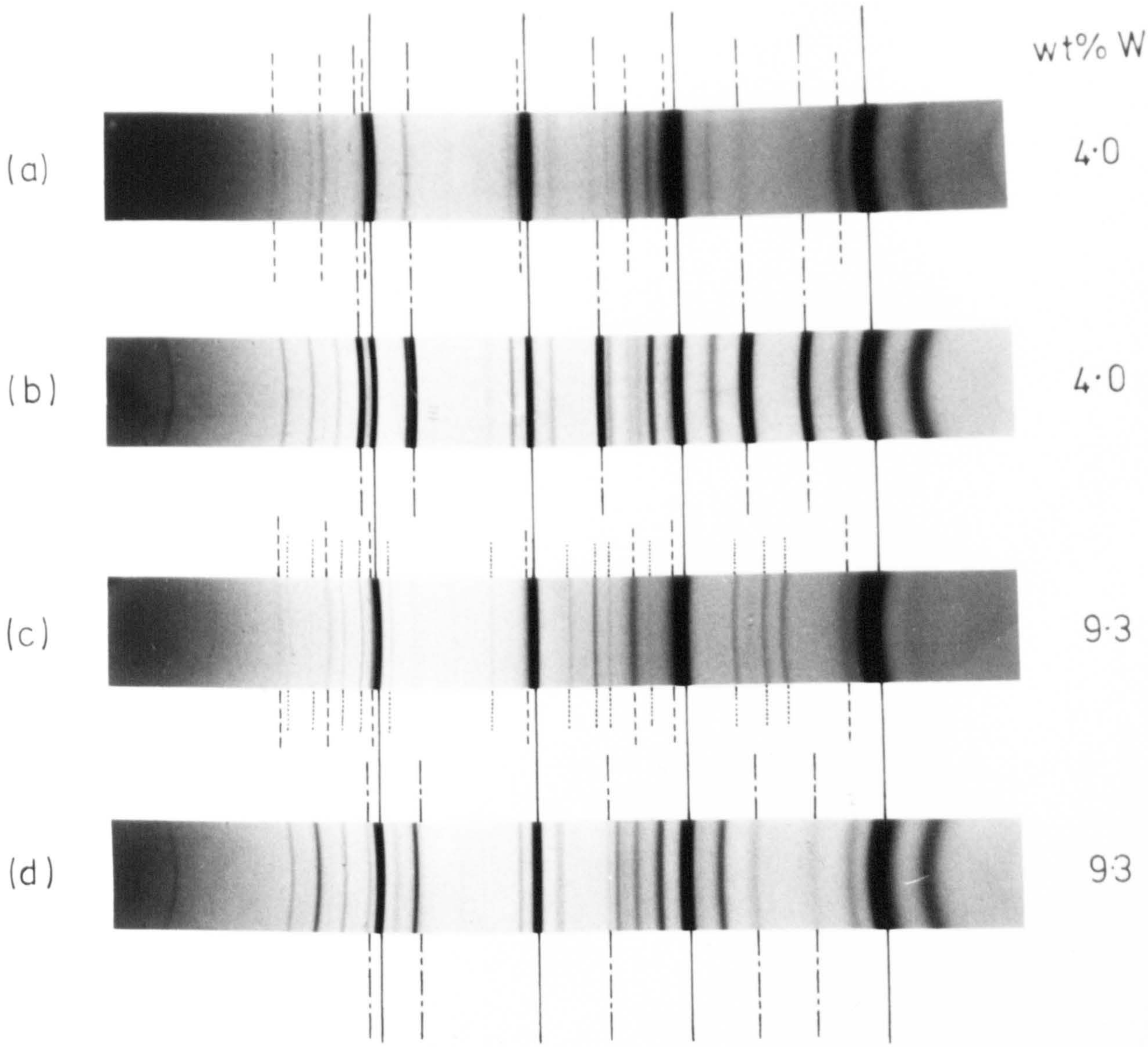

(a) & (c) nitrided for 8 h.

(b) & (d) nitrided for 4 d.

X-RAY PHOTOGRAPHS SHOWING PHASES PRECIPITATED IN Fe–W ALLOYS NITRIDED IN 8 % NH_3:H_2 AT 615 °C.

Table V.3

Precipitation during pressure-nitriding and quench-aging

run	nitriding temp. °C	$\sim p\,N_2$ atm.	aging temp. °C	time, days	hydrogen anneal	wt.% N	phases observed in α-iron matrix					
							η_3	η_1	δ	γ′	γ_A	α′
1	950	40	-	-	no	9.3	X					
2	950	40	-	-	no	5					X	
						2					X	
						1					X	
3	1150	40	720	1	no	9.3		X	X			
						5		X	X		X	
						2			X		X	X
4	950	40	600	1	yes	9.3		X	X			
						5		X	X			
						2			X		X	
				4		9.3		X	X			
						5		X	X			
						2			X			
5	950	40	600	2	yes	3.5			X			
						2			X			
						1			X		X	
						0.5			X		X	

Table V.3 (continued)

run	nitriding temp. °C	$\sim p_{N_2}$ atm.	aging temp. °C	time, days	hydrogen anneal	wt.%W	phases observed in -iron matrix					
							η_3	η_1	δ	γ'	γ_A	α'
6	950	15	610	3	yes	9.3		X				
						5			X			
						2			X			
7	950	6	575	6	yes	9.3		X				
						5			X			
						2		no phases observed				
8	950	40	560	4	yes	9.3		X	X			
						5			X			
						2			X	X		

Key to Table V.3

η_3 - $Fe_{12}W_{12}(O,C,N)$ or $Fe_6W_6N(O)$; cubic

η_1 - $Fe_3W_3N(O)$; cubic

δ - WN ; hexagonal

γ' - Fe_4N ; cubic

γ_A - nitrogen-austenite ; cubic

α' - nitrogen-martensite ; tetragonal

X - denotes phases present

are present in a mixture of ferrite, austenite and martensite or autotempered martensite. In the 9.3 wt.%W alloy there is some precipitation of η_3-nitride but most of the tungsten and nitrogen is in solution. Surprisingly the η-nitride has the same unit-cell dimensions as the original η-oxide and therefore is of composition $Fe_6W_6N(O)$ or $Fe_{12}W_{12}(N,O,C)$ and not Fe_3W_3N. Considerable quantities of precipitate are produced on subsequent aging and the low oxygen content prevents complication of the sequence by oxy-nitrides. The phase produced depends on the tungsten content of the alloy and the trend is more marked than in constant activity aging. The sequence of phases formed with decreasing tungsten content is $\eta_1 \longrightarrow \delta$ (runs 3, 4, 6, 7 and 8), with η_1 never being observed in alloys containing less than 5.05 wt.%W. In alloys nitrided at high nitrogen pressures η_1 is present in both 9.3 and 5.05 wt.%W specimens (runs 3 and 4) whilst at lower pressures (~15 and ~6 atm.N_2) the 5.05 wt.%W alloy contains only δ (runs 6 and 7) (see also Figures V.8 and V.9).

The same alloy nitrided in ~40 atm.N_2 but aged at 560°C (run 8) also contains only δ but this is probably due to a slightly lower pN_2 value than the one quoted, rather than the lower aging temperature. Relatively small amounts of Fe_2N are used as a nitrogen source (~ 0.060gm.) and variations in the volume of the sealed nitriding tube can cause errors in the assessment of the nominal pressure. This is particularly noticeable in the present study because the critical tungsten level at which the stable phase changes almost coincides with the composition of one alloy (5.05 wt.%W).

Fig. V.8

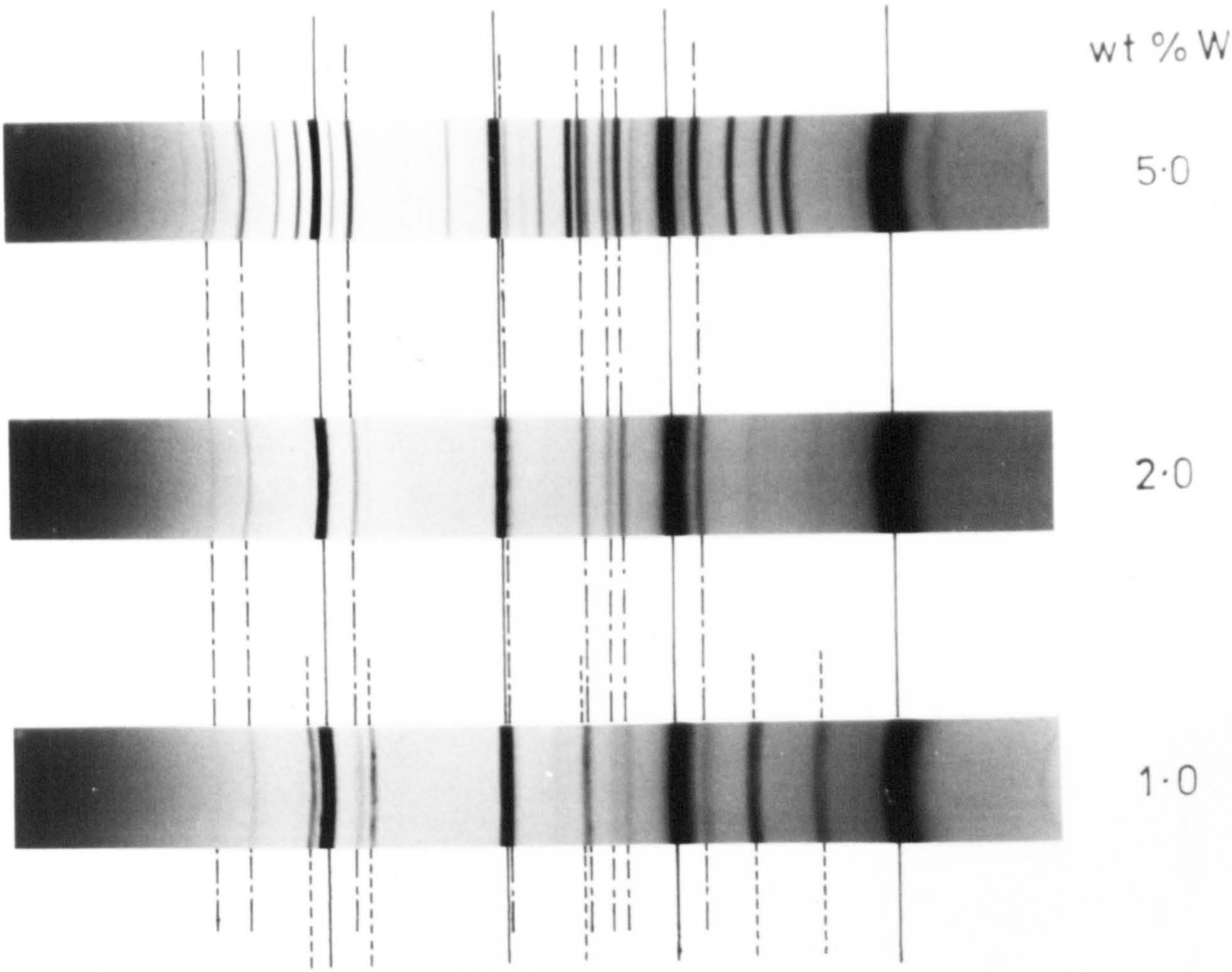

——————— α – Fe

- - - - - - - - - - γ_A – Fe

— · — · — · — δ – WN

unmarked η_1 – Fe_3W_3N

X-RAY PHOTOGRAPHS SHOWING PHASES PRECIPITATED IN Fe-W ALLOYS NITRIDED IN ~40 atm. N_2 AT 950 °C AND SUBSEQUENTLY AGED AT 610 °C FOR 4 DAYS.

Fig. V.9

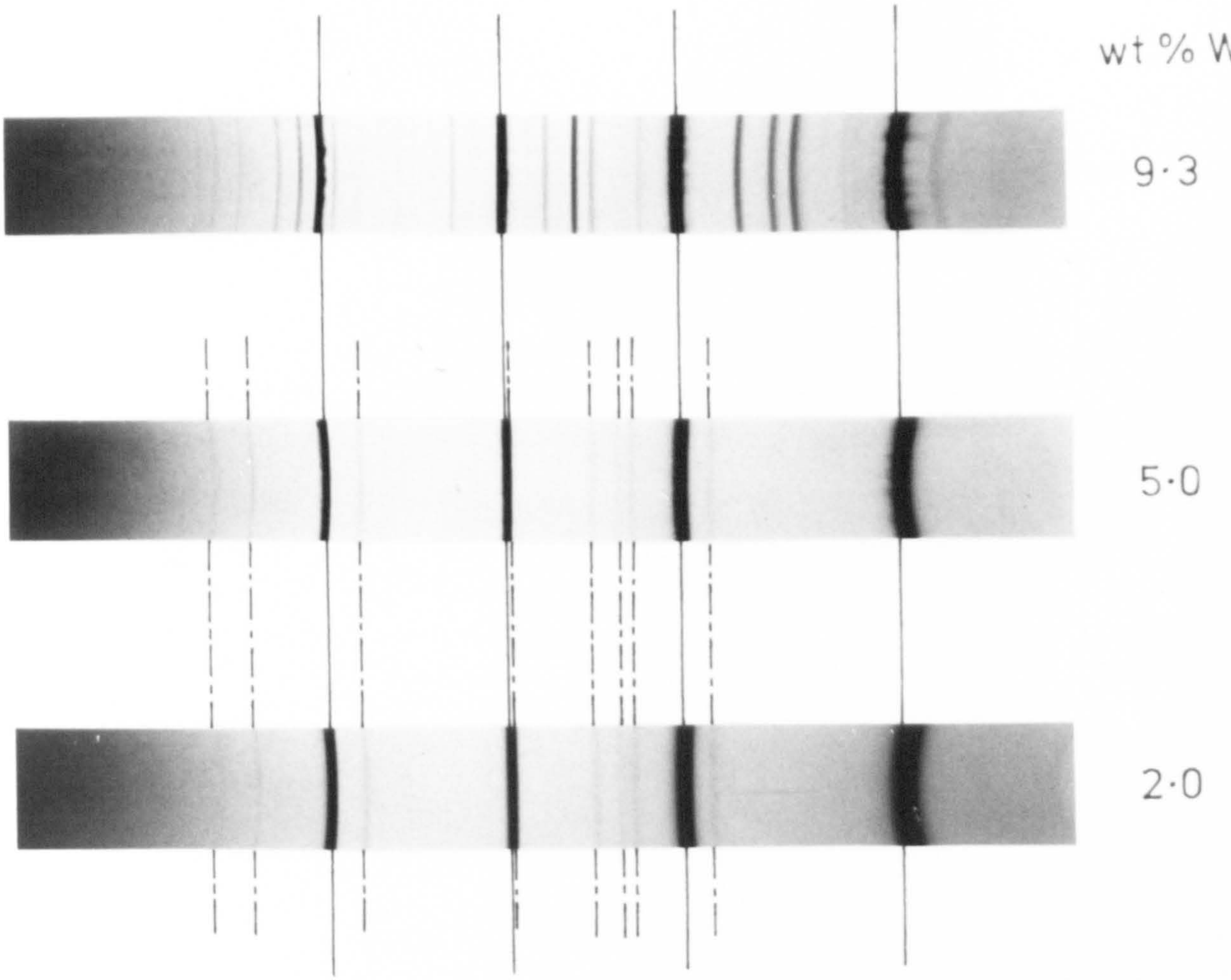

X-RAY PHOTOGRAPHS SHOWING PHASES PRECIPITATED IN Fe-W ALLOYS NITRIDED IN ~15 atm N_2 AT 950 °C AND SUBSEQENTLY AGED AT 610 °C FOR 3 DAYS.

Precipitation is more rapid than in constant activity aging and in the high alloys the tungsten activity quickly reaches the level at which δ becomes stable (runs 3 and 4). The only occasions when δ is not seen with η_1 in the 9.3 wt.%W alloy is when the alloy is nitrided in low nitrogen pressures and there is insufficient nitrogen to combine with all the available tungsten (runs 6 and 7).

The converse of the above situation is when the low tungsten alloys are nitrided at a pressure of ~40 atn. and contain nitrogen in excess of that required to precipitate all the tungsten. In the early stages of aging before any appreciable precipitation of tungsten occurs, most of the nitrogen is present in either austenite (above 590°C) or Fe_4N (below 590°C). If the nitrogen is in excess of that required for complete precipitation of tungsten plus saturation of ferrite, it stabilises either austenite or Fe_4N depending on the temperature (runs 5 and 8). Similarly if aging is interrupted before precipitation is complete (run 4) austenite is also present. Run 3 shows the presence of austenite in the 5.05 and 2.05 wt.%W alloys because the specimens were nitrided at a higher temperature (and therefore a slightly higher pressure) and so contain more nitrogen.

Because the alloys are two-phase ($\alpha + \gamma$) at the nitriding temperature the nitrogen is inhomogeneously distributed in the specimen. On subsequent aging most of the nitrides occur in regions which at high temperatures were austenite and on quenching are martensite or retained austenite (see Figure V.10).

Fig.V.10

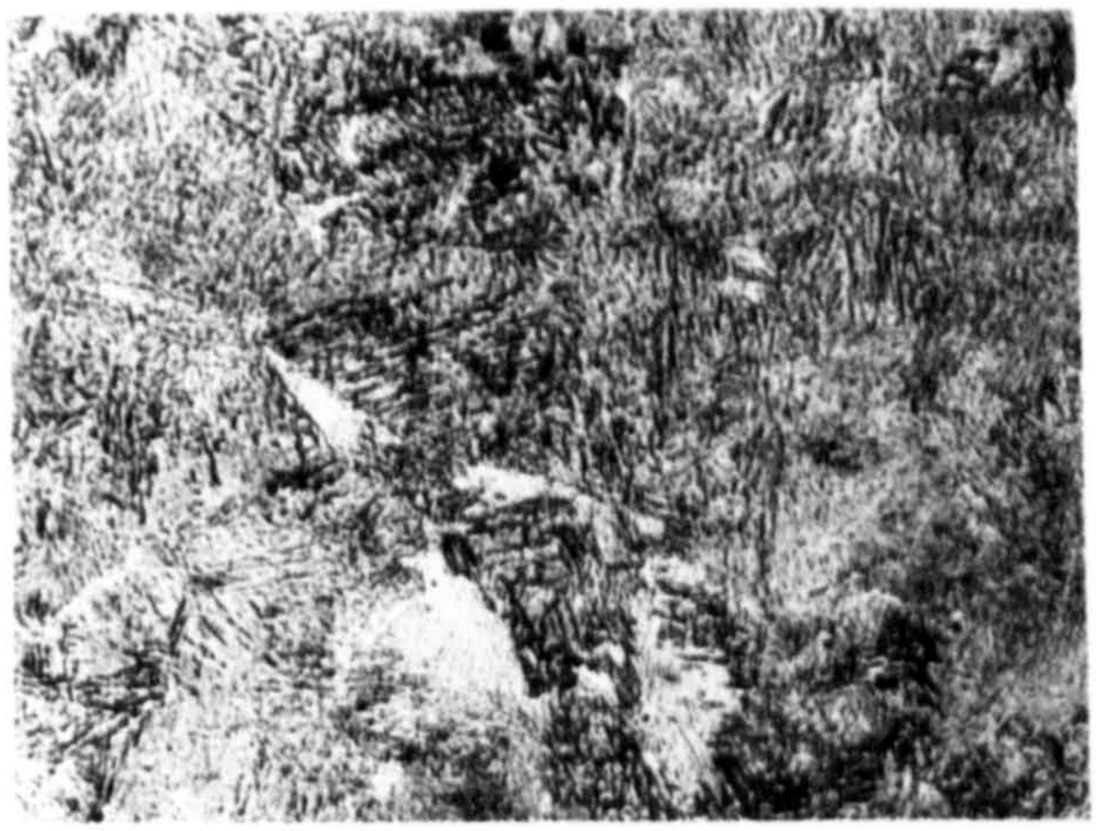

(a) Fe–5·05 wt.% W

4d. 600°C.

$\alpha + \delta + \eta$

X 190

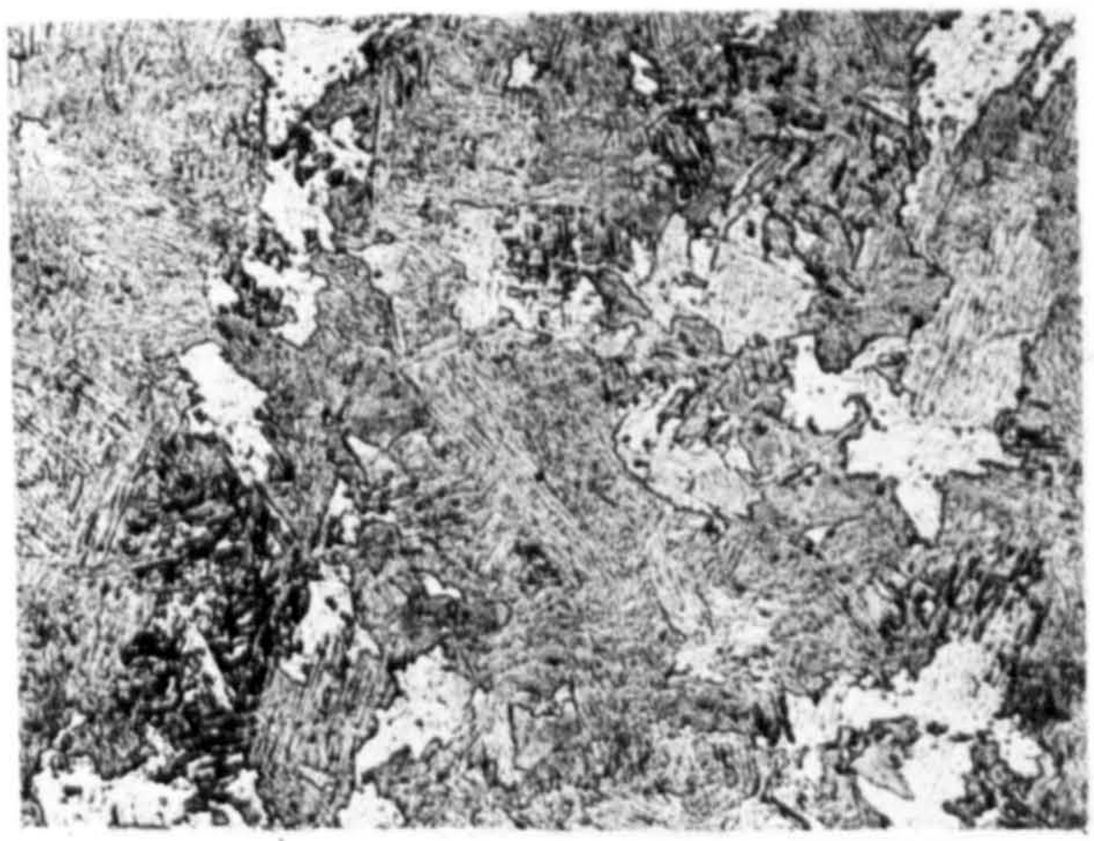

(b) Fe–2·05 wt.% W

4d. 600°C.

$\alpha + \delta$

X 190

(c) Fe–1·00 wt.% W

as nitrided

$\alpha + \gamma_A$ + auto-tempered α'

X 190

PHOTOMICROGRAPHS OF PRESSURE–NITRIDED AND QUENCH–AGED Fe–W ALLOYS [All specimens nitrided for 16h. in 40 atm. N_2 at 950°C.]

V.5 Discussion

No attempt has been made in this chapter to discuss all the experimental data in detail, but examples have been chosen to illustrate the effect of the different variables. It is clear that the nitride phase produced in Fe-W-N alloys depends upon the tungsten, nitrogen and oxygen activities in the alloy and the aging temperature. Of these the oxygen potential appears to have the most significant effect, but at a constant, low oxygen potential the activity of tungsten becomes more important.

The effect of substitutional solute activity on precipitation in other Fe-X-N systems has been previously demonstrated (Pipkin, 1967; Speirs, 1969; Roberts, 1970; Mortimer, 1971). In Fe-Mn-N alloys Pipkin, Grieveson and Jack were able to show how the precipitation sequence was in accordance with, and could be predicted from thermodynamic data applied to a pseudo-equilibrium model. Thus Figure V.11 shows a partial molar free energy V composition diagram for the manganese-nitrogen system on which are plotted the "curves" for the three manganese nitrides Mn_3N_2, Mn_5N_2 and Mn_4N. The nitrides are assumed to be stoichiometric and therefore the integral molar free energies of formation are at fixed compositions. The nitrogen potential greatly exceeds that required to precipitate all the nitrides and the relatively high diffusivity of nitrogen allows complete saturation of the specimen before appreciable precipitation occurs. Therefore the phase produced is controlled by the prevailing manganese activity. It is easily predicted

Fig. V.11

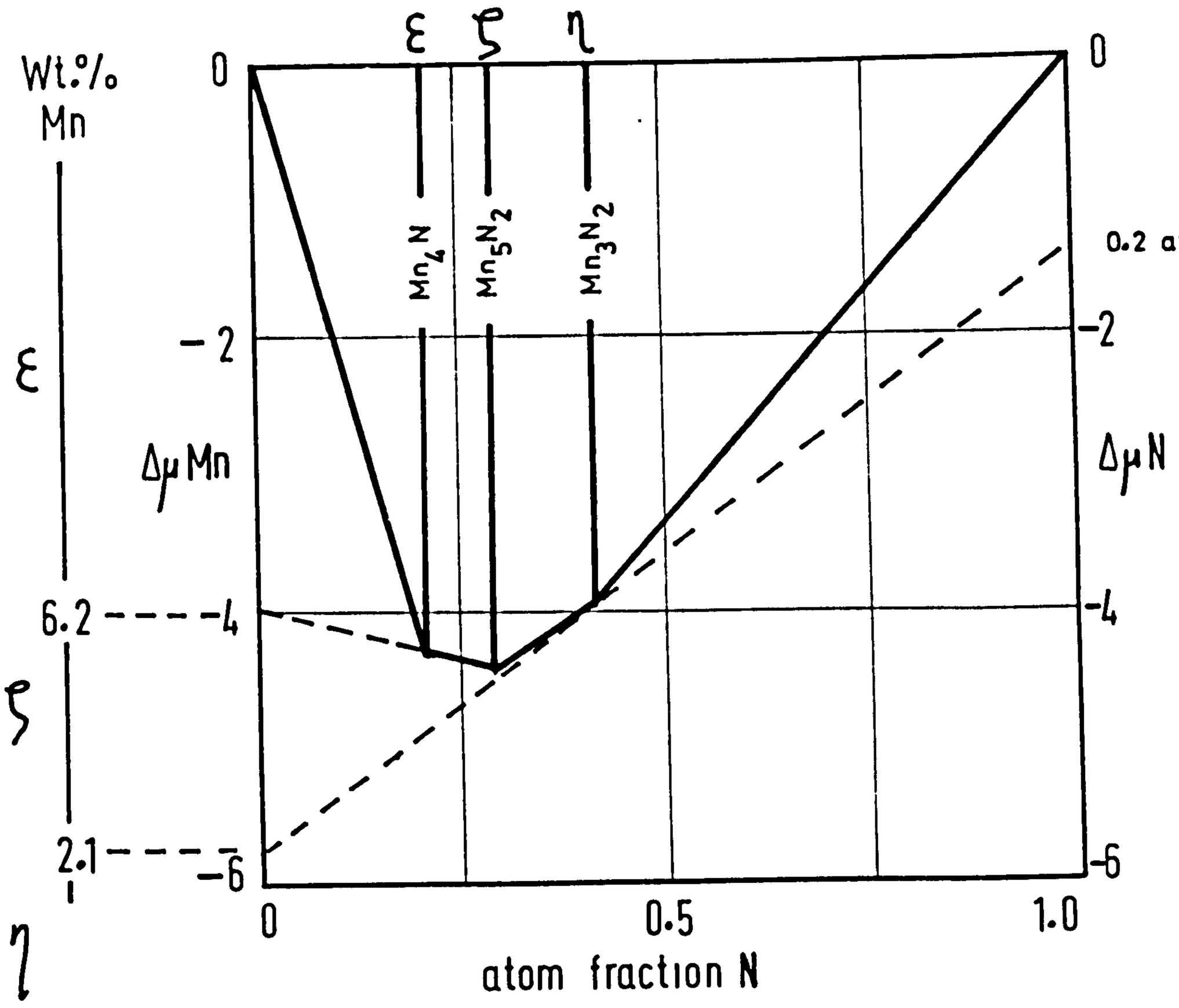

DIAGRAM TO ILLUSTRATE THE USE OF THERMODYNAMIC DATA TO PREDICT THE PRECIPITATION SEQUENCE OF NITRIDES IN Fe-Mn-N ALLOYS

(Figure V.11) that as the manganese activity decreases during precipitation, the critical levels at which Mn_5N_2 and Mn_3N_2 become stable are successively passed. The experimental data compiled by Pipkin are in good agreement with this model. Speirs was subsequently able to apply the argument qualitatively to his study of precipitation in Fe-Mo-N alloys.

In the Fe-W-N system the above theory is not generally applicable. It is approached in pressure-nitrided and quench-aged alloys where only "pure" nitrides are formed, but since one of them is an iron-tungsten-nitride (η_1) it should not strictly be included on the same diagram. However, if Mn_3N_2 and Mn_4N are replaced by WN and Fe_3W_3N respectively then the predicted precipitation sequence with decreasing tungsten activity will be $\eta_1 \rightarrow \delta$ which is actually observed. No thermodynamic data are available for tungsten nitrides and therefore the model can not be rigidly applied.

The presence of the highest nitride (δ-WN) in the low tungsten alloys and the lowest nitride (η_1-Fe_3W_3N) in the high tungsten alloys is shown in the metastable equilibrium diagrams of Figure V.12. The critical tungsten content at which η_1 is formed increases from < 5.0 wt.% to > 5.0 wt.% as the nitriding pressure is lowered from ~ 40 atm. to ~ 15 atm. of N_2 (Figure V.12 c. and d.). The formation of η_1 is given by the equation:

Fig. V.12

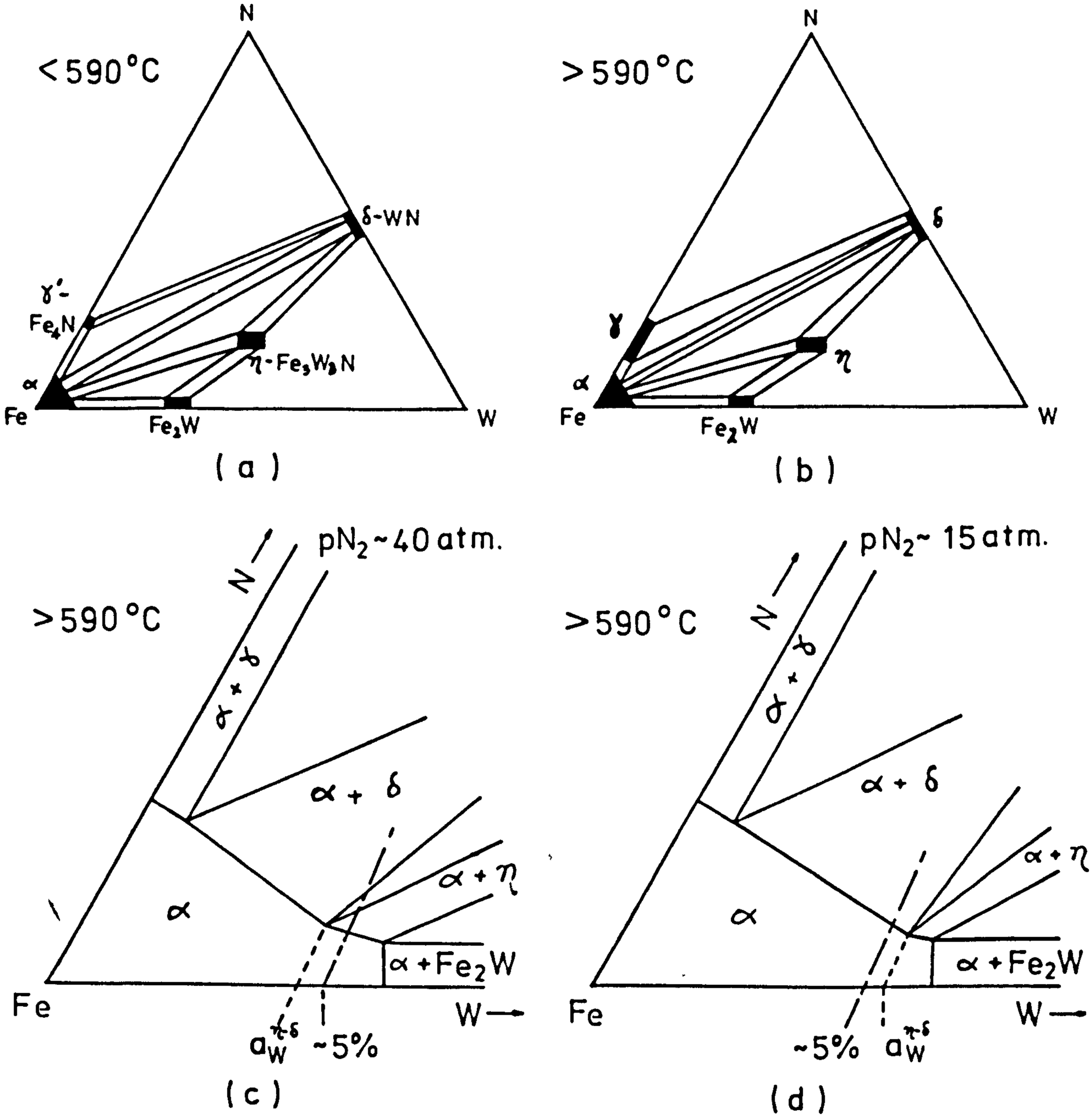

PROPOSED TERNARY DIAGRAMS FOR PRESSURE-NITRIDED AND QUENCH-AGED Fe-W-N ALLOYS (SCHEMATIC).

$$3Fe + 3\underline{W} + \underline{N} = Fe_3W_3N \quad \ldots\ldots (V).1$$

$$K = \frac{a_{Fe_3W_3N}}{a_{Fe}^3 \cdot a_{\underline{W}}^3 \cdot a_{\underline{N}}} \quad \ldots\ldots (V).2$$

assuming pure Fe and Fe_3W_3N

$$K = \frac{1}{a_{\underline{W}}^3 \cdot a_{\underline{N}}} \quad \ldots\ldots (V).3$$

$$\text{i.e. } a_{\underline{W}}^3 = \frac{1}{K.a_{\underline{N}}} \quad \ldots\ldots (V).4$$

Therefore if the initial activity of nitrogen on aging is decreased, (by lowering the nitrogen pressure during nitriding) then the critical tungsten activity at which η_1 forms will be increased.

The pseudo-ternary diagrams for high and low ammonia contents in constant activity aged alloys are shown in Figure V.13. The predominant phases produced in ammonia-hydrogen nitriding are the oxy-nitrides δ' and γ'. Again it is the higher (oxy-)nitride, δ -$W_{0.75}(N,O)$, which is found in the low tungsten alloys and the critical tungsten activity at which δ begins to form is increased at higher temperatures and lower nitrogen potentials (Figure V.13). Considering a series of Fe-W alloys nitrided at 615°C in 8%NH_3:H_2 according to Figure V.13b,

Fig. V.13

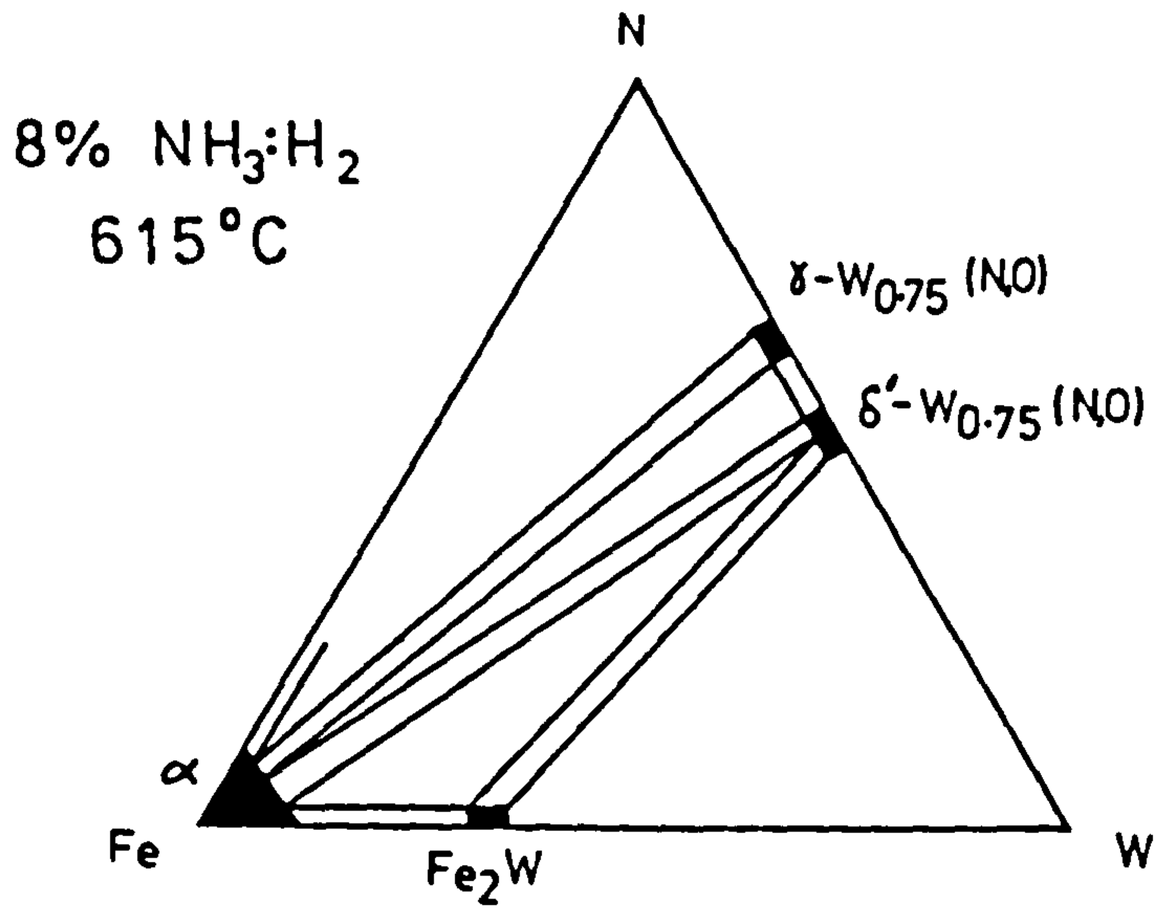

(a)

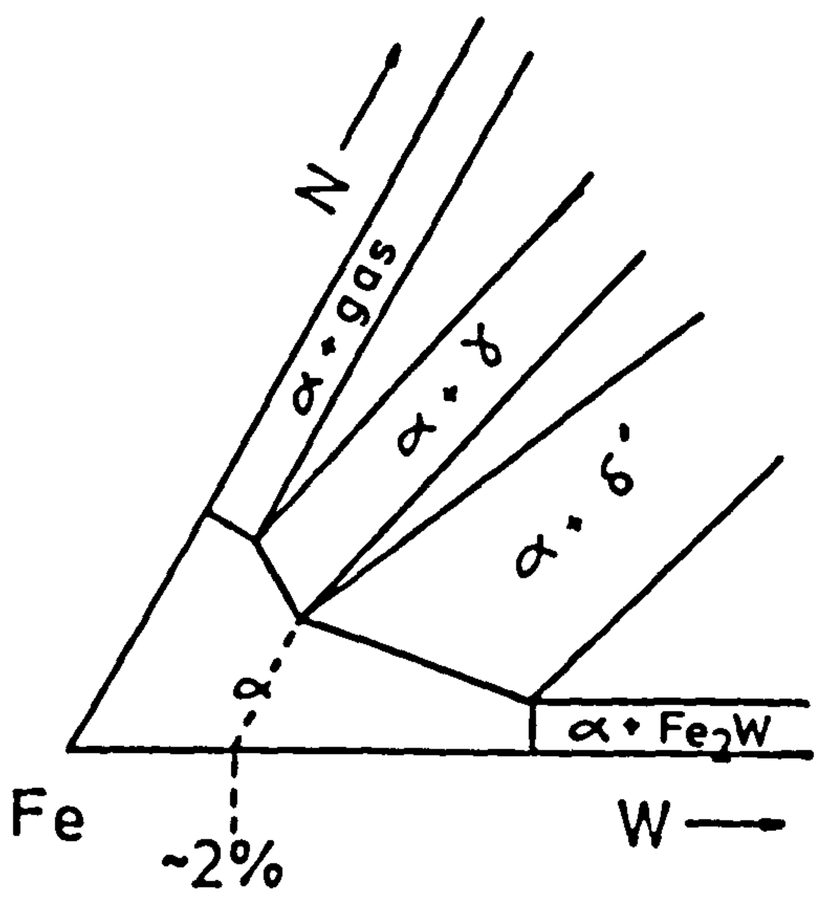

(b)

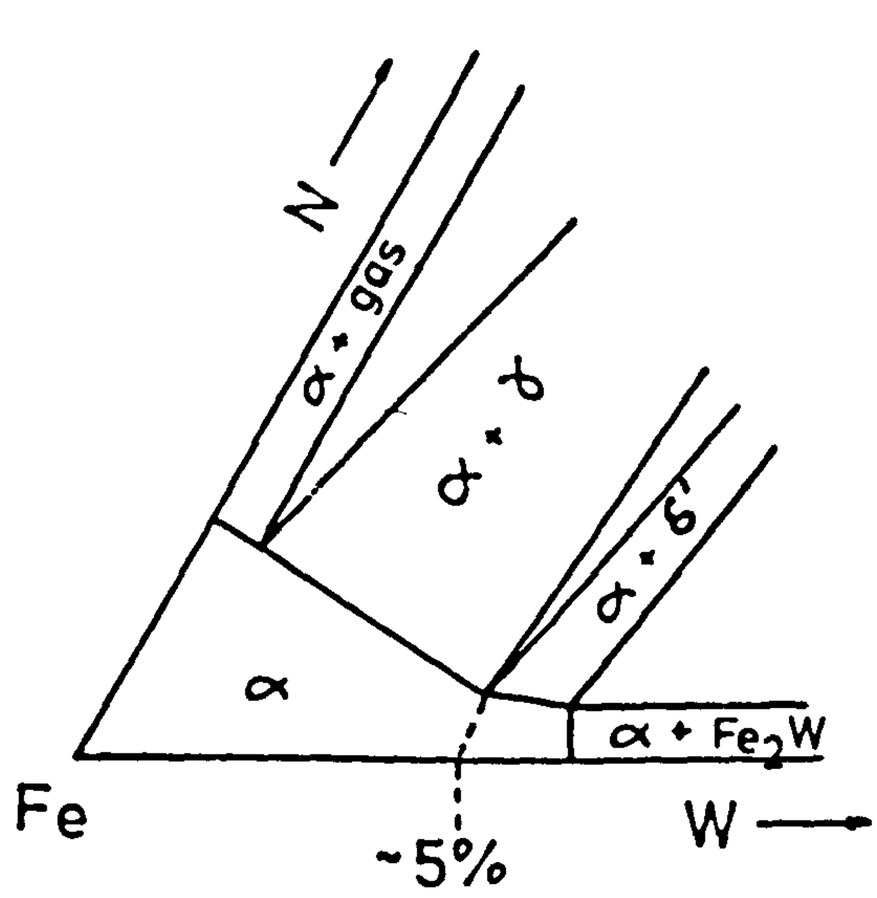

(c)

PROPOSED TERNARY DIAGRAMS FOR CONSTANT ACTIVITY AGED Fe–W–N ALLOYS (SCHEMATIC).

ferrites of composition greater than Fe-2 wt.%W after saturation with nitrogen will be at the appropriate point on the α-solvus to precipitate δ'. During precipitation the ferrite composition moves along the solvus until it reaches ~2 wt.%W at which point δ forms. Conversely, alloys of composition less than Fe-2 wt.%W precipitate only δ.

One surprising feature of constant activity aged alloys is the appearance of several phases apparently formed at the same tungsten activity in specimens containing Fe_2W. In particular δ was detected with δ' when some Fe_2W remained and therefore where the tungstent content in the ferrite should not have been low enough for δ to be the stable phase. One possible explanation is that the nitrides detected are in different regions of the specimen and different stages of nitriding are being observed, allowing unconverted Fe_2W to be in the same specimen as δ' and δ without the phases co-existing locally. However, run 10 (Table V.2) shows that δ can nucleate together with δ' in a 5.05 wt.%W alloy (which does not contain Fe_2W) and is subsequently replaced by δ' as aging continues. A probable explanation for this is that on aging, nitrogen diffuses into the ferrite and a concentration profile moves through the specimen until eventually the ferrite is in equilibrium with the gas. Therefore at all points within the specimen the activity of combined nitrogen gradually increases from zero to that of the gas. In cold-worked specimens nucleation is rapid and some precipitation occurs before the specimen reaches a constant nitrogen activity. It is

suggested that when precipitation from any small volume element within the specimen begins, the tungsten ferrite "sees" a low nitrogen activity and hence the system initially behaves as if it was at a low nitrogen potential. This results in δ being precipitated from a high tungsten ferrite (Figure V.13c), and it is only when the specimen is saturated with nitrogen that the system behaves as predicted by its true nitrogen potential (Figure V.13b) i.e. δ' grows and δ disappears.

V.6 Conclusions

1. A hexagonal oxy-nitride δ'-$W_{0.9}(N,O)$ is characterised and shown to be stable if sufficiently high oxygen and nitrogen potentials are maintained.

2. As many as six different tungsten or iron-tungsten nitrides and oxy-nitrides are precipitated in Fe-W-N alloys under various conditions of temperature, oxygen potential and solute activities. These are δ-$W_{0.75}(N,O)$, δ'-$W_{0.9}(N,O)$, δ''-oxy-nitride, δ-WN, η_1-$Fe_3W_3N(O)$ and η_3 (probably $Fe_6W_6N(O)$).

3. In addition, the iron-nitrogen phases γ_A-Fe, γ'-Fe_4N, α'-martensite and α''-$Fe_{16}N_2$ are precipitated under certain well-established conditions of temperature, nitrogen potential and heat-treatment.

4. The general observations can be satisfactorily interpreted in terms of schematic ternary phase diagrams.

Chapter VI

PRECIPITATION IN Fe-W-N ALLOYS: THE PRECIPITATION SEQUENCE

VI.1 Introduction

It is now well established that under certain conditions, homogeneous precipitation can be obtained in many ternary Fe-X-N systems. Constant activity aging not only provides a high nitrogen potential and therefore a high supersaturation, but also a continuous source of nitrogen. As precipitation proceeds neither the driving force with respect to nitrogen nor the supply of nitrogen decreases, and the extent of precipitation is controlled only be the substitutional solute content of the alloy. Homogeneous precipitation in Fe-W-N alloys can also occur under carefully controlled conditions which include nitrogen potential, tungsten activity, temperature and the physical state of the alloy.

Figure VI.1 shows the nitriding rates for various Fe-W alloys in 8%NH_3:H_2 at 615°C. The nitrogen potential is slightly lower than that required to stabilise nitrogen-austenite at this temperature and would produce a nitrogen-ferrite containing about 0.08 wt.%N in pure iron. Any increase in weight above about 0.08% is therefore attributable to precipitation of nitrogen. The high tungsten ferrites rapidly increase in weight due to the initial formation of substitutional-interstitial

Fig. VI.1

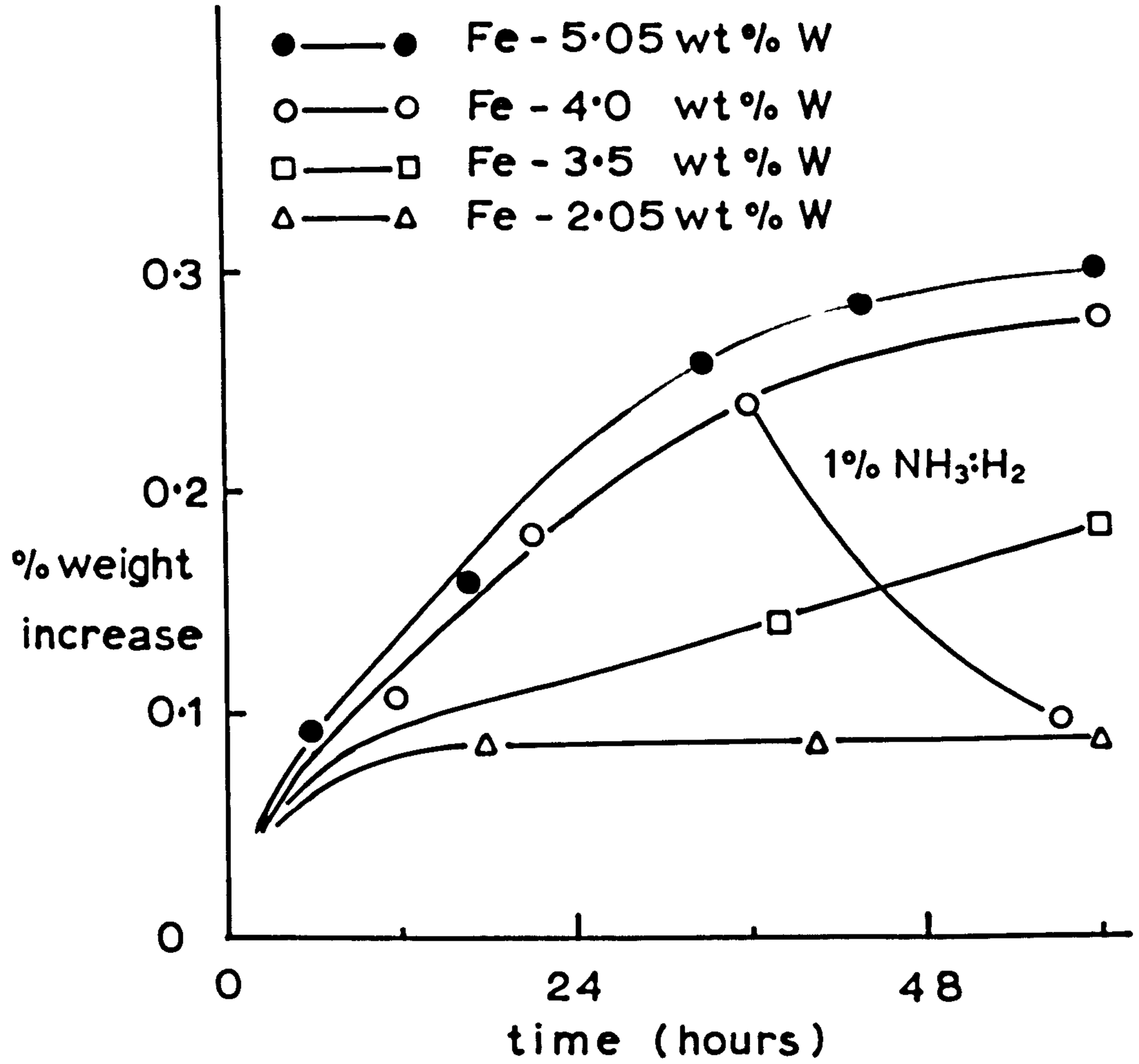

Nitriding rates of Fe - W alloys in 8% $NH_3:H_2$ at 615 °C

Guinier-Preston zones. Conversely precipitation in nitrided Fe-2.0 wt.%W is very restricted and within experimental error there is no detectable increase in weight other than that expected from nitrogen in solution. At intermediate tungsten compositions moderate reaction rates are observed.

VI.2 Homogeneous precipitation

The structures obtained in Fe-4.0 and Fe-5.0 wt.%W alloys after nitriding for short times under conditions described in Figure VI.1 are shown in Figure VI.2, together with typical diffraction patterns (Figure VI.3).

In Fe-5.05 wt.% tungsten the disc shaped clusters lying on $\{100\}$ matrix planes are about 200-300 Å diameter and 5-10 Å thick. Bright-field micrographs (Figure VI.2) exhibit characteristic matrix strain-field contrast (Ashby and Brown, 1963) and structure factor contrast (Hirsch, Howie, Whelan, Nicholson and Pashley, 1965). Electron diffraction patterns (Figure VI.3) show only small amounts of streaking in $[100]_\alpha$ matrix directions, which is surprising in view of results obtained from other systems, e.g. Fe-Mo-N (Speirs et.al., 1971; Driver et.al., 1972), Fe-Nb-N (Roberts, 1970) and Fe-V-N (Pope, 1972; see also Appendix II). The extent of visible streaking indicates a disc thickness of about 15 Å, a figure which seems high by comparison with the bright-field images. There are three possible reasons

Fig. VI.2

(a) Fe – 5·05 wt.% W
nitrided 6 h. at 615 °C.
in 8% NH_3:H_2

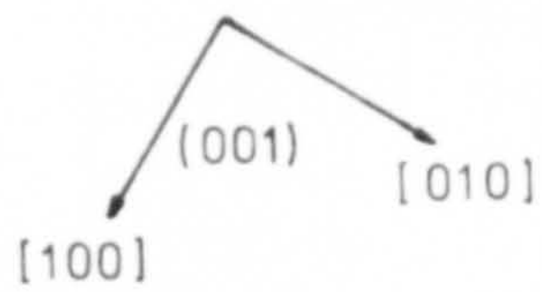

0·1 μ

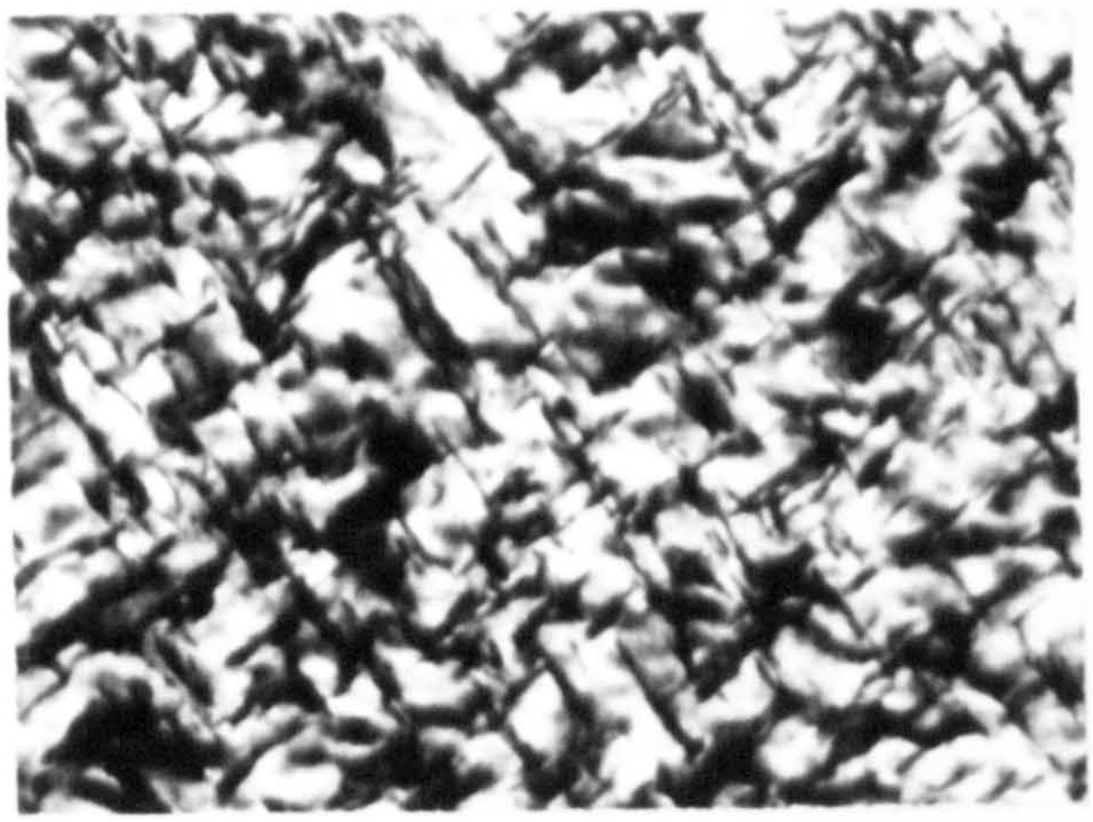

(b) Fe-5·05 wt.% W
as (a)

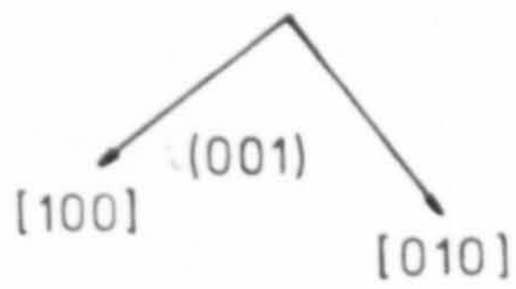

0·1 μ

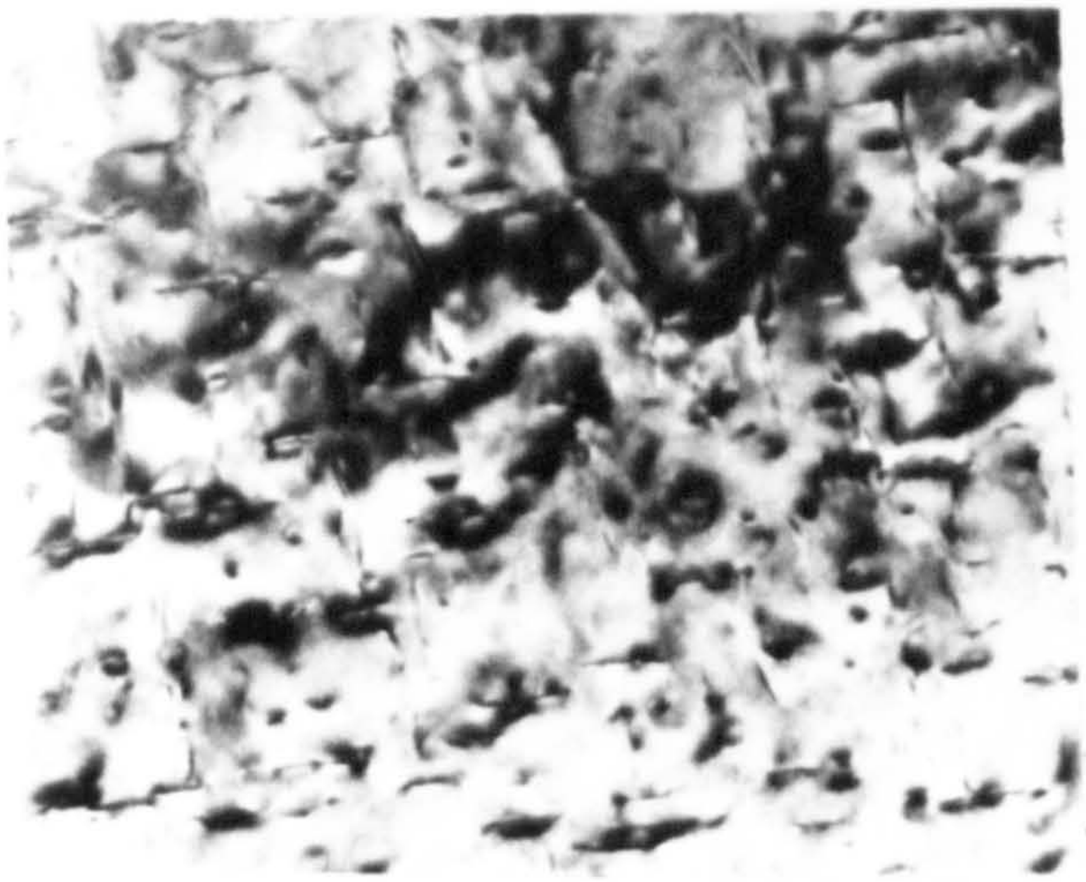

(c) Fe-4·0 wt.% W
nitrided 12 h. at 615 °C.
in 8 % NH_3:H_2

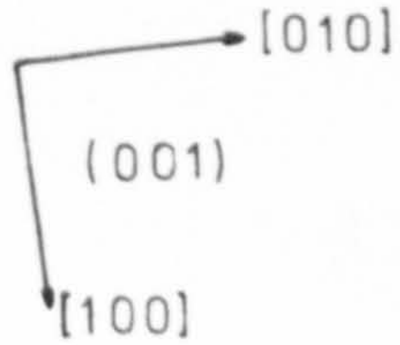

0·1 μ

ELECTRON MICROGRAPHS SHOWING THE EARLY STAGES OF PRECIPITATION IN CONSTANT ACTIVITY AGED Fe-W ALLOYS.

Fig. VI.3

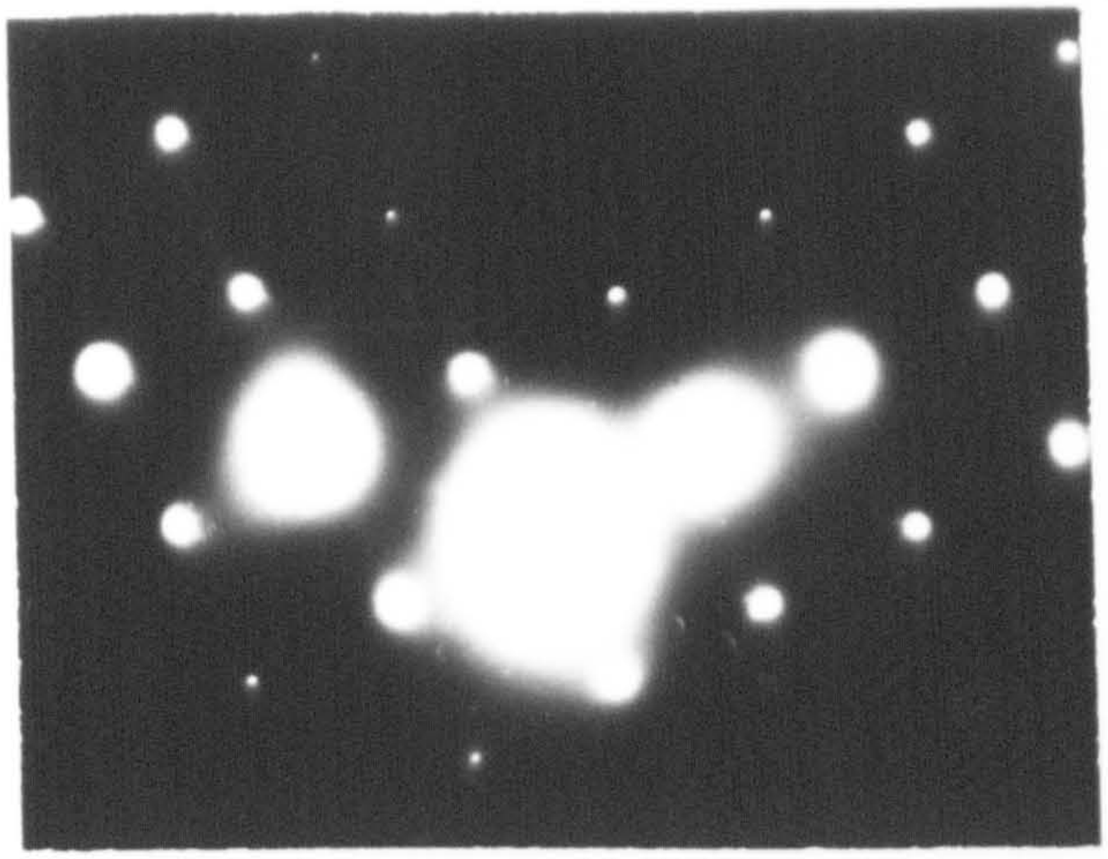

(a)

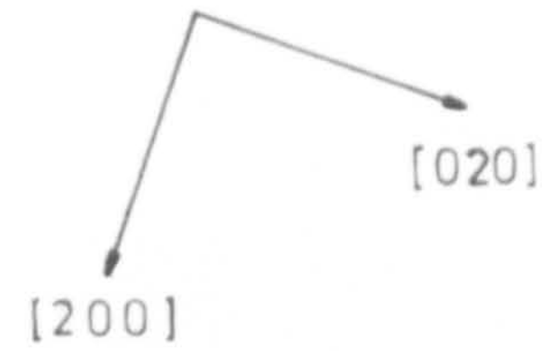

[001] zone

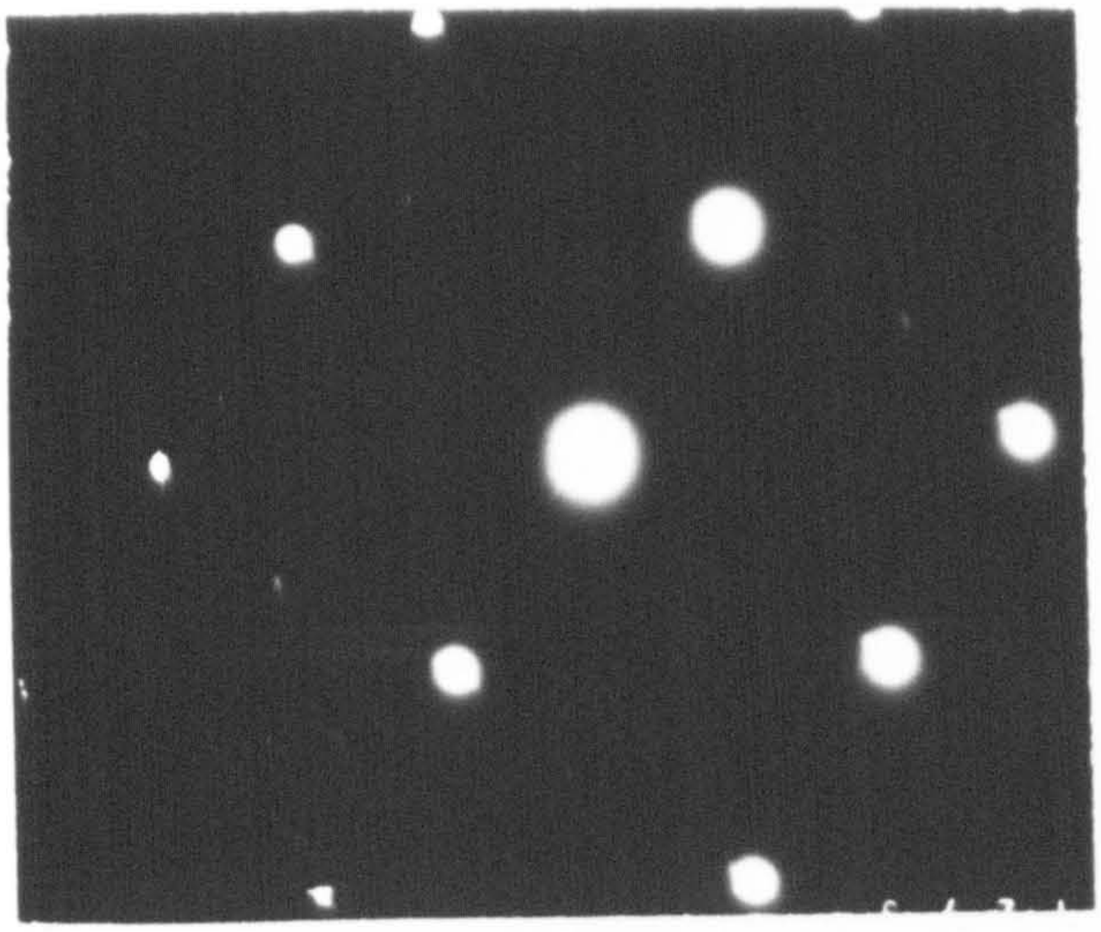

(b)

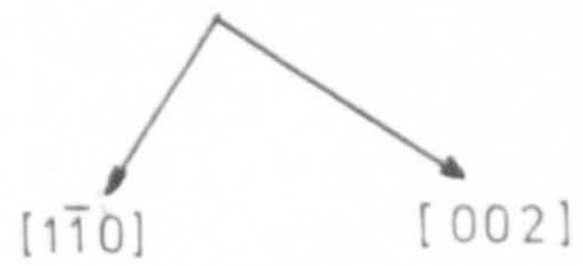

[110] zone

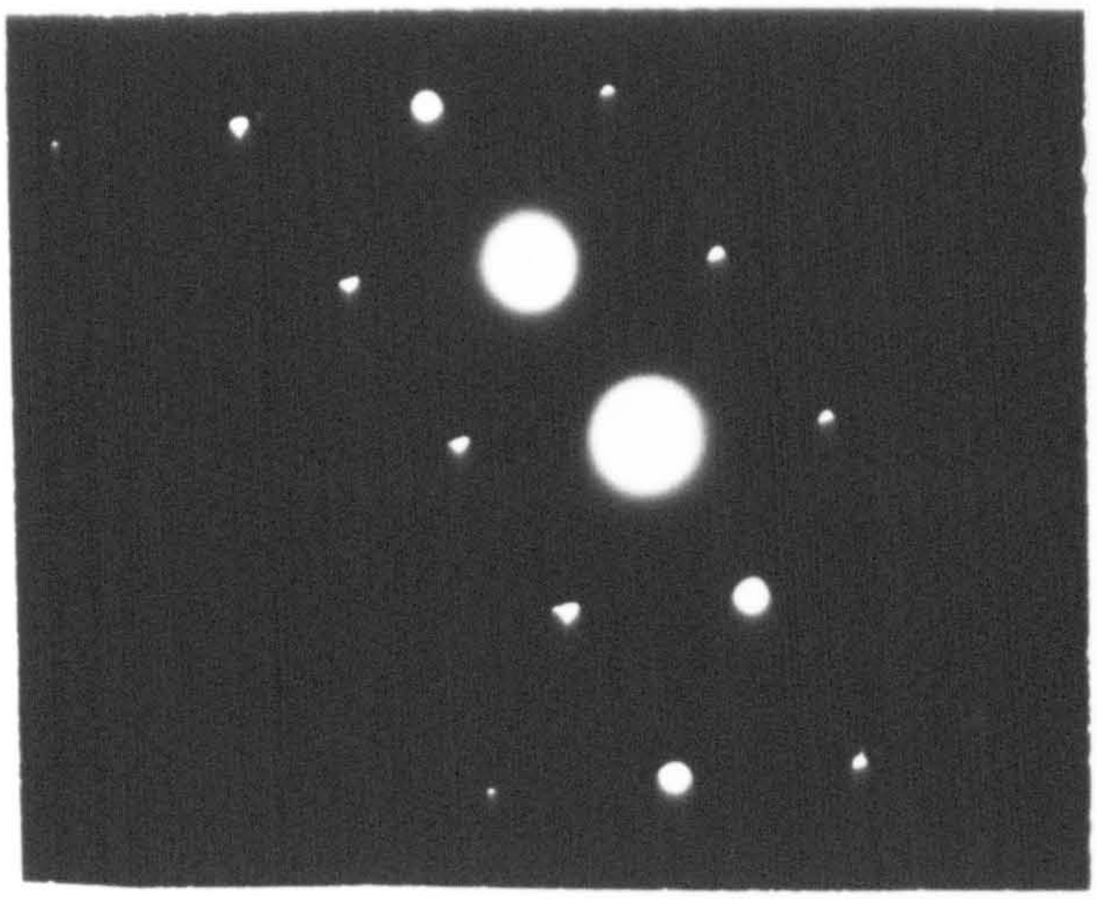

(c)

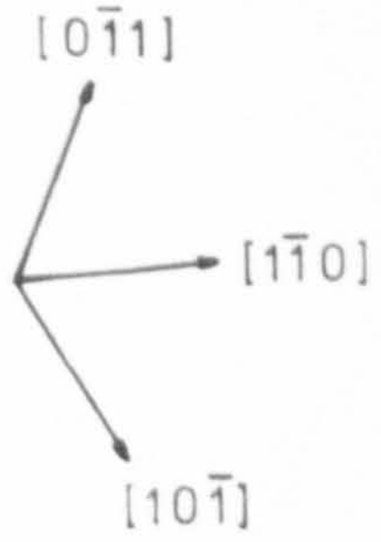

[111] zone

ELECTRON DIFFRACTION PATTERNS OBTAINED FROM Fe-5·05 wt.% W NITRIDED FOR 6 h. AT 615°C IN 8 % NH_3:H_2.

for the surprisingly small amount of streaking:

(i) Unlike other Fe-X-N systems a study of the first stage of precipitation in Fe-W-N alloys is restricted to small volume fractions of clusters and diffraction effects will be less noticeable.

(ii) It is thought that the zones contain an appreciable quantity of iron, in which case the effective atomic scattering factor of the zone metal-atom is reduced.

(iii) Electron diffraction streaking can be due to either matrix strain associated with disc-shaped coherent clusters, or purely shape effects from semi-coherent or partially coherent disc-shaped precipitates (Hirsch et.al. 1965). The former mechanism applies in the early stages of precipitation in Fe-W-N alloys and the extent of streaking is governed by the degree of strain. This is supported by observations in Fe-V-N alloys where the streaking is continuous even in alloys containing only 0.4 wt.%V (Pope, 1972), but is due to a much higher degree of matrix strain than is present in Fe-W-N alloys.

The atomic arrangement of a substitutional-interstitial solute atom cluster is shown schematically in Figure VI.4. When no nitrogen is present, the sixfold co-ordinated octahedral interstice in bcc iron has tetragonal symmetry, the B-B interatomic distance being $\sqrt{2}\,\underline{a}$ (Figure VI.4), whilst the A-A distance is only $\underline{a}$. When the site is occupied the filled octahedron becomes regular with equal B-B and A-A distances, the strain being essentially in only one direction. A cluster can be regarded as a "disc" of

Fig. VI.4

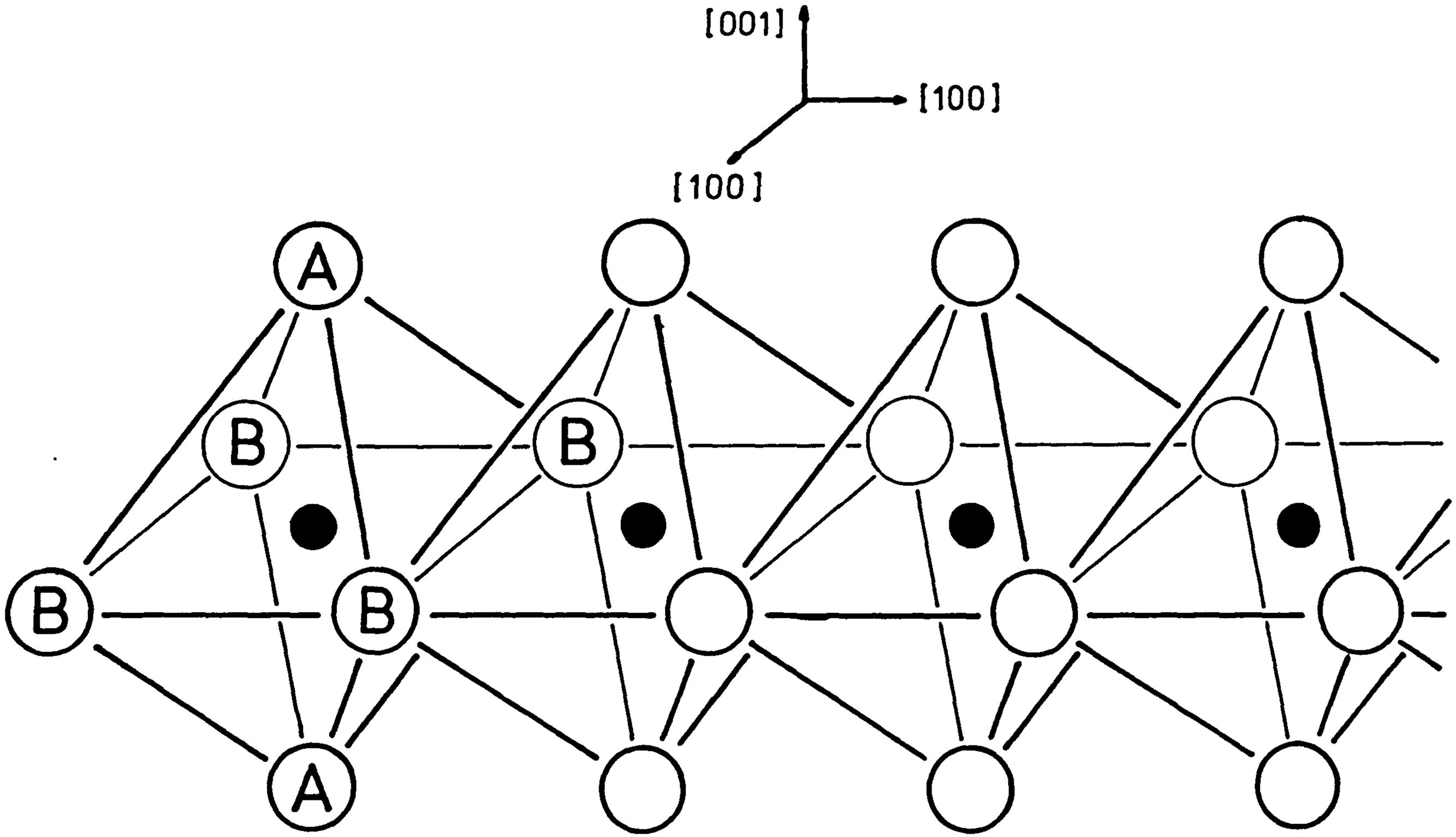

○ Random occupation of A or B metal atom sites by W and Fe

● Nitrogen in octahedral sites of only one type

SCHEMATIC MODEL OF ATOMIC ARRANGEMENT IN A SUBSTITUTIONAL – INTERSTITIAL GUINIER–PRESTON ZONE.

filled octahedra with some iron atoms replaced by those of tungsten. This arrangement is stabilised at about 600°C by the low mobility of tungsten and the high affinity of tungsten for nitrogen. Neither the composition of the zone nor the preferred tungsten sites (if any) are known.

An indication of the overall matrix strain due to substitutional-interstitial GP zones is given by matrix lattice parameter measurements. This is clearly demonstrated in Fe-V-N alloys (Pope, Krawitz and Jack, 1972) where nitrogen contents several times greater than the maximum solubility in pure ferrite produce proportional increases in the α-iron lattice parameter. Conversely in nitrided Fe-W alloys both the increase in lattice parameter and the total amount of nitrogen present in clusters are small.

A study of the early stages of precipitation in Fe-W-N alloys is difficult because the tungsten content at which GP zones are stable is relatively high. In addition there is no detectable pseudo-equilibrium between GP zones and enriched solid solution; that is, there is no stage during nitriding when precipitation is interrupted and GP zones are left (temporarily) in metastable equilibrium with a high tungsten ferrite. This would be shown by a discontinuity in the weight increase v time curves of Figure VI.1. Instead, after short nitriding times, the pre-precipitates transform to an ordered Fe-W-N intermediate phase, the onset of which is just apparent in Figure VI.3c.

VI.3 The structure and morphology of the intermediate phase

Continued nitriding of alloys with tungsten contents greater than about 3.5 wt.% produces a homogeneous distribution of intermediate precipitate (Figure VI.5). The intermediate precipitate in Fe-W-N alloys has been described as a two-dimensional superlattice of α-iron similar in structure to α''-$Fe_{16}N_2$ (Stephenson, Grieveson and Jack, 1972). The metal-atom arrangement is very similar to that of α''-$Fe_{16}N_2$ (see Figure I.4) and is formed in a similar manner, but chemically the two phases are different.

Figure VI.6 shows an electron diffraction pattern obtained from extracted intermediate phase indexed on the basis of a tetragonal unit cell with a dimension 5.74 Å, but whose c dimension is not determinable. The habit plane of the precipitate plates is $\{001\}$ and centred dark-field techniques show that only plates lying perpendicular to the electron beam contribute to the diffraction pattern, which is essentially that due to the $[001]$ zone of a single precipitate crystal. The precipitate is too thin to give $\{001\}$ and $\{h01\}$ reflections and even when tilted, gives no reflections other than $\{hk0\}$. Thus there are insufficient $\{001\}$ precipitate planes for diffracted electron waves to be reinforced and the atomic arrangement can be considered as essentially "two-dimensional". Certainly in $[100]$ directions the crystallinity extends over large distances since metal-atom ordering produces reflections which correspond to a superlattice of ferrite, the superlattice a

Fig. VI.5

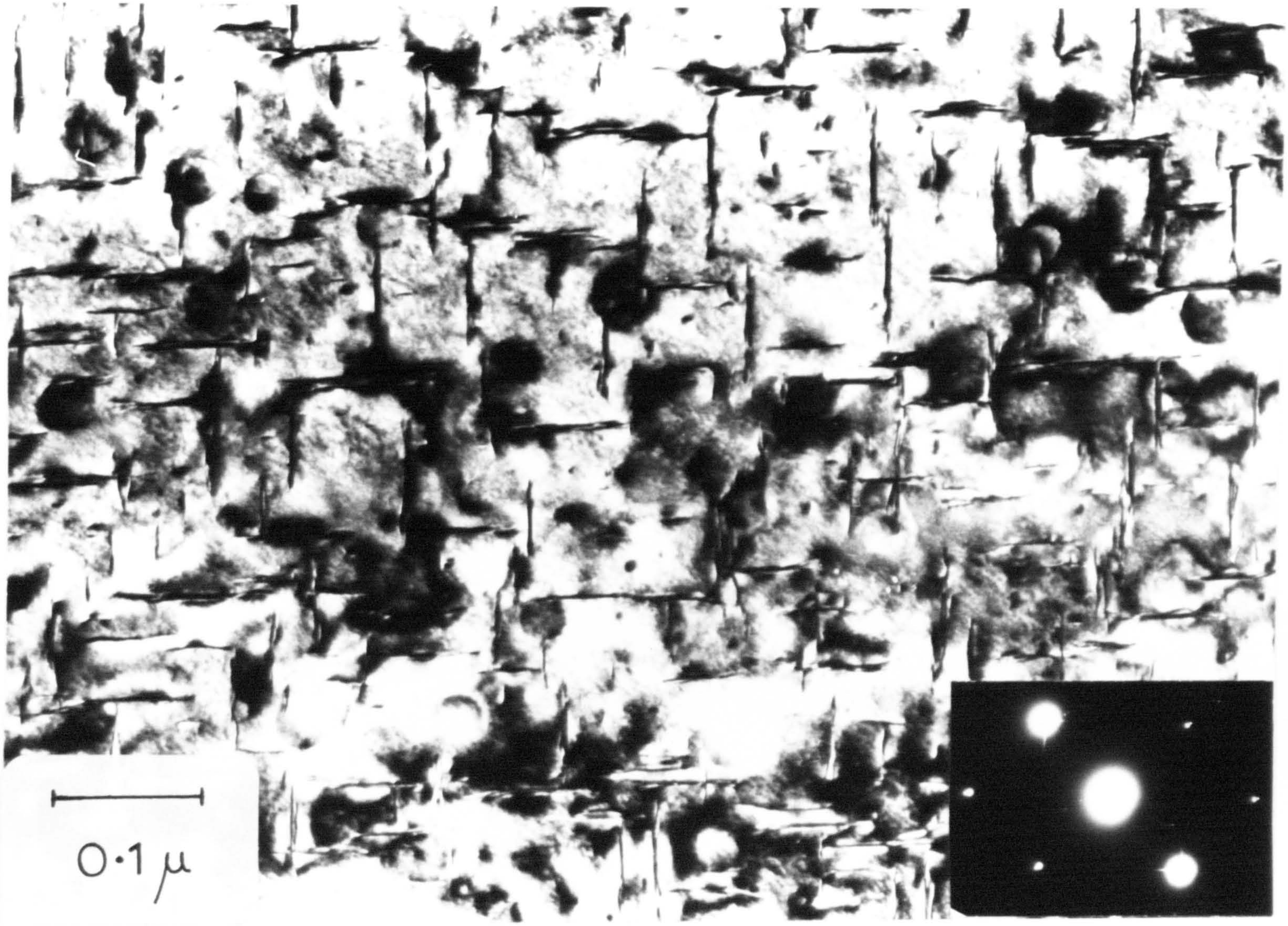

Fe-4·0 wt% W nitrided in 8% NH_3:H_2 at 615°C for 24 hrs

Fig. VI.6

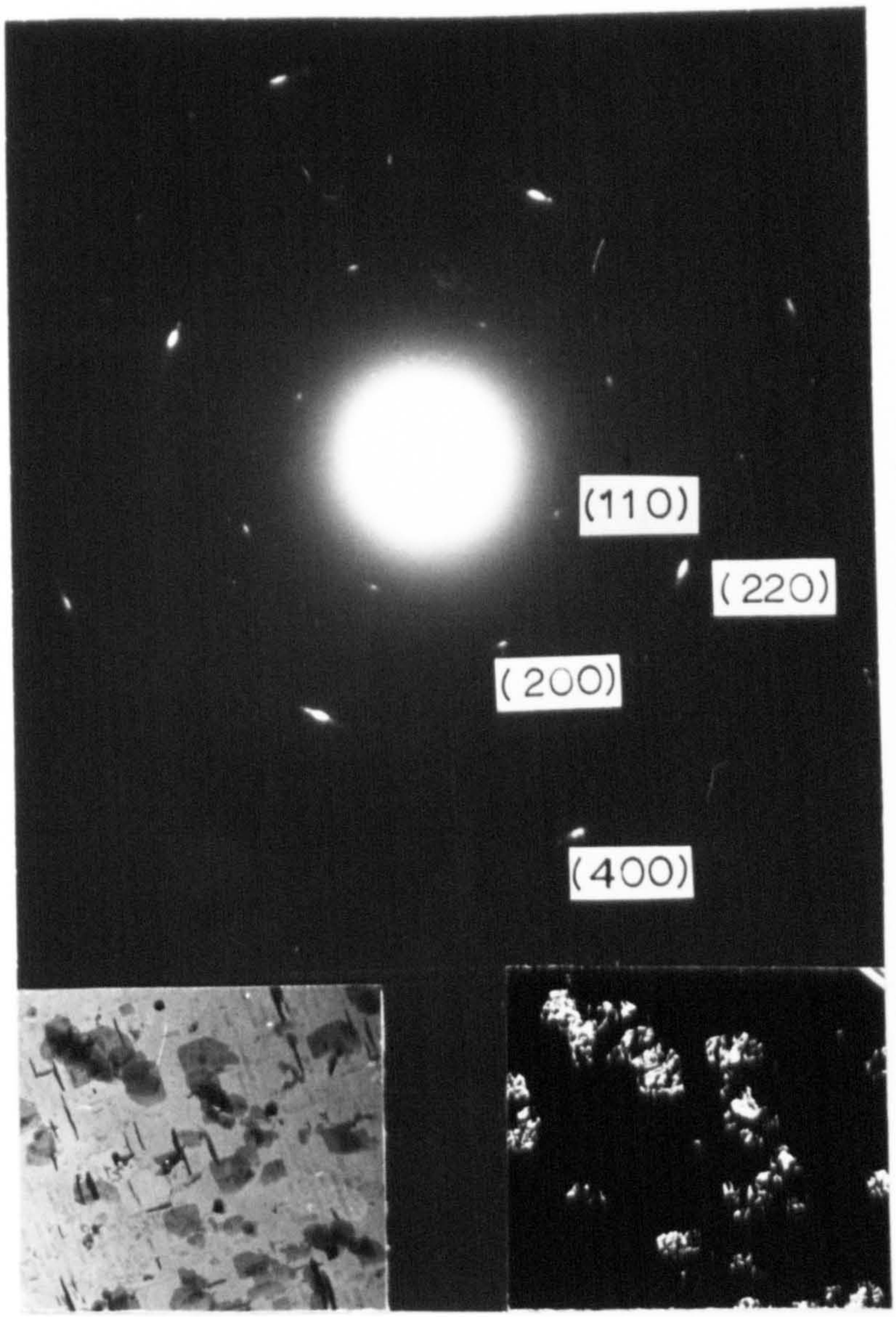

ELECTRON DIFFRACTION PATTERN OBTAINED FROM VERY THIN PLATELETS OF Fe-W-N INTERMEDIATE PHASE [indexed on the basis of a body centered tetragonal "$Fe_{16}N_2$ type" of unit cell].

dimension being twice that of ferrite.

"In situ" diffraction patterns of intermediate phase e.g. Figure VI.7, show streaking and characteristic superlattice spots. The streaks appear to be continuous in reciprocal space but they are very narrow due to the large precipitate diameter ($\geq 0.1\mu$) and are only seen to be continuous when an exact foil orientation is obtained.

The position of the streaks in reciprocal space is shown superimposed on the reciprocal lattice diagram of ferrite of Figure VI.8. The reciprocal lattice points corresponding to the precipitate $\{hk0\}$ planes are merely those points given by the appropriate reciprocal lattice vector for ferrite, but having only half of the magnitude. That is, the precipitate is considered as having a body-centred tetragonal unit cell of unknown c dimension, precipitated in ferrite according to the orientation relationship:

$$(001)\ \text{precipitate} \parallel (001)_\alpha \ ;\ [001]\ \text{precipitate} \parallel [001]_\alpha$$

i.e. the same as that of α''-$Fe_{16}N_2$.

The positions at which the network of streaks intersect in reciprocal space can be determined by considering several orientations of thin foils containing the three mutually perpendicular precipitate types. Thus the spot arrowed in the $[001]_\alpha$ pattern of Figure VI.7 is a $\{110\}$ superlattice type but is not present on the $[110]_\alpha$ pattern in the same figure. Inspection of Figure VI.8 shows that the reflection

Fig. VI. 7

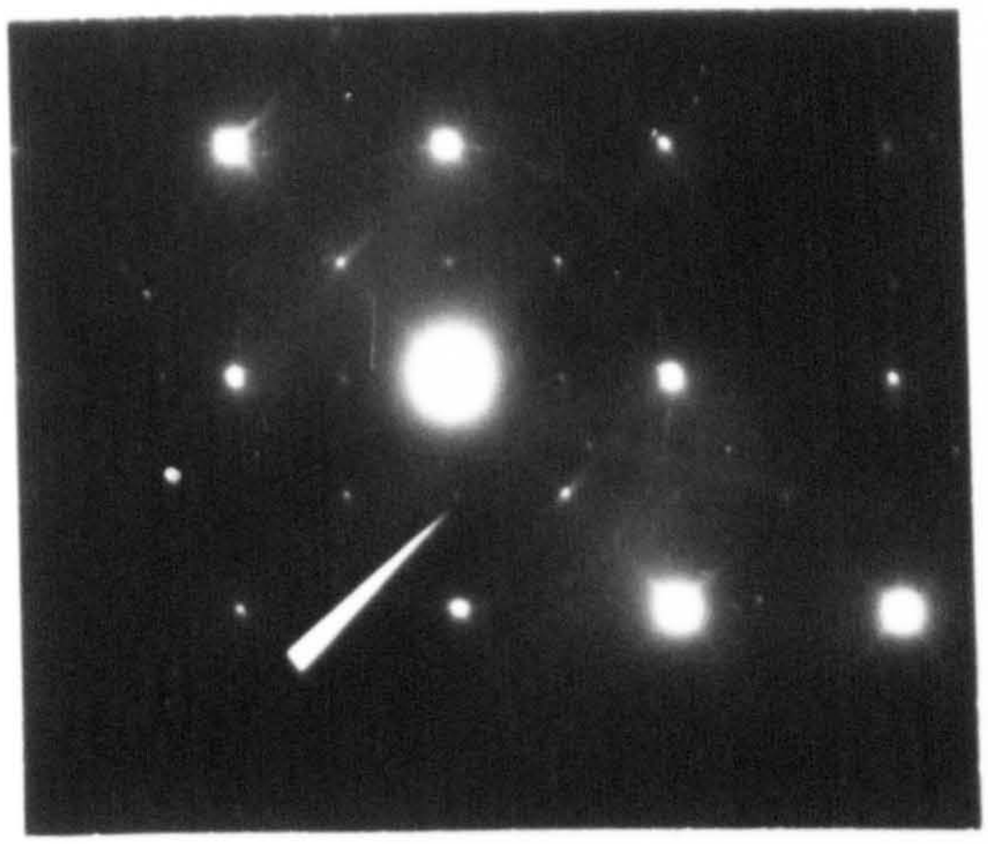

[001]

[111]

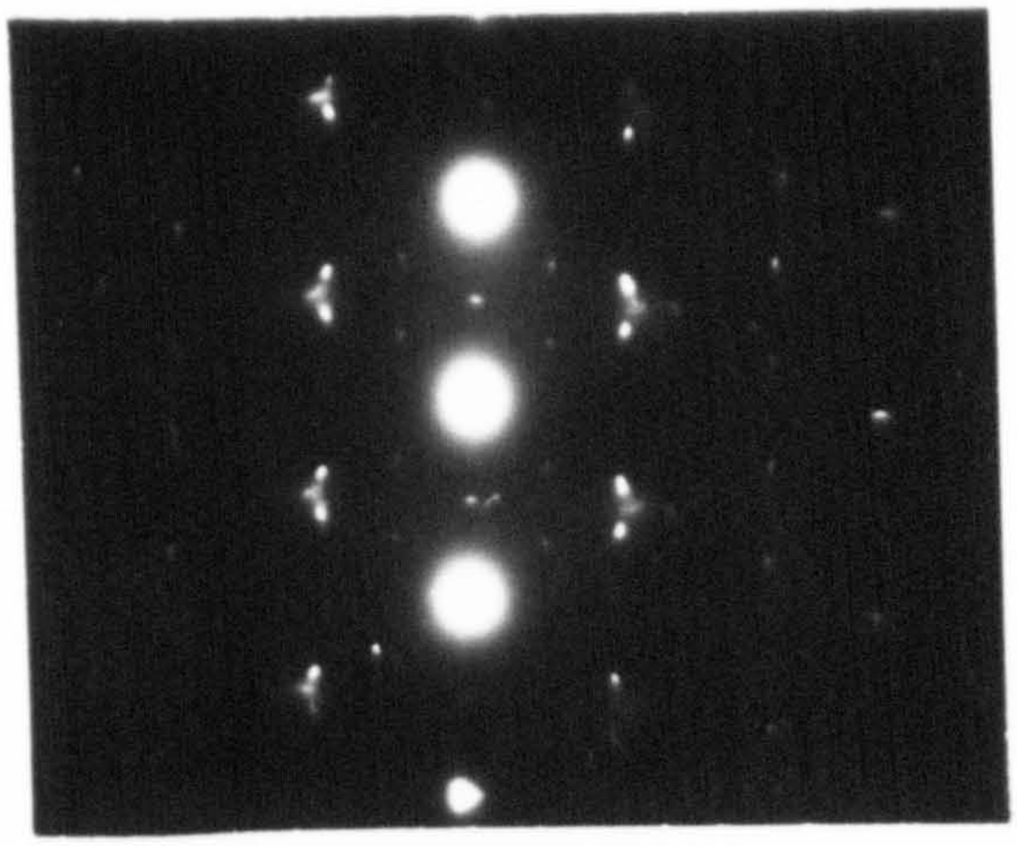

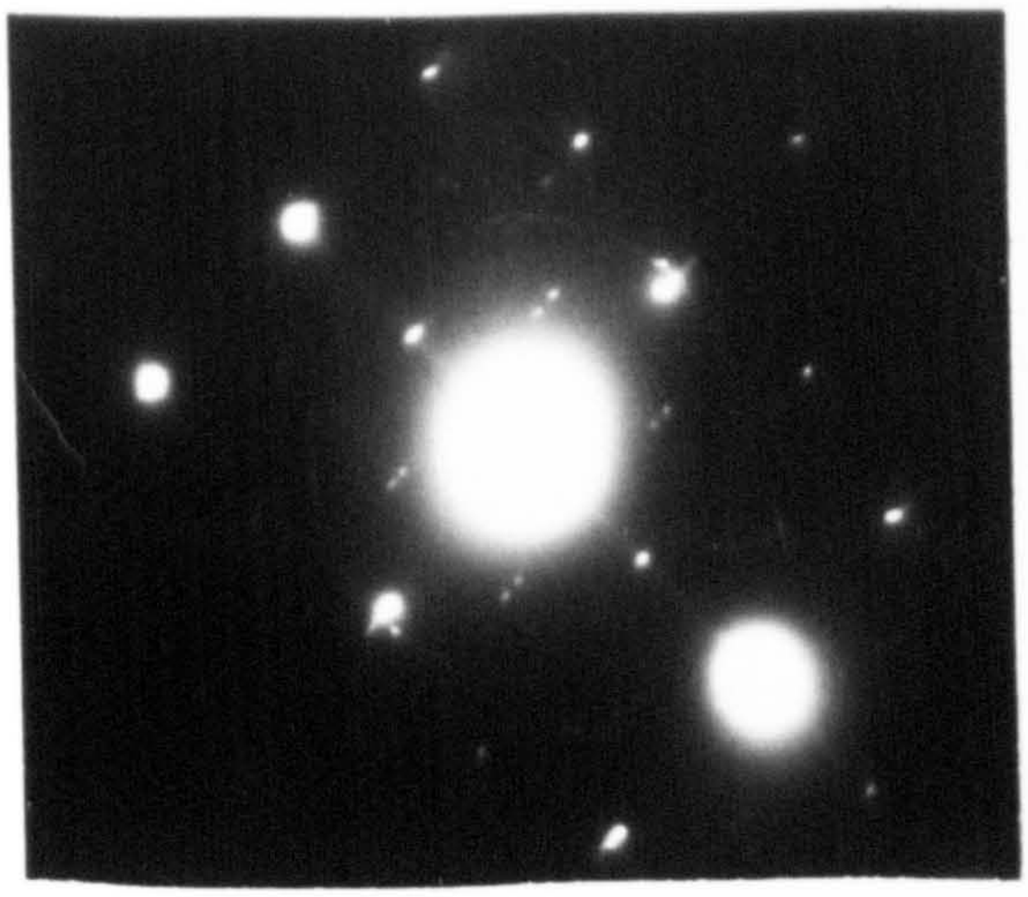

[110]

Fe - 5·05 wt % W nitrided in 8% NH_3:H_2

at 615°C for 48 hrs

Fig. VI.8

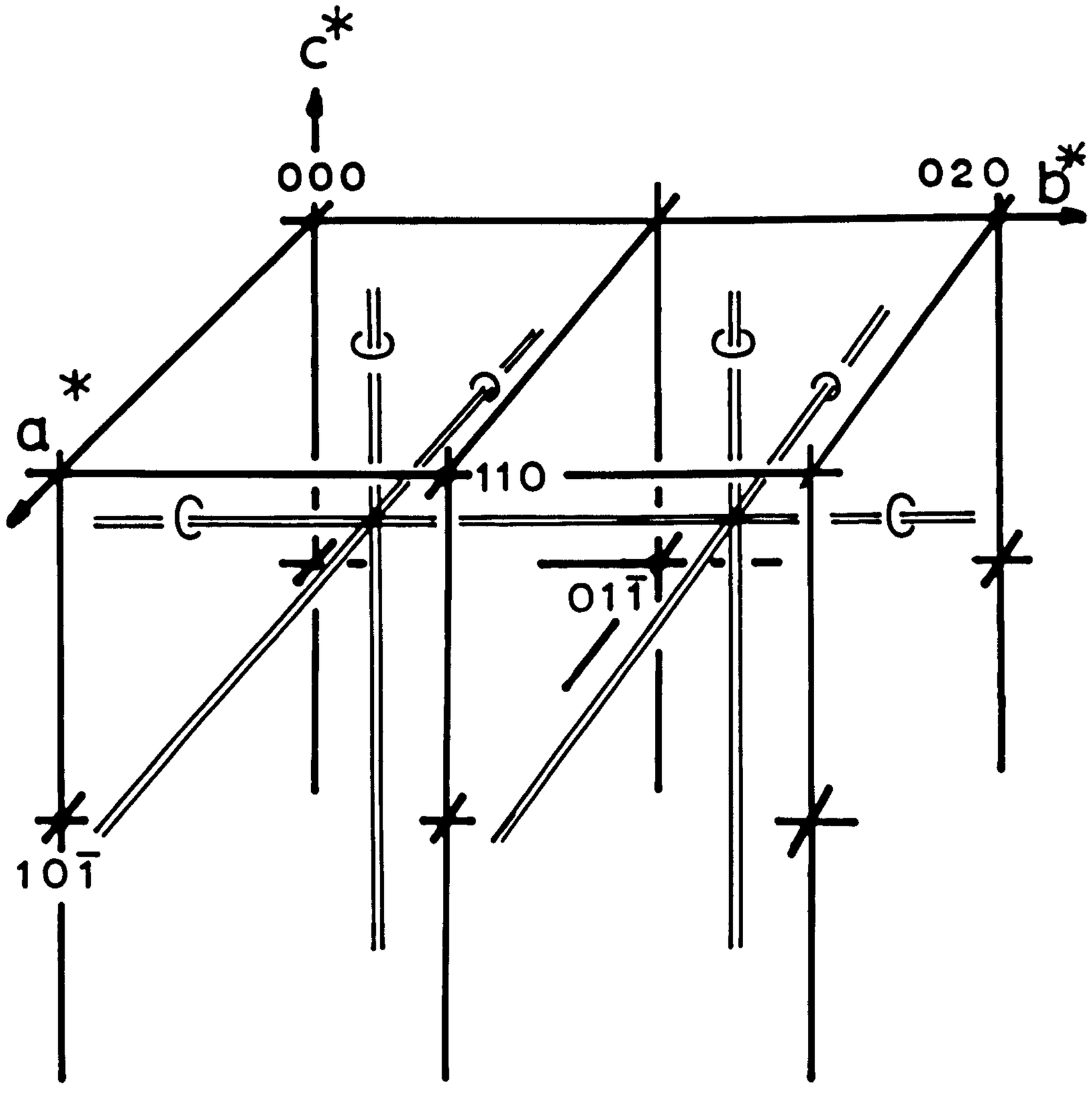

RECIPROCAL LATTICE OF FERRITE SHOWING THE POSITION OF SUPERLATTICE STREAKS

would be contained in a continuous streak if the orientation was exact, and its intersection with mutually perpendicular streaks is at a different point in reciprocal space. The slight deviation from an exact $[1\,1\,0]_\alpha$ zone is illustrated by the "splitting" of superlattice spots which converge as the exact Bragg condition is approached. All diffraction patterns are characterised by intense well-defined spots where rel-rods intersect the Ewald sphere and they become quite complex at less simple foil orientations e.g. the $[2\,1\,0]_\alpha$ zone shown in Figure VI.9. In this orientation one set of precipitates are parallel to the electron beam whilst the other two sets are incident at angles of 63.5° and 26.5° respectively. The streaks produced are perpendicular to the precipitate habit planes and can be distinguished on Figure VI.9 because one set produces elongated "spots" due to its low incident angle. In the micrographs of Figure VI.10 the dark-field image (d) using the elongated spot reveals the discs of low aspect area whilst that using the sharp spot shows the precipitates of high aspect area (Figure VI.10c). The micrograph (b) shows all three precipitate types because all three sets of streaks intersect at this point, which unfortunately is not clear on Figure VI.9 because of an intense spot due to the presence of an epitaxial surface oxide film (Keown and Dyson, 1966). All oxide spots marked $(hkl)_{ox}$ are produced by a [211] zone of Fe_3O_4 ($\underline{a}$ = 8.39 Å).

When the precipitate plates thicken, their $\underline{c}$ dimension becomes determinable and they can be isolated by dissolution of the matrix in 20% H_2SO_4. Figure VI.11 shows electron

Fig. VI.9

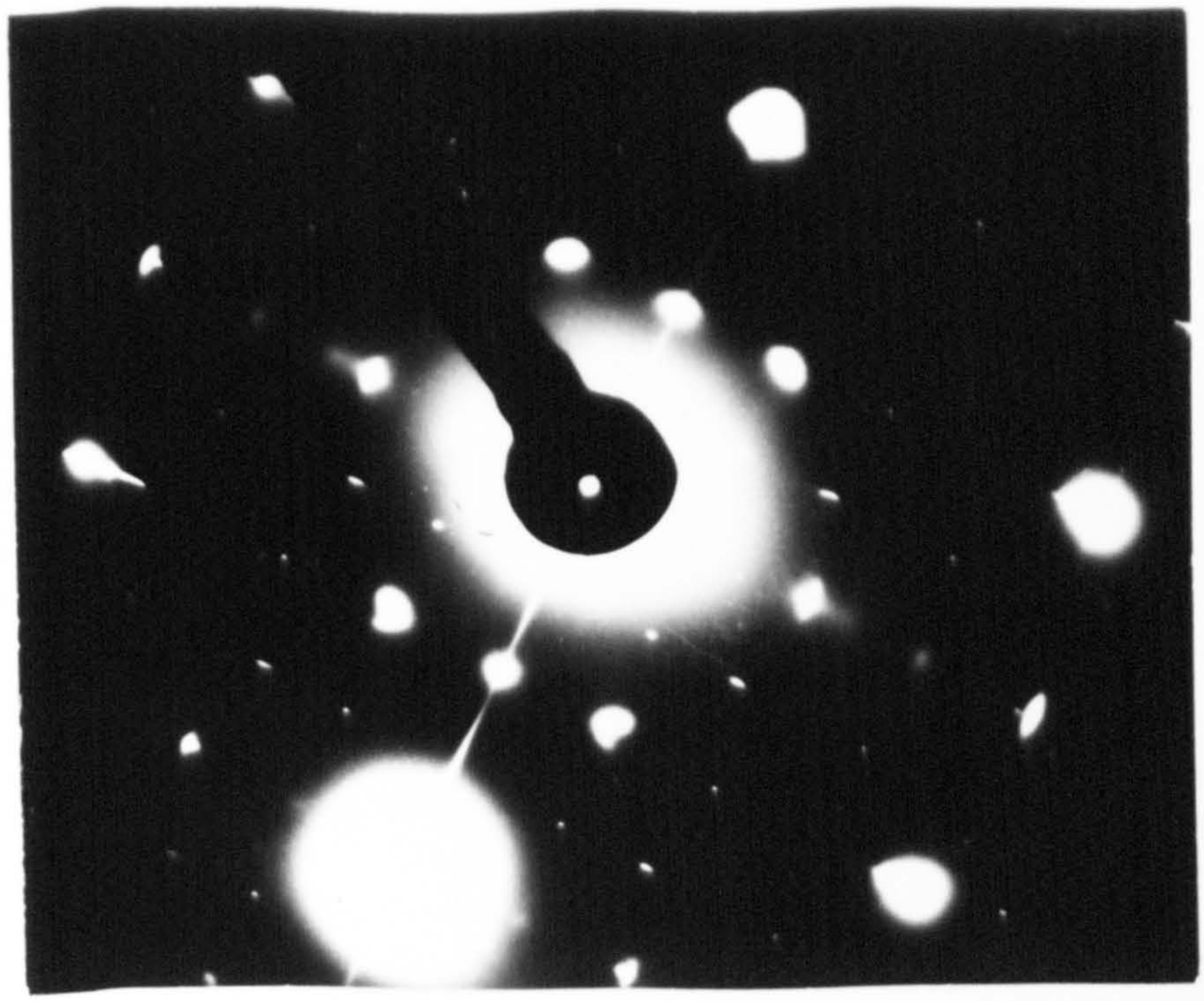

Beam parallel to $[120]_{\alpha}$ and $[211]_{Fe_3O_4}$

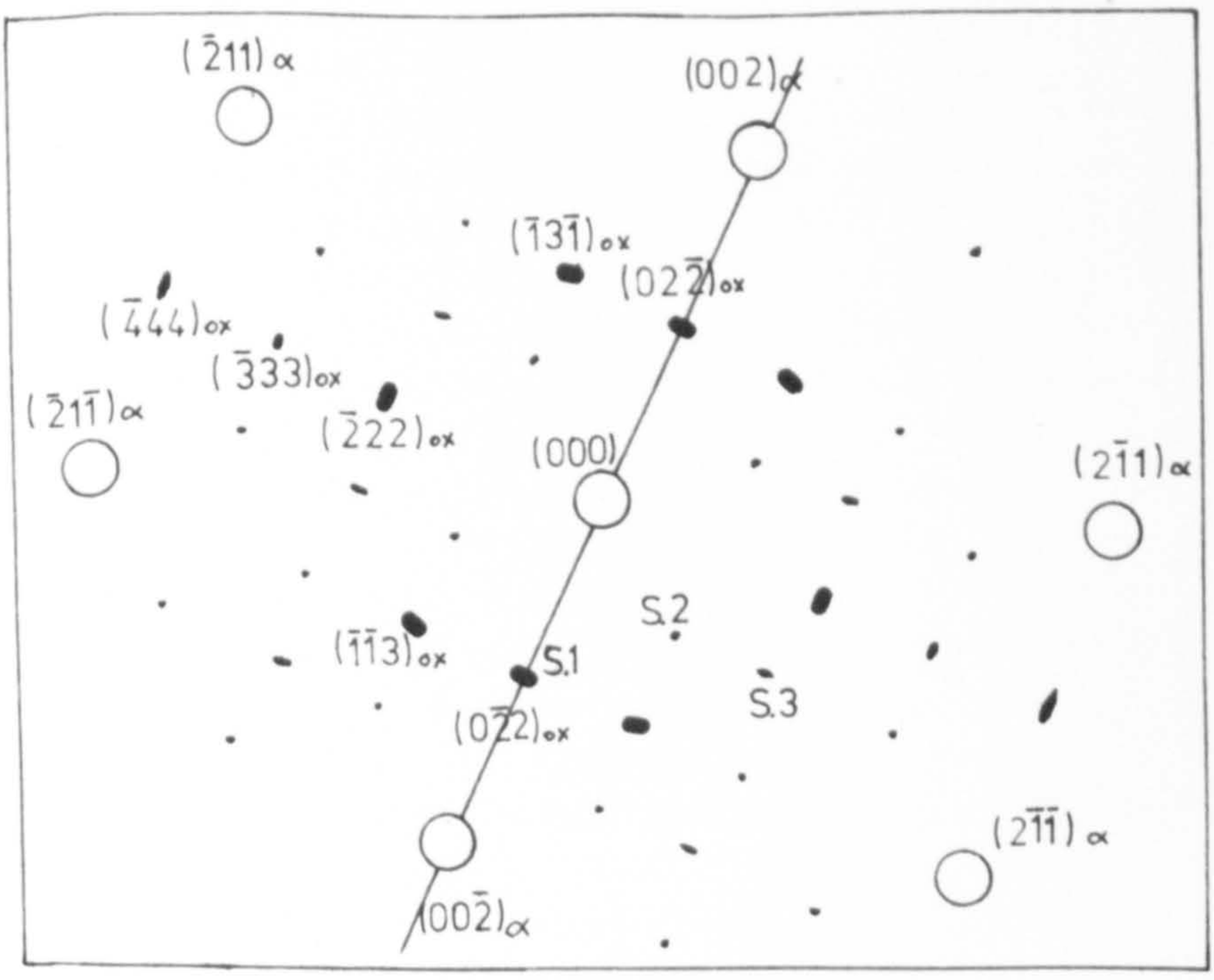

α - matrix
ox - epitaxial film of Fe_3O_4
remainder - intersection of rel-rods with Ewald sphere

ELECTRON DIFFRACTION PATTERN OBTAINED FROM Fe-4·0wt.%W NITRIDED FOR 24h. AT 615 °C. IN 8 % NH_3:H_2.

Fig. VI.10

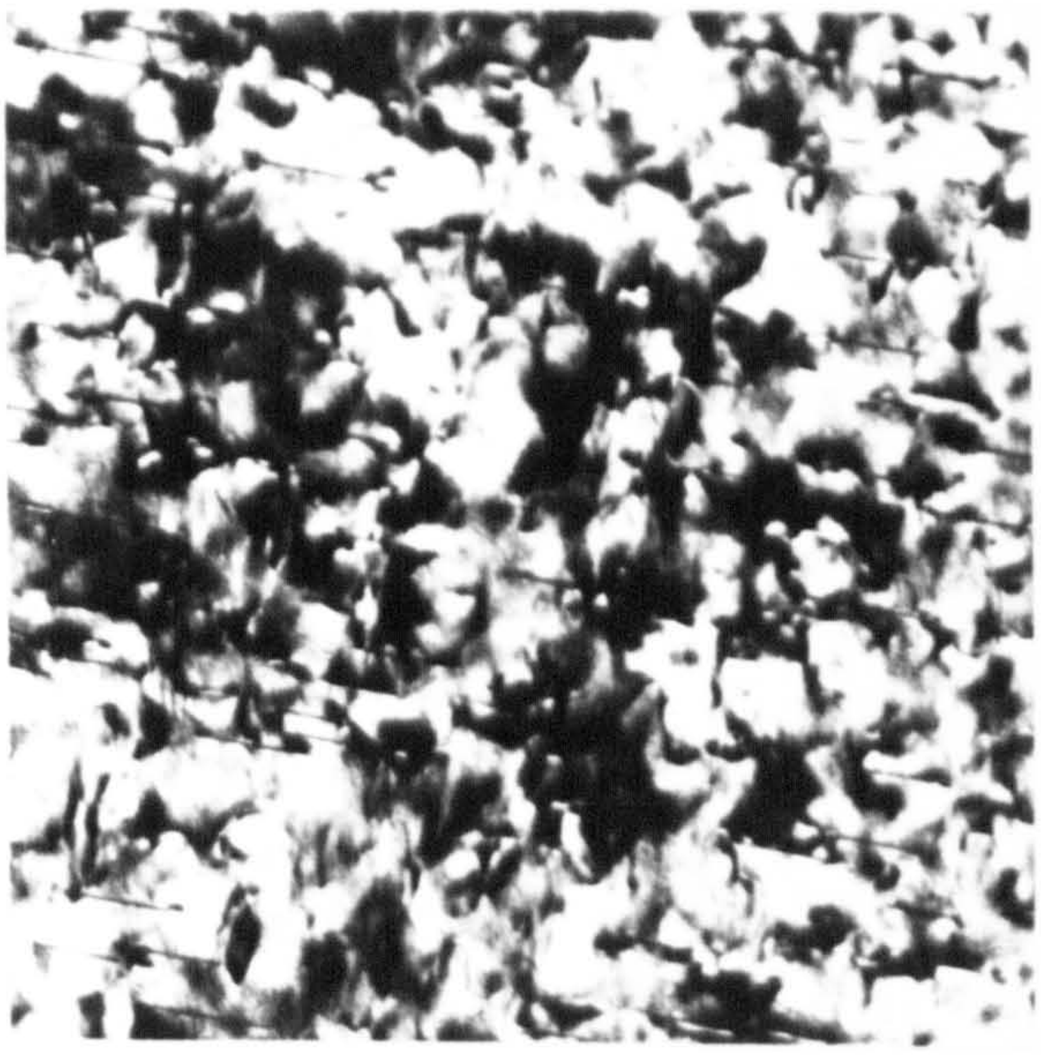

(a) Bright field

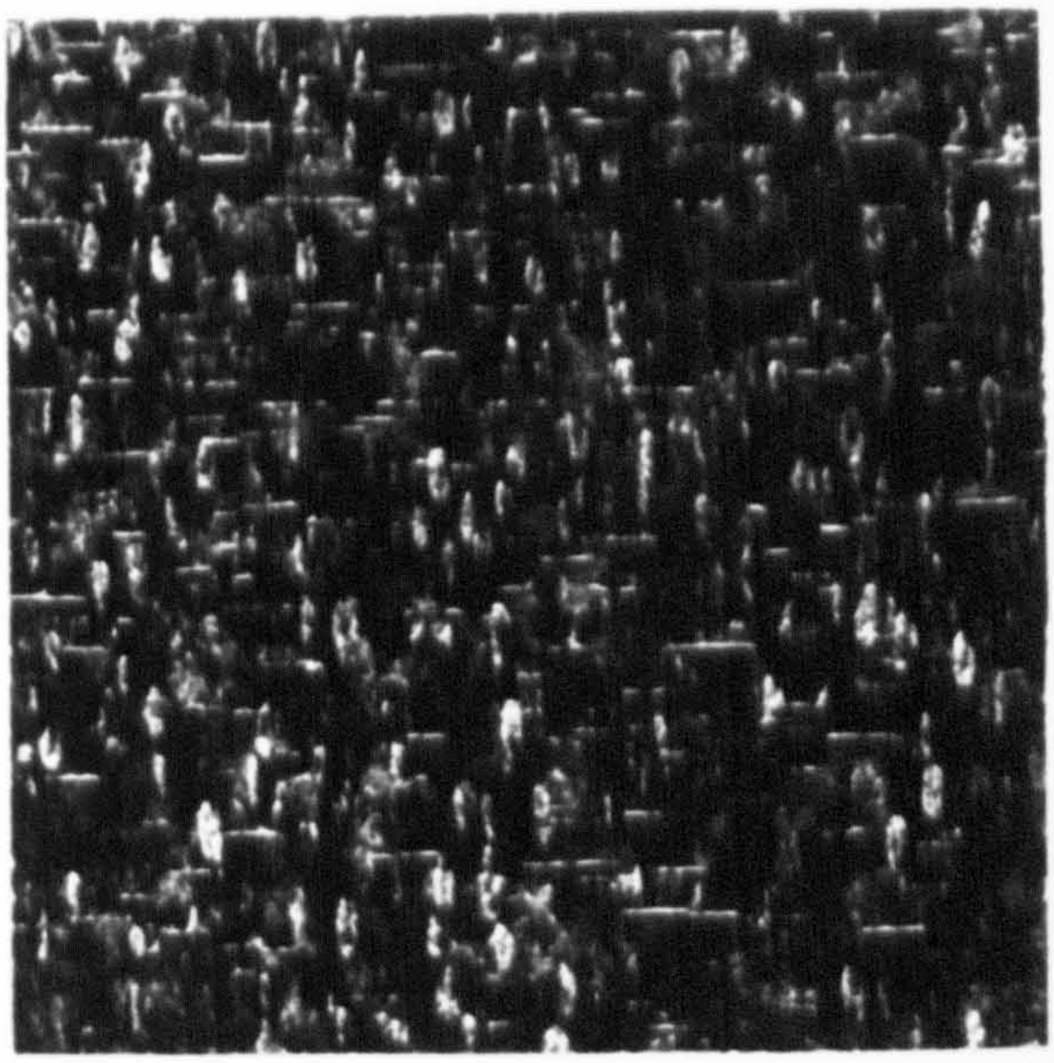

(b) C.D.F. using S.1

0·1μ

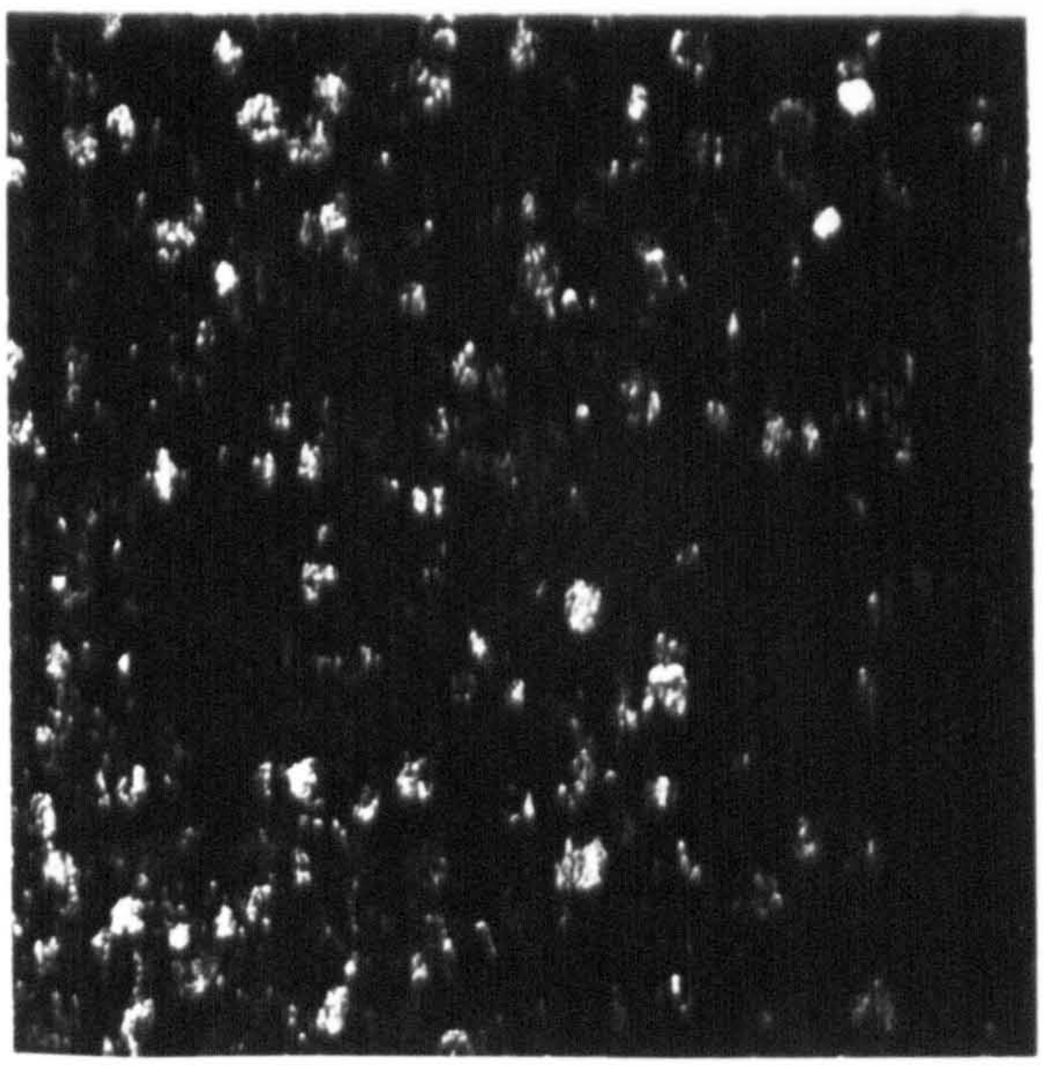

(c) C.D.F. using S.2

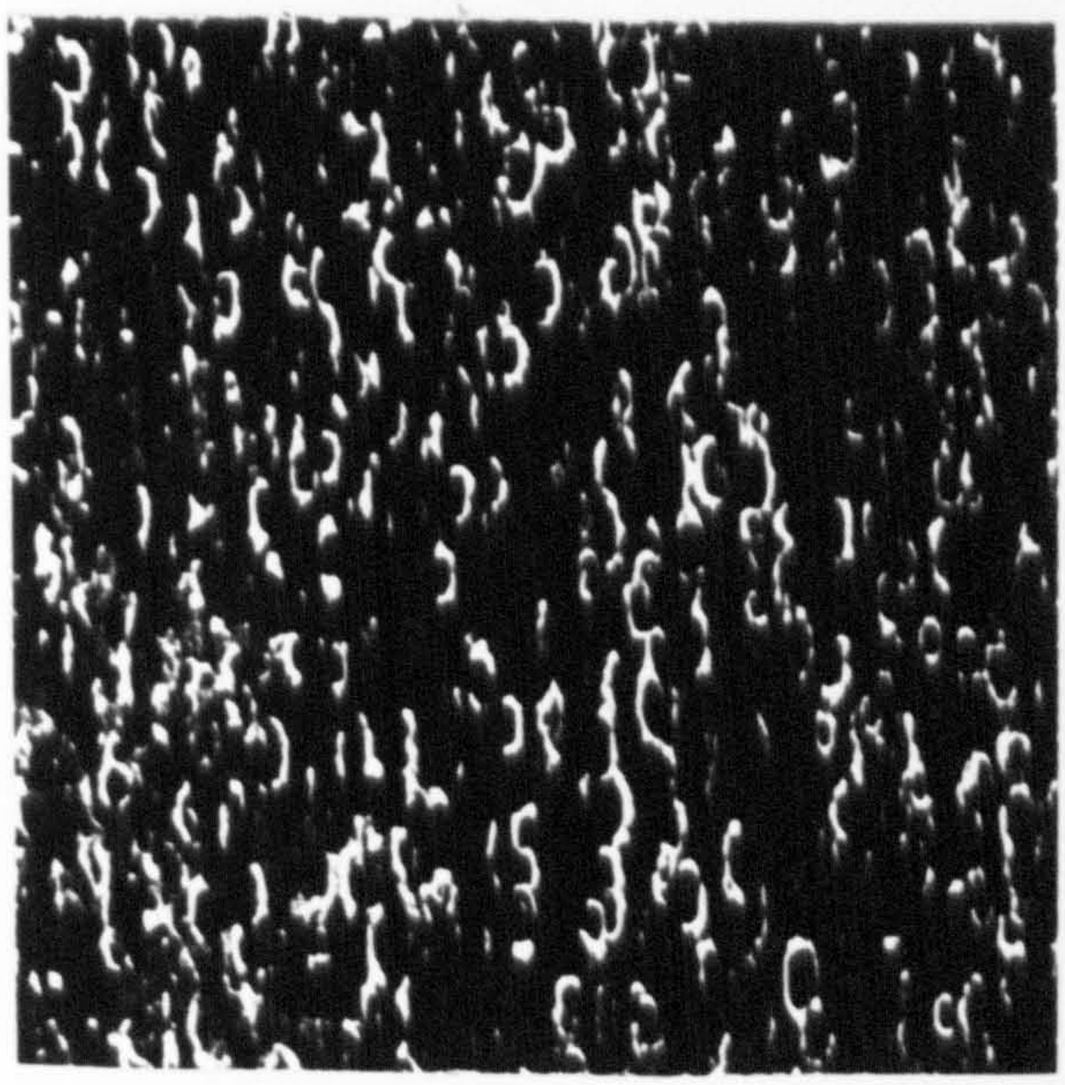

(d) C.D.F. using S.3

ELECTRON MICROGRAPHS OBTAINED FROM Fe–4·0wt. % W NITRIDED FOR 24h. AT 615 °C IN 8% NH_3:H_2

[S.1,2 & 3 refer to spots on the diffraction pattern of Figure VI.9]

and X-ray diffraction patterns of the phase at this stage. X-ray diffraction yields only reflections from $\{hk0\}$ planes because the small crystallite size in the $[001]$ direction causes irresolvable diffraction broadening, but ordering of the metal atoms is confirmed by the presence of super-lattice lines. However, electron diffraction patterns now show $\{hkl\}$ reflections which, on the body-centred tetragonal interpretation, give a $\underline{c}/\underline{a}$ ratio of about $\sqrt{2}$ and therefore the simplest unit cell is approximately cubic having an orientation relationship with the matrix of:

$$(110)\,\text{precipitate} \parallel (100)_\alpha \; ; \quad [001]\ \text{precipitate} \parallel [001]\,\alpha$$

i.e. the Baker-Nutting orientation relationship (1959) for f.c.c. carbides and nitrides in ferrite. The electron diffraction pattern of Figure VI.11 consists of reflections from three precipitate zones and is now indexed on the basis of a cubic unit cell, the reciprocal lattice points of which are shown relative to ferrite in Figure VI.12.

The presence of iron in the extracted precipitate was confirmed by compacting the extract and reducing in hydrogen at 800°C. The resultant alloy was shown by X-ray diffraction to consist of W(Fe) solid solution and Fe_2W_3. Although the test was only qualitative the iron content of the residue was estimated as being about 5-10 at.%. A previous determination using electron probe analysis of carbon extraction replicas gave a much higher value ($\sim$50%) but it is possible that considerable error was introduced due to the presence of corrosion products produced during extraction.

Fig. VI. 11

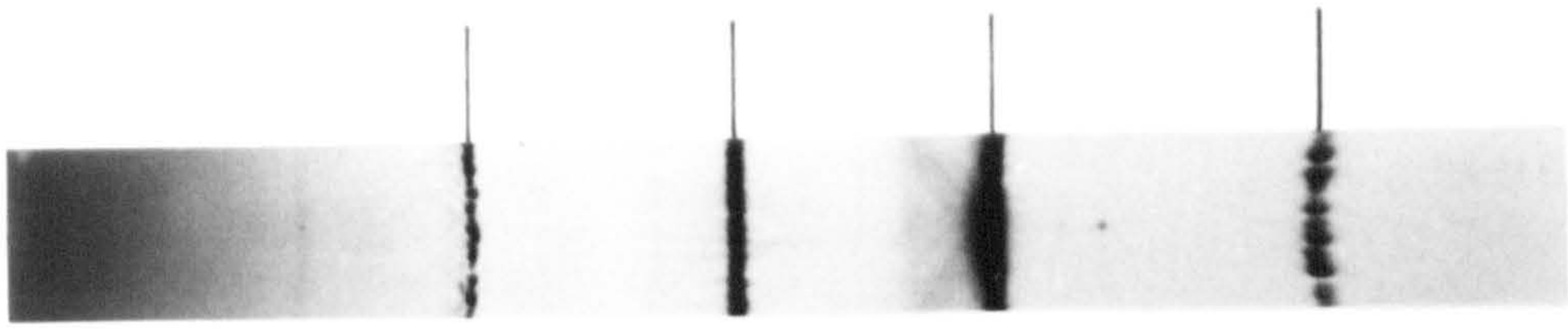

α-Fe

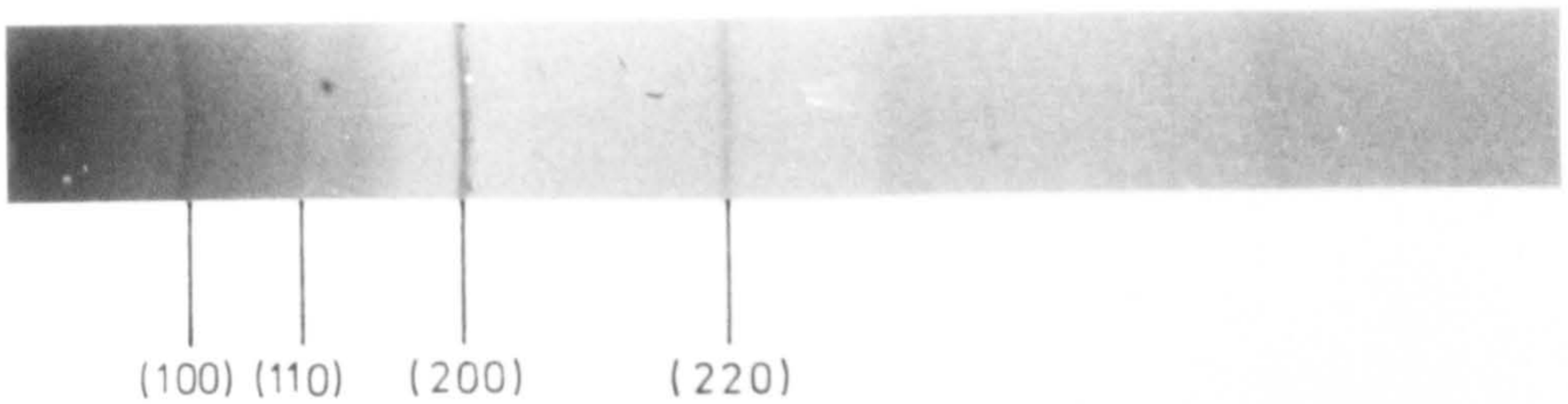

(100) (110) (200) (220)

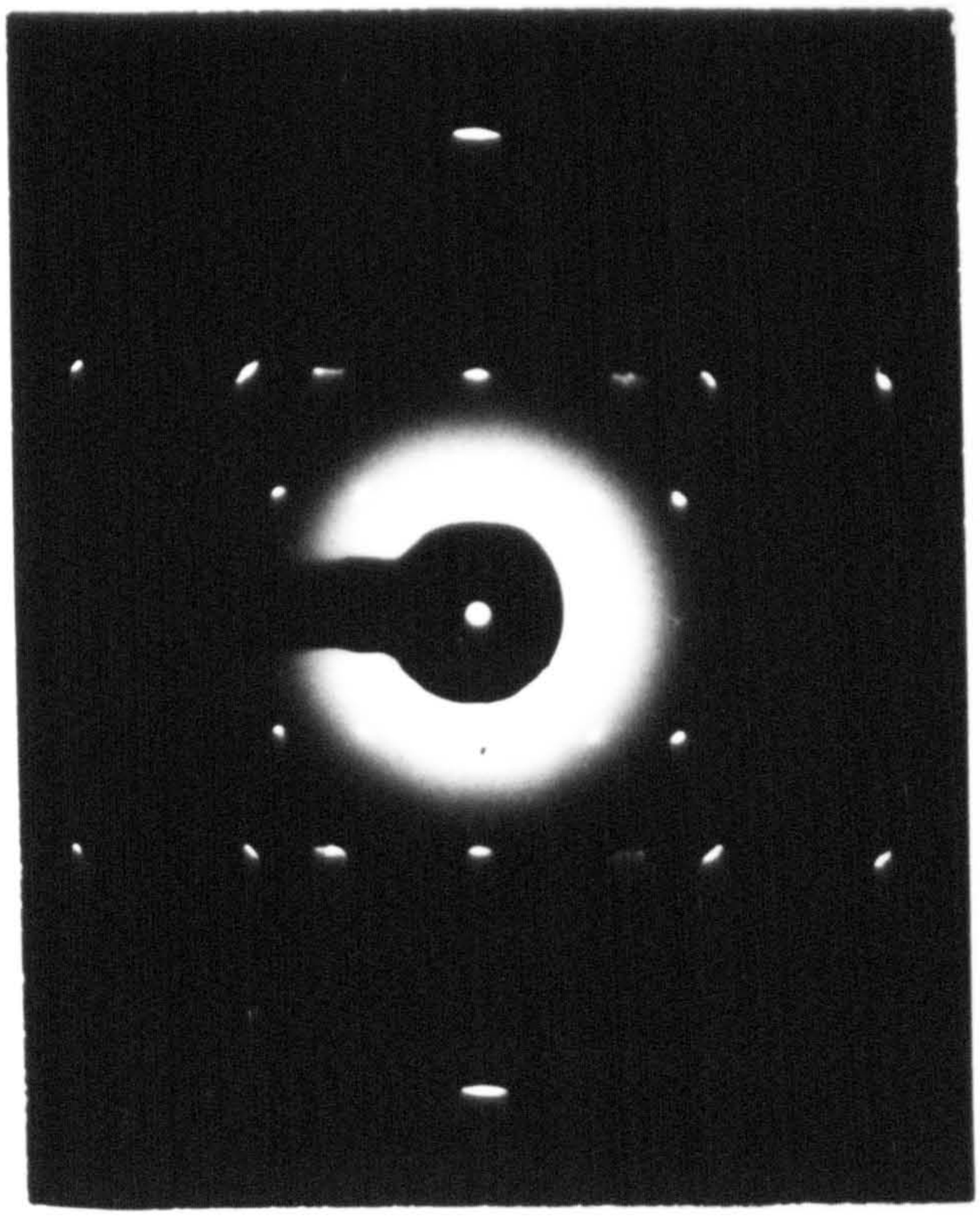

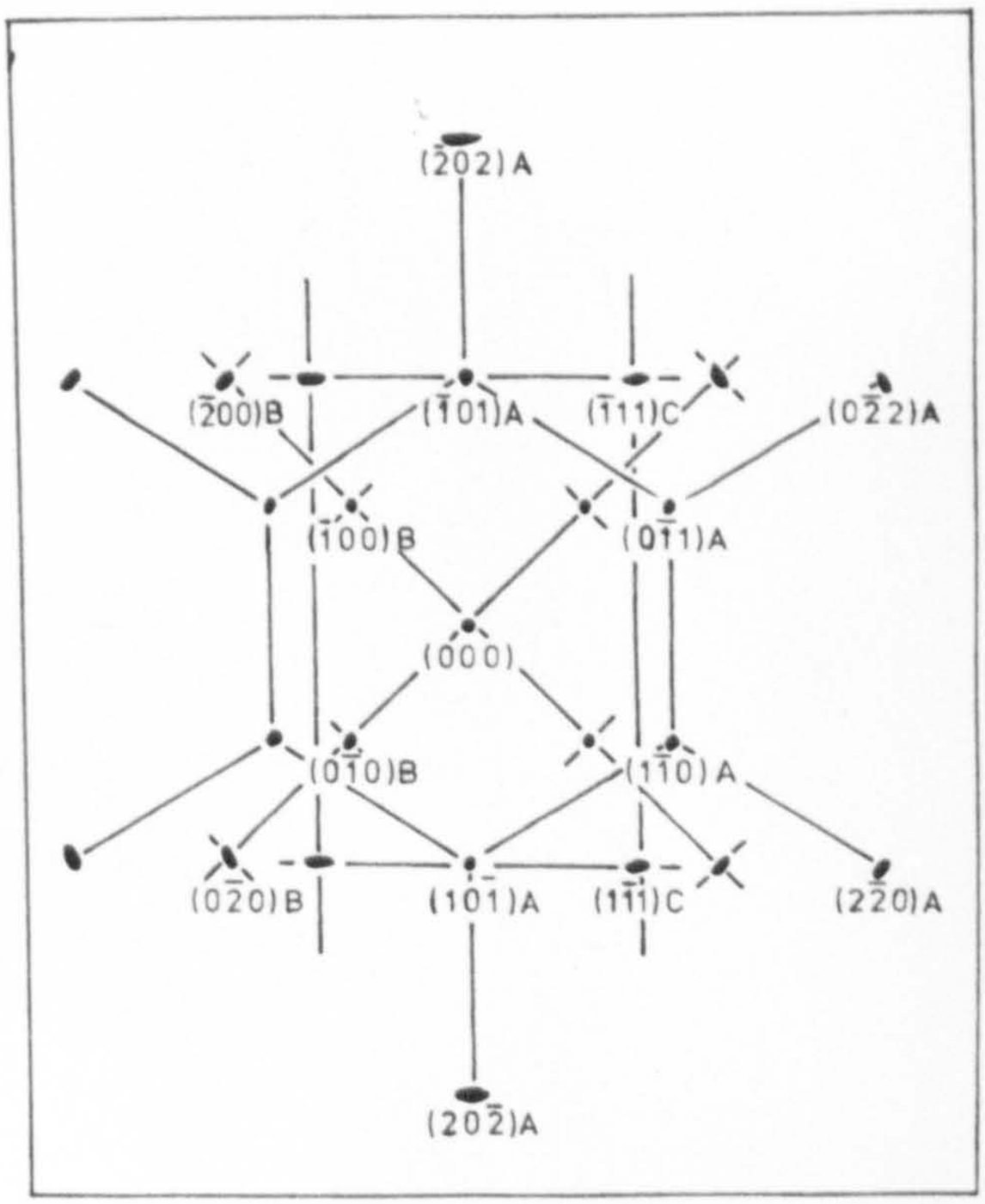

A [111] zone : B [001] zone : C [110] zone

X-RAY AND ELECTRON DIFFRACTION PATTERNS OF EXTRACTED Fe-W-N INTERMEDIATE PHASE [indexed on the basis of a close-packed cubic unit cell].

Fig. VI. 12

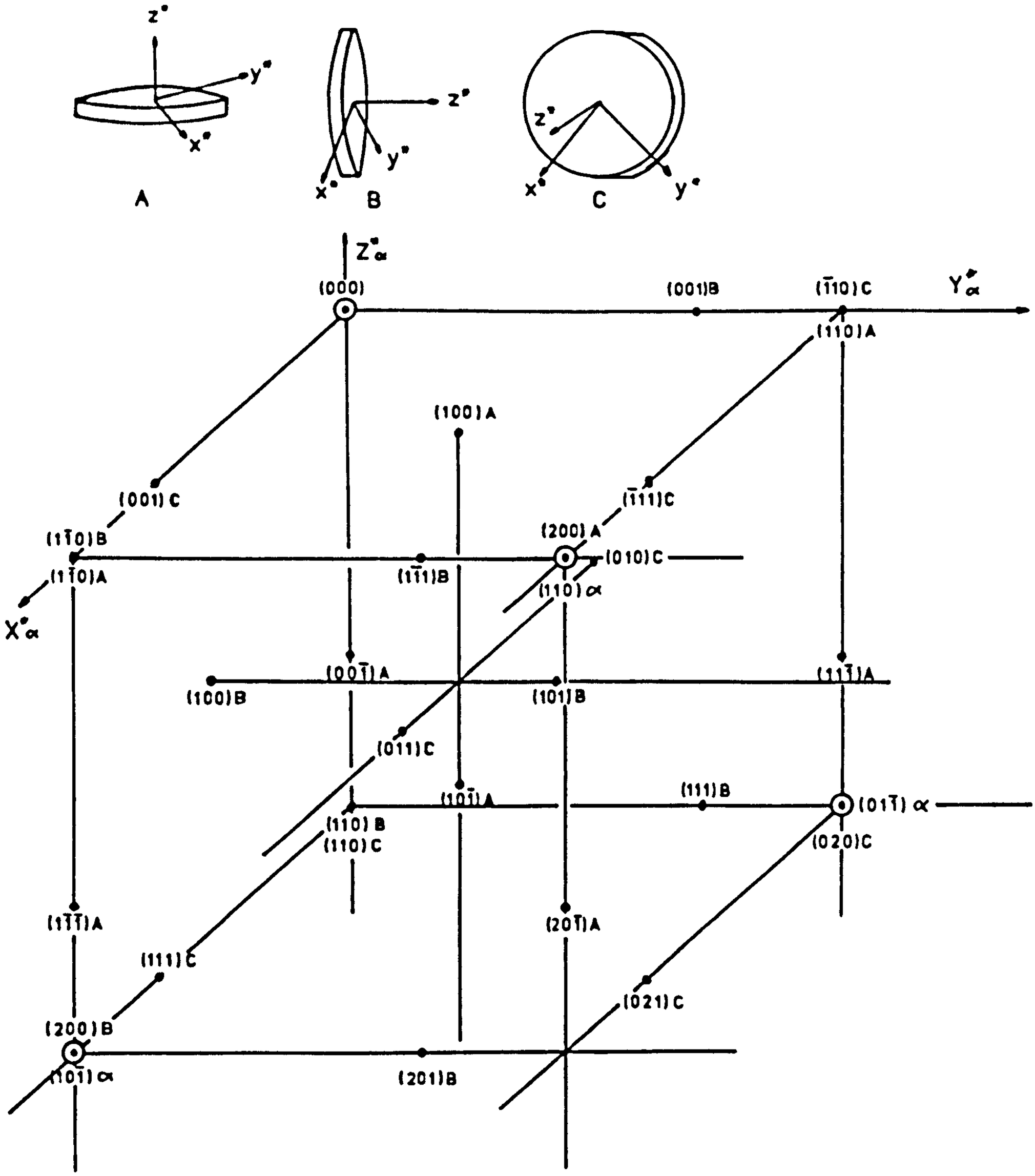

RECIPROCAL LATTICE CONSTRUCTION FOR FERRITE CONTAINING THREE MUTUALLY PERPENDICULAR ORIENTATIONS OF Fe-W-N INTERMEDIATE PHASE [Indexed on the basis of a close-packed cubic unit cell].

It is clear from the intensity of the superlattice reflections that there must be ordering of the two metal atoms and/or possibly defects. The most probable explanation is that iron atoms partially occupy the (000) positions of a face centred cubic arrangement of tungsten atoms. The alternative is that these positions are partially or totally vacant, but this would make the structure similar to γ-$W_{0.75}(N,O)$ and the nitrogen content should be about three times greater. In addition γ-$W_{0.75}(N,O)$ can not exist at low oxygen potentials whereas the intermediate phase can.

The shifts in metal-atom positions necessary for transformation of the original clusters to intermediate phase are illustrated in Figure VI.13. Precipitation proceeds by continuous replacement of iron atoms by those of tungsten accompanied by the clustering and ordering of nitrogen. In this manner the precipitate is formed without any change in the overall metal-atom arrangement, and the process merely continues until the most stable composition is attained. In systems such as Fe-Cr-N (Mortimer, 1971) and Fe-V-N (Pope, 1972) where the equilibrium nitride is face centred cubic, the process continues until the equilibrium phase is produced directly. However in the present system, where the equilibrium composition is near to WN and the structure is simple hexagonal (see Chapter V), the continuous ordering process ceases before stable equilibrium is attained. The equilibrium phase in these alloys nucleates at grain boundaries and grows discontinuously, and the intermediate precipitate persists in its metastable

Fig. VI.13

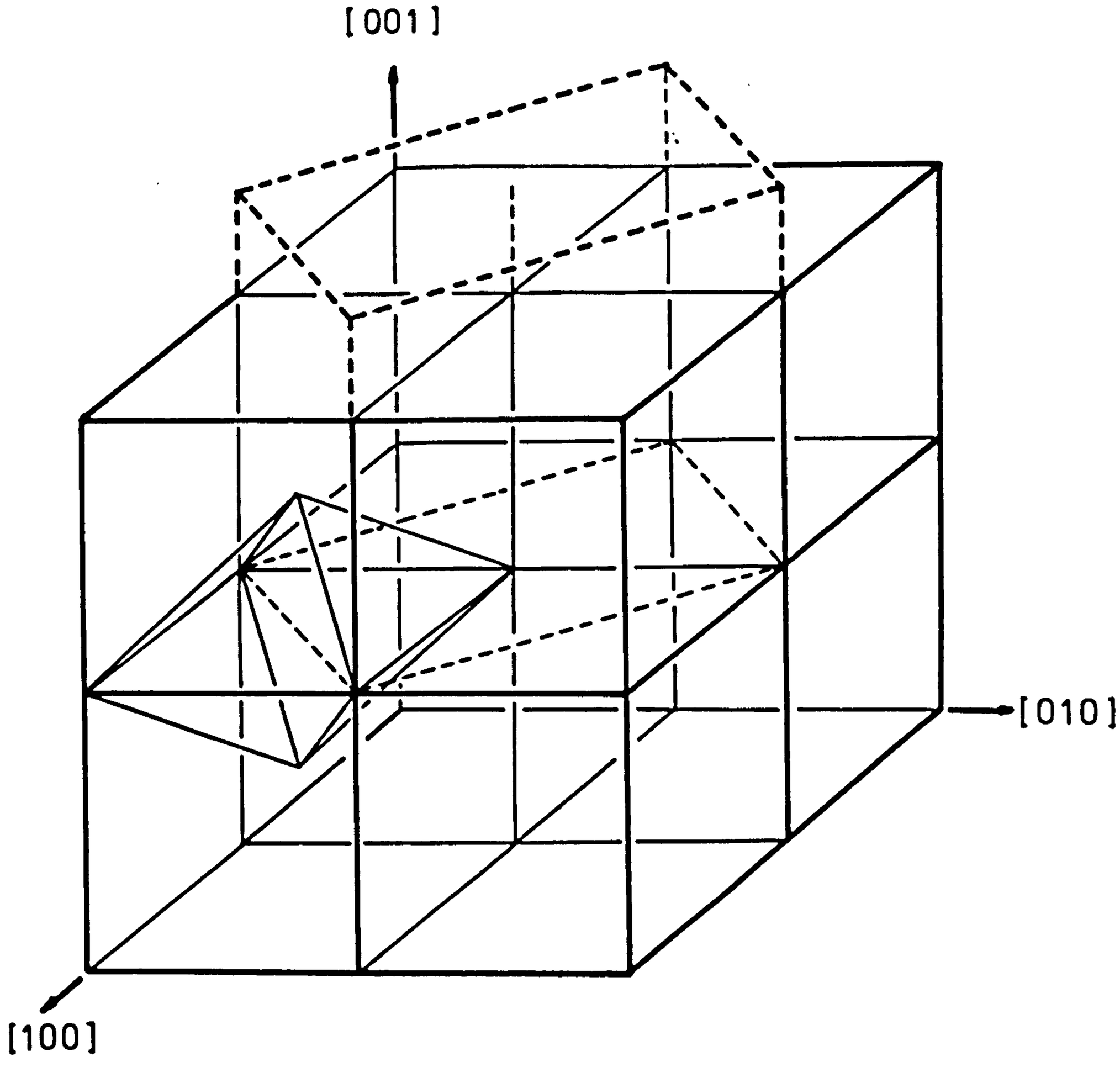

——— Fe atom lattice containing undistorted "zone-octahedra"

------ Close-packed cubic unit cell

SCHEMATIC DIAGRAM ILLUSTRATING THE CHANGE IN METAL-ATOM STRUCTURE DURING CONTINUOUS ORDERING

form until it is consumed by equilibrium phase growth.

VI.4 Heterogeneous precipitation

Figure VI.1 shows that with less than 4.0 wt.%N, nitrogen diffuses into the specimen at a significantly faster rate than it precipitates. With 3.5 wt.%N the rate of weight increase up to about 0.1 wt.%N is greater than that above 0.1 wt.%N whilst with only 2.0 wt.%N the rate of increase above the nitrogen solubility is virtually zero. This is because precipitation is now heterogeneous and since the number of nuclei is reduced considerably, the rate of precipitation is low.

Figure VI.14 shows micrographs of Fe-3.5 wt.%N alloys nitrided in 8%NH_3:H_2 at 615°C for 36 hours. The alloy contains about 0.14 wt.%N and since the precipitation reaction is slow compared to nitrogen diffusion into the specimen, then at 615°C most of this nitrogen (0.09 wt.%) must be present in solution in ferrite. A combination of auto-tempering during the quench and retaining the specimens at room temperature allows decomposition of the supersaturated nitrogen-ferrite, producing Fe-N GP zones. The high nitrogen potential employed in these experiments produces the high concentration of nitrogen required for homogeneous precipitation in nitrogen-ferrite (see Chapter 1). Thus Figure V.14a shows heterogeneous precipitation of Fe-W-N intermediate phase produced at 615°C in a background of ferrite containing Fe-N GP zones produced at about 20°C.

Fig. VI.14

(a)

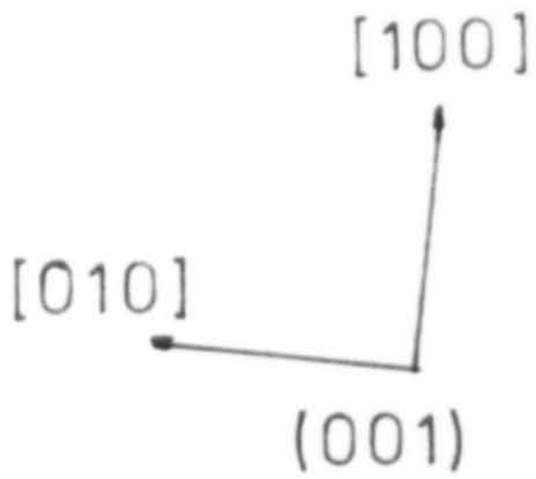

0·2μ

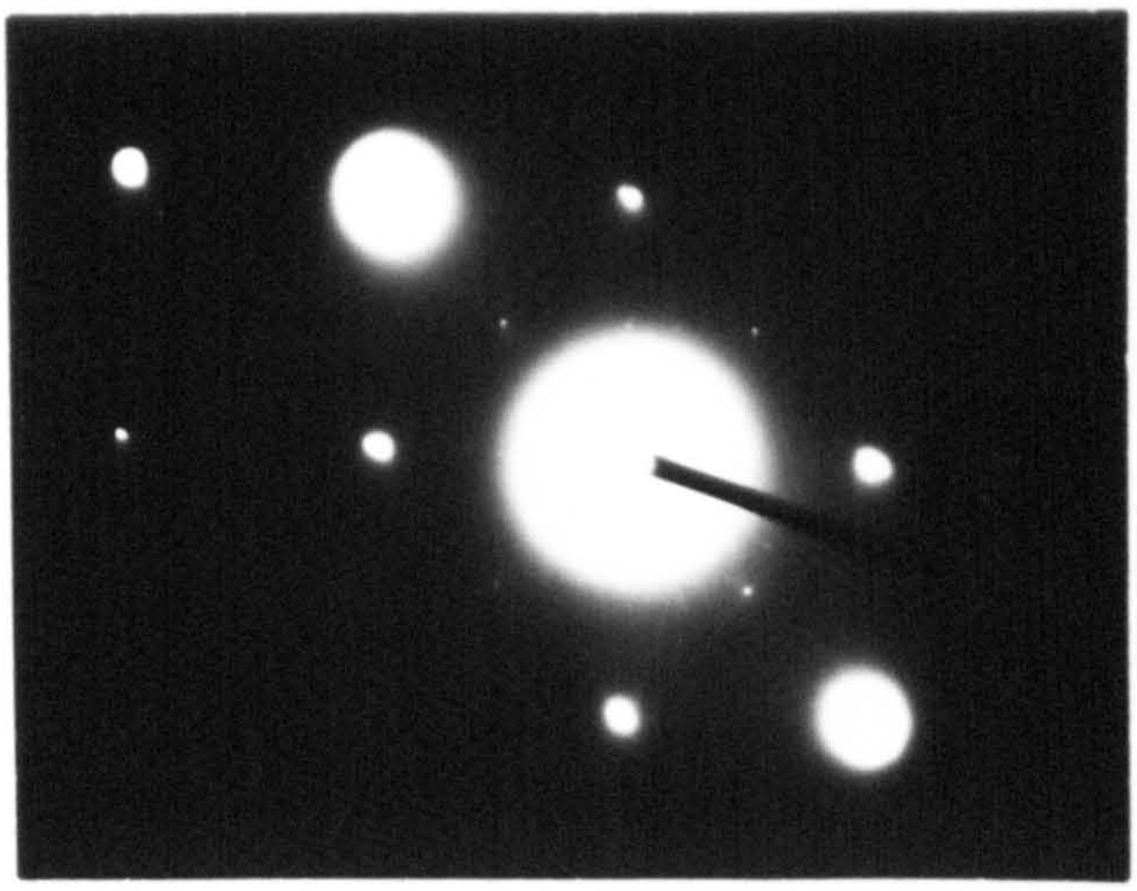

(b) SADP from area shown in (a)

(c) Carbon extraction replica

1·0μ

ELECTRON MICROGRAPHS SHOWING HETEROGENEOUS PRECIPITATION OF Fe-W-N INTERMEDIATE PHASE IN Fe–3·5 wt.% NITRIDED IN 8% NH_3:H_2 AT 615 °C. FOR 36 h.

The intermediate phase precipitates have an irregular disc shape and are usually formed as clusters of three plates on a single nucleus very similar in appearance to ε-carbide plates in aged carbon-ferrite (Hale and McLean, 1963) and α''-$Fe_{16}N_2$ plates in aged nitrogen-ferrite (Hale and McLean, 1963; Lehtinen, 1972). Electron diffraction patterns obtained from the region containing the large precipitates in Figure VI.14a show characteristic super-lattice spots despite the low volume fraction of precipitate (Figure VI.14b). The distribution of precipitates is seen more clearly in Figure VI.14c and is predominantly on dislocations. The surface of the foil from which this extraction replica was produced is near to $(100)_\alpha$ and the section of the dislocation lines on which precipitation is dense lie in the $(100)_\alpha$ ferrite plane. General observations indicated that precipitation on dislocations was more predominant when this condition was fulfilled.

Further nitriding of the alloy shown in Figure VI.14 produces additional nucleation and growth until ultimately a dense network of interlocked precipitates is produced (Figure VI.15a). There is some indication that the continued nucleation of intermediate phase occurs by an autocatalytic mechanism similar to that discussed by Lorimer (1970) for the precipitation of θ' in Al-Cu alloys, in which as one plate grows, nucleation of an adjacent plate is induced in the strain field of the first. A prerequisite of such a mechanism is the existence of strain in the matrix at the periphery of the precipitate and this is clearly seen in Figure VI.10a. The particles probably grow by

Fig. VI.15

(a) Fe 3·5 wt.% W nitrided in 8 % NH_3:H_2 at 615 °C. for 78 h.

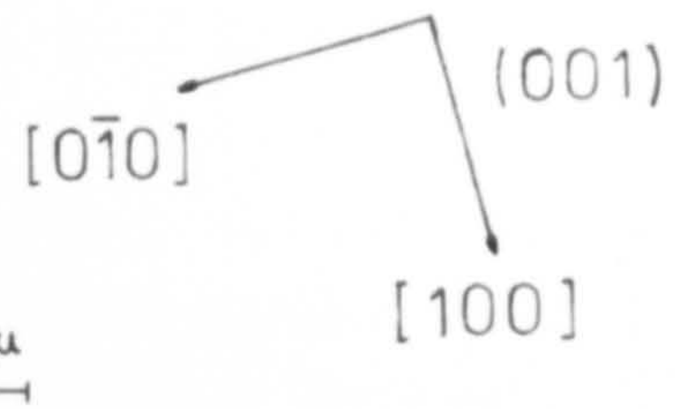

0·2 μ

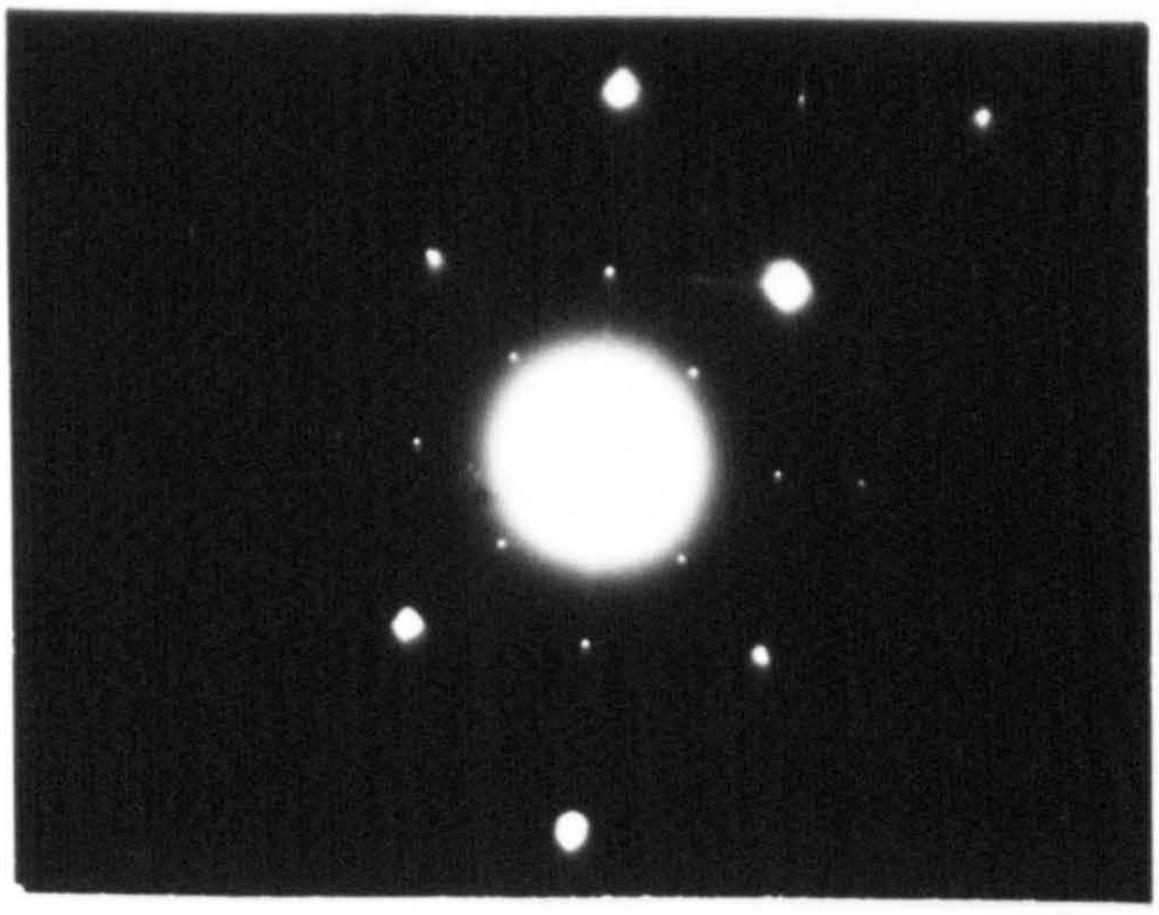

(b) SADP from (a)

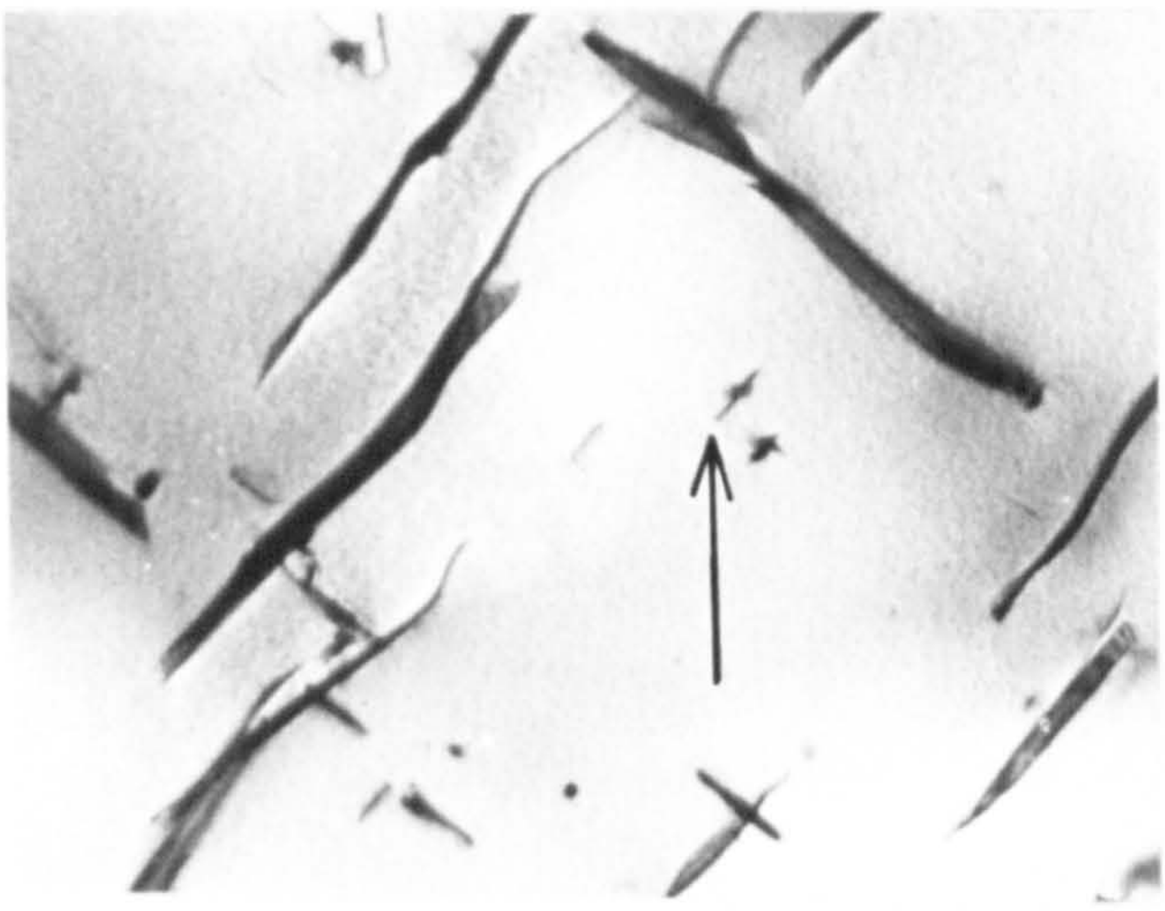

(c) Fe-2·05 wt.% W nitrided in 8 % NH_3:H_2 at 615 °C for 78h. and subsequently aged at 250 °C for 20 min.

[large precipitate is α''-$Fe_{16}N_2$]

0·2 μ

ELECTRON MICROGRAPHS SHOWING HETEROGENEOUS PRECIPITATION OF Fe-W-N INTERMEDIATE PHASE

a ledge mechanism similar to that described by Mitchell (1971) for hafnium nitride in molybdenum, in which coarsening occurs by the successive formation of extrinsic steps and intrinsic loops which grow radially, generating matrix strain near to the circumference of the disc.

With only 2.0 wt.% W the rate of heterogeneous precipitation is reduced dramatically. Figure VI.15c shows small amounts of Fe-W-N intermediate phase produced after nitriding for 78 hours, which have been detected only by subsequently aging the specimen at 250°C in order to transform the fine distribution of Fe-N GP zones to a coarse dispersion of α''-$Fe_{16}N_2$.

Cahn (1957) predicts that for a given phase precipitation on dislocations becomes energetically more favourable as the supersaturation increases. In the present system as the tungsten content is increased up to about 3.5 wt.% precipitation on dislocations becomes more evident but at the supersaturations at which homogeneous precipitation occurs the latter is so extensive that dislocation nucleation is not commonly observed. Thus the influence of dislocation is greatest at moderate supersaturations (Kelly and Nicholson, 1963).

The observations are consistent with the existence of a zone solvus but in this case since there are two solutes the supersaturation required for homogeneous precipitation must be achieved by exceeding an activity product. The tungsten content above which homogeneous precipitation occurs

will therefore depend on the nitrogen potential.

VI.5 Discontinuous precipitation

The final stage of precipitation is the heterogeneous nucleation of equilibrium nitride at grain boundaries, and transformation of the microstructure by discontinuous precipitation. The reaction interface is a high angle boundary at which simultaneous dissolution of the intermediate phase and precipitation of the equilibrium phase occurs. Figure V.16 shows lamellae of δ'-$W_{0.9}(N,O)$ growing in the direction indicated and "dragging" a grain boundary at which the intermediate phase is consumed. Matrix recrystallisation is clearly demonstrated in the matrix bright field-dark field micrographs which show that the interlamellar ferrite is of the same orientation as the grain from which the precipitate originates. There is no dissolution of the intermediate phase at large distances ahead of the boundary.

Extraction replicas from alloys containing continuous and discontinuous precipitation reveal the habit plane of the equilibrium δ' plates to be $(001)_{\delta'}$, and the plates grow extensively in all directions lying in the basal plane of the hexagonal unit cell. The pseudo single crystal electron diffraction pattern of Figure V.1 was obtained from such a plate lying perpendicular to the electron beam. Figure VI.17 shows a series of micrographs obtained from a thin foil which was successively tilted until the projected

Fig. VI.16

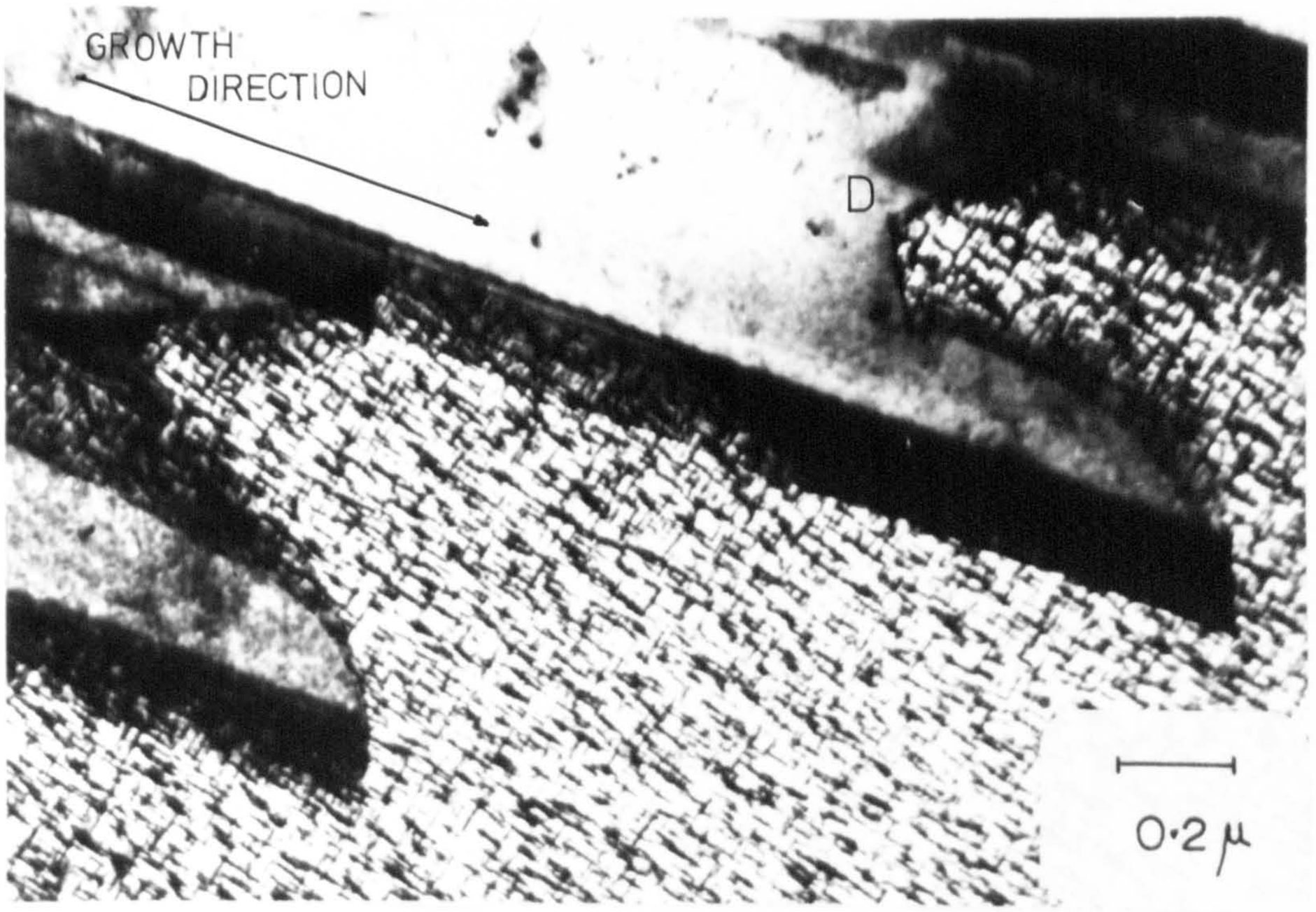

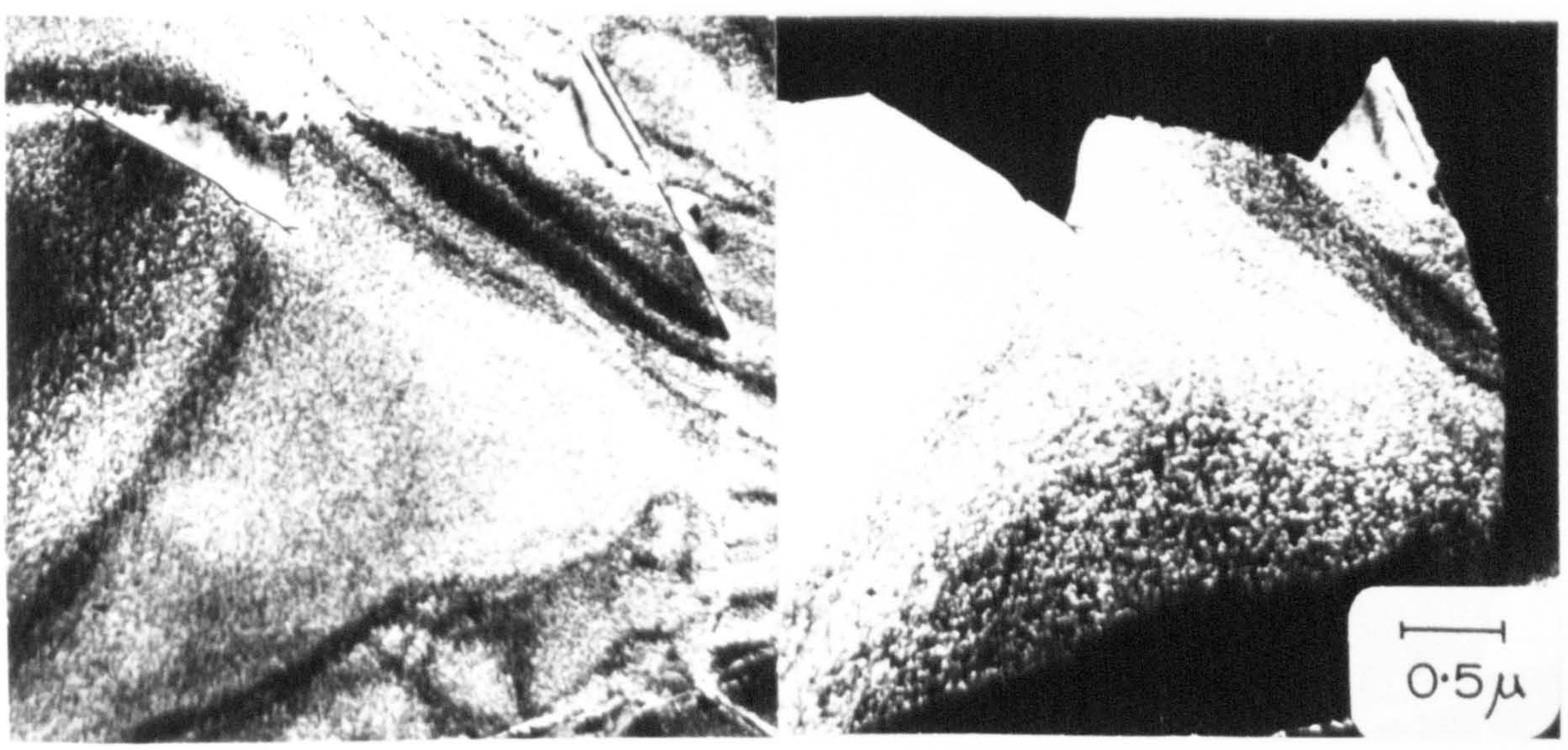

Discontinuous and continuous precipitation in Fe-4·0 wt % W nitrided in 8% NH_3:H_2 at 615 °C

Fig. VI.17

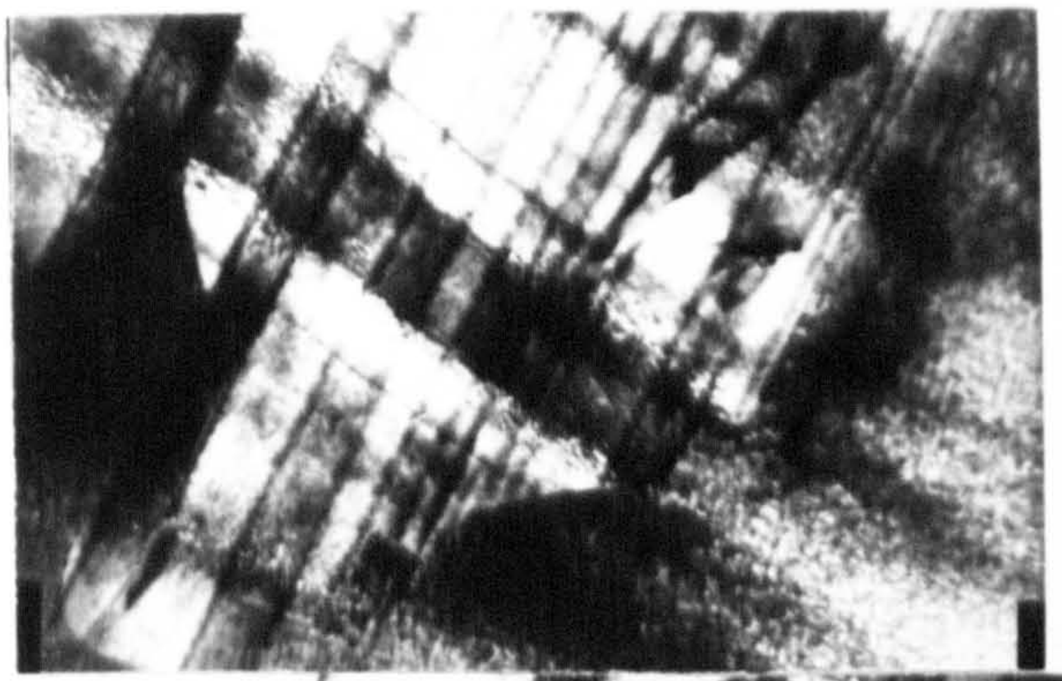

(a) 0° tilt

tilt axis parallel to lamellae

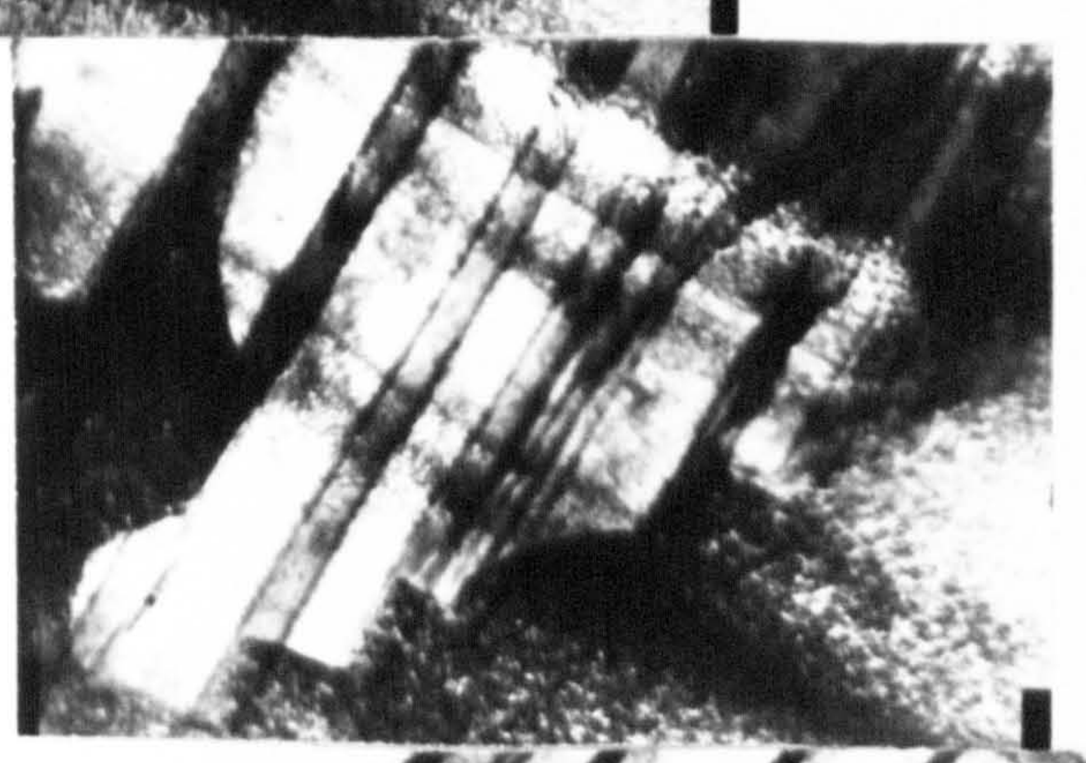

(b) 15° tilt

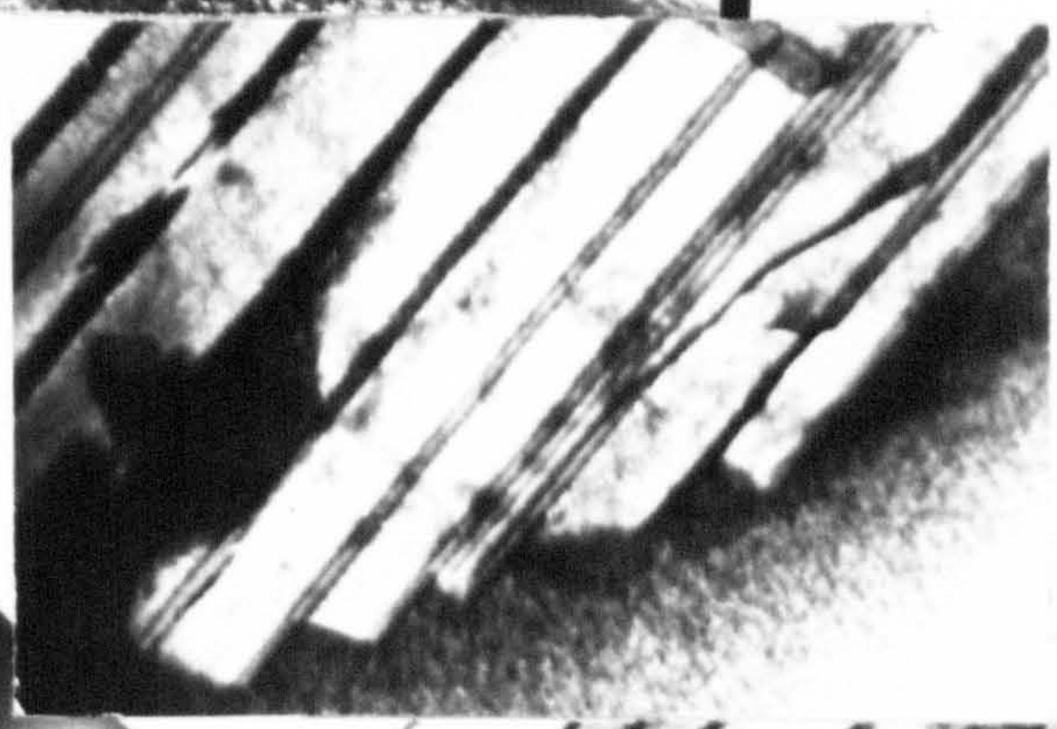

(c) 30° tilt

(e) SADP from interlamellar ferrite of (d) [110]

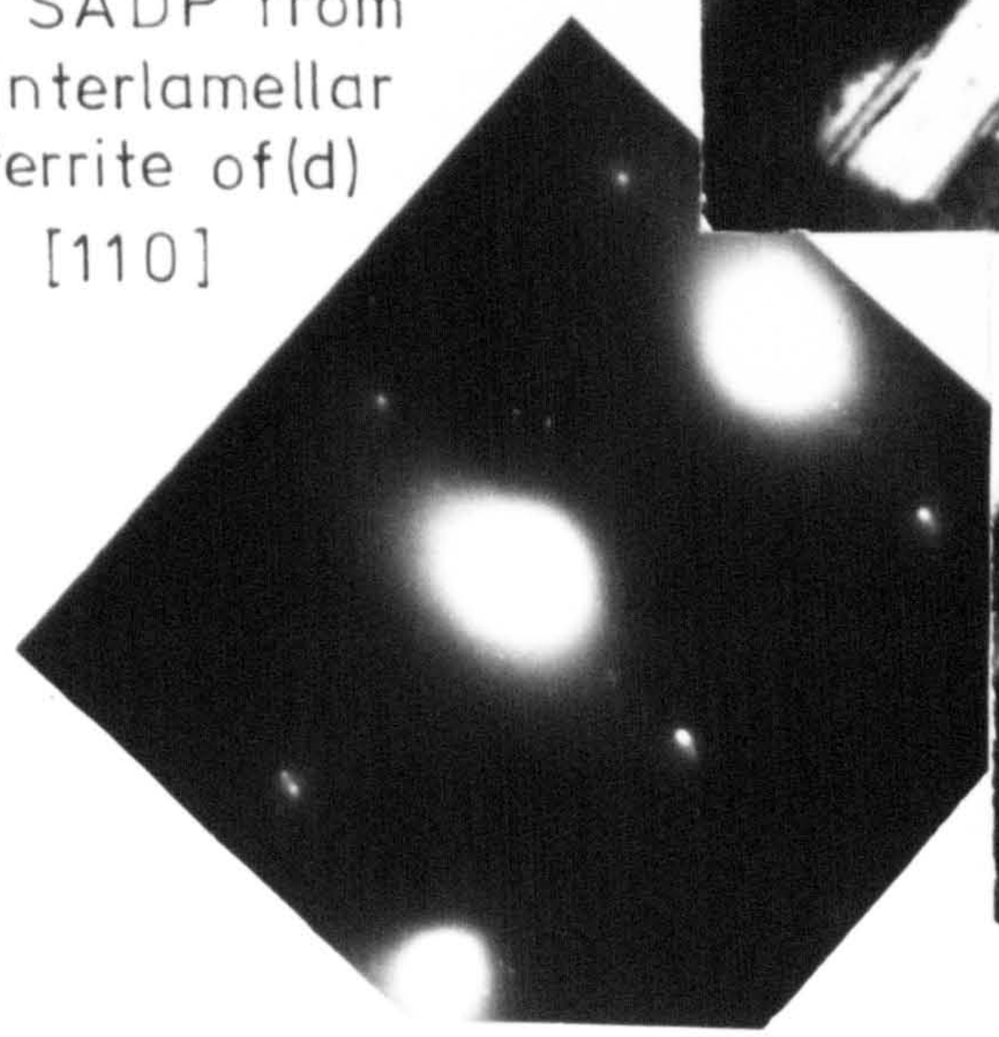

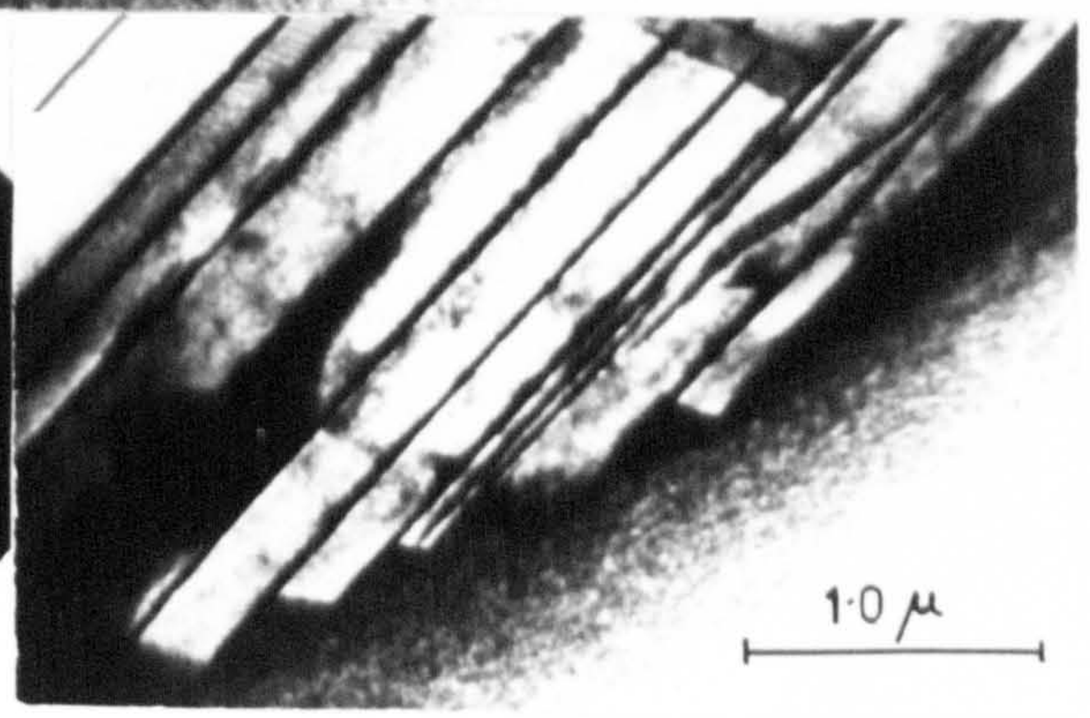

(d) 45° tilt

DISCONTINUOUS PRECIPITATION IN Fe – 4·0 wt.% W NITRIDED IN 8 % NH_3:H_2 AT 615 °C. FOR 24 h.

precipitate width was a minimum i.e. the plates are ultimately lying with their habit planes parallel to the electron beam. The S.A.D.P. accompanying Figure VI.17d was obtained from the interlamellar matrix and shows that the precipitate habit planes, as expected, are parallel to the $\{110\}_\alpha$ ferrite planes.

Unfortunately a diffraction pattern of the two parallel zones was not obtained; however Figure VI.18 shows a pattern from a specimen alligned such that $(311)_\alpha$ and $(02\bar{1})_{\delta'}$ are both nearly perpendicular to the electron beam, and the measured angle between $(\bar{1}21)_\alpha$ and $(200)_{\delta'}$ is about 5°. This is consistent with the orientation relationship;

$$(0001)_{\delta'} \parallel (011)_\alpha \quad ; \quad [11\bar{2}0]_{\delta'} \parallel [100]_\alpha$$

(Pitsch and Schrader, 1958)

which is illustrated in Figure VI.19a.

Preferential nucleation of cells at a boundary between α-grains A and B may be explained in a similar manner to that in the much studied Pb-Sn system (Turnbull, 1955).

Considering two ferrite grains A and B separated by a high angle boundary as shown in Figure VI.19b. δ' nucleates adjacent to the boundary in grain A with an orientation relationship which minimises the interfacial energy between δ' and $A\alpha$. For δ' to grown into $A\alpha$ the reaction requires volume diffusion of tungsten atoms in grain A. Instead δ' branches and grows into grain B causing the $A\alpha$ -$B\alpha$ boundary to move so as to maintain the desired

Fig. VI.18

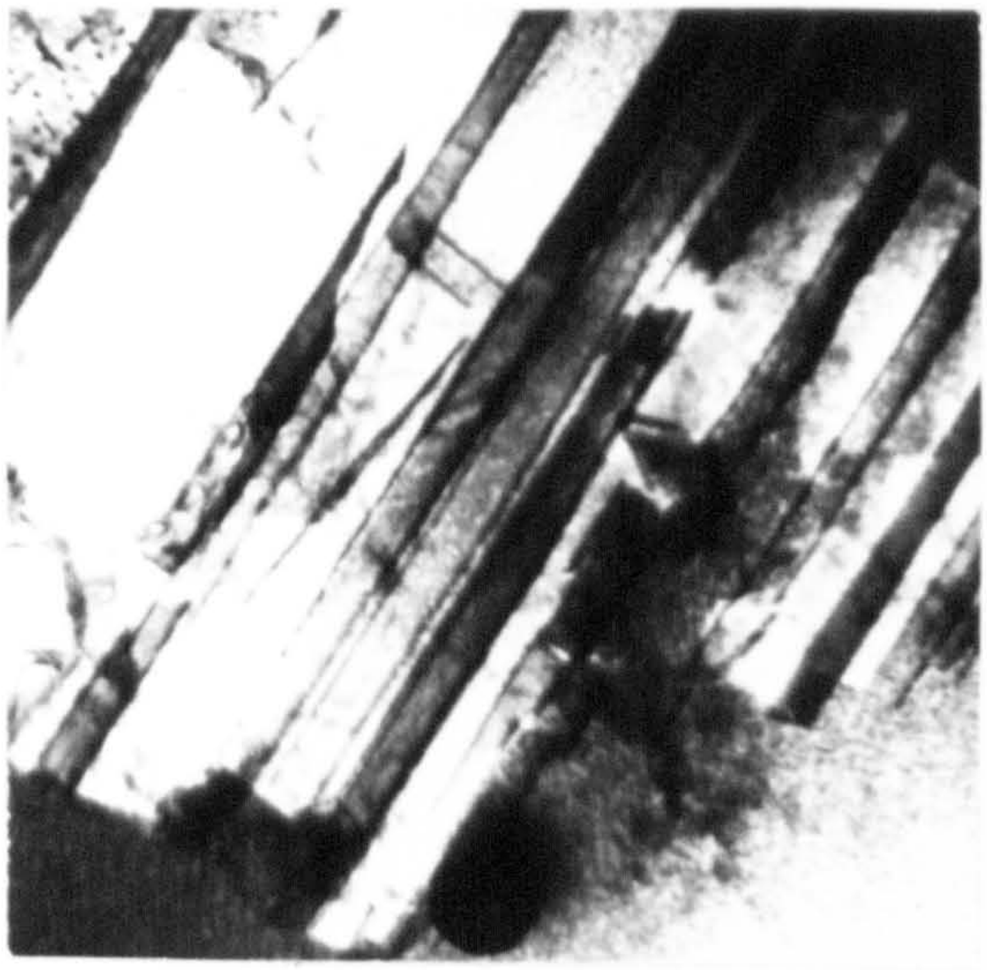

(a) Fe – 4·0 wt % W nitrided in 8 % NH_3 : H_2 at 615 °C for 24 h.

1·0 μ

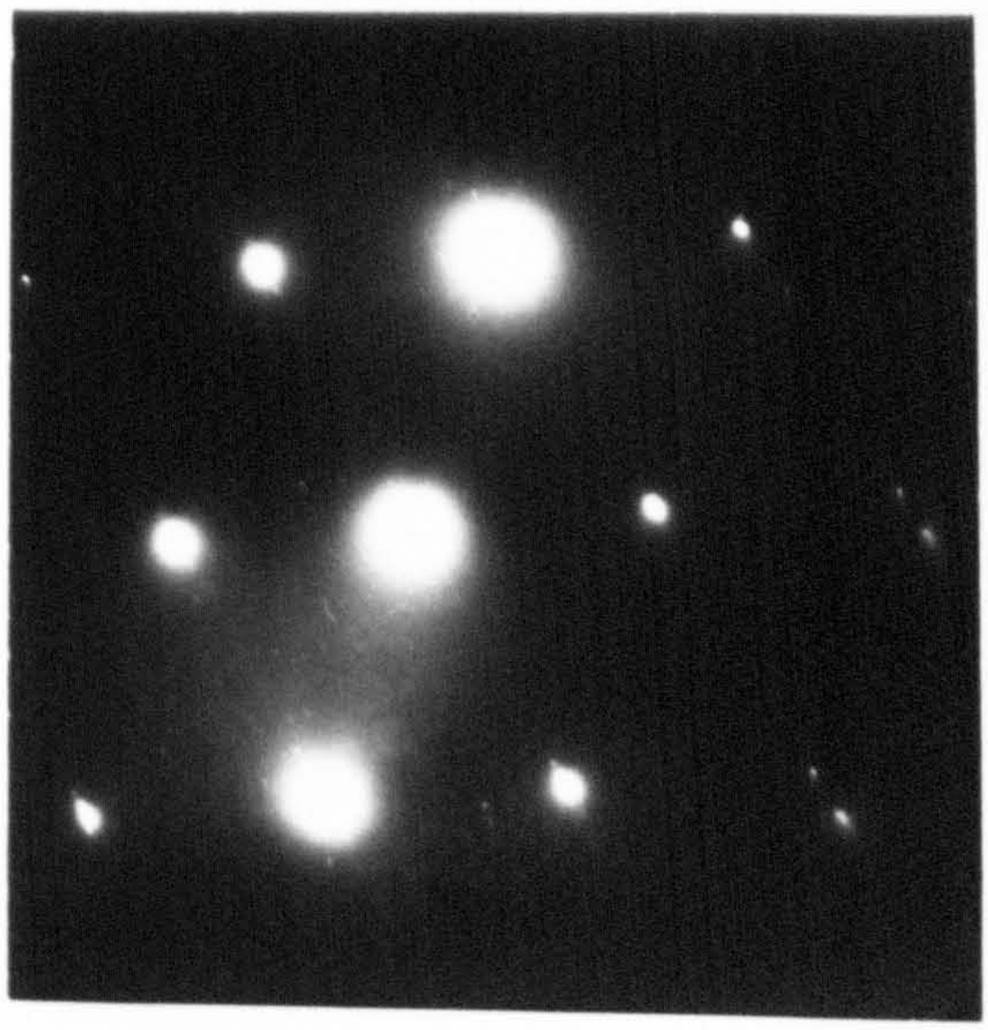

(b) SADP from (a)

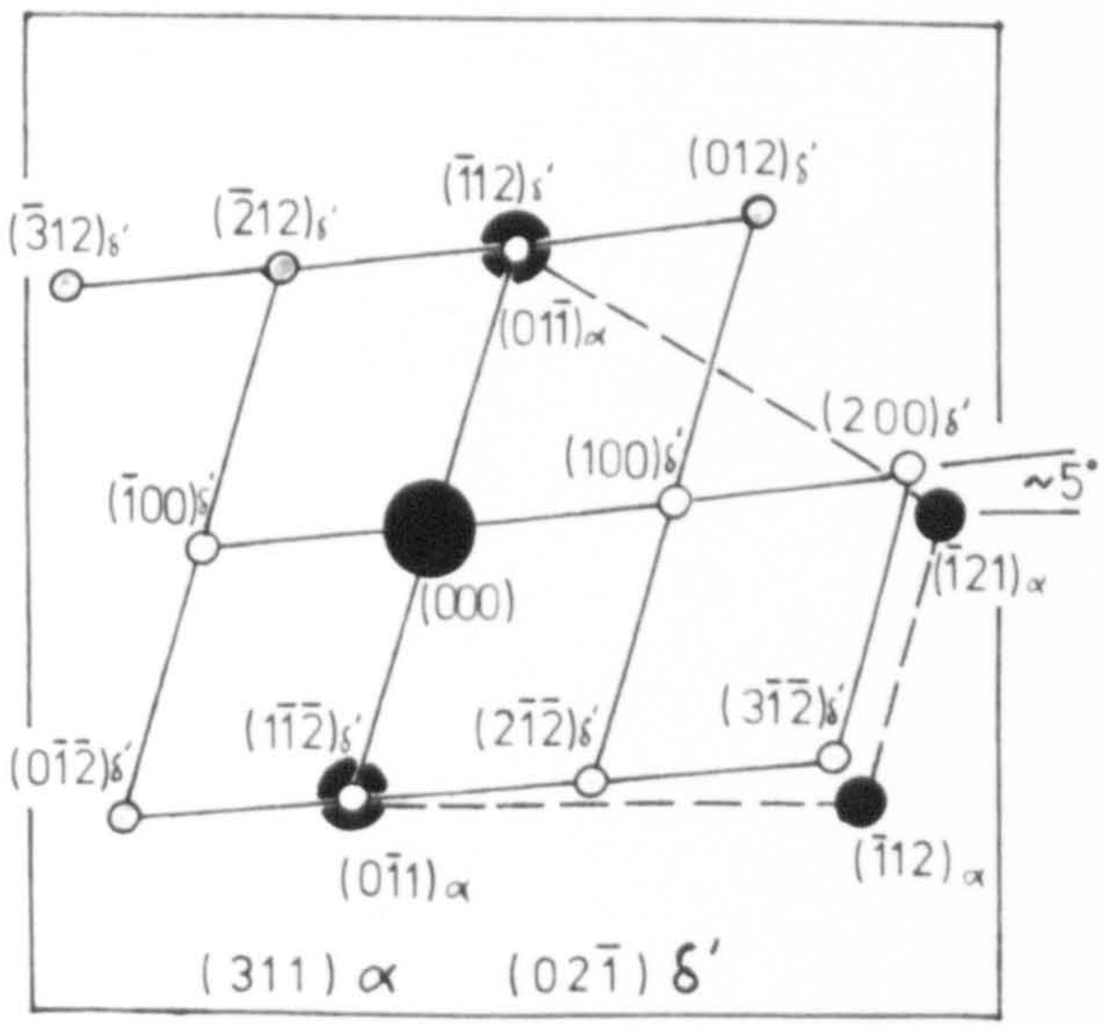

(c) Fe – 2·05 wt % W nitrided in 8% NH_3 : H_2 at 615 °C for 24 h. and subsequently aged at 650 °C for 24 h.

1·0 μ

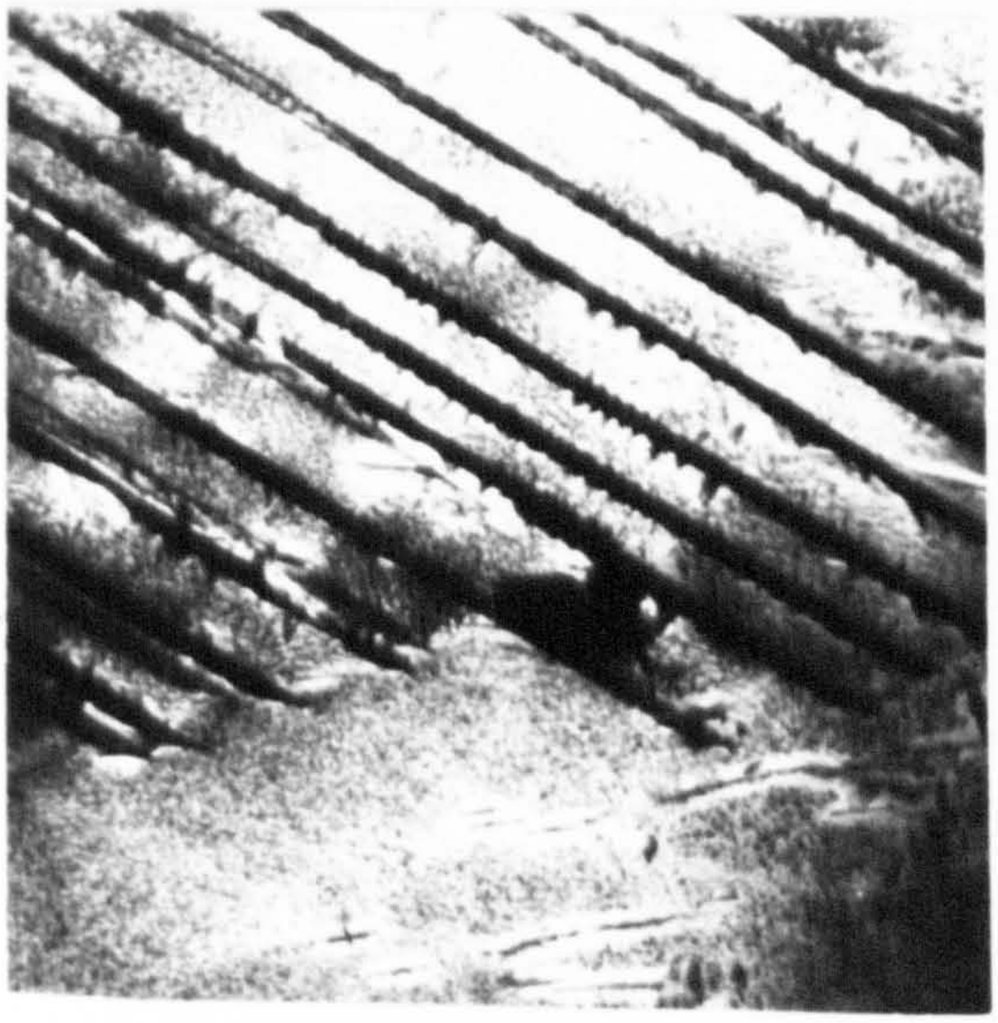

DISCONTINUOUS PRECIPITATION OF δ'–$W_{0\cdot9}$(N,O) IN NITRIDED Fe – W ALLOYS.

Fig. VI. 19

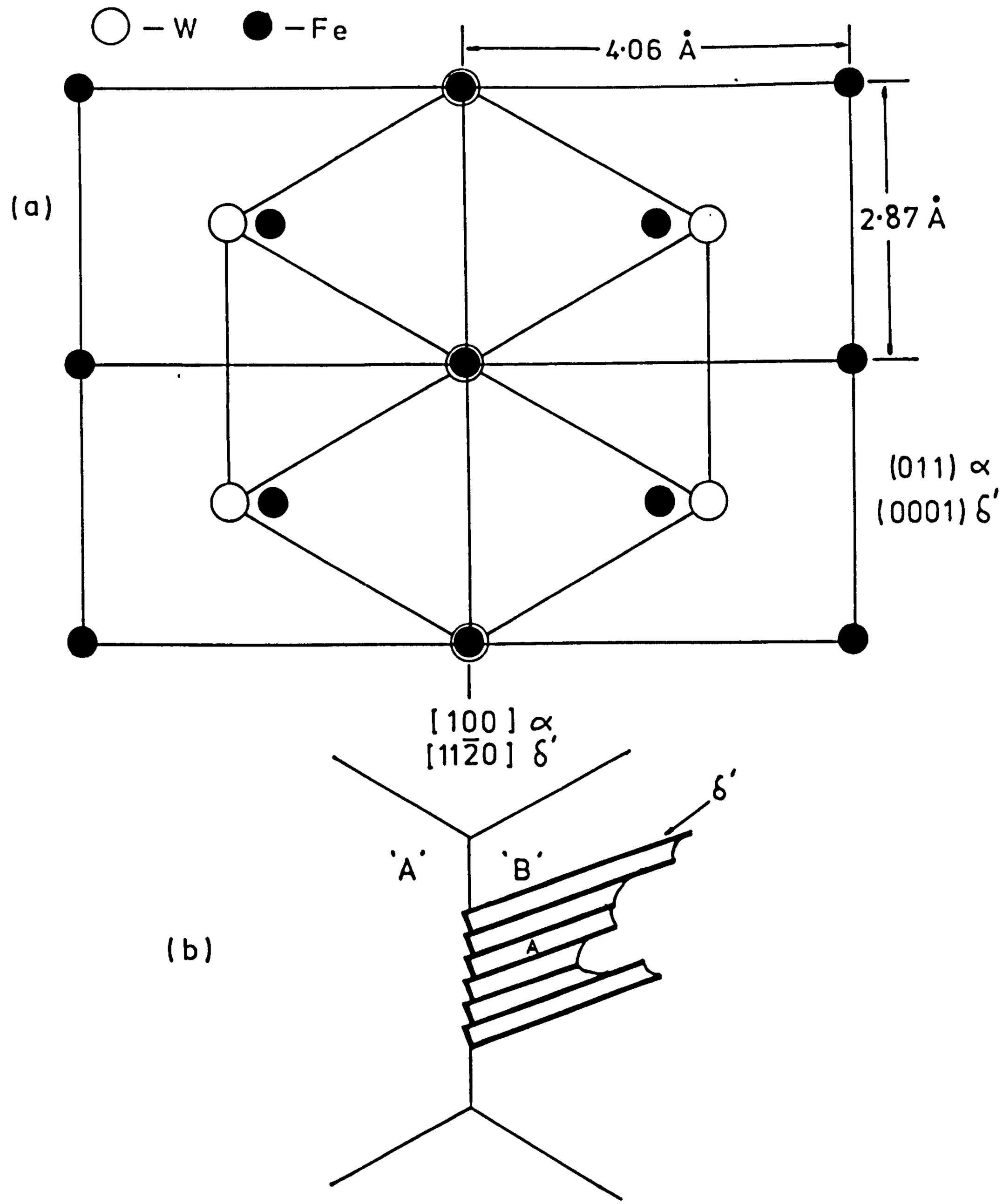

PRECIPITATION OF δ'-$W_{09}(N,O)$ IN α-Fe DURING CONSTANT ACTIVITY NITRIDING.

orientation relationship and produce a diffusion short circuit.

Previous studies of discontinuous precipitation have involved measuring reaction rates for precipitation in a supersaturated solid solution. In such cases the diffusion coefficient controlling the transport of solute atoms has been shown to be several orders of magnitude greater than the experimentally determined volume diffusion coefficients (Turnbull, 1955), and the kinetics of the process can be described in terms of two parameters, the grain boundary diffusion coefficient and the net free energy decrease during recrystallisation (Cahn, 1959). In the Pb-Sn system only about 60% of the thermodynamic excess of Sn in solution is precipitated by diffusion along the migrating boundary as it traverses the grain, the remainder being left in solution and eventually precipitating via the slower lattice diffusion to adjacent lamellae (Turnbull and Treaftis, 1955).

Subsequent studies of discontinuous precipitation in systems where the initial decomposition of the supersaturated solid solution is by prior continuous precipitation, showed that on the basis of the Turnbull theory the kinetics more closely followed those expected for predominant lattice diffusion. However for Al-Ag alloys, Aaronsson and Clark (1968) showed that the reaction was D_B controlled when account was taken of the considerable reduction in driving force for discontinuous precipitation, due to the low solute activity in equilibrium with the continuous precipitate.

The kinetics of precipitation were not studied in the present work but by the argument of Aaronsson and Clark it would appear that the thermodynamic excess available for discontinuous precipitation is greater in the low tungsten alloys e.g. Fe-2.05 wt.%W, because the activity of tungsten prior to cellular growth in the higher alloys is rapidly reduced to that in equilibrium with the intermediate phase. The most noticeable difference between discontinuous precipitation with and without prior continuous precipitation is revealed in Figure VI.18d. In this alloy, without prior continuous precipitation of intermediate phase (the fine homogeneous distribution has been produced at room temperature) considerable branching of lamellae is evident whereas with high tungsten contents (Figure VI.16 and VI.17) this is never observed. When the advancing boundary passes through a random solid solution some of the solute remains and segregation is incomplete (cf. Pb-Sn alloys). The remaining solute eventually diffuses through the lattice to adjacent laths causing additional growth. Conversely, as the moving boundary passes through a depleted solution containing intermediate precipitate, partial segregation has already occurred and the solute is located in small regions of high concentration, allowing virtually complete segregation by a grain boundary diffusion mechanism.

One commonly observed feature is the association of parts of the migrating boundary with the broad faces of lamellae in order to reduce the total boundary surface area. This leads to pinning of the moving boundary at interlamellar debris (D on Figure VI.16); such particles are probably

formed when the moving boundary is suitably orientated locally for nucleation in the special orientation relationship (Tu and Turnbull, 1968).

The predominating form of precipitation during aging (continuous or discontinuous) is that which provides the highest rate of change of free energy i.e. that for which $d\Delta G/dt$ is greatest (Kelly and Nicholson, 1963). Thus although allowing a greater overall decrease in net free energy, discontinuous precipitation is restricted in the early stages of nitriding in favour of the higher rate of decrease which accompanies rapid formation of the metastable intermediate precipitate. It is only in the later stages that discontinuous precipitation of the equilibrium nitride predominates.

VI.6 High temperature aging of nitrided alloys

Aging of nitrided alloys in the range 650-800°C in vacuum produces coarsening of the intermediate precipitate and growth of the equilibrium phase.

(a) The intermediate phase

Alloys containing less than about 4.0 wt.%N do not form GP zones during nitriding, but exhibit slow heterogeneous precipitation. Consequently the matrix always contains nitrogen in equilibrium with the gas phase, and if the concentration is high ($>\sim$0.06 wt.%) the solution decomposes homogeneously at room temperature.

When such an alloy is subsequently aged at 650°C the high concentration of nitrogen is again present in solution and additional precipitation of Fe-W-N intermediate phase occurs. The high concentration of nitrogen remains in the matrix until it is precipitated as intermediate phase and if the treatment is interrupted before precipitation is complete, Fe-N GP zones are again formed on cooling to room temperature (Figure VI.20a).

Figure VI.20b shows the microstructure obtained after aging a partially nitrided Fe-5.05 wt.%W alloy at 650°C. Prior to aging, the alloy contains Fe-W-N GP zones and the microstructure is that shown in Figure VI.2a. During aging the GP zones transform to intermediate phase and coarsen, in this case from 200 Å diameter zones to 1000 Å diameter precipitates, at which point electron diffraction patterns exhibit "superlattice spots". In contrast to the previously discussed low tungsten-ferrites no substantial amount of nitrogen is available for additional precipitation at 650°C.

(b) The equilibrium phase

Alloys overage to the equilibrium condition by one of two methods depending on the residual concentration of nitrogen in ferrite after initial nitriding. Discontinuous precipitation of δ'-$W_{0.9}(N,O)$ during constant activity aging is a slow process and therefore after homogeneous precipitation has ceased, the matrix rapidly attains equilibrium with respect to the nitrogen activity of the gas phase. Subsequent high temperature aging leads

Fig. VI. 20

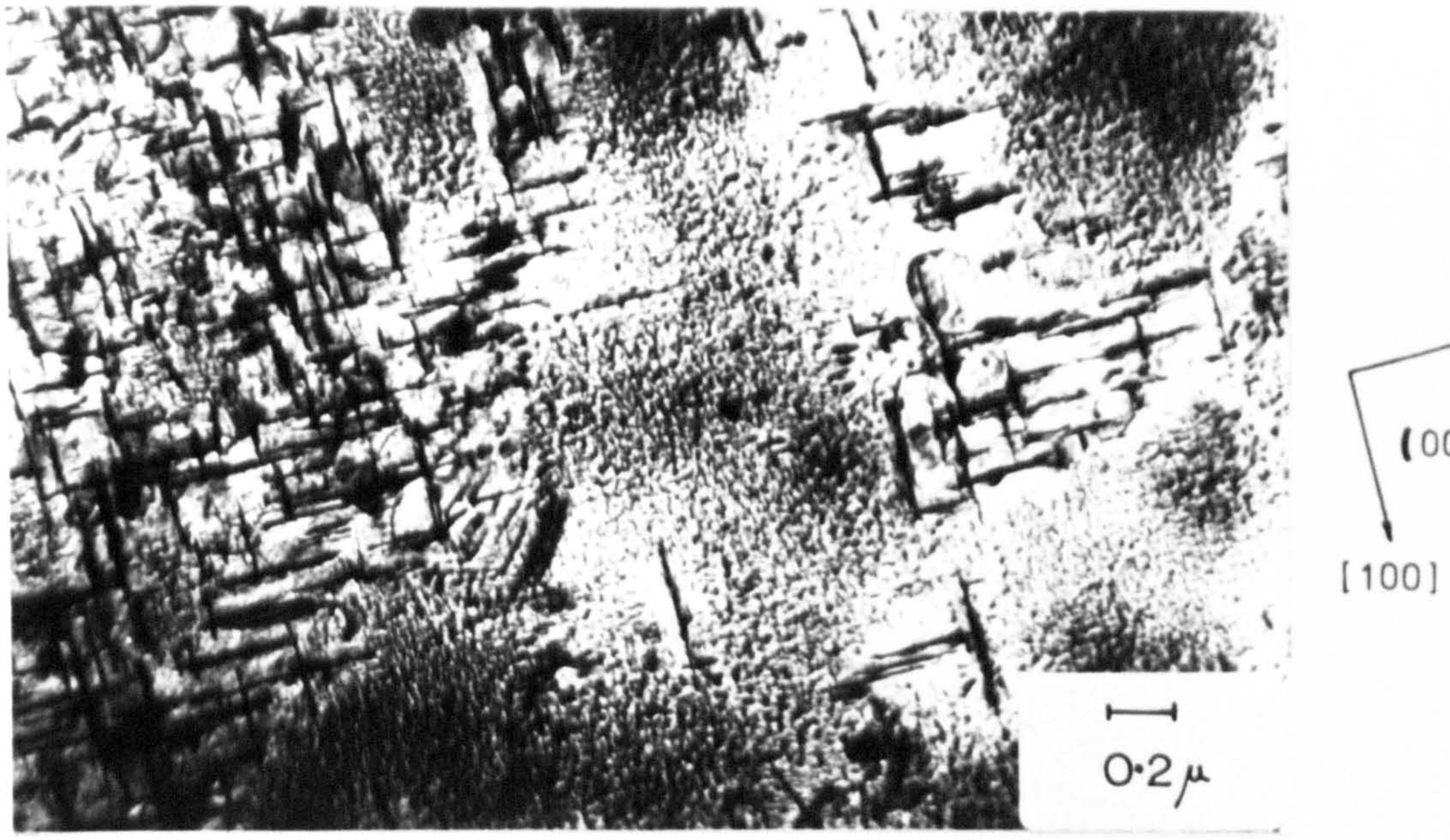

Fe 3·5 wt % W NITRIDED IN 8 % NH_3:H_2 AT 615 °C FOR 24 h. AND SUBSEQUENTLY AGED AT 650 °C FOR 48 h.

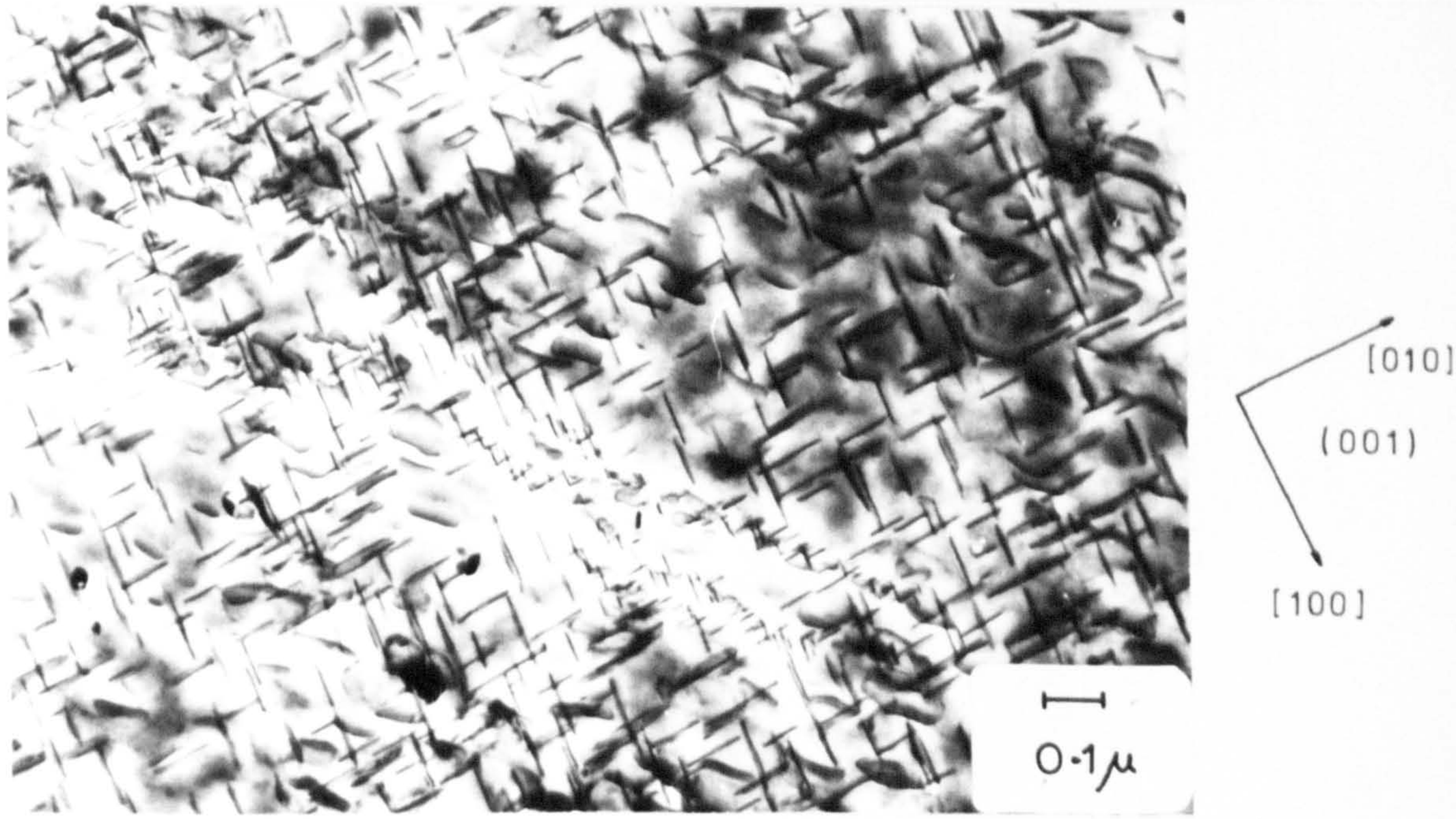

Fe 5·05 wt % W NITRIDED IN 8 % NH_3:H_2 FOR 8 h. AND SUBSEQUENTLY AGED AT 650 °C FOR 24 h.

to the formation of nitrogen-austenite if the temperature exceeds some critical value which depends on the nitrogen concentration of the ferrite. The solubility of nitrogen in α-Fe decreases from about 0.1 wt.% at 600°C to zero at 910°C and hence the higher the nitrogen content (i.e. the higher the nitrogen potential used during nitriding), the lower will be the $\alpha \rightarrow \gamma$ transformation temperature.

Figure VI.21 shows micrographs of nitrided Fe-5.05 wt.% W alloys aged below and above the $\alpha \rightarrow \gamma$ transformation temperature respectively. At 650°C (Figures VI.21a and VI.21b) cellular discontinuous precipitation has occurred by the same mechanism as discussed in the previous section, that is, recrystallisation without any change in crystal structure of the matrix:

$$\alpha\text{-Fe} + \text{intermediate phase} \rightarrow \alpha\text{-Fe} + \text{equilibrium phase}$$

At 750°C (Figures VI.21c and Vi.21d) a network of nitrogen-austenite is nucleated at ferrite grain boundaries and advances into the grains, consuming the intermediate precipitate and reprecipitating the equilibrium phase in a non-lamellar distribution. The austenite eventually becomes depleted of nitrogen due to precipitation of nitrides and re-transforms to ferrite:

$$\alpha\text{-Fe} + \text{intermediate phase} \rightarrow \gamma\text{-Fe} \rightarrow \alpha\text{-Fe} + \text{equilibrium phase.}$$

Fig. VI.21

a. X 220

b. X 2350

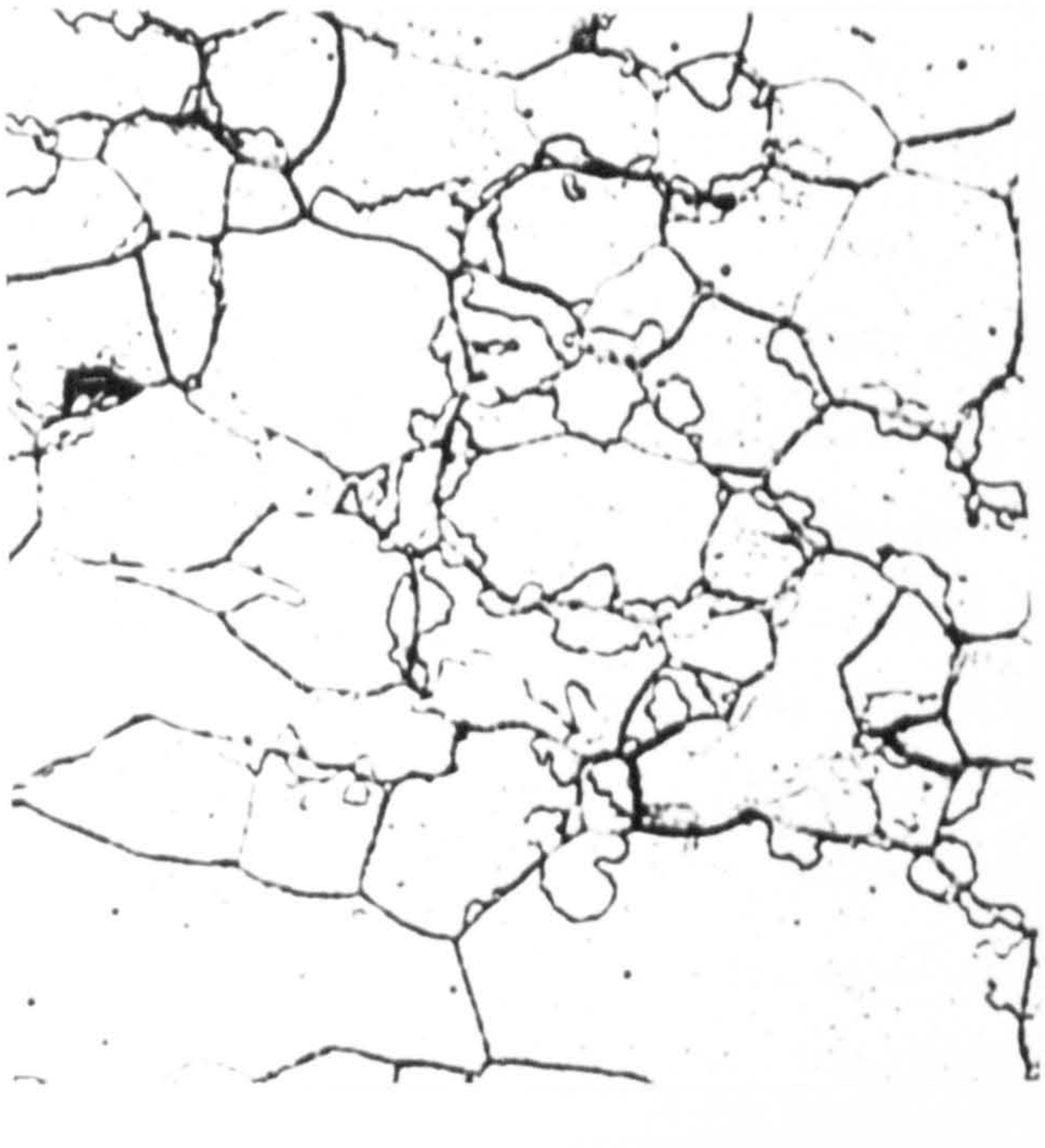

c. X 320

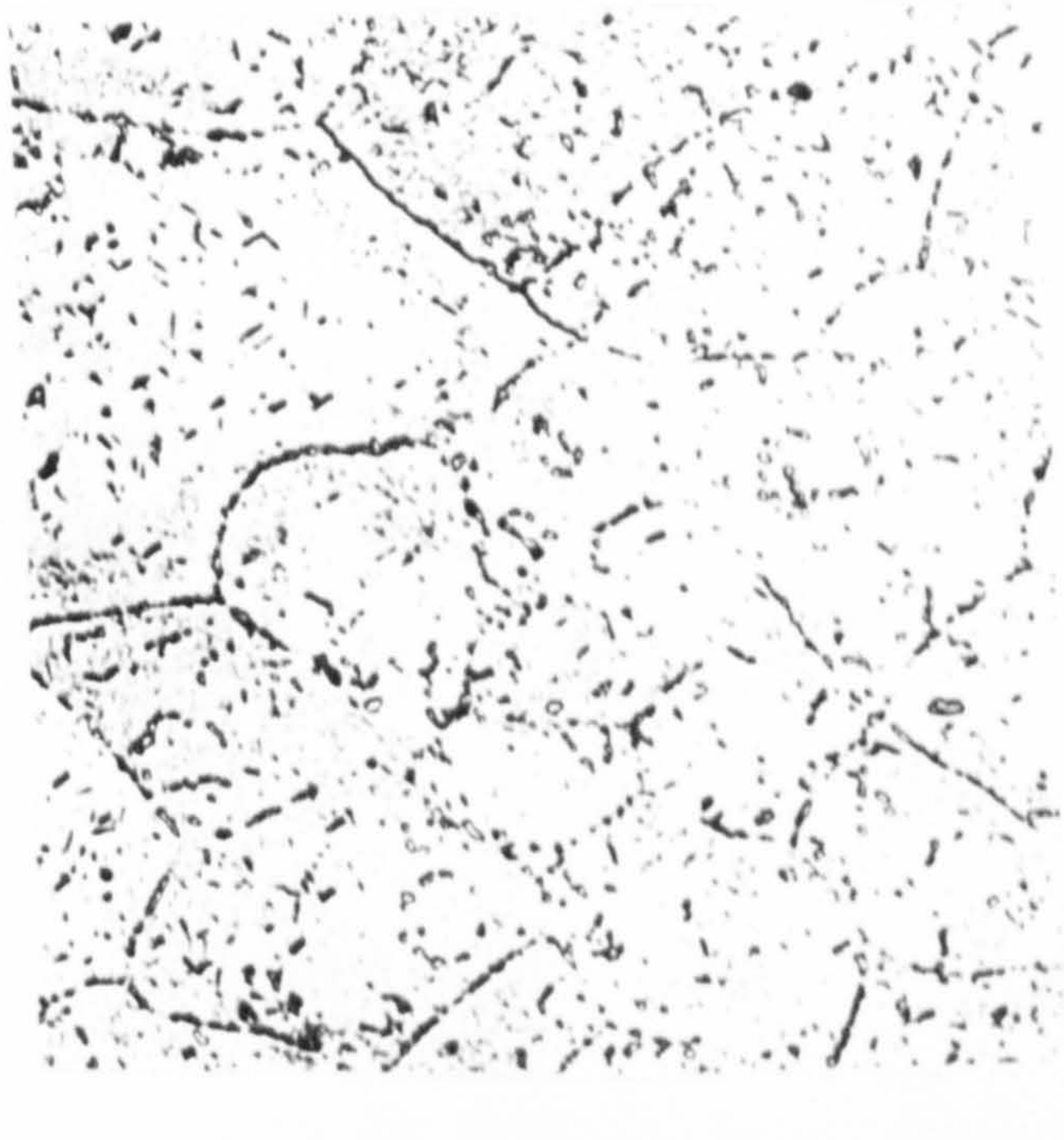

d. X 480

Fe - 5wt% W alloys nitrided for 48 hrs at 605° C in 9% NH_3 - H_2 and subsequently aged in vacuum.

a. 116 hrs at 650°C

b. 116 hrs at 650 °C

c. $2\frac{1}{4}$ hrs at 750°C

d. 98 hrs at 750 °C

The δ' oxy-nitride is produced only when precipitation proceeds in a nitriding atmosphere which also provides a continuous oxygen supply. The sequence of phases observed when a specimen is overaged in vacuum can be explained using the equilibrium diagram constructed from the pressure nitriding observations of Chapter V. Figure VI.22 shows the phases present at various stages of averaging at 750°C; the observations can be summarised as follows:

α-Fe	$\rightarrow$ γ-Fe	$\rightarrow$ α-Fe	$\rightarrow$ α-Fe
+ intermediate	+ δ-WN	+ δ-WN	+ η_1-$Fe_3W_3N(O)$
phase	+ η_1-$Fe_3W_3N(O)$	+ η_1-$Fe_3W_3N(O)$	+ η_3-$Fe_6W_6(N,O)$
0 h.	2h.	25h.	100h.

Immediately after nitriding the alloy consists of a homogeneous distribution of intermediate phase particles in a matrix of almost saturated nitrogen-ferrite. On heating to 750°C austenite is nucleated and some intermediate phase dissolves increasing the tungsten content of the matrix. At the advancing γ-α interface, where the precipitation reaction occurs, local variations in the matrix tungsten content exist. In accordance with Figure V.14, δ-WN is nucleated when the tungsten in solution is low, but has only a temporary existence since the alloy is of sufficiently high tungsten content for the resultant equilibrium phase to be η_1-$Fe_3W_3N(O)$. The presence of the lower nitride η_3 probably reflects the oxygen content of the alloy since such phases are known to accommodate more oxygen than their M_6N

Fig. VI.22

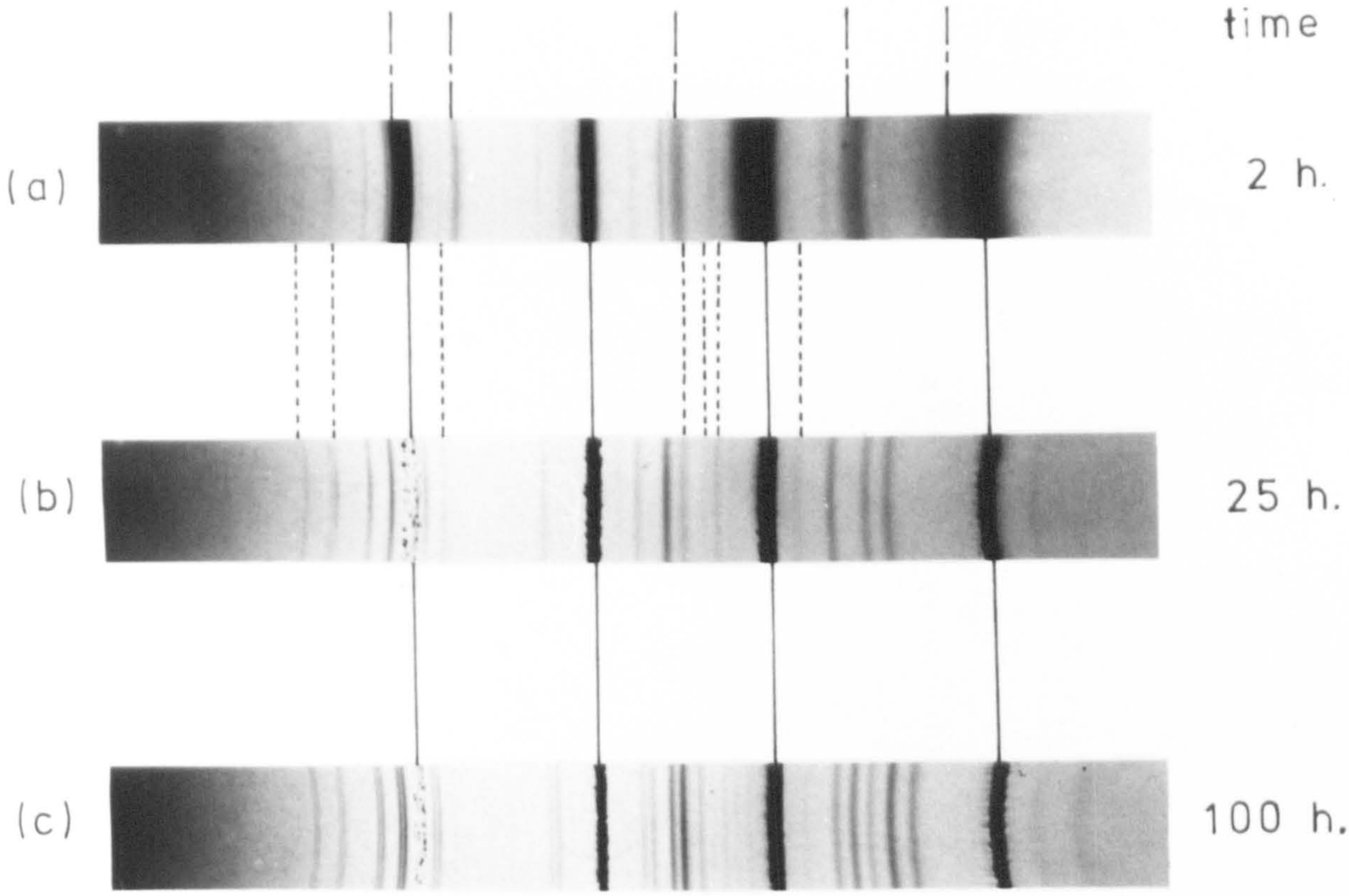

——— γ - Fe

——— α - Fe

..... δ - WN

unmarked η_1 - Fe_3W_3N

η_3 - Fe_6W_6N

(a) — ($\alpha + \gamma + \alpha' + \delta + \eta_1$)

(b) — ($\alpha + \delta + \eta_1$)

(c) — ($\alpha + \eta_1 + \eta_3$)

X-RAY DIFFRACTION PATTERNS SHOWING PHASES PRECIPITATED IN NITRIDED Fe-5·05% W (9% NH_3:H_2 A 600 °C FOR 2 DAYS) SUBSEQUENTLY AGED IN VACUUM AT 750 °C

equivalents (Nutter, 1969). It appears that the prior intermediate phase provides a source of oxygen which is insufficient for the formation of δ'-$W_{0.9}(N,O)$ but is in excess of that which can be accommodated by η_1-$Fe_3W_3N(O)$. The amount of η_1 produced is controlled by the tungsten concentration of the alloy (since there is excess nitrogen), and it is probably significant that the η_3-oxy-nitride is only present after long times when the residual oxygen-tungsten ratio has increased.

Chapter VII

THE STABILITY OF THE INTERMEDIATE PRECIPITATE AND THE CONDITIONS FOR FORMATION OF G.P. ZONES

VII.1 Introduction

The concept of metastable equilibrium can be used whenever the approach to true thermodynamic equilibrium is slow compared to some other reaction, e.g. carbon steels invariably contain cementite although this is metastable with respect to graphite. The Fe-N system shows particularly good examples of metastable equilibrium since even the so-called "equilibrium nitrides" are metastable with respect to $N_2(g)$ at 1 atmosphere. Dijkstra's internul friction results (1949) for aging of nitrogen-ferrite are reproduced in Figure VII.1 and show quite clearly two stage precipitation behaviour. Q^{-1}_{max} is proportional to the concentration of nitrogen in solution and the plateaux in the aging curve represent regions of metastable equilibria.

The first precipitate α''-$Fe_{16}N_2$ is the least stable phase and is therefore in metastable equilibrium with a relatively high nitrogen activity compared to γ'-Fe_4N which is formed after longer aging times. At 1 atmosphere pressure even Fe_4N is unstable and if aging were continued nitrogen would be evolved and the alloy would eventually consist of only a very dilute solution of nitrogen in α-Fe.

Fig. VII.1

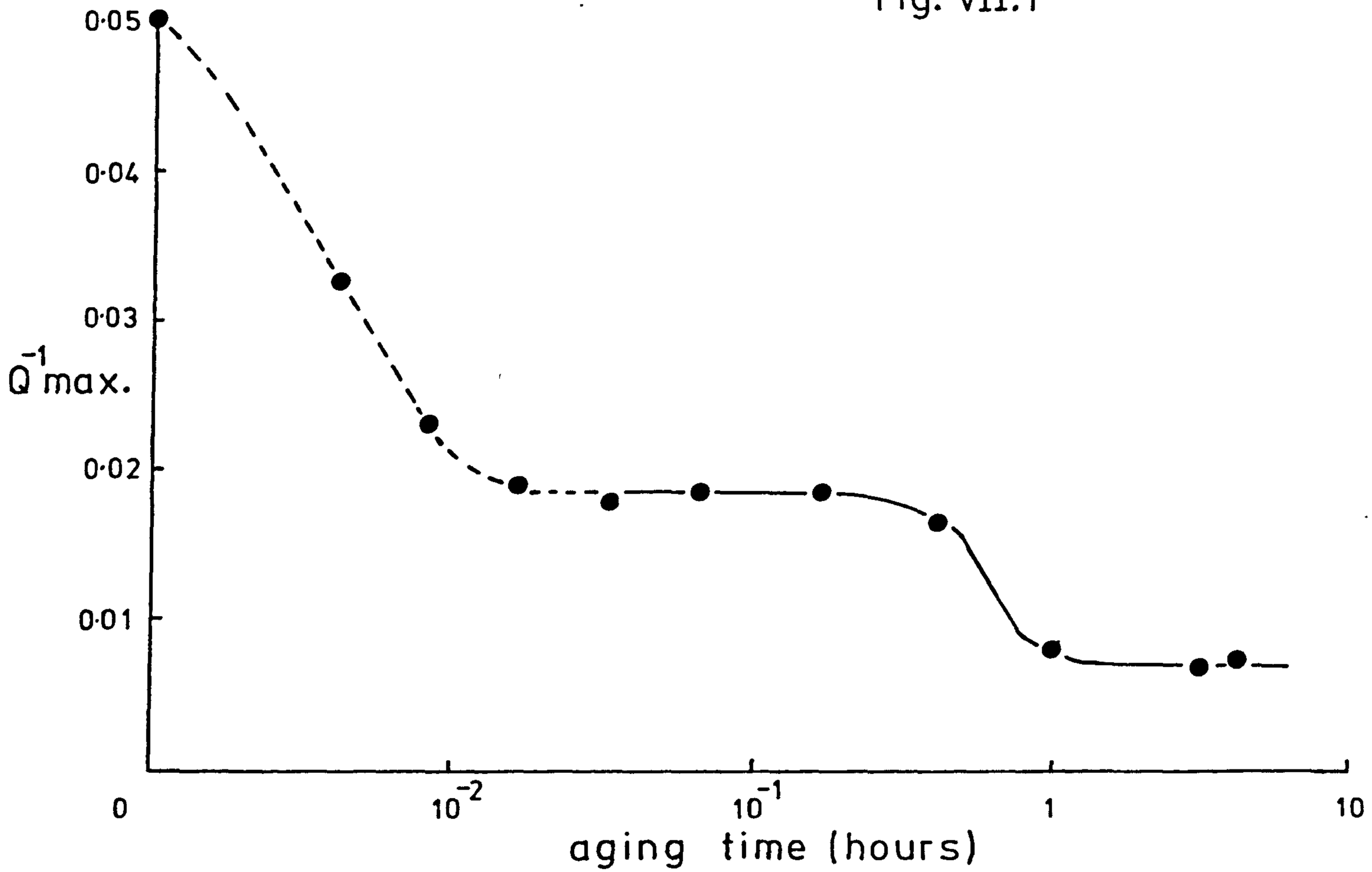

INTERNAL FRICTION V AGING TIME FOR Fe~0·05 wt.% N AGED AT 250 °C

[from Dijkstra, 1949]

Thus in true thermodynamic terms the low temperature aging of Fe-N alloys at 1 atmosphere $N_2(g)$ is a three stage process.

The precipitation of intermediate phase in nitrided Fe-W alloys is rapid compared to the approach to true equilibrium, and so the application of metastable equilibrium concepts is valid. Both metallography and weight changes indicate that discontinuous precipitation of the equilibrium phase is slow and any change in the nitriding conditions which affects the intermediate precipitate or the matrix is quickly registered.

VII.2 The stability of the intermediate precipitate

Figure VII.2 illustrates an experiment carried out to examine the effect of changes in the nitrogen activity on the alloy in the nitrided state. The standard nitriding curve for Fe-5.05 wt.%W in 8%NH_3:H_2 at 615°C shows a weight increase of 0.32% at saturation. Under these conditions after complete precipitation, the matrix α-Fe contains about 0.09 wt.%N, leaving 0.23 wt.%N present as intermediate phase. Assuming all the tungsten to be precipitated, the composition of the phase is determined as (Fe)W1.75 N, where the concentration of iron is not known precisely but is small. When the nitrogen activity is reduced, the specimen saturates at some smaller nitrogen content characteristic of the nitrogen potential.

Fig.VII.2

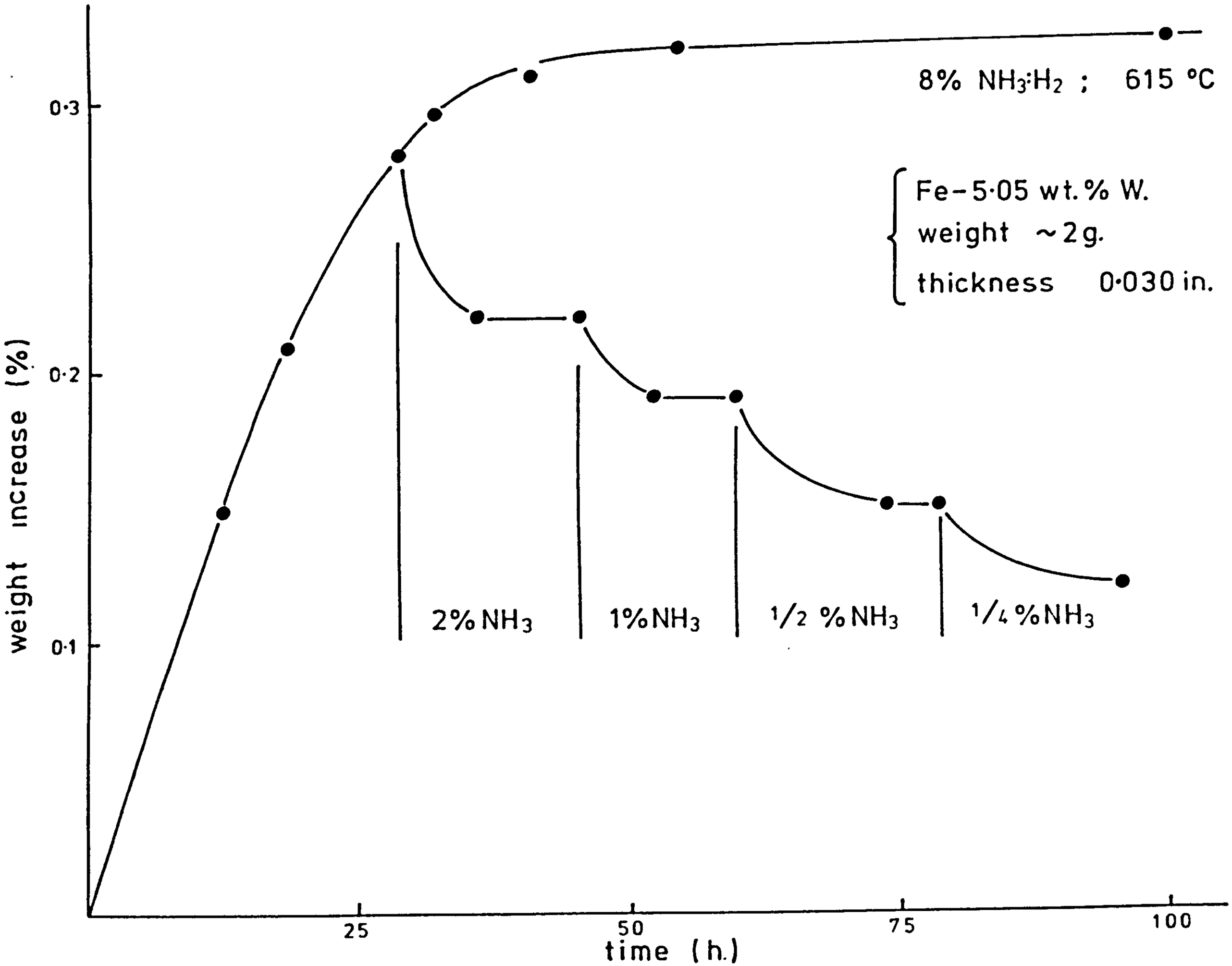

WEIGHT INCREASE V. TIME FOR Fe-5·05 wt.% W. AT VARIOUS NITROGEN POTENTIALS.

The equilibrium constant K_1 for the formation of the intermediate phase is given by:

$$(Fe) + 1.75\,\underline{W}^{\alpha} + \underline{N}^{\alpha} = (Fe)\,W_{1.75}N \qquad \ldots\ (VII).1$$

$$K_1 = \frac{a_{(Fe)W_{1.75}N}}{a_{Fe} \cdot a_{\underline{W}^{\alpha}}^{1.75} \cdot a_{\underline{N}^{\alpha}}} \qquad \ldots\ (VII).2$$

$$= \frac{1}{a_{\underline{W}^{\alpha}}^{1.75} \cdot a_{\underline{N}^{\alpha}}} \qquad \ldots\ (VII).3$$

where $a_{\underline{W}^{\alpha}}$ is the activity of tungsten

$a_{\underline{N}^{\alpha}}$ is the activity of nitrogen

$a_{Fe} = a_{(Fe)\,W_{1.75}N} = 1$

If Henry's Law is obeyed for tungsten in α-Fe up to about 1 at.%, then:

$$\underline{a_{W^{\alpha}} = k_h \cdot \%\,\underline{W}^{\alpha}} \qquad \ldots\ (VII).4$$

where $\%\underline{W}^{\alpha}$ is the wt.%W in α-Fe

and K_h is Henry's Law constant for W in α-Fe

The nitrogen activity of an ammonia : hydrogen gas mixture (see Chapter II) is given by:

$$a_{\underline{N}^{\alpha}} = K_2 \, p_{NH_3} / p_{H_2}^{3/2} \qquad \ldots\ldots (VII).5$$

where p_{NH_3} is the partial pressure of ammonia

p_{H2} is the partial pressure of hydrogen

K_2 is an equilibrium constant

Substituting (VII).4 and (VII).5 into (VII).3 gives:

$$K_1 = \frac{1}{(k_h \cdot \%\underline{N}^{\alpha})^{1.75} \cdot K_2 \cdot p_{NH_3} / p_{H^2}^{3/2}} \qquad \ldots\ldots (VII).6$$

$$\text{i.e.} \quad (\%\underline{N}^{\alpha})^{1.75} = K_3 \cdot p_{H_2}^{3/2} / p_{NH_3} \qquad \ldots\ldots (VII).7$$

$$\text{hence:} \quad 1.75 \log \%\underline{N}^{\alpha} = \log K_3 + \log p_{H_2}^{3/2} / p_{NH_3} \qquad \ldots\ldots (VII).8$$

where K_3 is the reciprocal of $(k_h^{1.75} \cdot K_1 \cdot K_2)$

If the assumptions are valid and the plateaux on Figure VII.2 correspond to metastable equilibrium between tungsten, nitrogen and the intermediate phase, then a plot of $\log \%\underline{W}^{\alpha}$ v $\log\left(p_{H_2}^{3/2}/p_{NH_3}\right)$ should be linear of slope equal to 0.57.

The tungsten concentration of the matrix is given by the difference between the total tungsten contant (5.05 wt.%), and that present in the precipitate, the latter being determined from the total weight increase assuming the composition of the precipitate to be constant. The derived data are listed in Table VII.1.

Figure VII.3 shows the required plot of slope 0.55 and in view of the limitations of the procedure the agreement is surprisingly good. The plot describes the conditions under which the intermediate phase is stable at 615°C. The results predict that even with only 1 atmosphere $N_{2(g)}$ the precipitate is stable with an alloy content of $\geq$ 4 wt.%W. Conversely, in 8%NH_3:H_2 the phase is stable with only 0.4 wt.%W although electron microscopy of nitrided Fe-0.5 wt.%W failed to detect any intermediate precipitate.

The intermediate precipitate in Fe-W-N alloys is analagous to other intermediate configurations in conventional age-hardening systems e.g. θ in Cu-Al, but whereas in a binary system the two parameters which describe the solvus are solute activity and temperature, in a ternary system the solvus for a precipitate involving both solutes is determined

Table VII.1

Weight increase data for Fe-5.05 wt.%W in various nitriding potentials at 565°C

$NH_3:H_2$	$\%\underline{N}^{\alpha\text{-eq}}$	weight increase (%)	N precipitated (wt.%)	$\%\underline{W}$
8:92	0.09	0.32	0.23	-
2:98	0.02	0.22	0.20	0.70
1:99	0.01	0.19	0.18	1.10
0.5:99.5	0.005	0.15	0.15	1.80
0.25:99.75	0.003	0.12	0.12	2.45

Fig. VII. 3

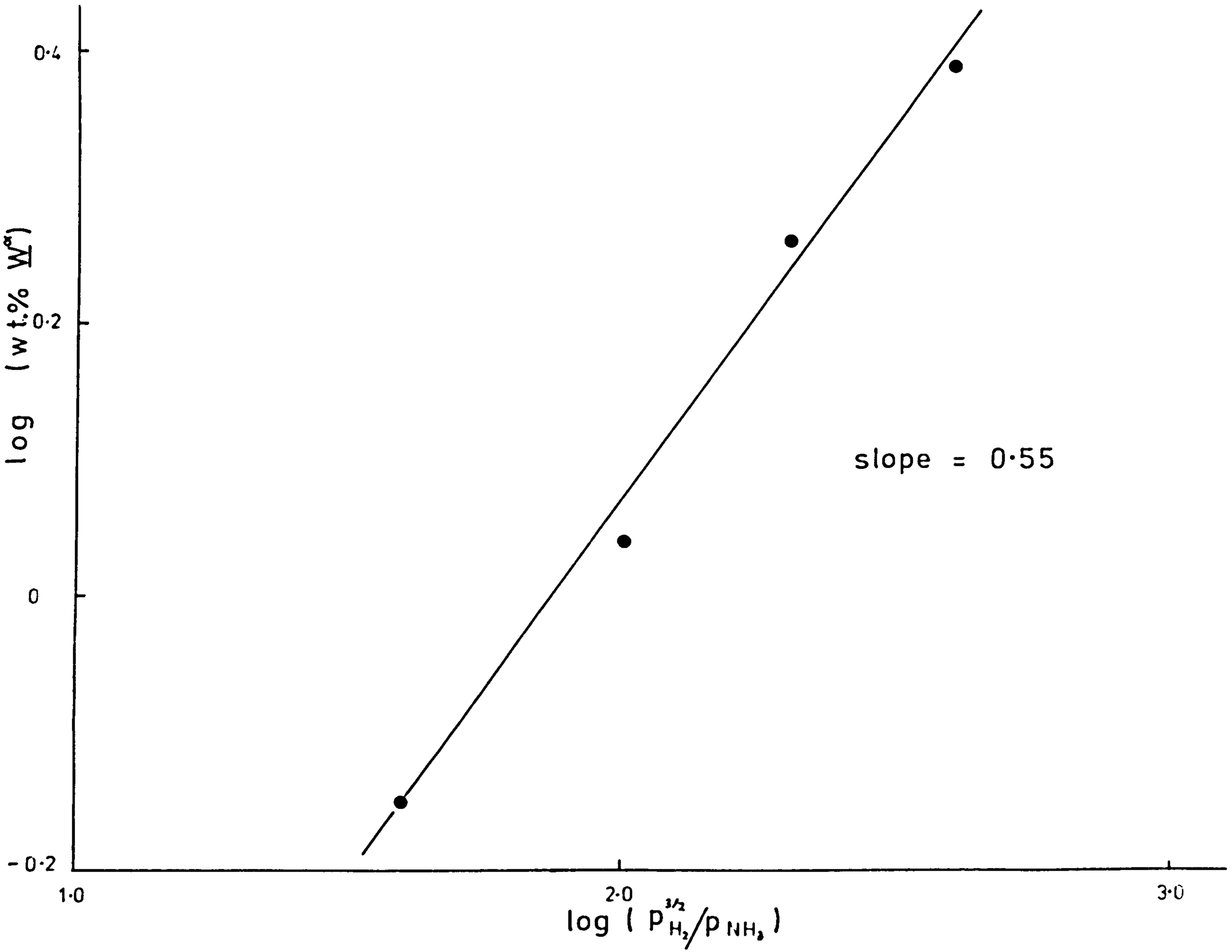

THE SOLUBILITY OF Fe-W-N INTERMEDIATE PHASE AT 615 °C

by two solute activities together with the temperature. In this case the temperature has been maintained constant but since one of the solutes is controlled by a gas phase, dissolution of the precipitate is achieved by varying the solute activity.

VII.3 Internal friction observations in Fe-5.05 wt.%W-0.1 wt.%N

Dijkstra's results (1949, see Figure VII.1) illustrate the use of internal friction in studying precipitation in Fe-N alloys.

The physical origin of the low temperature (20-40°C) internal friction peak in Fe-N and Fe-C alloys (Snoek, 1941) is due to the tetragonal symmetry of the unfilled octahedral interstices in bcc iron and their cubic symmetry when filled with carbon or nitrogen. As long as no external stress is applied to the specimen the distribution of interstitial atoms is random, and the c-axes of the locally distorted unit cells are equally and randomly oriented along the three cube directions of the matrix. If a stress is applied, the interstitial atoms move to octahedral positions whose directions of distortion are aligned along the $\langle 100 \rangle_\alpha$ direction nearest to the stress axis. When the stress is removed the distribution of filled interstitial sites again becomes random, but since migration is time dependent there is a phase lag between strain and stress during oscillation. The extent of damping is measured as a function of temperature at a constant frequency of oscillation and a maximum value

is obtained at some characteristic temperature.

Internal friction theory predicts that the magnitude of damping (Q^{-1}) is proportional to the concentration of either carbon or nitrogen in solution, provided the concentrations are small. This has been verified by Dijkstra (1947) for the range of solubilities in α-Fe. It is the degree to which stress and strain are out of phase which is the direct measure of internal friction and the damping parameter Q^{-1} is given by:

$$Q^{-1} = \tan \phi = \delta/\pi \qquad \ldots\ (VII).9$$

where ϕ is the angle of lag

δ is the logarithmic decrement during natural decay,

and is given by:

$$\delta = \ln \frac{An}{An+1} = \frac{1}{n} \ln \frac{A1}{An+1} \qquad \ldots\ (VII).10$$

where An is the amplitude of the n^{th} ascillation

An+1 is the amplitude of the $(n+1)^{th}$ oscillation

thus:

$$Q^{-1} = \frac{1}{n\pi} \ln \frac{A1}{An+1} \qquad \ldots\ (VII).11$$

According to Dijkstra (1949) for a single relaxation process occurring in "pure" Fe-N or Fe-C alloys, there is a 1 : 1 correlation between internal friction peak height

Q^{-1}_{max}, and wt.% solute in solution in α-Fe, i.e.

$$Q^{-1}_{max} = \text{wt.\%}\ \underline{C}^{\alpha} \text{ or } \underline{N}^{\alpha} \ (\pm 10\%) \qquad \ldots\ (VII).12$$

When the alloy contains a substitutional solute in addition to nitrogen there no longer exists a single relaxation process. In such a case some of the interstitial atoms are located in octahedra comprised of Fe atoms plus one or more substitutional solute atoms. Thus the energy barrier which must be surmounted when the nitrogen atom migrates can be modified either physically, if the metal-atom radii are different, or chemically if the respective metal atom-nitrogen interactions are different.

Extensive investigations of ternary Fe-X-N systems have shown the presence of additional peaks in the Q^{-1} v. temperature curves, which have generally been interpreted in terms of atomic jumps to and from different local environments. Most of these additional peaks occur at higher temperatures than the "normal" nitrogen peak, the increased temperature signifying a higher activation energy for the relaxation process. The systems studies include Fe-Mn-N (Dijkstra and Sladek, 1952; Ritchie and Rawlings, 1967; Fast, Meijering and Verrijp, 1961), Fe-Mo-N (Dijkstra and Sladek, 1952), Fe-Cr-N (Dijkstra and Sladek, 1952; Ritchie and Rawlings, 1967), Fe-Si-N (Leak, Thomas and Leak, 1955), Fe-V-N (Dijkstra and Sladek, 1952; Jamieson and Kennedy, 1966; Köster and Horn, 1966; Pope, 1972)

and Fe-Ti-N (Szabó-Miszenti, 1970) and cover a wide range of metal atom-nitrogen interactions. In general, the temperature of the "abnormal" internal friction peak increases with the magnitude of the substitutional solute-nitrogen interaction, but results are not always comparable for alloys nitrided in different ways. In particular Pope (1972) has shown that for Fe-V-N prepared by constant activity aging, the absence of any "normal" nitrogen peak in alloys containing GP zones is associated with a microstructure showing extensive matrix strain.

The results reported in the present section (Figure VII.4) are from Fe-5.05 wt.%W nitrided for 6 hours in 8%NH_3:H_2 at 615°C. The alloy is nitrided only to about one-third completion and at this stage still has about 2-3 wt.%W in solution. In addition, the concentration of nitrogen varies across the diameter of the wire, but the results of Chapter VI indicate that the specimen contains only GP zones throughout. A "normal" internal friction peak is obtained because an appreciable volume fraction of unstrained matrix remains, but since some tungsten is still in solution the peak is composite and is comprised of a "normal" peak plus at least one "interaction" peak.

The composite peak (Figure VII.4a) could not be successfully resolved, principally due to its size, the amount of nitrogen in solution being less than 0.01 wt.% (compare Figure VII.4 with the scale of Figure VII.1). However it is clear that the contribution from the "interaction" peak is small, and the peak temperature is in the region of 35°C.

Fig. VII.4

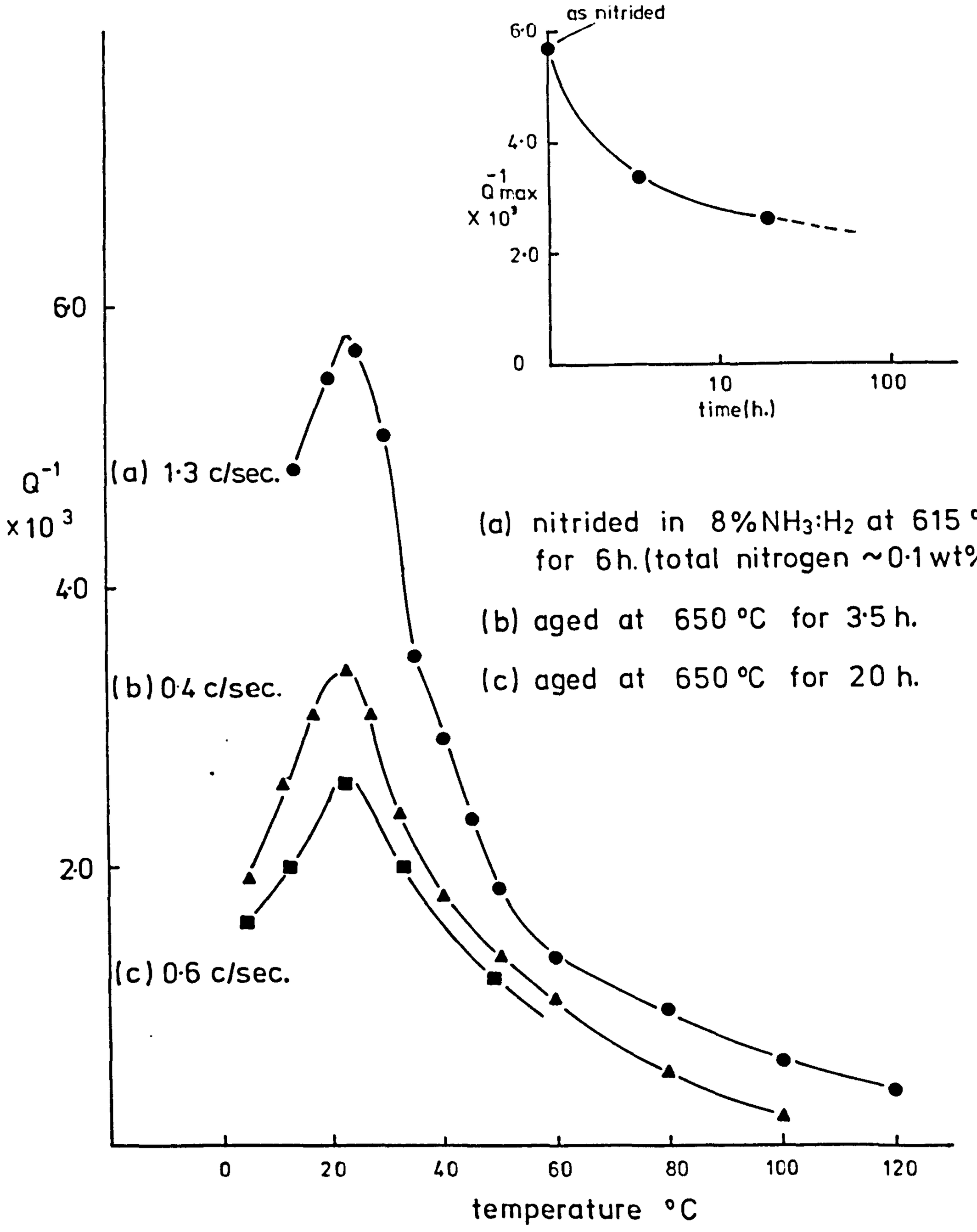

INTERNAL FRICTION DATA FOR PARTIALLY NITRIDED AND AGED Fe–5·05 wt.% W.

In previous investigations in other systems most authors have found several additional peaks, but often one predominates. A similar situation probably exists for the present alloys so it is impossible to be precise, but general indications are that the effect of tungsten on the internal friction of Fe-N alloys is less marked than most other alloy element "nitride formers". The relationship between the height of the composite peak and wt.% nitrogen is uncertain, but because of the small interaction it should not differ greatly from that of pure Fe-N.

Immediately after nitriding the nitrogen in solution is less than about 0.01 wt.% (only one-tenth of that of pure α-Fe in equilibrium with the same gas mixture) indicating that at this stage precipitation is rapid compared to the rate at which nitrogen is entering the specimen. Apparently a high activity of nitrogen is required for nucleation of clusters (equivalent to about 0.06 wt.%N at 615°C) but this need not be maintained during growth. This observation emphasises an important difference between substitutional-interstitial GP zones and those obtained, for example, in Cu-Al alloys. The conditions under which Fe-W-N zones become unstable are not the limiting conditions for their formation and therefore reversion is not observed.

During aging at 650°C the peak height ($Q^{-1}max$) initially decreases at a high rate. After 20 hours (Figure VII.4) $Q^{-1}max$ is approaching a constant value which represents the nitrogen activity in (metastable)

equilibrium with the intermediate precipitate. Although aging is not strictly complete it is nevertheless evident that the equilibrium value of Q^{-1}_{max} will be about $2.0\text{-}2.5 \times 10^{-3}$ indicating an approximate nitrogen concentration in α-Fe ($\%N^{\alpha}$) of about $2\text{-}3 \times 10^{-3}$ wt.%. This value would be produced in pure α-Fe at 615°C using a nitrogen potential equivalent to 0.25%$NH_3:H_2$ and from Figure VII.3, also at 615°C, the equilibrium activity of tungsten is about 2.5 wt.%. In fact the specimen contains only 0.1 wt.%N which on aging will combine with about 2.0 wt.%W leaving approximately 3.0 wt.%W remaining in α-Fe, and therefore the internal friction results are quite consistent with the solubility data presented in the previous section.

VII.4 The conditions for homogeneous precipitation

The range of temperature, tungsten activity and nitrogen activity under which homogeneous precipitation can be obtained is very restricted, and in the same way as for the formation of the intermediate precipitate, the parameters are inter-dependent. The results of Chapter VI show quite clearly that for constant nitriding conditions, there exists a critical tungsten activity above which homogeneous precipitation can be obtained. Likewise for a constant tungsten activity, a critical nitrogen activity must be exceeded. Figure VII.5 illustrates the conditions under which GP zones precede the formation of the intermediate precipitate in nitrided Fe-5.05 wt.%W. In Figure VII.5a

Fig. VII.5

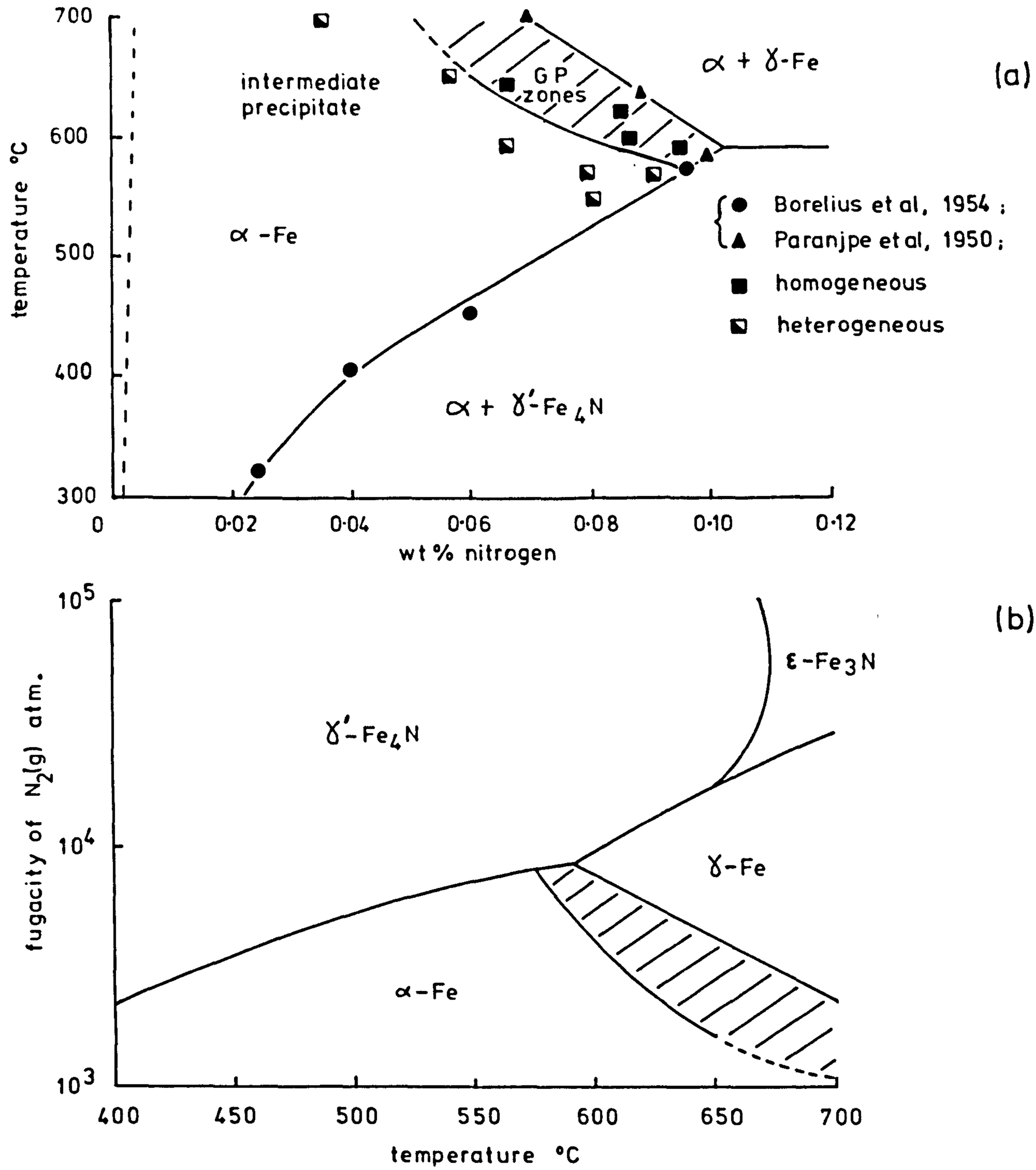

CONDITIONS FOR HOMOGENEOUS PRECIPITATION IN Fe-5·05 wt.%W–N ALLOYS SUPERIMPOSED ON

(a) THE BINARY Fe-N DIAGRAM

(b) THE Fe-N FUGACITY–TEMPERATURE DIAGRAM

[from Lehrer, 1930]

the nitrogen potentials describing the solvus have been converted to equivalent nitrogen concentration in pure α -Fe, and plotted on the low nitrogen end of the Fe-N diagram.

The figure illustrates the limited range of conditions for homogeneous precipitation. Temperatures and nitrogen activities at the $\alpha - \gamma'$ and $\alpha - \gamma$ boundaries can not be exceeded because in the case of the former γ'-Fe_4N is precipitated, and in the case of the latter, $\alpha \rightarrow \gamma$ matrix recrystallisation allows equilibrium phase precipitation at the advancing interface. The upper temperature limit although not accurately determined is at least 650°C but is unlikely greatly to exceed this value because the substitutional solute is then becoming more mobile and so equilibrium phase precipitation is facilitated. Figure VII.5b shows the solvus plotted on a fugacity-temperature diagram for the Fe-N system.

Homogeneous precipitation is detected by a high nitriding rate and high micro-hardness values ($\sim$650 VHN) as well as by electron microscopy observations. Not all specimens defining the solvus on Figure VII.5 were examined metallographically and so the determination also relies on these other criteria. It is perhaps surprising that as the temperature is increased lower solute supersaturations are required for the formation of zones, in apparent contrast to binary age-hardening systems.

The total free energy change ΔG_T^B associated with

the formation of a stable nucleus of a phase β in a solid solution of a phase α is the sum of three components namely ΔG_V the volume free energy change, ΔG_S the surface free energy change, and ΔG_E the strain free energy change

$$\Delta G_T^{\beta} = \Delta G_V + \Delta G_S + \Delta G_E \quad \ldots\ldots (VII).13$$

Substitutional-interstitial GP zones in bcc iron introduce an exceptionally high strain and this is probably reflected in the large supersaturation required for their formation. However the term $(\Delta G_S + \Delta G_E)$ although large would not be expected to vary significantly over the range 580-650°C.

If equilibrium soncepts can be applied to the GP zone solvus the following argument might explain the unusual observations. If the formation of GP zones can be represented by

$$xFe + yW + zN = Fex\ Wy\ Nz$$

the volume free energy of formation will be

$$\Delta G_V = \Delta G_V^{\circ} + RT \ln \frac{a_{Fe_x W_y N_z}}{a_{Fe}^{x} \cdot a_{W}^{y} \cdot a_{N}^{z}} \quad \ldots\ldots (VII).14$$

where the symbols have their usual meanings.

Assuming unit activity for $Fe_xW_yN_z$ and Fe, Equation (VII).14 becomes

$$\Delta Gv = \Delta G_v^o - RT \ln \left[a_W^y \cdot a_N^z\right] \quad \ldots\ldots (VII).15$$

The activity of nitrogen is controlled by the gas phase but the activity of tungsten is not controlled and the expression for ΔGv becomes

$$\Delta Gv = \Delta G_v^o - RT \ln \left[(\gamma_W \cdot N_W)^y \cdot a_N^z\right] \quad \ldots\ldots (VII).16$$

where γ_W is the activity coefficient of tungsten and N_W is its atom fraction. γ_W can be further separated into two components namely γ_W^W the activity coefficient in a binary Fe-W alloy, and γ_W^N the effect of nitrogen on the tungsten activity coefficient, and

$$\gamma_W = \gamma_W^W \cdot \gamma_W^N \quad \ldots\ldots (VII).17$$

The effect of γ_W^W is to decrease the tungsten activity relative to its value for an ideal solid solution of W in Fe (i.e. the system is expected to exhibit large negative deviations from ideality in view of its tendency to form intermetallic compounds). However as the temperature is increased the system tends towards ideal behaviour and therefore γ_W^W increases. Similarly nitrogen decreases the activity coefficient of tungsten by a small amount, but

to a lesser extent at higher temperatures, and γ_W^N also increases with temperature. Thus by decreasing the effect of both solutes on the activity coefficient of tungsten in α-Fe, an increase in temperature raises the value of γ_W in Equation (VII).16 and it is possible that the nitrogen activity can be lowered without a net decrease in the term $[(\gamma_W . N_W)^y \cdot a_N^z]$.

The existence of a critical tungsten activity for any standard nitriding conditions leads to the occurrence of precipitate free zones at grain boundaries. Figure VII.6 is an example in Fe-4.0 wt.%W nitrided in 8%NH_3:H_2. Grain boundary precipitation of equilibrium phase δ'-$W_{0.9}(N,O)$ is not extensive in the early stages of nitriding but isolated particles are observed. The growth of these particles is controlled by the rate at which tungsten diffuses to the grain boundary from within the grain and a concentration profile develops. For this nitriding treatment the critical tungsten concentration for GP zone formation is between 3.5 and 4.0 wt.%, and at the appropriate point on the profile homogeneous precipitation is prevented (Figure VII.6b).

VII.5 Nitriding kinetics

The rate of any chemical reaction is controlled by the rate of the slowest step which can be either the transport of reactants to the reaction interface ("diffusion control") or the transfer of atoms across the interface

Fig.VII.6

(a)

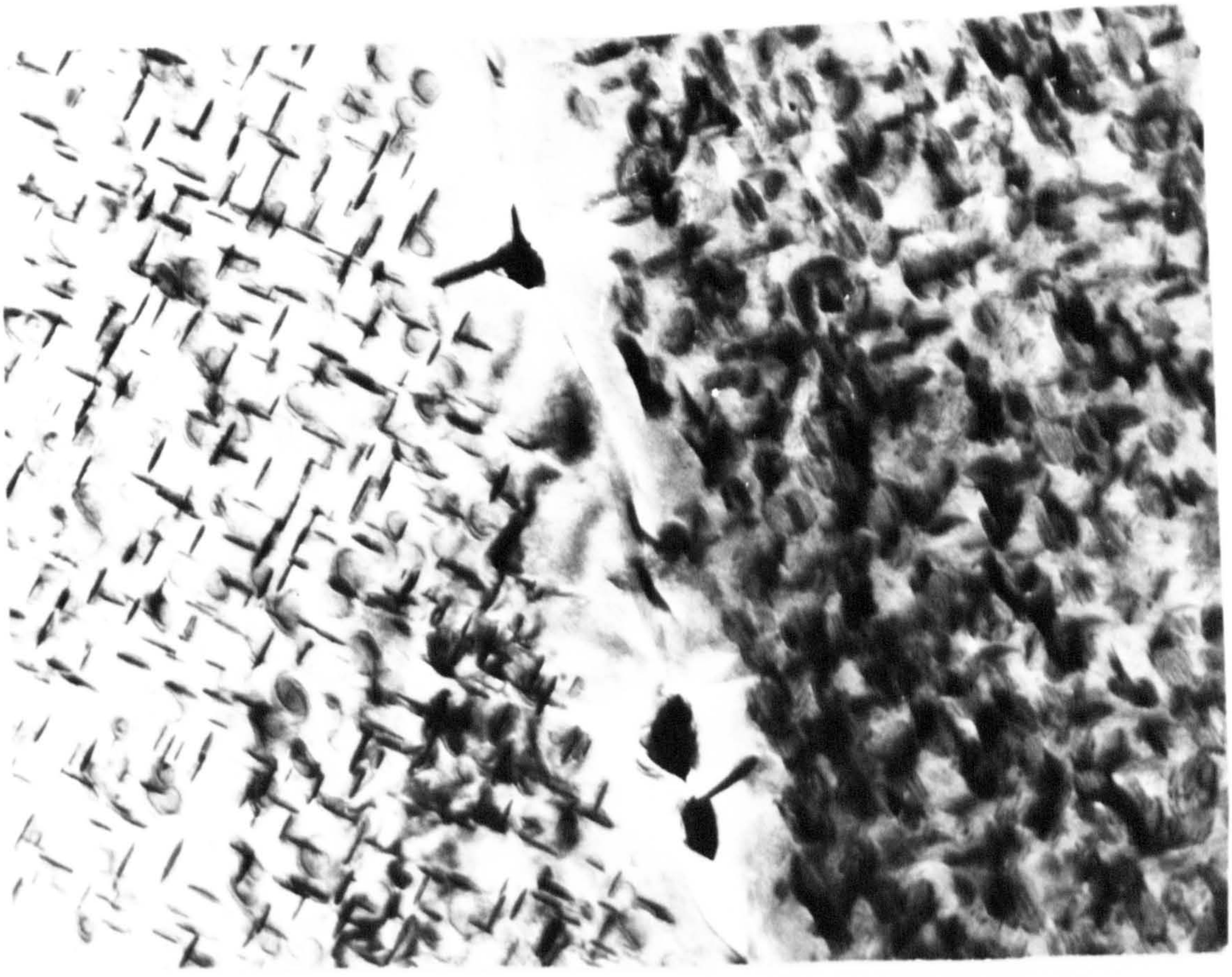

0·1μ

(b)

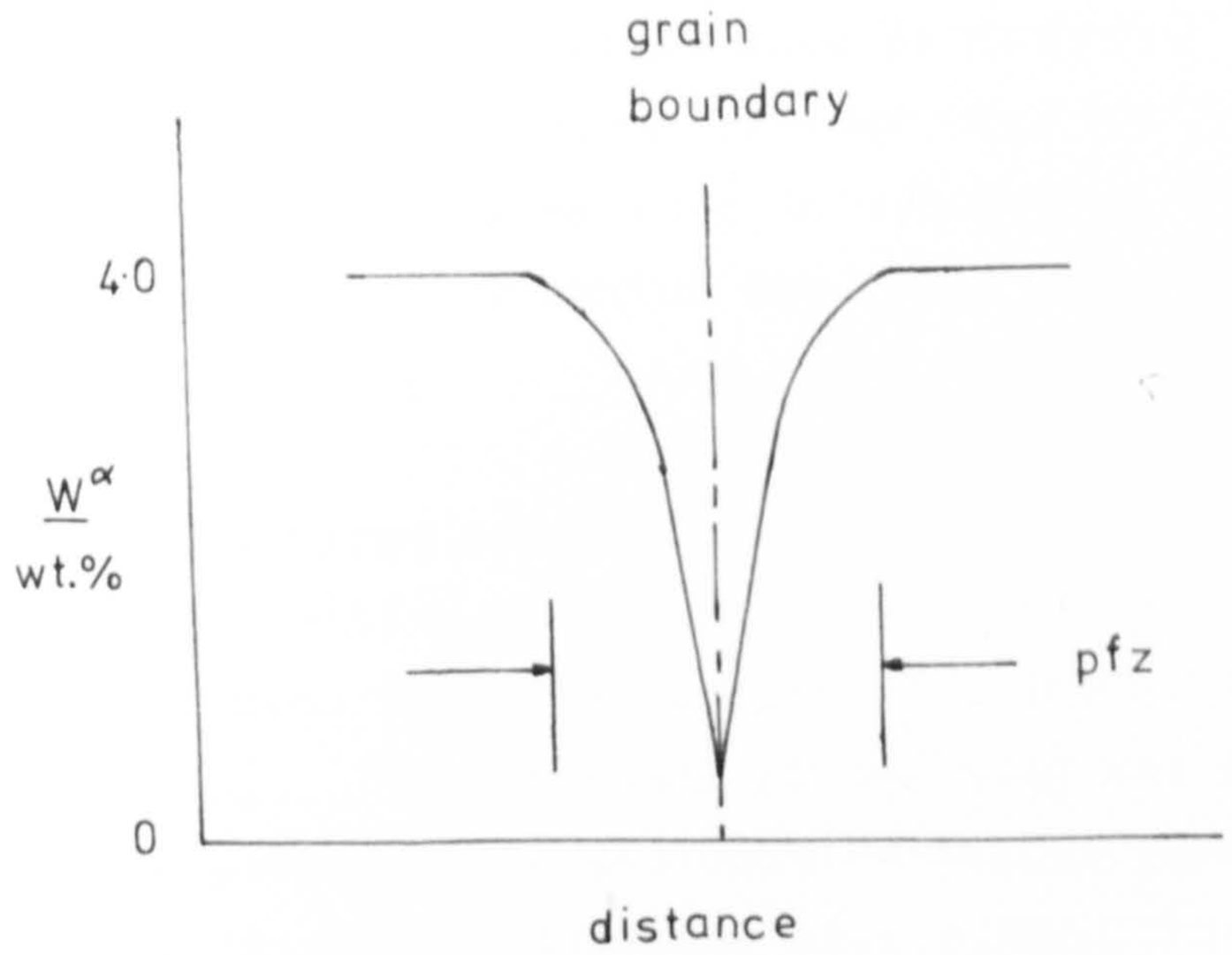

PRECIPITATE FREE ZONES IN Fe–4·0 wt.% W
NITRIDED IN 8 % NH_3:H_2 AT 615 °C

("chemical reaction control").

The transport process in nitriding iron alloys is complex, involving two distinct mechanisms, namely the influx of nitrogen into the specimen and the subsequent precipitation of both solutes. The diffusion coefficient of nitrogen in α-Fe is six or seven orders of magnitude greater than those of metal atoms at nitriding temperatures (Darken, 1958), and for comparable diffusion path lengths the slowest species is always the substitutional solute. However, the distances over which each species must diffuse are not necessarily the same, and assuming the overall reaction rate to be controlled by the diffusivity of one of the species, two possible extremes can be envisaged.

(a) If the rate at which substitutional solute atoms diffuse to a growing precipitate is greater than the rate of nitrogen influx, then the latter will be rate controlling.

(b) If the reverse is true then the rate controlling step is metal-atom diffusion.

An intermediate situation can exist when the two rates are comparable.

The first example in which nitrogen diffusion is rate controlling, is characterised by the gradual increase in thickness from the surface of a hardened case during nitriding. The hardness of the case and the amount of solute precipitated per unit volume of case remains constant during nitriding, implying that within the nitrided layer precipitation is substantially complete, and the overall

nitriding rate is measured by the movement of the nitriding front. The hardness and the solute content of the core remain in the "as annealed" condition until swept by the reaction front. This type of behaviour has been observed in Fe-Ti-N alloys (Jack, 1970), Fe-V-N alloys (Pope, 1972) and Fe-Cr-N alloys (Mortimer, 1971) and is associated with a high precipitate density and hence a small substitutional solute diffusion path length. General observations in several systems, in particular Fe-Mo-N (Driver, 1971), show that the particle density increases with supersaturation, which implies a dependence of critical nucleus size on free energy in accordance with classical nucleation theory. It is therefore not surprising that case hardening is observed in systems involving the more stable nitride formers (V and Ti) especially at higher solute activities. Standard treatments in the Fe-Ti-N, Fe-V-N and Fe-Cr-N systems based on the work of Hepworth et.al. (1965) for internally oxidised Fe-Al alloys, give satisfactory explanations of internal nitriding kinetics based on the diffusivity of nitrogen being rate controlling.

In Fe-W-N alloys even with homogeneous precipitation the inter-particle spacing is about ten times greater than that in nitrided Fe-Ti and Fe-V alloys. This necessitates longer times for diffusion of tungsten, and modifies the rate controlling mechanism. Using specimens up to 2mm. thickness, almost uniform hardening is observed during nitriding because nitrogen diffuses into the centre of the specimen before growth occurs to any appreciable extent in the outer layers. Thus precipitation in the centre occurs

at almost the same time as at the surface.

When precipitation is heterogeneous the specimen can be saturated with nitrogen (in solution) prior to the onset of precipitation. Since the latter is so slow the matrix remains saturated at all times during subsequent precipitation.

The weight increase v. time curves for Fe-5.05 wt.%W nitrided under various conditions are reproduced in Figure VII.7a. Curve (i) shows the relatively rapid nitriding rate associated with homogeneous precipitation, whilst curves (ii) and (iii) are typical of those observed for heterogeneous precipitation and clearly show that the rate of influx of nitrogen into the specimen greatly exceeds the precipitation rate. The plateaux on curves (ii) and (iii) at short times represent incubation periods for nucleation of Fe-W-N intermediate phase during which equilibrium between the nitriding atmosphere and α-Fe is established. Figure VII.7b shows typical sigmoidal y v. log t curves for the three conditions where y(t) the fraction transformed is defined as the ratio of the number of atoms per unit volume in the final configuration at time t, to the number available for transformation at t = 0. For curves (ii) and (iii) t = 0 is taken as the end of the incubation period. Curve (i) does not represent true values of y because at any stage in the reaction it is impossible to distinguish between nitrogen in solution in α-Fe and nitrogen precipitated as intermediate phase. During nitriding the concentration of nitrogen in solution

Fig. VII. 7

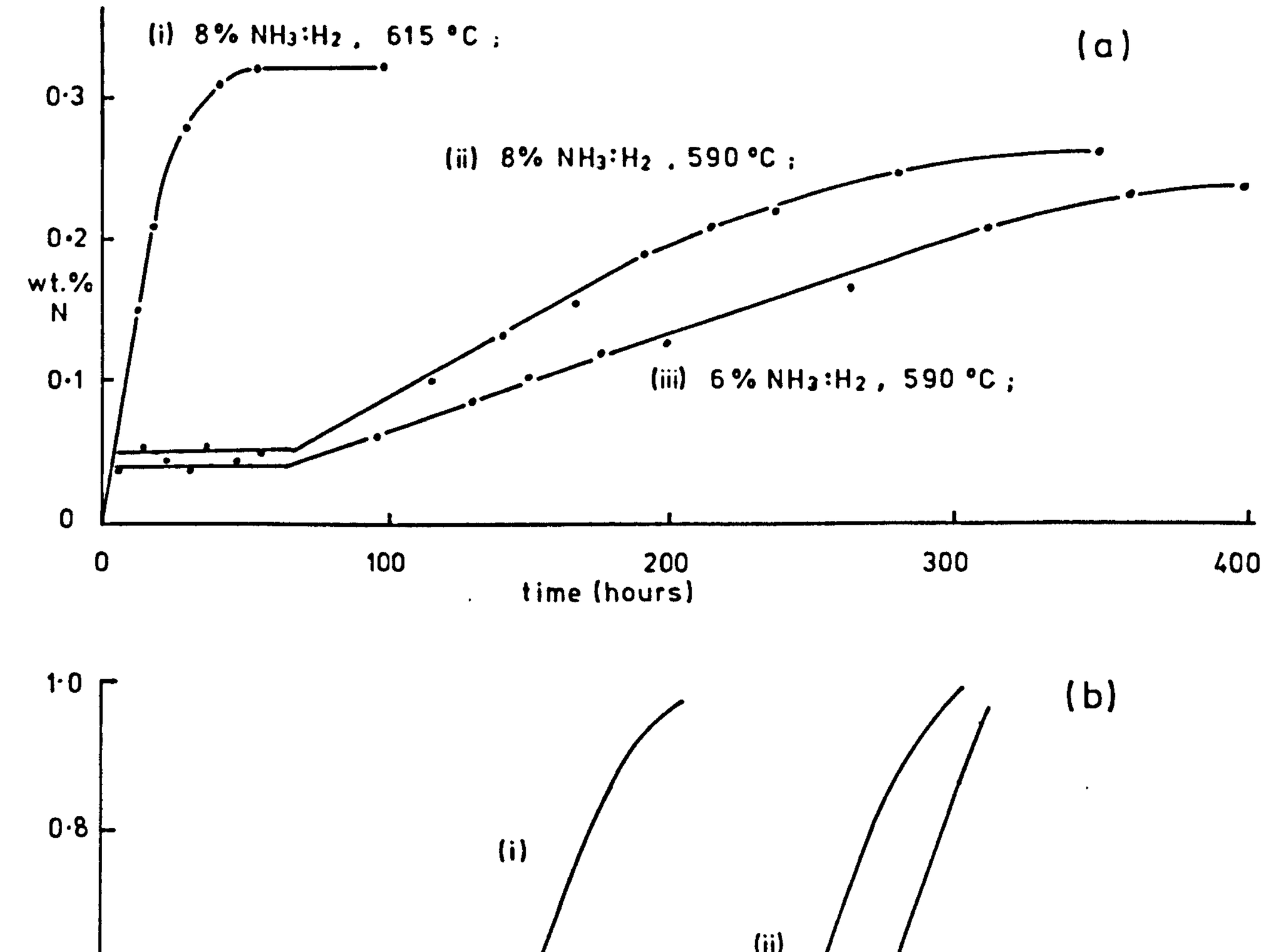

NITRIDING KINETICS FOR Fe–5·05 wt.% W

gradually increases until at some point in the later stages the matrix becomes saturated. This problem does not arise in the other examples because at all times allowance can be made for nitrogen in solution.

It is found empirically that an equation of the general form

$$dy / dt = k^n t^{n-1} (1-y) \quad \ldots\ldots (VII).18$$

describes the isothermal kinetics of a wide variety of precipitation reactions in metals (Burke, 1965), where k and n are assumed to be true constants independent of y. The term $(1-y)$ is included to account for the decrease in reaction rate due to impingement or competition for solute. If the above assumptions are valid, (VII).18 can be integrated to give

$$\ln \left[1/(1-y) \right] = kt^n \quad \ldots\ldots (VII).19$$

in which $1/n$ has been taken into the constant.
An equivalent form is

$$y = 1 - \exp (-kt)^n \quad \ldots\ldots (VII).20$$

this being the generalised form of a particular equation derived by Johnson and Mehl (1939). k and n are empirical parameters which define the isothermal kinetics of a precipitation reaction when (VII).20 is obeyed. Figure VII.8a is a Johnson-Mehl plot of log.log 1/1-y v.

Fig.VII.8

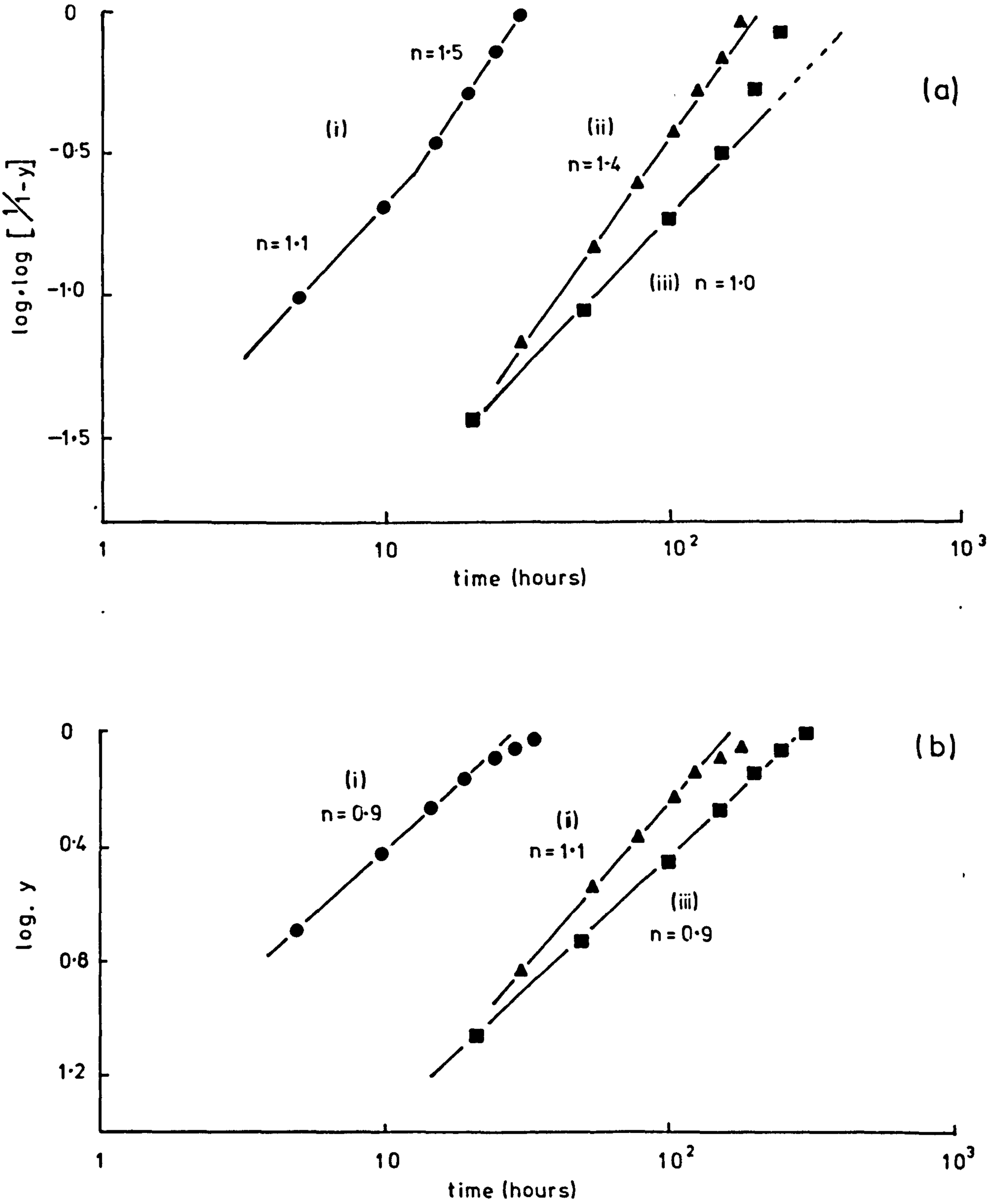

NiTRIDING KINETICS FOR Fe-5·05 wt.% W

log t for the three previous examples, the straight line portions demonstrating the limited extent to which (VII).20 applies.

One of the factors on which the instantaneous reaction rate depends is the time dependence of the rate of nucleation. Since this is generally unknown, rigorous mathematical solutions to various models can be obtained only in idealised cases which involve arbitrary assumptions concerning the nucleation kinetics. Various models have been suggested which produce equations conforming to the Johnson-Mehl equation up to about $y = 0.5$ (Zener, 1949; Wert, 1950; Ham, 1958, 1959; Burke, 1961). An approximate treatment of the model which is most likely to represent a continuous precipitation process (Burke, 1965) gives

$$y \simeq 1 - \exp\left[- \frac{8\sqrt{2}}{3} \pi N D^{3/2} \left(\frac{C_I - C_E}{C_\beta - C_E} \right)^{1/2} t^{3/2} \right] \quad \ldots \text{(VII).21}$$

where N is the number of particles per unit volume,
D is the solute diffusion coefficient,
C_β is the solute concentration of the particle,
C_E is the matrix concentration in equilibrium with the particle, and
C_I is the solute concentration of the matrix.

The model assumes the diffusion controlled growth of a fixed number of crystals from a slightly supersaturated solid solution, and if it is satisfied a Johnson-Mehl plot should be a straight line of slope 3/2.

Curve (i) for homogeneous precipitation shows a change in slope from approximately 1.1 to 1.5 at about $y = 0.4$. As discussed previously this is not a true value of y because in the early stages of nitriding all the nitrogen introduced into the specimen and observed by the weight increase is not being precipitated. Other observations have shown that after times corresponding to $y \sim 0.5$ the α-Fe is substantially saturated and so most of the subsequent weight increase represents nitrogen being precipitated. It therefore seems possible that the change in behaviour of curve (i) corresponds to the point where nitrogen uptake represents the true precipitation rate and thereafter the reaction conforms to the approximate model. The expression for the empirical rate constant k in (VII).21 can be evaluated using values of C_ε and C_β determined from previous experiments (Chapter VII.2), and a value of $N = 10^{16} cm^{-3}$ determined by electron microscopy. This gives a value for the diffusion coefficient of W in α-Fe at $615^{\circ}C$ of about $2.0 \times 10^{-15} cm^2.sec^{-1}$ which is in reasonable agreement with that obtained from extrapolated high temperature data, $10^{-14} cm^2.sec^{-1}$ (Fridberg, Törndahl and Hillert, 1969).

Metallographic examination of specimens containing heterogeneously precipitated intermediate phase (Chapter VI) suggests that nucleation is at least partly catalysed by the presence of pre-existing precipitates. It is thus impossible to suggest a mathematical kinetic model to account for curves (ii) and (iii), since the time dependence of nucleation is unknown.

The choice of impingement factor $(1-y)$ in (VII).18 is somewhat arbitrary and better agreement is sometimes obtained by using $(1-y)^2$ (Austin and Ricketts, 1939). The present results are less consistent using this equation and so it seemed possible that better agreement might be obtained by neglecting impingement i.e. equivalent to using a factor of $(1-y)^0$. The rate equation now becomes

$$dy/dt = k'^{n'} \cdot t^{n'-1} \qquad \ldots\ldots (VII).22$$

which integrates to

$$y = k'^{n'} \cdot t^{n'} \qquad \ldots\ldots (VII).23$$

where, once again, $1/n'$ has been included in the constant.

Figure VII.8b shows plots of log y v. log t which give values of n' near to unity for all conditions. This simply means that y is directly proportional to t over a large range of y, which is evident from the nitriding curves (Figure VII.7a). Physically, neglecting the impingement factor implies that the growth of precipitates is not impaired by either particle impingement or competition for solute until a late stage in the reaction. This may be because the nitrogen activity remains constant but perhaps a more reasonable conclusion is that the catalytic effect of the growing precipitates on additional nucleation counteracts the expected decrease in growth rate.

In principle, constant activity nitriding offers advantages in studying the kinetics of solid state metallurgical reactions because of the direct relationship between weight increase and reaction progress. The treatment of the present results is approximate, but is offered to emphasise the changes in kinetic behaviour which occur during the nitriding of different alloy-ferrites. It is increasingly obvious that in all respects each system studied behaves differently in detail although all have common features. Thus Fe-Ti (Jack, 1970) and Fe-V (Pope, 1972) are known to case harden over the range of solute concentrations studied, whilst Fe-Mo (Speirs, 1969; Jack, Lidster, Grieveson and Jack, 1971) and Fe-W harden "uniformly". The nitriding behaviour of Fe-Cr (Mortimer, 1971) is critically dependent on the solute activities, case hardening being observed at high nitrogen and chromium activities, with "uniform" hardening and ultimately slow heterogeneous precipitation as the supersaturation is decreased. As well as producing greater supersaturations, higher solute contents also lead to a larger substitutional solute flux which also encourages case hardening.

Chapter VIII

LOW TEMPERATURE AGING OF TUNGSTEN-NITROGEN-FERRITES

VIII.1 Introduction

Even at temperatures where diffusion rates of substitutional atoms are negligible, alloying elements have a marked effect on the para-precipitation of iron nitrides from supersaturated nitrogen-ferrite. In Fe-Mn-N (Pipkin, 1967), Fe-Mo-N (Speirs, 1969), Fe-Si-N (Roberts, 1970) and Fe-Cr-N (Mortimer, 1971) all results are explicable in terms of the thermodynamics of the systems (Pipkin, Grieveson and Jack; see Pipkin, 1967). The metallography of aged Fe-W-N alloys shows structures which are different from those observed in previous systems, but additional experiments demonstrate that the observations are consistent with previous proposals.

VIII.2 Experimental

The results of Chapter VII enabled suitable conditions to be determined under which tungsten-ferrites could be saturated with nitrogen without precipitation of tungsten. Accordingly, alloys were nitrided in 12%NH_3:H_2 at 570°C and quenched before aging for various times at 150°C and 250°C.

In addition, specimens were nitrided at 470°C and 520°C in order to study the effect of tungsten on the activity coefficient of nitrogen. 2g specimens cut from 0.030in. strip were electropolished and carefully weighed before and after nitriding. Physical defects e.g. dislocations interact strongly with dissolved nitrogen and so all alloys were pre-annealed for 2 hours at 900°C in purified hydrogen.

VIII.3 Discussion of previous results

For Fe-Si alloys nitrided under constant conditions and subsequently aged at low temperatures, Roberts (1970) observed that as the Si content increases

(a) The sizes of γ'-Fe_4N, and to a lesser extent α''-$Fe_{16}N_2$ precipitates decrease;
(b) the transition from α'' to γ' precipitation occurs at shorter aging times; and
(c) the quantity of precipitate is reduced.

In Fe-Mn-N and Fe-Mo-N alloys Pipkin (1967) and Speirs (1969) observed opposite effect and the explanation is in terms of the effect of the substitutional solute on the nitrogen activity coefficient.

During nitriding, for a given nitrogen activity ($p_{NH_3}/p_{H_2}^{3/2}$) in the nitriding gas, the nitrogen concentration in solid solution in α-Fe containing element X varies according to the activity coefficient of nitrogen,

$$K\left(p_{NH_3}/p_{H_2}^{3/2}\right) = a_{\underline{N}} = f_N^X \cdot [\text{wt.\%}\underline{N}] \qquad \ldots\ldots \text{(VIII).1}$$

where K is the equilibrium constant (see Chapter II) and f_N^X is the activity coefficient of nitrogen in the alloy using the infinitely dilute solution of nitrogen in α-Fe as the standard state, i.e. $f_N^X = 1$ for pure iron.

Addition of an element such as Si, which increases the activity coefficient of nitrogen, decreases the dissolved nitrogen concentration for a given gas mixture, and therefore decreases the total amount of subsequent low-temperature precipitate. Conversely, Mn, Mo and Cr decrease f_N and produce the opposite effect. Figure VIII.1 shows the way in which f_N^X varies for various elements at 1600°C; the effect is greater at lower temperatures where the systems deviate further from ideality.

The observed variation of precipitate distribution is explained by classical nucleation theory, which gives the critical radius for nucleation of a spherical particle (Heal and Hardy, 1954) as:

$$r^* = \frac{-2\sigma}{\Delta Gv} \qquad \ldots\ldots \text{VIII).2}$$

where ΔGv is the free energy change per unit volume,
σ is the surface energy per unit area of particle-matrix interface,

and where any strain energy contribution is neglected.

Fig. VIII.1

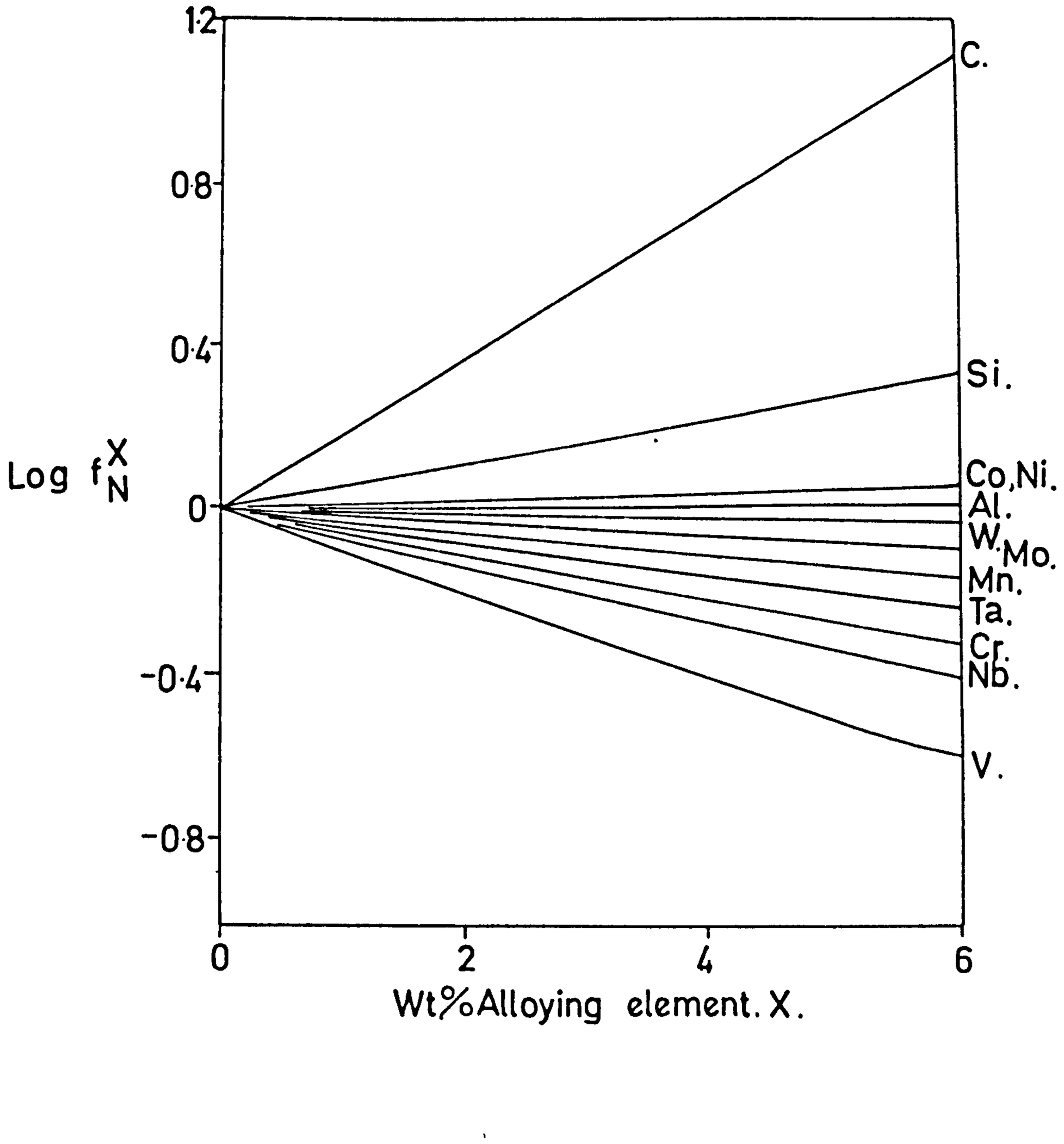

THE EFFECT OF ALLOYING ELEMENTS ON THE ACTIVITY COEFFICIENT OF NITROGEN IN IRON AT 1600°C.

[from Schenck et.al.(1958) & Pehlke and Elliott (1960).]

The driving force per unit volume for precipitation is

$$\Delta G_v = \frac{-RT}{\Omega} \ln \left(\frac{a_1}{a_2} \right) \quad \ldots\ldots (VIII).3$$

where a_1 is the solute activity in the supersaturated solid solution at T^oK,

a_2 is the activity in equilibrium with the precipitated phase at the same temperature,

and Ω is the molar volume of the precipitate.

After nitriding in a constant activity gas mixture, both "pure" iron and iron-alloys have the same nitrogen activity but different nitrogen concentrations. When the system deviates further from ideality at the lower aging temperatures the further change in f_N^X alters the relative nitrogen activities (since the concentrations remain constant), producing a change in ΔG_v (equation (VIII).3) and hence in r^* (equation (VIII).2). Elements such as Si which increase f_N produce a decrease in r^* and hence a fine distribution, whereas Mn, Mo and Cr, which decrease f_N cause an increase in r^* and produce a coarser dispersion of iron nitrides.

Classical nucleation theory also explains the effect of the substitutional element on the rate of precipitation of γ'-Fe_4N (Roberts, Grieveson and Jack; see Roberts, 1970). The maximum total free energy change for nucleation (ΔG^*) is given by

$$\Delta G^{*} = \frac{16\pi}{3} \cdot \frac{\sigma^3}{\Delta Gv^2}$$

$$= \frac{4}{3}\pi (r^{*})^2 \sigma. \qquad \ldots\ (VIII).4$$

The rate of nucleation of precipitates from supersaturated solid solution (Becker, 1938) is

$$I = Ko \exp - \left(\frac{\Delta G^{*} + Q}{RT}\right) \qquad \ldots\ (VIII).5$$

where Ko is the maximum possible nucleation frequency, and Q is the activation energy for solute diffusion. Equation (VIII).5 predicts a higher initial nucleation rate if f_N^X is increased, and a lower initial rate for additions which decrease f_N^X, in agreement with observations.

VIII.4 The effect of tungsten on f_N

Since the conditions for homogeneous precipitation are so restricted it is possible to obtain supersaturated tungsten-nitrogen-ferrites and hence determine reasonably accurate values of the nitrogen activity coefficient.

Specimens were nitrided at 570, 520 and 470°C to produce tungsten-nitrogen ferrite with a given nitrogen potential and the weight increases recorded as shown in Table VIII.1.

Table VIII.1

The effect of tungsten on the activity coefficient of nitrogen in α-Fe

Temperature ^{o}C	$\%NH_3:H_2$	wt.%W	wt.%N	f_N	e_N^W
570	12:88	0	0.097	1.0	0.008
		1	0.099	0.98	
		2	0.102	0.95	
		5	0.105	0.92	
520	15:85	0	0.055	1.0	0.013
		1	0.055	1.0	
		2	0.060	0.92	
		5	0.064	0.86	
470	20:80	0	0.051	1.0	0.011
		1	0.053	0.96	
		2	0.053	0.96	
		5	0.058	0.88	

Surprisingly, the effect of tungsten is very small, with correspondingly large possible errors in the value of f_N. Figure VIII.2a shows plots of $\log f_N^W$ v wt.%W obtained at the three temperatures together with that at 1600°C (Pehlke and Elliott, 1960). The error limits are shown for a 2% uncertainty in the weight increases on nitriding i.e. about 20ppm of nitrogen.

In view of the magnitude of the interaction and the possible errors, Figure VIII.2a is not unreasonable, and and approximate value of f_N^W is given by:

$$\log f_N^W = \text{wt.\%W} \cdot \frac{d \log f_N^W}{d \% W}$$

$$= \underline{\text{wt.\%W} \cdot e_N^W} \quad \ldots\ldots (VIII).6$$

As expected, the value of e_N^W is smaller (i.e. less negative) at higher temperatures (Figure VIII.2b), and it is clear that the effect of tungsten on the activity coefficient of nitrogen in α-Fe is less than that of Si, Mn, Mo and Cr.

VIII.5 The metallography of aged alloys

The distribution of α-$Fe_{16}N_2$ and γ'-Fe_4N in nitrogen-ferrites containing 0, 1, 2 and 5 wt.%W and aged at 150°C and 250°C is shown in the optical micrographs

Fig.VIII.2

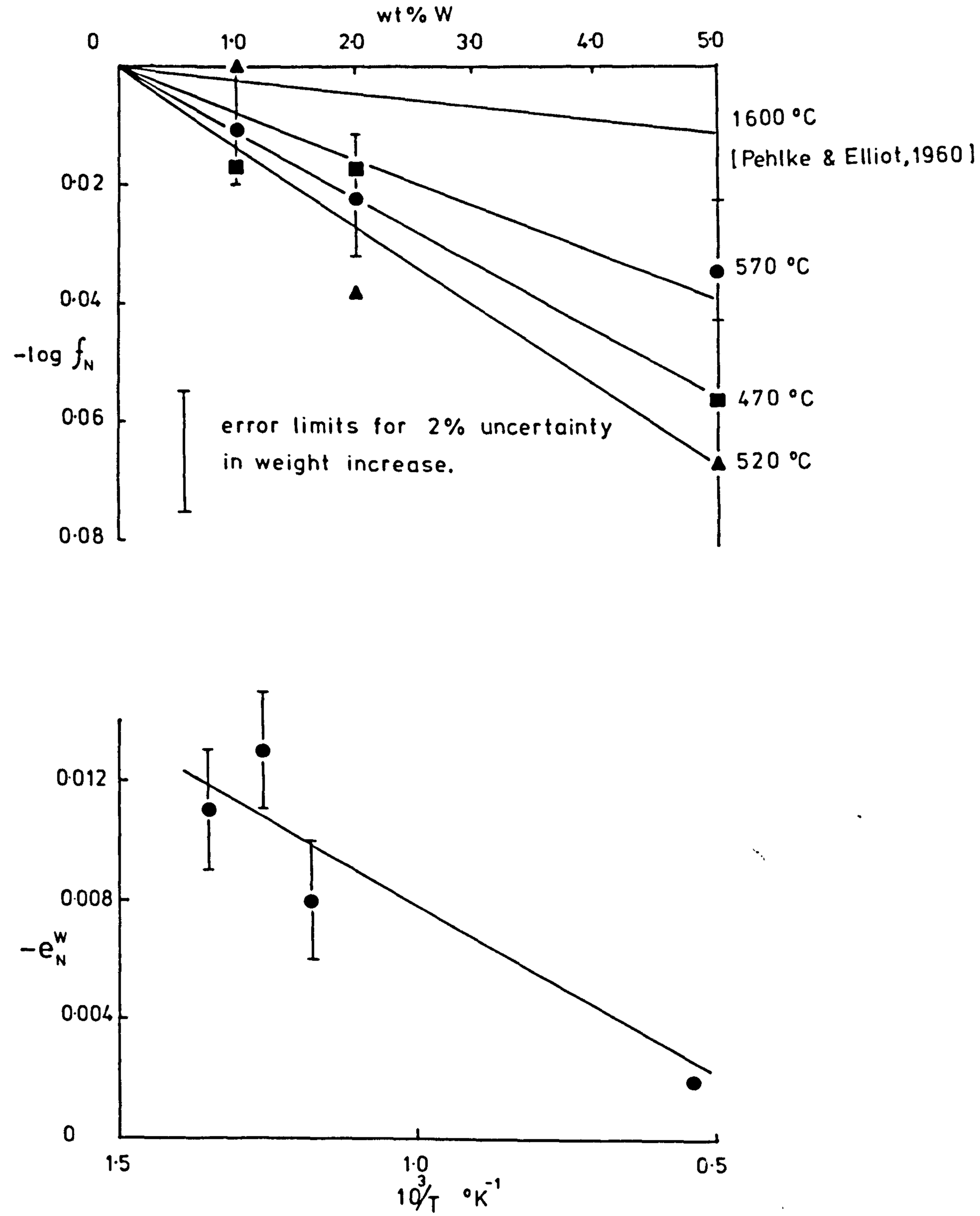

THE EFFECT OF TUNGSTEN ON THE ACTIVITY COEFFICIENT OF NITROGEN IN α-Fe [f_N].

of Figures VIII.3 and VIII.4.

In contrast to all other systems studied, there appears to be no significant effect of tungsten on the quantity or distribution of iron nitrides. In alloys aged for 24 hours at 150°C (Figure VIII.3) and 20 minutes at 250°C the metallography shows mainly the first stage precipitate α'', together with minor proportions of the equilibrium γ'. There is some indication that at higher tungsten concentrations the $\alpha'' \rightarrow \gamma'$ transition is inhibited. The dense distribution of α'' reflects the relatively high nitrogen concentration (0.1 wt.%) and, as expected, a finer dispersion is obtained at the lower aging temperature.

γ' formation appears to be complete after 3 hours at 250°C (Figure VIII.4) and at this time and after 24 hours there is no striking difference in the microstructures of all alloys. The small excess of γ' which would be expected in the 5 wt.%W alloy is perhaps detectable, but the overall conclusion is, as predicted by the previously determined interaction coefficients, that the effect of tungsten on the para-precipitation of α''-$Fe_{16}N_2$ and γ'-Fe_4N is negligible.

The deeply-etched grain boundaries in the 5 wt.%W alloy indicate that some precipitation of δ'-$W_{0.9}(N,O)$ occurs during nitriding at 570°C. Although this might be expected to produce abnormally high weight increases, the previous section indicates that any anomalies are insignificant.

Fig.VIII.3

0 % W

10 μ

1 wt.% W

2 wt.% W

5 wt.% W

Fe-W ALLOYS NITRIDED IN 12 % NH_3:H_2 AT 570 °C AND AGED FOR 24 HOURS AT 150 °C.

[α''-$Fe_{16}N_2$ + γ'-Fe_4N precipitated]

Fig.VIII.4

0 % W

10μ

1 wt.% W

2 wt.% W

5 wt.% W

Fe-W ALLOYS NITRIDED IN 12% NH_3:H_2 AT 570 °C AND AGED FOR 3 HOURS AT 250 °C.

[γ'-Fe_4N precipitated]

VIII.6 Conclusions

Nitriding tungsten-ferrite at 570°C and aging tungsten-nitrogen-ferrites at 150°C and 250°C shows that:

(a) tungsten reduces the activity coefficient of nitrogen in α-Fe, but only to a very small extent;

(b) the consequent effect of tungsten on the para-precipitation of iron-nitrides is negligible.

Chapter IX

GENERAL DISCUSSION OF THE TUNGSTEN-NITROGEN INTERACTION IN IRON

The existence of a pronounced interaction between tungsten and nitrogen in iron is amply verified by the present work.

Such an interaction can not, of course, exist unless tungsten and nitrogen in their elemental forms have a mutual affinity for each other. The initial studies described in the present thesis confirm the existence of stable nitrides and oxy-nitrides, although no explanation for the apparent reluctance of pure tungsten to react completely with gaseous nitrogen can be given. Nevertheless it is clear that the problem is concerned with the reaction kinetics and not with the thermodynamic stability of the nitrides. The significant effect of oxygen on the formation of tungsten nitrides is clearly demonstrated.

When the elements are present in solution in iron, the interaction is more apparent in spite of the low solute activities. Thus in pressure-nitrided and quench-aged alloy's there is no restriction to the formation of the "pure" nitride δ-WN. The frequent occurrence of the ternary iron-tungsten-nitrogen η-phases indicates that the solvent species does not always remain uninvolved in the interaction, and in particular the formation of ternary phases from ostensibly "pure" tungsten is most surprising (Appendix I).

The behaviour of tungsten and nitrogen remaining in supersaturated solid solution in α-Fe is demonstrated quantitatively by internal friction methods and activity coefficient measurements. Comparison with equivalent data for other systems indicates a relatively small interaction.

Homogeneous precipitation is well-established in many nitrogen-alloy-ferrites with a precipitation sequence: GP zones $\longrightarrow$ metastable intermediate phase $\longrightarrow$ equilibrium nitride. It is now recognised that each system behaves differently with respect to the occurrence of each stage in the sequence. In Fe-V-N and Fe-Cr-N alloys the intermediate stage remains uncharacterised, whilst in the Fe-W-N system the GP zone stage has only transitory existence but the intermediate precipitate persists for long periods.

Transformation from GP zones is achieved by small atomic movements without any change in the overall metal-atom arrangement. This is accompanied by a gradual loss of coherence and if the equilibrium nitride is face-centred cubic it can be formed directly by this mechanism. In contrast, if like WN the equilibrium phase is simple-hexagonal, an intermediate phase is produced. All types of system eventually precipitate equilibrium phase discontinuously but this occurs much more easily in Fe-W-N and Fe-Mo-N alloys. When an alloy consists of homogeneously distributed equilibrium phase, the driving force for discontinuous precipitation is merely the reduction in particle-matrix interfacial energy. However in cases where the continuous precipitate is metastable the transformation to discontinuous

equilibrium phase also reduces the chemical free energy.

The stability of the Fe-W-N intermediate phase is examined in the present work and is shown to depend upon the activity product $\left[a_{\underline{W}}^{1.75} \cdot a_{\underline{N}} \right]$

The conditions for homogeneous precipitation have been determined for several systems but have yet to be fully explained. Observations with Fe-W-N alloys suggest that the supersaturation required for the formation of GP zones need not be maintained during their growth, but if aging is continued under these circumstances the zones rapidly transform to intermediate precipitate. As a result of this, true reversion has not been observed either by increasing the temperature or by reducing the nitrogen potential. It is clearly shown that for a given nitrogen potential a critical tungsten activity is required and it seems reasonable to suggest that the zone solvus is defined by an activity product $\left[a_{\underline{W}}^{x} \cdot a_{\underline{N}}^{y} \right]$ in the same way as the intermediate phase.

Because of the effect of both solutes on the substitutional solute activity coefficient, the conditions will be more clearly indicated by the product

$$\left[(\gamma_M \cdot N_M)^x \cdot a_N^{\,y} \right]$$

where γ_M is the metal solute activity coefficient and N_M the atom fraction. This would satisfactorily explain the

absence of homogeneous precipitation in nitrided Fe-Si alloys, where the activity coefficient for silicon in a typical alloy at nitriding temperatures (Fe-2 wt.% Si at 600°C) is exceptionally low ($\gamma_{Si} \sim 10^{-7}$; see Roberts, 1970).

The magnitude of the metal-nitrogen interaction also affects the nitriding kinetics of strip specimens. In Fe-W-N alloys where the interaction is relatively weak the density of GP zones is correspondingly lower than in systems where larger supersaturations are possible. The longer tungsten diffusion paths consequent upon this prohibit case hardening in these alloys.

The general interpretation of precipitation phenomena in nitrided Fe-W alloys is supported by observations in two other alloys (Appendices II and III) and of course parallel and previous work at Newcastle.

Appendix I

THE FORMATION OF Fe-W-N η-PHASES ON TUNGSTEN WIRE

A.I.1 Introduction

Pressure nitriding tungsten wire using Fe_2N as a nitrogen source produced thin films of a ternary Fe-W-N η-phase on the specimen surface. As far as the study of pure binary nitrides was concerned, the problem was overcome by using θ-$Mn_{N_{0.9}}$ as a nitrogen source (see Chapter IV) but it was of some interest to examine the apparently anomalous formation of ternary phases.

A.I.2 Experimental results

From experiments carried out using 99.9%W and 99.97%W wire nitrided under various conditions, the following observations were made.

(a) 99.97%W wire usually produced less η-phase, together with some δ-WN

(b) Nitriding 99.9%W in 25%N_2:H_2 at a total gas pressure of one atmosphere at 900°C, produced trace quantities of η_3-phase (see Figure AI.1a). This experiment was conducted in a flowing gas mixture in the total absence of iron (except any present in solid solution in the tungsten).

Fig. AI.1

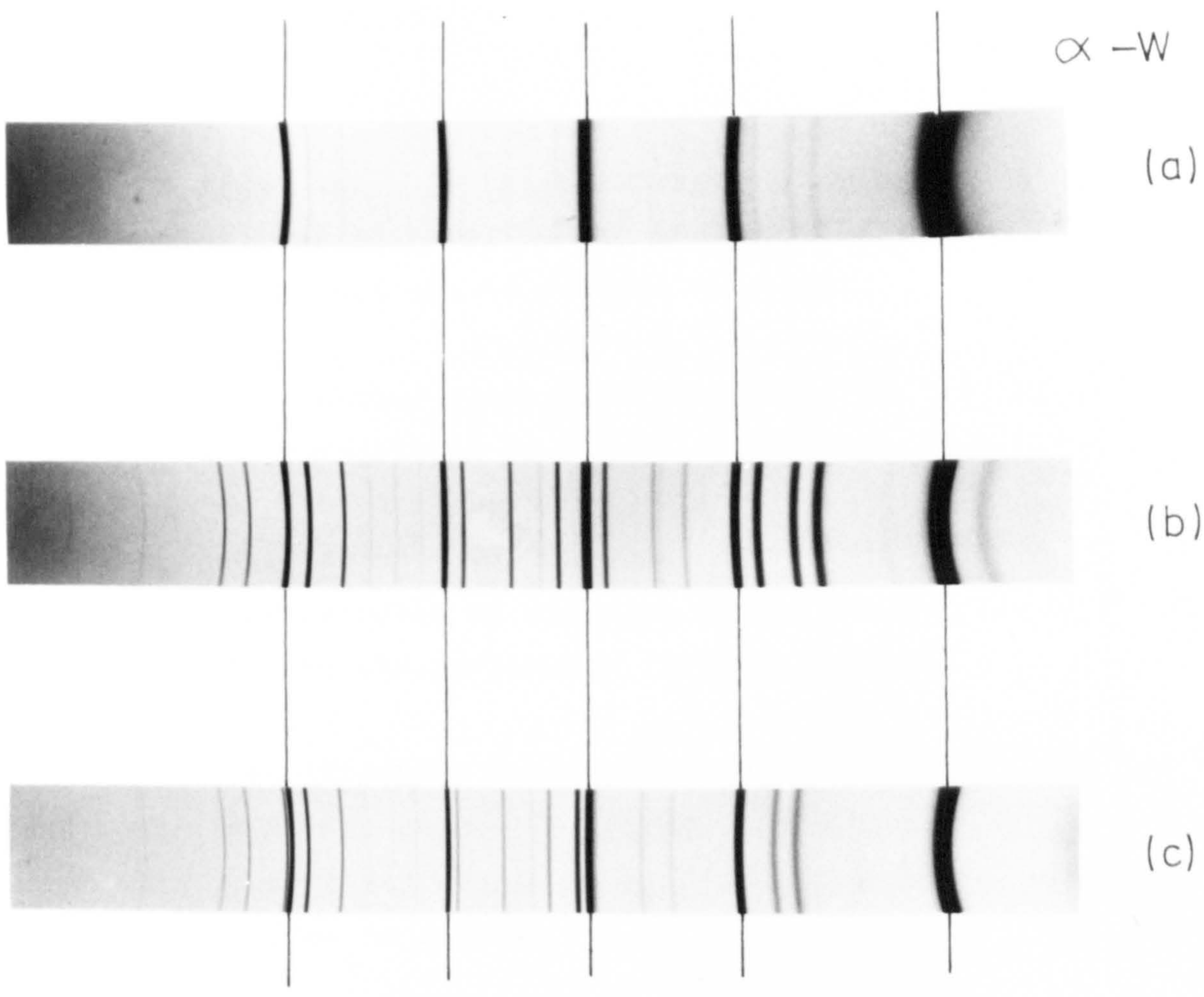

(a) 99·9% W nitrided in 25% N_2:H_2 at 900 °C.

(η_3 : a = 10·937 Å)

(b) 99·9% W nitrided in ~40 atm. N_2 at 900 °C using Fe_2N as a nitrogen source.

(η_3 : a = 10·937 Å)

(c) 99·9% W nitrided in ~40 atm. N_2 at 900 °C using Fe_2N as a nitrogen source.

(η_1 : a = 11·098 Å)

EXAMPLES OF Fe-W-N η-PHASE FORMATION ON NITRIDED TUNGSTEN WIRE.

(c) In pressure nitriding experiments no weight decrease was detected in the decomposed Fe_2N pellet other than that due to evolved nitrogen.

(d) Either η_1-Fe_3W_3N (a = 11.098 Å) or η_3 of probable composition Fe_6W_6N (a = 10.937 Å) could be produced, but both phases were never present together (Figure AI.1b and c). Experiments at 900°C using 20, 40 and 60 atmospheres of nitrogen failed to show any systematic variation in the particular η-phase formed.

(e) Nitrided specimens which showed both η-phase and δ-MN were etched in 70%HNO_3/30%HF mixtures and subsequent X-ray examination gave a sequence of phases from surface to centre:

$$\eta \rightarrow \delta \rightarrow \alpha\text{-N}$$

A.I.3 Discussion

Prevention of η-phase formation when θ-$Mn_4N_{0.9}$ is used as a nitrogen source suggests that iron from the Fe_2N pellet is somehow transported to the specimen. However, η-phase formation in nitrogen-hydrogen gas mixtures shows that externally supplied iron is not necessary. The most probable solution is that nucleation of the ternary phase can occur using only the dissolved iron impurity, but the phase subsequently grows by surface absorption of extremely fine iron particles carried by the gas as the

Fe_2N pellet decomposes. Only very small quantities of surface phases are necessary for X-ray detection.

The problem of which η-phase is produced is equally confusing. Variations in nitrogen pressure have no effect and it can only be assumed that slight variations in other experimental conditions, in particular oxygen potential, are critical.

The fact that the pure nitride δ-WN is found in between the surface ternary phase and the tungsten metal, suggests that the presence of iron prevents formation of δ, and the latter can only be nucleated when the outer regions of the tungsten specimen have been depleted of iron by growth of η.

Appendix II

PRECIPITATION IN CONSTANT ACTIVITY AGED Fe-0.5 wt.%W-0.16 wt.%V

A.II.1 Introduction

Nitriding Fe-W alloys of composition $\leq$ 2 wt.%W in 8%NH_3:H_2 at 615°C for relatively short times produces no detectable precipitation of tungsten, and the weight increases correspond to the equilibrium amount of nitrogen in solution in α-Fe. Of the three available alloys in this composition range (0.5, 1.0 and 2.05 wt.%W) the 1.0 and 2.05 wt.%W specimens contain about 0.09 wt.%N after nitriding and have micro-hardness values of about 250-320 VHN, depending on the aging time at room temperature. The 0.5 wt.%W alloy increases in weight by about 0.13% and has a micro-hardness of 400-420 VHN, and the specimen does not overage at room temperature. Chemical analysis of the alloy has shown it to contain 0.16 wt.%V.

A.II.2 Results and discussion

Electron microscope observations from the nitrided alloy are summarised in Figure A.II.1.

Under the standard nitriding conditions for Fe-W alloys, the high nitrogen potential always leads to a high matrix concentration of nitrogen after fully nitriding.

Fig. AII. 1

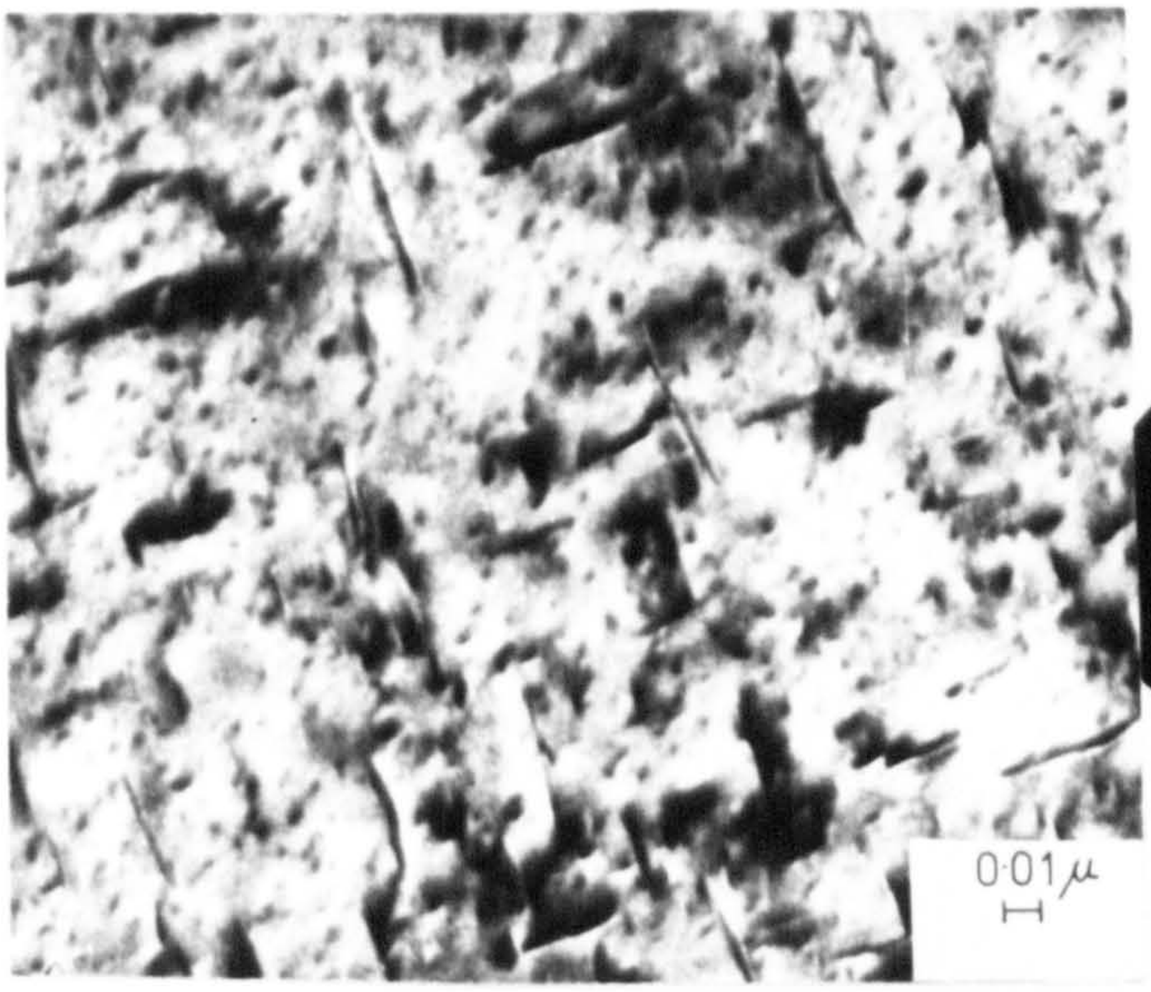

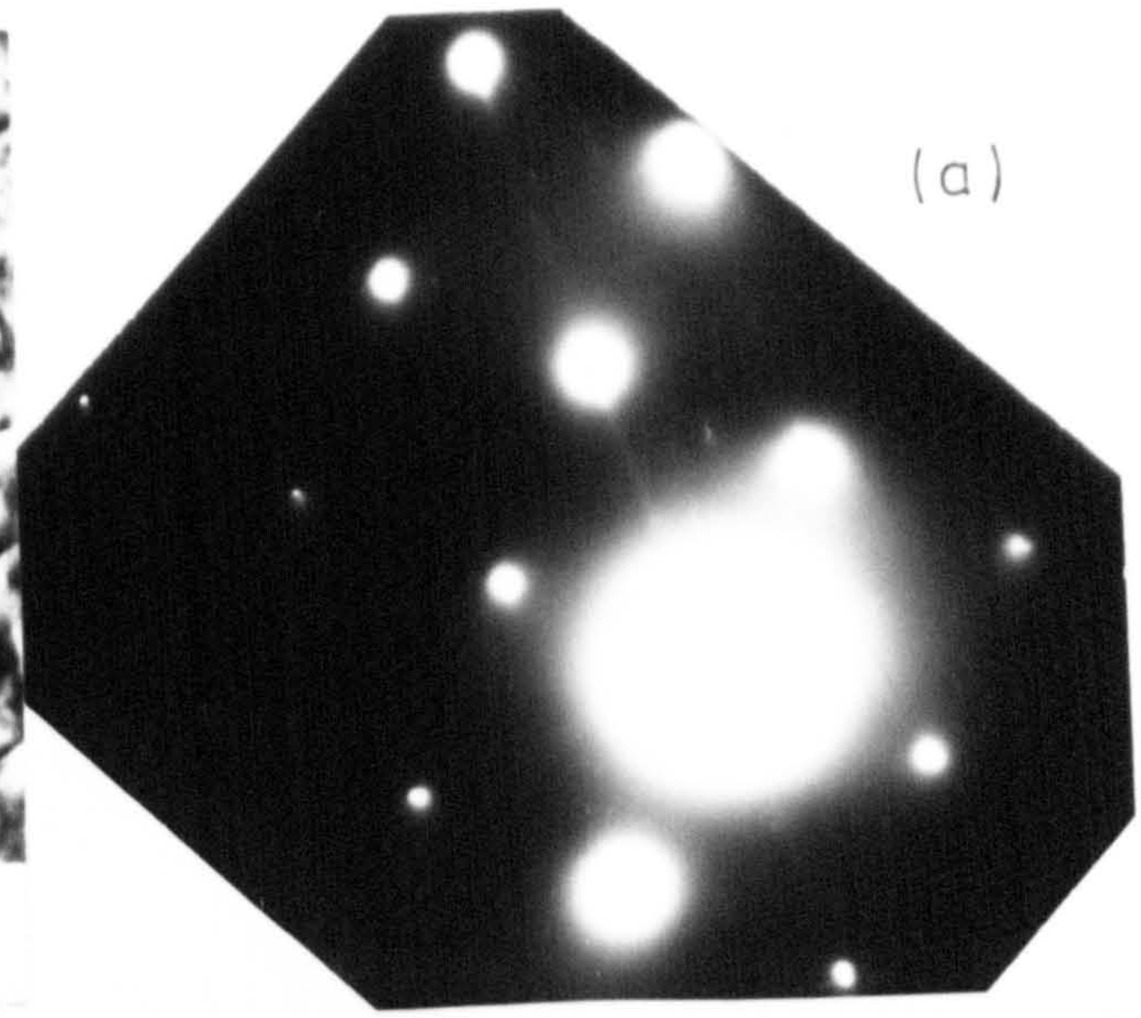

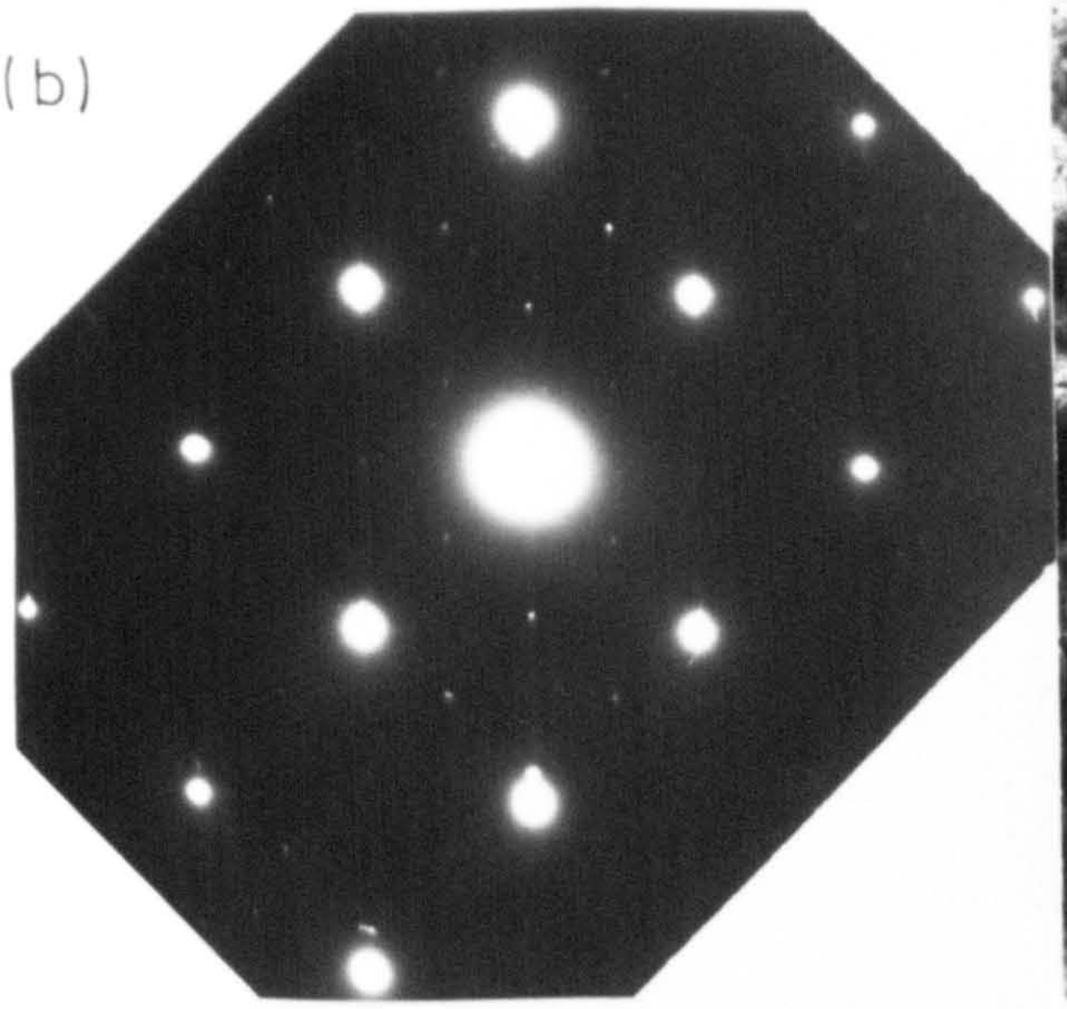

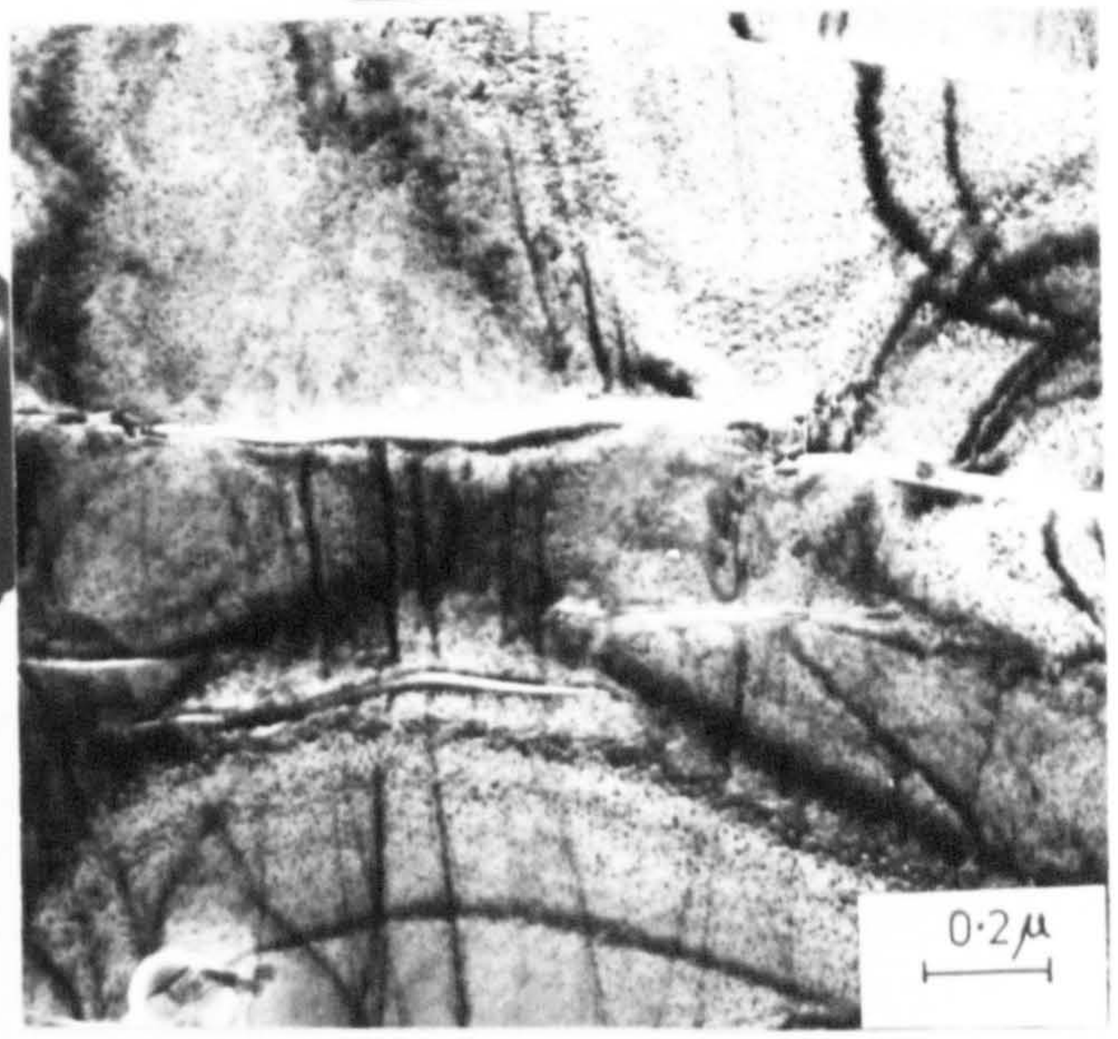

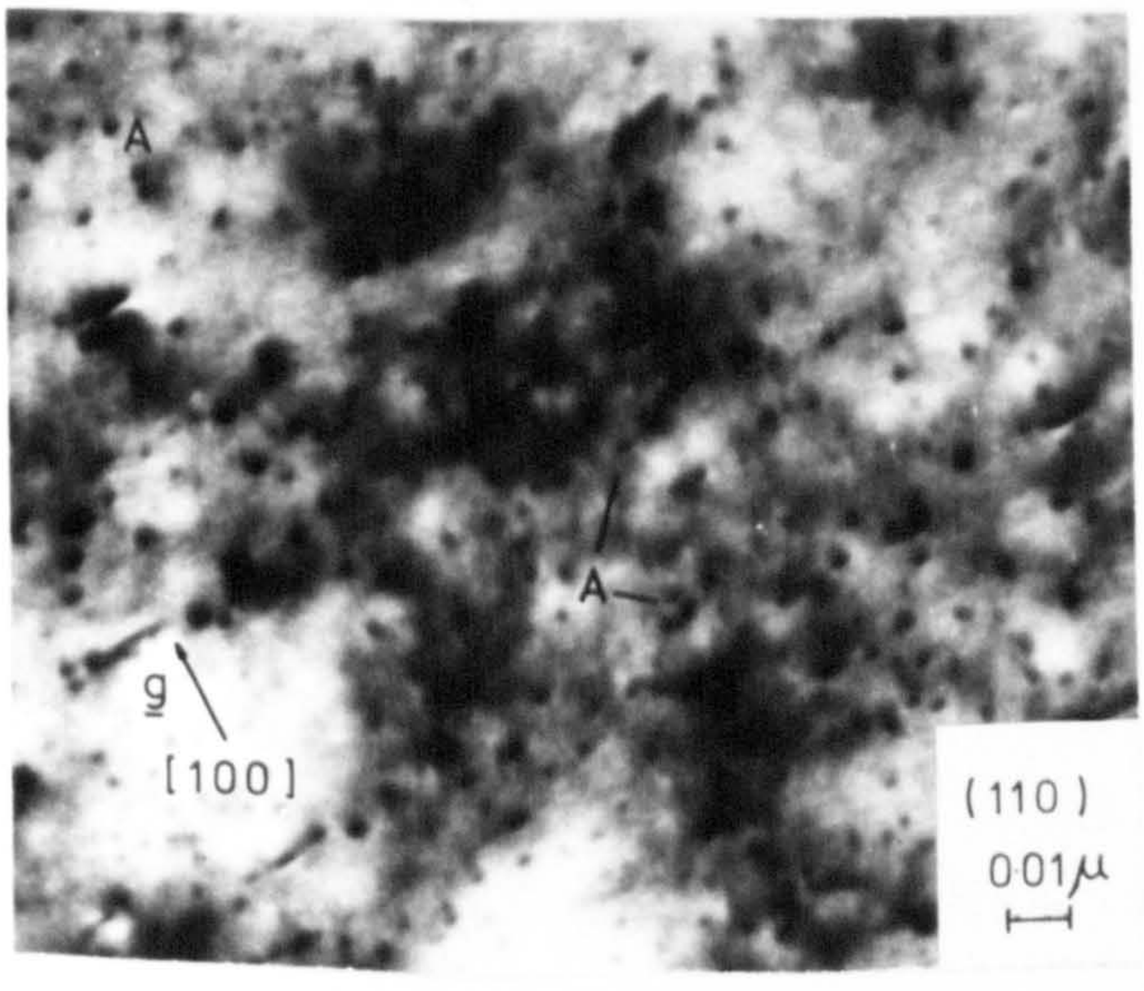

(c)

(a) nitrided in 8% NH_3:H_2 at 615 °C ; aged 2 d. at 25 °C

(b) nitrided as (a); aged at 250 °C for 20 minutes.

(c) nitrided in 5% NH_3:H_2 at 570 °C.

ELECTRON MICROSCOPY OF Fe–0·5 wt.% W – 0·16 % V NITRIDED AND AGED UNDER VARIOUS CONDITIONS.

The consequence of this has been demonstrated in Fe-N alloys of low tungsten content i.e. the supersaturated matrix always decomposes at room temperature to produce α-$Fe_{16}N_2$. Thus in Figure A.II.1a the large plates (200-400 Å diameter) have been produced at room temperature and do not contain vanadium, and they contribute little to the almost continuous diffraction streaking.

This is confirmed by aging at 250°C for a short time, when the matrix nitrogen precipitates as large particles of α''-$Fe_{16}N_2$ (Figure A.II.1b). The precipitate diffraction spots in this figure are produced by α'' but the streaking produced by the five background clusters remains.

The high temperature Fe-V-N precipitation is more usefully studied by using lower nitrogen potentials which lead to smaller matrix nitrogen supersaturations and eliminate rapid low temperature decomposition (Figure A.II.1c). High magnification microscopy on this alloy reveals typical strain-field contrast from small coherent plate-like clusters (A on the figure). In general the clusters are about 15-20 Å diameter although a few larger ones exist and the extent of streaking indicates a thickness of only one metal-atom plane.

The Fe-V-N system has been more fully studied by Pope, Grieveson and Jack (see Pope, 1972) who show that with only 0.4 wt.%V the strain fields overlap and the structure is irresolvable. Matrix lattice parameter measurements

indicate the presence of exceptionally high nitrogen concentrations in solution and internal friction studies show no nitrogen to be present in unstrained "normal" Fe-N interstitial sites. The size and coherence of the clusters in the present alloy support the conclusion that they are truly in solution.

It is notable that in a study of nitrided Fe-W alloys the presence of impurities can have a greater effect than the principle solute. The large interaction between vanadium and nitrogen in α-Fe ensures that both the size of the clusters and the nitrogen pressures required for their formation are at least an order of magnitude less than those for tungsten.

Appendix III

PRECIPITATION IN NITRIDED Fe-3 wt.%Mo - 1 wt.%Ni

A.III.1 Introduction

By reducing nickel molybdate in commercially "pure" hydrogen at temperatures up to 1000°C, Nutter (1969) produced an interstitial alloy having the β-manganese structure and of composition $Ni_8Mo_{12}N_4$. Analysis showed the phase to contain only trace quantities of carbon and oxygen and it was concluded that β^m-$Ni_8Mo_{12}N_4$ is an exceptionally stable nitride produced by nitrogen present in the cylinder hydrogen.

In view of the stability of the phase it was reasoned that an alloy of suitable composition might produce Fe-Ni-Mo-N GP zones as a precursor to the stable equilibrium phase. Accordingly an alloy was prepared from Fe-2.95 wt.%Mo base metal, having a nominal composition of Fe-3 wt.%Mo -1 wt.%Ni.

A.III.2 Results and discussion

Figure A.III.1 shows typical micrographs from a specimen containing 0.30 wt.%N nitrided in 8%NH_3:H_2 at 590°C. The specimen contains fine GP zones together with a much coarser distribution of intermediate phase and appropriate regions of each grain exhibit a gradation

Fig. AIII.1

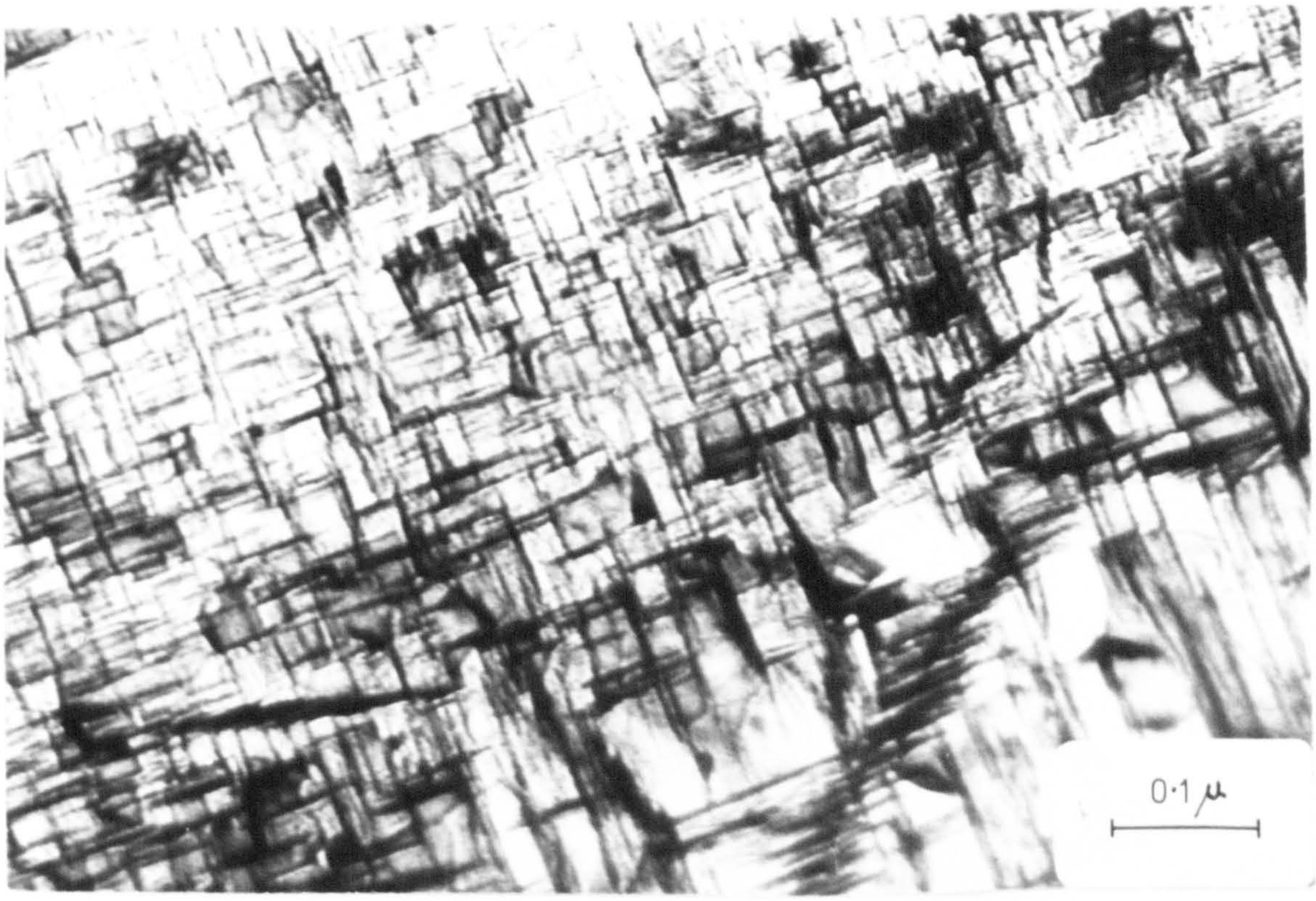

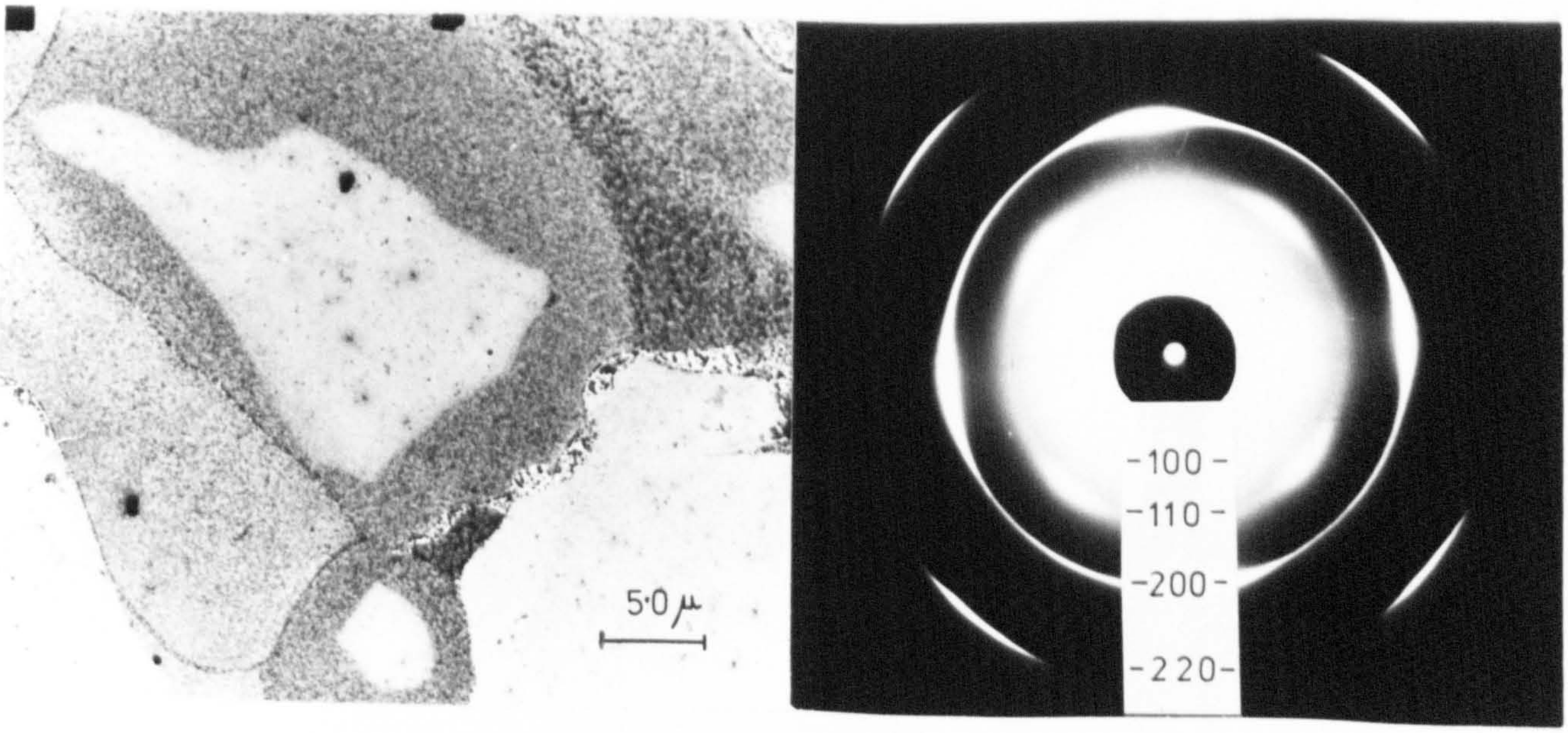

THE TRANSFORMATION FROM G.P. ZONES TO ORDERED INTERMEDIATE PRECIPITATE IN Fe – 3wt.% Mo – 1wt.% Ni NITRIDED IN 8% NH_3 : H_2 AT 590 °C. (0·30 wt% N)

Fig. AIII.2

INTERMEDIATE PHASE PRECIPITATION IN Fe-3 wt.% Mo-1 wt.% Ni NITRIDED IN 8% NH_3:H_2 AT 590 °C.

in particle size and distribution. Carbon extraction replicas show a transformation front, roughly following the contours of the grain boundary, which proceeds from the boundary to the centre of each grain transforming the zones to intermediate phase. A second and much slower transformation to equilibrium phase follows, in exactly the same manner as in Fe-W-N alloys.

Electron diffraction patterns obtained from the intermediate phase show its structure to be exactly analagous to that in Fe-W-N alloys i.e. the structure is close packed cubic but with a superlattice.

The Fe-Mo-N system has been extensively studied (Speirs, 1969; Jack, Lidster, Grieveson and Jack, 1971; Driver and Papzion, 1972) but largely using Fe-5 wt.% Mo specimens which on constant activity aging show only GP zones. By partially nitriding and aging at higher temperatures in the absence of nitrogen, Driver and Papazion (1972) showed by electron diffraction and field ion microscopy that the zones transform to γ-$Mo_2N(O)$ containing about 10 at %Fe. They concluded that ordering of nitrogen atoms was a possibility but no evidence was found for metal-atom ordering. The present results show that if lower supersaturations are used (less molybdenum), the transformation occurs isothermally and virtually all the molybdenum can be precipitated as intermediate phase. The high volume fraction allows characterisation of superlattice reflections from which Fe-Mo metal-atom ordering is deduced.

The lattice parameter of the intermediate phase, determined by electron diffraction, is 4.09 Å, significantly less than that of "pure" γ-Mo_2N(O) (a = 4.17 Å; Hägg, 1930a) implying about a 20% substitution of molybdenum by iron or nickel. The superlattice reflections probably arise by the ordering of Fe and/or Ni atoms in the (000) positions of what would otherwise be face-centred cubic γ-Mo_2N(O), producing a phase exactly equivalent to the Fe-Mo-N intermediate precipitate. It seems that the phase also contains excess nitrogen since at saturation, weight increases indicate a Mo:N ratio of one. At this stage, the alloy contains appreciable quantities of the equilibrium nitride δ-MoN, but a certain amount of intermediate phase (and possibly even GP zones) still remains.

Transformation to intermediate phase is more apparent in lower molybdenum alloys because for any standard nitriding treatment, the supersaturation is lower. For the conditions used in this experiment the critical molybdenum concentration for GP zone formation is about 2-3 wt.% and after only a small amount of precipitation the zones become unstable. Since nitrogen diffuses into the grain from the boundary, the reaction is more advanced in the peripheral regions of the grain.

A.III.3 Conclusions

Electron microscopy of nitrided Fe-3 wt.%Mo - 1 wt.%Ni shows that:

(a) the stable nitride β^m-$Ni_8Mo_{12}N_4$ is not precipitated even after overaging, and the alloy behaves essentially as a ternary Fe-Mo-N alloy;

(b) the transformation

GP zones ⟶ intermediate phase ⟶ equilibrium nitride

occurs isothermally and continusouly when the molybdenum concentration is low;

(c) the intermediate phase contains either iron or nickel or both in ordered metal-atom sites.

REFERENCES

Aaronson, H.I. and Clark, J.B. 1968, Acta Met. 16, 845.

Ashby, M.F. and Brown, L.M. 1963, Phil. Mag. 8, 1649.

Austin, J.B. and Ricketts, R.L. 1939, Trans. A.I.M.E. 135, 396.

Baird, J.D. and Jamieson, A. 1963, N.P.L. Symposium No. 15.

Baird, J.D. and Jamieson, A. 1966, J.I.S.I. 204, 793.

Baird, J.D. and Mackenzie, C.R. 1964, J.I.S.I. 202, 427.

Baker, R.G. and Nutting, J. 1959, "Precipitation Processes in Steel". I.S.I. Special Report No. 64.

Becker, R. 1938, Ann. Phys. 32, 128.

Bell, T., Hetherington, G. and Jack, K.H. 1962, Phys. and Chem. of Glasses 3, 5 and 141.

Booker, G.R., Norbury, J. and Sutton, A.L. 1957, J.I.S.I. 187, 205.

Borelius, G., Berglund, S. and Avsan, O. 1950, Arkiv Fysik 2, 551.

Brunauer, S., Jefferson, M.E., Emmet, P.H. and Hendricks, S.B. 1931, J. Am. Chem. Soc. 53, 1778.

Burke, J. 1961, Phil. Mag. 6, 1439.

Burke, J. 1965, "The Kinetics of Phase Transformations in Metals." Pergamon.

Cahn, J.W. 1957, Acta Met. 5, 169.

Cahn, J.W. 1959, Acta Met. 7, 18.

Darken, L.S. 1958, N.P.L. Symposium No. 9.

Davenport, A.T. and Honeycombe, R.W.K. 1967, "Precipitation in Iron-Tungsten-Carbon Alloys." B.I.S.R.A. Report.

Dijkstra, L.J. 1947, Philips Res. Rep. 2, 357.

Dijkstra, L.J. 1949, Trans. A.I.M.E. 224, 1119.

Dijkstra, L.J. and Sladek, R.J. 1953, Trans. A.I.M.E. 197, 69.

Driver, J.H. and Papazion, J. 1972, to be published in Acta Met.

Evans, D.A. 1957, Ph. D. Thesis, University of Durham.

Evans, D.A. and Jack, K.H. 1957, Acta Cryst. 10, 769.

Fast, J.D., Meijering, J.L. and Verrijp, M.B. 1961, Met. Corr. Ind. 36, 431.

Forrest, P.G. and Hopkin, L.M.T. 1963, N.P,L. Symposium No. 15.

Fraker, A.C. 1967, Ph. D. Thesis, North Carolina State University, U.S.A.

Fridberg, J., Torndahl, L.E. and Hillert, M. 1969, Jernkont, Ann. 153, 263.

Grieveson, P. 1960, M. Sc. Thesis, University of Durham.

Hägg, G. 1930a, Z. Phys. Chem. (B) 7, 339.

Hägg, G. 1930b, Z. Phys. Chem. (B) 11, 152.

Hale, K.F. and McLean, D. 1963, J.I.S.I. 201, 337.

Ham, F.S. 1958, J. Chem. Phys. of Solids 6, 335.

Ham, F.S. 1959, J. Appl. Phys. 30, 1518.

Hansen, M. 1958, "Constitution of Binary Alloys". McGraw-Hill.

Hardy, H.K. and Heal, T.J. 1954, "Progress in Metal Physics". 5.

Hepworth, M.T., Smith, R.P. and Turkdogan, E.T. 1965, Trans. A.I.M.E. 236, 1278.

Hirsch, P.B., Howie, A., Nicholson, R.B., Pashley, D.W. and Whelan, M.J. 1965, "Electron Microscopy of Thin Crystals". Butterworths.

Hopkin, L.M.T. 1965, J.I.S.I. 203, 583.

Jack, D.H. 1970, Unpublished work, University of Newcastle upon Tyne.

Jack, D.H., Lidster, P.C., Grieveson, P. and Jack, K.H. 1971, Conference on Metallurgical Thermochemistry Sheffield.

Jack, K.H. 1948, Proc. Roy, Soc. (A) 195, 34.

Jack, K.H. 1951a, Proc. Roy. Soc. (A) 208, 200.

Jack, K.H. 1951b, Proc. Roy. Soc. (A) 208, 216.

Jack. K.H. and Maxwell, D. 1952, J.I.S.I. 170, 254.

Jamieson, R.M. and Kennedy, R. 1966, J.I.S.I. 204, 1208.

Johnson, W.A. and Mehl, R.F. 1939, Trans. A.I.M.E. 135, 416.

Keh, A.S. and Wriedt, H.A. 1962, Trans. A.I.M.E. 224, 560.

Kelly, A. and Nicholson, R.B. 1963, "Progress in Materials Science". 10, No. 3.

Keown, S.R. and Dyson, D.J. 1966, J.I.S.I. 204, 832.

Khitrova, V.I. and Pinsker, Z.G. 1959, Kristallografiya 4, 545. Soviet Physics - Crystallography 4, 513.

Khitrova, V.I. and Pinsker, Z.G. 1962, Kristallografiya 6, 882. Soviet Physics - Crystallography 6, 712.

Kiessling, R. and Liu, Y.H. 1951, J. Metals 3, 639.

Kiessling, R. and Peterson, L. 1954, Acta Met. 2, 675.

Köster, W. and Horn, W. 1966, Arch. Eisen. 37, 245.

Krainer, H. 1950, Arch. Eisen. 21, 39.

Kuo, K. 1953, Acta Met. 1, 301.

Leak, D.A., Thomas, W.R. and Leak, G.M. 1955, Acta Met. 3, 501.

Leciejewicz, J. 1964, J. Less Common Metals 7, 318.

Lehrer, E. 1930, Z. Electrochem. 36, 383.

Lehtinen, B. 1972, "Conference on Interstitials in Steel" Hagfors, Sweden.

Lorimer, G.W. 1970, Fizika 2, 33.

Mehl, R.F., Barret, C.S. and Jerabek, H.S. 1934, Trans. A.I.M.E. 113, 211.

Mitchell, J.B. 1971, Acta Met. 19, 1063.

Mortimer, B., Grieveson, P. and Jack, K.H. 1972, Sand. J. Met. 1, 203. see also Mortimer, B. 1971, Ph. D. Thesis, University of Newcastle upon Tyne

Nutter, K. 1969, Ph. D. Thesis, University of Newcastle upon Tyne.

Paranjpe, V.G., Cohen, M., Bevers, M.B. and Floe, C.F. 1950, Trans. A.I.M.E. 188, 261.

Pehlke, R.D. and Elliott, J.F. 1960, Trans. A.I.M.E. 218, 1088.

Pitsch, W. and Schrader, A. 1958, Arch. Eisen. 29, 715.

Pipkin, N.J. 1967, Ph. D. Thesis, University of Newcastle upon Tyne.

Pope, M., Grieveson, P. and Jack, K.H. 1973, Scand. J. Met. 2, 29 see also Pope, M. 1972, Ph. D. Thesis University of Newcastle upon Tyne.

Pope, M., Krawitz, A., and Jack, K.H. 1972, to be published - see Pope, M. 1972.

Ritchie, I.G. and Rawlings, R. 1967, Acta Met. 15, 491.

Roberts, W. 1970, Ph. D. Thesis, University of Newcastle upon Tyne.

Schenk, H., Frohberg, M. and Graf, H. 1958, Arch. Eisen, 29, 683.

Schönberg, N. 1954a, Acta Chem. Scand. 8, 204.

Schönberg, N. 1954b, Acta Chem. Scand. 8, 932.

Schönberg, N. 1955, Acta Met. 3, 14.

Seitz, F. 1943, "The Physics of Metals". McGraw-Hill.

Snoek, J.L. 1941, Physica 8, 711.

Speirs, D.L. 1969, Ph. D. Thesis, University of Newcastle upon Tyne.

Speirs, D.L., Roberts, W., Grieveson, P. and Jack, K.H. 1971, Proc. of the 2nd International Conference on the Strength of Metals and Alloys, 2, 601. (American Society of Metals.)

Stephenson, A., Grieveson, P. and Jack, K.H. 1973, Scand. J. Met. 2, 39.

Szabó-Miszenti, G. 1970, Acta Met. 18, 477.

Tu, K.N. and Turnbull, D. 1968, "The Mechanism of Phase Transformations in Crystalline Solids". Institute of Metals Monograph no. 33.

Turnbull, D. 1955, Acta Met. 3, 55.

Turnbull, D. and Treaftis, H.N. 1955, Acta Met. 3, 43.

Wert, C. 1950, J. App. Phys. 21, 5.

Westgren, A. 1933, Jernkont. Ann. 117, 1.

Wreidt, H.A. and Zwell, L. 1962, Trans. A.I.M.E. 224, 1242.

Zener, C. 1959, J. App. Phys. 20, 962.